



**University of
Leicester**

**Strategies To Reduce Morphine Tolerance In Cancer:
Evaluation Of The Bifunctional Opioid
UFP-505**

Thesis submitted in partial fulfillment of the requirements for the degree of
Doctor of Philosophy

Written by:
NIKOLAOS DIETIS

Supervisors:
D.G. Lambert
D. J. Rowbotham

FEBRURARY 2012



University of Leicester

Strategies To Reduce Morphine Tolerance In Cancer: Evaluation Of The Bifunctional Opioid UFP-505

Thesis submitted in partial fulfillment of the requirements for the degree of
Doctor of Philosophy

Written by:
NIKOLAOS DIETIS

Supervisors:
D.G. Lambert
D. J. Rowbotham

FEBRURARY 2012

Funded by a HOPE Against Cancer studentship



Strategies To Reduce Morphine Tolerance In Cancer: Evaluation Of The Bifunctional Opioid UFP-505

Nikolaos Dietis

Morphine is a gold-standard analgesic acting at MOP (μ) opioid receptors, producing analgesia and tolerance when administered chronically to patients (e.g., cancer patients). If DOP (δ) opioid receptors are blocked at the same time that MOP is activated then analgesia with reduced tolerance results. UFP-505 (H-Dmt-Tic-Gly-NH-Bzl) is a synthetic pseudopeptide that interacts with MOP and DOP receptors (bifunctional). In a series of different models, we have characterized the pharmacological profile of UFP-505 and we evaluated its antinociceptive properties *in vivo*.

In Chinese Hamster Ovary (CHO) cells stably expressing human MOP or DOP receptors, UFP-505 presented a full agonism and ultra-low partial agonism respectively. UFP-505 caused a concentration-dependent internalization of MOP receptors, in contrast to morphine. Additionally, UFP-505 caused DOP receptor internalization similar to the full DOP agonist DPDPE. In a series of tail-flick assays using Wistar rats, acute intrathecal (i.t.) 10nmol UFP-505 produced strong antinociception, similar to 10nmol i.t. morphine. After 3 days of repeated administration, UFP-505 did not produce antinociceptive tolerance, in contrast to morphine. In neuronal tissue of treated animals, UFP-505 caused varying changes to opioid receptor mRNA levels, similar to morphine. In the same model, UFP-505 induced MOP and DOP receptor internalization, whereas morphine failed to internalize the MOP receptors. UFP-505 also induced the internalization of MOP and DOP receptors in a novel CHO cell line stably expressing both receptors (produced as part of this project), in contrast to morphine.

Collectively this thesis has made a significant contribution to the field in that: 1) an extensive pharmacological *in vitro* and *in vivo* characterization is made; 2) a MOP-agonist/DOP-partial agonist is shown to produce strong antinociception with no tolerance.

Further work on bifunctional opioids may lead to a better understanding of the mechanisms of analgesic tolerance and ligands like UFP-505 are good examples of prototypes for further development.

ACKNOWLEDGMENTS

This thesis would not have been possible without the guidance and support of my supervisors, **Professors David Lambert** and **David Rowbotham**. I would especially like to thank David Lambert for his invaluable contribution to my development as a researcher, his continuous encouragement during the project and his practical and psychological support in rough times. For me he will always be an exemplar of an academic and supervisor.

My gratitude goes to the Leicestershire & Rutland charity **HOPE Against Cancer** for their generous funding of this project and for providing me with a stipend that allowed me to support myself and my family for the duration.

I am indebted to my colleague, collaborator, friend and gym-buddy **Dr John McDonald**, with whom I've spent most of my time at Leicester. He has always been there for me, answering my irritatingly numerous questions, introducing me to new laboratory techniques, supporting me psychologically with my personal life and sharing his extensive knowledge on Arnold Schwarzenegger's techniques for weight-lifting.

It is a pleasure to thank my Italian collaborators who supported this research, **Drs Giro Calo** and **Remo Guerrini** for their work on UFP-505 and their contribution to the publications that arose from this thesis, my friend and colleague **Stefano Molinari** for the great time we had and for his lessons on Italian swearwords and, **Dr Giovanni Vitale** and his fantastically friendly team (**Valentina, Monica** and **Chiara**) for providing their lab in Modena and sharing their knowledge for the *in vivo* experiments of UFP-505, as well as for welcoming me to their beautiful country. Ciao a tutti!

Also, I would like to thank my colleagues and friends at the University of Leicester; **Dr Benjamin Hunt** for his welcoming during my first year and his guidance to molecular biology techniques, **Sonja Khemiri** for endured my religious aphorisms during numerous cloning attempts and for accepting my outrageous enlightenment to name a new cell line from the initials of our names (SONIC), and all the research nurses and administrators at the **Department of Anaesthesia** for their fantastic support and for creating the warmest environment to work in.

I would also like to thank the many people that played an important role to my education and helped me reach this level, especially **Professor Mark Darlison** who was the first supervisor that really believed in my potential and gave me an excellent support during my MRes degree, and all the lecturers at the University of Leicester, the **Nottingham Trent University** and the **University of Portsmouth**, with whom I've worked with and provided their guidance through my studies.

I would like to finish with the most important piece of my life; my family, to whom I owe everything I have achieved so far. Mostly my wife **Giota**, who still tolerates my flaws, tells me that "things will go better" when I need it most, and always provides her love and support unconditionally. My brother-in-law **Rafael**, for providing abundant joy and relaxation during these three years. My brother **Teo**, for his understanding and for sending me a brand-new laptop to write-up my thesis when my PC stopped working although living thousands of kilometres apart. My **parents** for their love and financial support through the rough times and my **parent-in-laws** for always believing in me and being there when needed most.

“There is nothing impossible to him who will try”

ALEXANDER THE GREAT

*“Healing is a matter of time, but curing is sometimes
a matter of opportunity”*

HIPPOCRATES

LIST OF CONTENTS

CHAPTER 1. INTRODUCTION	1
<hr/>	
1.1. Opioid Receptors	1
1.1.1. General Classification & Nomenclature	1
1.1.2. History of Opioid Receptors	8
1.1.3. Distribution and Function of Opioid Receptors	9
1.1.4. Receptor Structure	11
1.1.5. Opioid Receptor Signalling	13
1.1.5.1. General Opioid Receptor Signalling Pathway	13
1.1.5.2. The Role of G α Subunit to Analgesia	17
1.1.6. Receptor Desensitization and Internalization	18
1.1.7. Alternative Splicing	21
1.1.8. Dimerization of Opioid Receptors and Molecular Interactions	24
1.2. Opioid Ligands	30
1.2.1. Endogenous Ligands	30
1.2.2. Exogenous Opioid Ligands and Morphine	30
1.2.3. Pain Pathways and Processing	33
1.2.4. Molecular Basis of Analgesic Tolerance: Morphine as an Example	38
1.3. Cancer Pain	40
1.3.1. Clinical Description	40
1.3.2. Current Therapies and Limitations	40
1.3.3. Pain Undertreatment	43
1.4. The “Multi-Targeting” Concept	45
1.4.1. Bivalent and Bifunctional Ligands	45
1.4.2. MOP and DOP Receptor Interaction Studies	48
1.4.3. Multiple Receptor Selectivity	64
1.5. UFP-505	65
1.6. Aims of the Thesis	66
<hr/>	
CHAPTER 2. GENERAL METHODS	68
<hr/>	
2.1. General Theory of Ligand Biding	69
2.2. Properties and Handling of Radioligands	70
2.2.1. Characteristics of Radioligands	70
2.2.2. Efficiency of Detection of Radioactivity (β -counting)	71
2.3. The Role of Non-Specific Binding	71
2.4. Saturation Binding Assay.....	73

2.4.1.	Theory	73
2.4.2.	Methodology	75
2.5.	Displacement Binding Assay	76
2.5.1.	Theory	76
2.5.2.	Methodology	77
2.6.	GTPγ³⁵S Assay	78
2.6.1.	Theory	78
2.6.2.	Methodology	80
2.7.	Cyclic Adenosine Monophosphate Assay	81
2.7.1.	General Theory	81
2.7.2.	Assay Theory	81
2.7.3.	Methodology	83
2.8.	Receptor Internalization Studies	85
2.8.1.	General Theory	85
2.8.2.	Methodology	85
2.9.	<i>In Vivo</i> Nociception Assays	86
2.9.1.	Particulars of the Study	86
2.9.2.	Animal Handling	86
2.9.3.	Catheterization of Animals	87
2.9.4.	Tail-Flick Assay	88
2.9.4.1.	Theory	88
2.9.4.2.	Experimental Design	90
2.9.4.3.	Methodology for Acute Experiments	91
2.9.4.4.	Methodology for Repeated Administration Experiments	91
2.9.5.	Hot-Plate Assay	92
2.9.5.1.	Theory	92
2.9.5.2.	Experimental Design and Methodology	92
2.9.6.	Tissue Removal	93
2.10.	Production of a Double-Expression System	94
2.10.1.	Theory	94
2.10.2.	Concentration-Death Plot	94
2.10.3.	Stable Transfection	95
2.10.4.	Subcloning	96
2.10.5.	Reverse Transcription PCR	97
2.10.5.1.	General Theory	97
2.10.5.2.	TaqMan Probes	99
2.10.5.3.	Cells-To-Ct TM	100
2.10.5.4.	Methodology for RT-PCR	102
2.11.	Statistical Analysis Methodology	103

CHAPTER 3. <i>IN VITRO</i> PHARMACOLOGICAL CHARACTERIZATION OF UFP-505	104
3.1. Introduction	105
3.2. Aims	107
3.4. Saturation Binding Assays	107
3.5. Displacement Binding Assays	110
3.6. GTP γ ³⁵ S Assays	112
3.7. Antagonist Affinity of UFP-505 in a GTP γ ³⁵ S Assay	115
3.8. Inhibition of Forskolin-Stimulated cAMP Formation.....	116
3.9. GTP γ ³⁵ S Assay in Rat Nervous Tissue	119
3.10. Discussion	121
CHAPTER 4. STUDIES OF OP`IOID RECEPTOR INTERNALIZATION...	126
4.1. Introduction	127
4.2. Aims	129
4.3. UFP-505 Induces Internalization of Recombinant MOP Receptors Expressed in CHO Cells	129
4.4. UFP-505 Also Induces Internalization of Recombinant DOP Receptors Expressed in CHO Cells	133
4.5. Full Saturation Curves After Pretreatment of CHO _{hMOP} And CHO _{hDOP} Cells With 10 μ M UFP-505 For 1 Hour	134
4.6. Discussion	138
CHAPTER 5. <i>IN VIVO</i> CHARACTERIZATION OF UFP-505 IN RATS	143
5.1. Introduction	144
5.2. Aims	144
5.3. Acute Intrathecal Administration of UFP-505 Produces Analgesia: Acute Administration	145
5.4. Subchronic Intrathecal Administration of UFP-505 10nmol Does Not Produce Tolerance When Compared to Morphine 10nmol	150
5.5. Subchronic Subcutaneous Administration of Morphine 5mg/kg Produces Tolerance in a Hot-Plate Assay	158
5.6. Discussion	159
CHAPTER 6. <i>IN VITRO</i> STUDIES OF NEURONAL TISSUES EXTRACTED FROM RATS TREATED WITH UFP-505 AND REFERENCE LIGANDS	166
6.1. Introduction	167

6.2.	Aims	167
6.3.	Loss of Cell-Surface Opioid Receptors in the Spinal Cord and the Frontal Cortex in Rats Treated Acutely with Intrathecal UFP-505 or Morphine	168
6.4.	Changes in Opioid-Receptor mRNA Expression in Neuronal Tissue Taken From Acutely and Chronically Opioid Treated Rats	171
6.5.	Discussion	175

CHAPTER 7. ESTABLISHMENT AND STUDIES OF A NOVEL CHO_{hMOP/hDOP} CO-EXPRESSION SYSTEM.....	181
--	------------

7.1. Introduction	182
7.2. Aims	182
7.3. The Concentration-Death Plot	183
7.4. Selection of an Appropriate Monoclonal CHO _{hMOP/hDOP} Cell Batch	184
7.5. Displacement Binding Assay of Various Ligands in CHO _{hMOP/hDOP} Cells	189
7.6. Receptor Internalization in CHO _{hMOP/hDOP} Cells	190
7.7. Discussion	192

CHAPTER 8. GENERAL DISCUSSION	197
--	------------

8.1. Summary of Main Findings	199
8.2. Putting The Thesis Findings Into Context With Exiting Literature	204
8.2.1. Other UFP-505 Data	204
8.2.2. Data in the Literature for Other Bifunctional Compounds	208
8.2.3. Receptor Internalization and Analgesic Tolerance	212
8.2.4. <i>In Vivo</i> Studies of Analgesic Tolerance With Bifunctional Ligands	215
8.3. Unexpected and Contentious Issues Arising From this Thesis	218
8.3.1. Residual DOP Agonism for UFP-505	218
8.3.2. Reduction of Morphine Analgesia at 2 Hours After Acute Administration: Acute Tolerance or Metabolism?	219
8.3.3. Tolerance After Repeated Administration of Naltrindole and Morphine	221
8.3.4. Downregulation of NOP mRNA After Acute Administration of Morphine or UFP-505	222
8.3.5. Relationship Between mRNA Levels and Receptor Expression in CHO _{hMOP/hDOP} Cells	224
8.3.6. Binding Affinity of Ligands in CHO _{hMOP/hDOP} Cells	225
8.4. Limitations of Study and Suggestions for Further Experiments	227
8.4.1. <i>In Vivo</i> Characterization	227
8.4.2. Double-Expression Recombinant System	228
8.5. Importance of the Thesis Findings	229
8.6. Future Work	231

APPENDIX	232
A1. Sources of Materials	232
A2. Cell Culture And Membrane Preparation	233
A3. Displacement Binding Curves for MCI compounds in CHO_{hMOP} Cells	234
A4. Methodology for the Electrically-Stimulated Isolated Tissue	237
A5. Conversion of Tail-Withdrawal Latencies to % of Maximum Possible Effect	238
A6. Receptor Internalization in CHO_{hMOP/hDOP} Cell Line: Is It Consistent with Single-Expression Internalization Data?	239
A7. Plasmid Information for the Production of The CHO_{hMOP/hDOP} Cell Line	240
A8. Attempts To Produce a pcDNA3.1/Hygro(+)-OPRD1 Plasmid in The Lab	241
A8.1. Restriction Enzyme Digestion of Plasmids	241
A8.2. DNA Purification and Ligation of Products	242
A8.3. Bacterial Transformation, Gene Identification and Purification	243
A8.4. Limitations and Setbacks Encountered	245
A9. Publications Arising From This Thesis	246
A9.1. Full Papers	246
A9.2. Reviews	246
A9.3. Abstracts	247
A9.4. Presentations	247
A10. Awards Relating To This PhD Thesis	248
REFERENCES	249

LIST OF FIGURES AND TABLES

Figure	Page
1.1	3
1.2	5
1.3	6
1.4	12
1.5	14
1.6	16
1.7	20
1.8	22
1.9	31
1.10	32
1.11	35
1.12	36
1.13	37
1.14	42
1.15	45
1.16	46
1.17	65
2.1	69
2.2	72
2.3	73
2.4	74
2.5	76
2.6	79
2.7	82
2.8	88
2.9	89
2.10	90
2.11	99
2.12	100
3.1	106
3.2	108
3.3	109
3.4	110
3.5	111
3.6	113
3.7	114
3.8	115
3.9	117
3.10	118
3.11	119
3.12	123
3.13	124
4.1	130
4.2	131

4.3	132
4.4	134
4.5	136
4.6	137
4.7	140
5.1	146
5.2	148
5.3	149
5.4	151
5.5	152
5.6	153
5.7	154
5.8	155
5.9	156
5.10	157
5.11	159
5.12	161
6.1	169
7.1	184
7.2	185
7.3	188
7.4	189
7.5	190
7.6	191
8.1	200
8.2	213
A	236
B	240
C	243
D	245

Table	Page
1.1	10
1.2	47
1.3	49
1.4	51
2.1	75
2.2	78
2.3	81
2.4	83
2.5	84
2.6	95
2.7	101
2.8	101
2.9	102
2.10	102

3.1	114
3.2	118
3.3	120
6.1	170
6.2	172
6.3	173
6.4	174
7.1	186
7.2	194
7.3	196
8.1	205
8.2	210
8.3	211
A	237

LIST OF ABBREVIATIONS

ΔCt	Cycle threshold difference
AC	Adenylyl cyclase
ATP	Adenosine triphosphate
B_{max}	Maximum receptor density
BSA	Bovin serum albumin
CHO	Chinese hamster ovary
cAMP	adenosine-3',5'cyclic monophosphate
CHO_{hDOP}	Chinese hamster ovary cells transfected with human DOP receptor
CHO_{hKOP}	Chinese hamster ovary cells transfected with human KOP receptor
CHO_{hMOP}	Chinese hamster ovary cells transfected with human MOP receptor
CHO_{hNOP}	Chinese hamster ovary cells transfected with human NOP receptor
Cpm	Counts per minute
Ct	Cycle threshold
CTOP	H-D-Phe-Cys-Tyr-D-Trp-Orn-Thr-Pen-Thr-NH ₂
DAMGO	[D-Ala ² ,MePhe ⁴ ,Gly-ol ⁵]enkephalin
Dmt	2',6'-dimethyl-L-tyrosine
DNA	Deoxyribonucleic acid
DOP	Delta opioid peptide
DPDPE	[D-Pen ² ,D-Pen ⁵]enkephalin
Dpm	Disintegrations per minute
DPN	Diprenorphine
EC₅₀	Effective concentration for 50% of effect
EDTA	Ethylenediaminetetraacetic acid
EM1	Endomorphin 1; Tyr-Pro-Trp-Phe-NH ₂
E_{max}	Maximum effect
GABA	γ-aminobutyric acid
GDP	Guanosine diphosphate
GOI	Gene of interest
GPCRs	G protein coupled receptors
GpI	Guinea pig ileum
GRK	G-protein receptor kinase
GTP	Guanosine triphosphate
GTPγ³⁵S	Guanosine-5'-O-(3-[³⁵ S]thio)triphosphate
HEPES	(N-(2-Hydroxyethyl)piperazine-N'-(2-ethanesulphonic acid))
i.c.v.	Intracerebroventricular(ly)
i.p.	Intraperitoneal(ly)
i.t.	Intrathecal(ly)
IUPHAR	International Union of Pharmacology

i.v.	Intravenous(ly)
K_d	Dissociation constant
K_i	Ligand affinity constant
KOP	Kappa opioid peptide
LT	Latency time
M6G	Morphine-6-glucuronide
MOP	Mu opioid peptide
mRNA	Messenger ribonucleic acid
Mvd	Mouse vas deferens
NMDA	<i>N</i> -Methyl- <i>D</i> -aspartic acid
N/OFQ	Nociceptin
NT	Naltrindole
NSAID	Non-steroidal antinflammatory drug
NSB	Non-specific binding
OPRD1	Opioid receptor delta 1 gene
OPRM1	Opioid receptor mu 1 gene
PAG	Pariaquaeductal gray
PCR	Polymerase chain reaction
PKA	Protein kinase A
PKC	Protein kinase C
PTX	Pertussis toxin
RT	Room temperature
RT-PCR	Reverse transcription polymerase chain reaction
s.c.	Subcutaneous
Tic	1,2,3,4-tetrahydroisoquinoline-3-carboxylic acid
UFP-101	[Nphe ¹ ,Arg ¹⁴ ,Lys ¹⁵]Nociceptin-NH ₂
UFP-505	H-Dmt-Tic-Gly-NH-CH ₂ -Ph
UFP-512	H-Dmt-Tic-NH-CH(CH ₂ -COOH)-Bid
WHO	World health organization

CHAPTER 1.
GENERAL INTRODUCTION

Chapter 1. General Introduction

1.1. Opioid receptors

1.1.1. General classification & nomenclature

The International Union of Basic and Clinical Pharmacology (IUPHAR) Committee on Receptor Nomenclature and Drug Classification, has established the IUPHAR-Database of Receptors, which issues general guidelines on receptor nomenclature that are widely accepted throughout the scientific community. According to IUPHAR, receptors are categorised in families, sub-families, types and sub-types (Sharman *et al*, 2011).

G-protein coupled receptors (GPCRs) are the largest *family* of receptors, with more than 10.000 receptor-members (thus often called “superfamily of receptors”). All GPCRs possess three common main characteristics: 1) a seven-transmembrane domain structure and 2) an affinity for guanine nucleotide-binding (G) proteins and 3) activation is initiated upon ligand binding.

The GPCR family-members are further classified into four main sub-families, which share a number of characteristics (other than those of the general family). These sub-families are called ‘*Classes*’ of GPCRs, *i.e.* the A, the B and the C class are the three main subfamilies of GPCRs with a total of six classes recorded by IUPHAR (figure 1.1). It is common practice that these classes of GPCRs take a name of the main receptor member that mostly attributes its characteristics or was first studied. For example, class A of GPCRs is also called the rhodopsin-like receptor class, class B the secretin-like receptor class, class C the metabotropic glutamate-like receptor class. Despite the fact that there are indications of evolutionary relationship among these

classes of receptors and that they have many structural and signal-transduction pathway similarities, these classes do not share any phylogenetic similarities and therefore the difference in their characteristics is regarded as fundamental.

G-PROTEIN COUPLED RECEPTORS					
Class A	Class B	Class C	Class D	Class E	Class F
Amine	Calcitonin	mGlutamate	Fungal pheromone A	cAMP	Frizzled
Peptide	Corticotropin-RF	Calcium-sensing like	Fungal pheromone B		Smoothened
Hormone	Gastric-IP	Pheromone	Fungal pheromone M		
Rhodopsin	Glucagon	GABA-B			
Olfactory	Growth-HRH	Taste			
Prostanoid	Parathyroid H				
Nucleotide	Secretin				
Cannabinoid	Vasoactive PP				
Platelet-AF	Diuretic H				
Gonadotropin-RH	EMR1				
Thyrotropin-RH	Latrophilin				
Melatonin					
Viral					
Lipid					
Leuotriene B4					

Figure 1.1. *Classification of G-protein coupled receptor family of receptors as described by the GLIDA (GPCR-Ligand Database). The six classes of GPCRs do not share significant sequence homology. Sub-families of GPCRs under each class (main ones shown in the figure), share a common evolutionary development reflected by a substantial sequence homology (up to 70%). Sub-families are named here by the type of ligand (i.e. peptide, glucagon) or a common receptor characteristic (i.e. tissue expressed). There are some receptors that have not yet been classified in one of the sub-families (orphaned receptors; not shown in this table).*

Class A is the largest of the GPCR subfamilies, comprising more than 80% of all GPCRs. Due to this large quantity, further classification based on phylogenetic analysis (in a sense of evolutionary development) has been particularly useful. Class A of GPCR is divided in a total of 19 *subfamilies*.

The peptide subfamily of GPCR includes four different receptors that have phylogenetic similarities. These are the opioid, somatostatin, neuropeptide and GPR1-orphan receptors. Apart from the latter, the first three receptors are comprised of different receptor *types*. These receptor types are linked by two main characteristics: 1) share a structural homology and 2) they acquire similar receptor function properties.

Regarding the opioid receptors, there are three main opioid receptor types that strictly cover the above criteria of a GPCR subfamily. These are the mu (μ ; MOP), the delta (δ ; DOP) and the kappa (κ ; KOP) opioid receptors. The three primary receptor types (MOP, DOP and KOP) share high amino-acid homology (figure 1.2) and are naloxone sensitive, with the latter characteristic being used as a distinctive tool for opioid receptor characterisation. Additionally to these three opioid receptors, a fourth receptor has also been identified and is considered as an opioid receptor, called the nociceptin/orphanin-FQ (N/OFQ; NOP) receptor. The NOP receptor has the lowest homology among opioid receptors and, strictly speaking, is not a classical opioid receptor, as non-selective opioid antagonists, such as naloxone, display negligible affinity. For these reasons, the wide scientific community considers the NOP receptor as highly evolved from the subfamily of classical opioid receptors (Lambert, 2008; Sharman *et al*, 2011). Although IUPHAR characterises the N/OFQ receptor as a “non-opioid branch of the opioid receptors”, it is widely accepted by the scientific community as an “opioid” receptor with distinct biology from the main three classical opioid receptors (distribution, function, pharmacology). We will call this a ‘non-classical’ opioid receptor in this thesis.

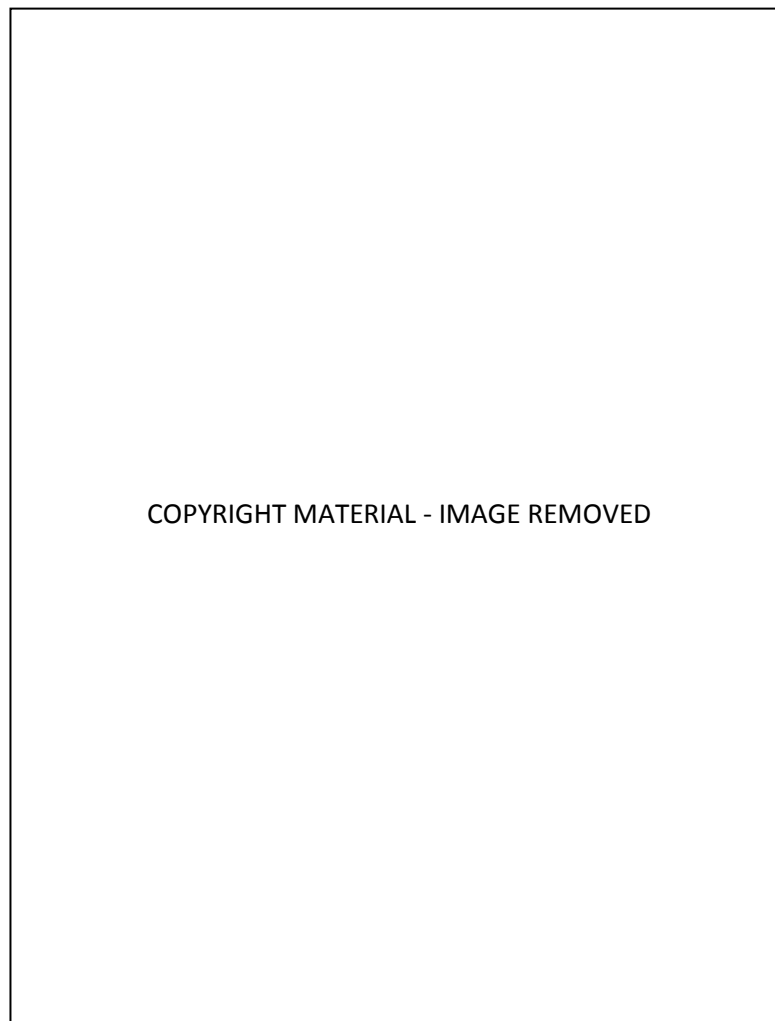


Figure 1.2. *Human DOP, MOP and KOP receptor amino acid composition, as show by comparison. The transmembrane-domain parts (TM) are underlined and numbered (modified from (Knapp et al, 1995).*

From the late '60s up to the time of formal molecular identification of single MOP, DOP, KOP and NOP receptor genes by cloning, a number of additional opioid receptor *subtypes* have been proposed, which initiated a long debate on further opioid receptor classification. This debate was initiated and powered by observed pharmacological variations within each classified opioid type, but these claims were later opposed by molecular biology findings of the single-gene/single-receptor concept.

The debate itself started as early as 1965, when Portoghese and colleagues suggested that it may be necessary to propose the existence of more than one opioid receptor type or that multiple modes of interaction of ligands with opioid receptors were possible (Portoghese, 1965). Since then, based on the pharmacology of a large number of opioid ligands, an equally large number of opioid receptor subtypes have been proposed, named as *putative* subtypes (figure 1.3). The first direct suggestions for the existence of opioid subtypes started with the μ receptor, the main target for the production of clinical analgesia (Pasternak *et al*, 1980; Wolozin & Pasternak, 1981) and this came about from the observations that some μ ligands could differentially affect the analgesic response and the unwanted respiratory depression. These sites were named μ_1 and μ_2 receptors. Similar pharmacological findings for the DOP and the KOP receptors have fuelled the proposal of a vast number of putative opioid subtypes – for the MOP into μ_1 -3, the DOP into δ_1 -2/ δ complexed/non-complexed, and for the KOP into κ_1 -3.

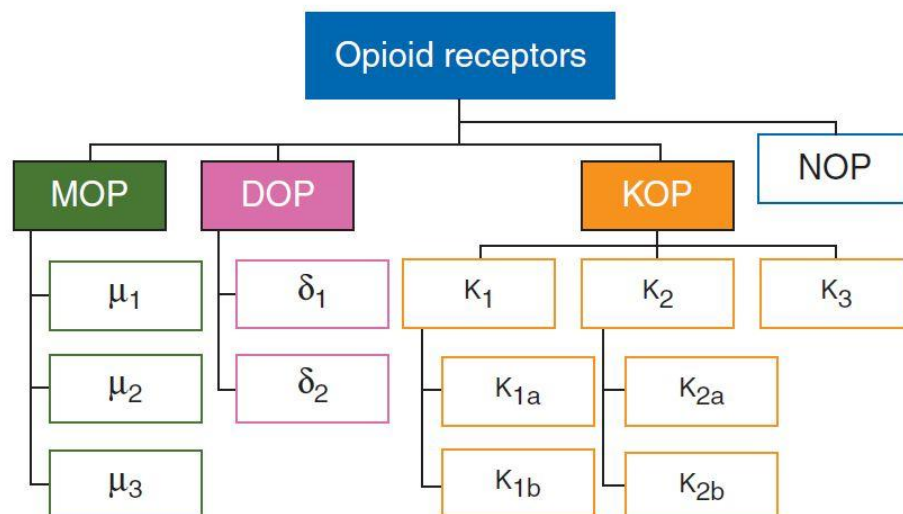


Figure 1.3. Pharmacological classification of the opioid receptor family, presenting the different proposed putative opioid receptors. The distinct pharmacology, reduced sequence homology and different function of the NOP receptor lead IUPHAR to name it as “a non-opioid branch of the opioid family”.

Nevertheless, subsequent to the molecular identification of the primary opioid receptor types by cloning and the use of this information to produce knock out animals, hard evidence for the suggested putative subtypes is lacking. Indeed, knock out of a single gene (and hence receptor) results in a loss of all function associated with that receptor. For example, in studies with MOP knock out rodents, both analgesia and respiratory (Kieffer 1999, Sona *et al.* 1997) has been abolished. This suggests that further sub-classification of the primary opioid receptor types is unwise, although the pharmacological distinction of analgesia and respiratory depression can be observed.

A simple count of the putative receptor subtypes reported in the bibliography gives a total of 11 receptors (classical and non-classical; figure 1.3). Yet, knockout of each of the individual receptor gene removes all of the receptor function associated with that particular receptor (Burmeister *et al.*, 2008; Kieffer, 1999; Kitchen *et al.*, 1997; Nitsche *et al.*, 2002; Rizzi *et al.*, 2011; Simonin *et al.*, 2001; Ueda *et al.*, 1997; Zhu *et al.*, 1999). The logical conclusion of this rather simple statement is that there are only four opioid receptor types (μ , δ , κ , and N/OFQ), recognized by IUPHAR as MOP, DOP, KOP, and NOP (which, unless referring to the pharmacological subtypes, will be used for the remainder of this thesis). In an attempt to reconcile the conflicting pharmacological and molecular evidence, there are four possible reconciliatory explanations for the pharmacological opioid receptor subtypes observed and which are discussed in this Chapter: alternative splicing-splice variants, receptor dimerization, receptor-protein interactions and functional selectivity.

1.1.2. History of opioid receptors

The existence of receptors for opiate drugs was first proposed in 1954 based on pharmacological studies with synthetic opiates (Beckett & Casy, 1954). In the early '70s, high-affinity stereospecific binding sites for different opiate drugs were discovered in the brain using naloxone (Pert & Snyder, 1973), etorphine (Simon *et al*, 1973) and dihydromorphine (Terenius, 1973) among others. In 1976, Martin *et al*. presented the first definitive evidence that the opioid receptor was not homogeneous implying the existence of opioid receptor types (Martin *et al*, 1976). They proposed two opioid receptors named after the prototypic drugs used in their studies, i.e. the μ receptor (mu for morphine) and the κ receptor (kappa for ketocyclazocine).

In 1977, pharmacological analysis of the effects of opioid peptides in the mouse vas deferens led to the discovery of the third or δ receptor (delta for 'deferens') (Lord *et al*, 1977). In parallel, a search for the endogenous ligands for these receptors led to the discovery of the enkephalins by Hughes (Hughes *et al*, 1975) as natural ligands for δ , β -endorphins by Cox (Cox *et al*, 1976) as natural ligands with activity at μ and dynorphins by Goldstein (Goldstein *et al*, 1979) as natural ligands for κ receptors. The search for selective endogenous μ ligands intensified in 1997 with the identification of the endomorphins (Zadina *et al*, 1997) but the precursors for these small peptides remain elusive. In 1992 the groundbreaking opioid studies of Kieffer and Evans (Evans *et al*, 1992; Kieffer *et al*, 1992) led to the cloning of the δ receptor, with the μ (Chen *et al*, 1993; Thompson *et al*, 1993; Wang *et al*, 1993; Zastawny *et al*, 1994), the κ (Li *et al*, 1993; Meng *et al*, 1993) and the nociceptin/orphanin FQ peptide receptor GPCR (Bunzow *et al*, 1994; Mollereau *et al*, 1994) soon to follow.

1.1.3. Distribution and function of opioid receptors

The distribution and the functional characteristics of opioid receptors have been the focus of studies since the late '80s and early '90s. Basic classification, distribution, function and pharmacology of the opioid receptors are summarised in Table 1.1.

The MOP receptors primarily, as well as some DOP and KOP receptors, are located in the thalamus, neocortex, nucleus accumbens, amygdala, colliculi and in the superficial layers of the dorsal horn of spinal cord and the raphé nuclei (Besse *et al*, 1990; Hawkins *et al*, 1988; Mansour *et al*, 1987). The main target for analgesia is the MOP receptor. Indeed, in an elegant study by Kieffer and colleagues, mice in which the MOP gene was deleted did not display morphine-induced analgesia (Kieffer, 1999). However, the MOP receptors have also been characterised to have additional differential functions apart from analgesia. These can include diverse functions as respiratory, cardiovascular, intestinal transit, feeding, mood, thermoregulation, hormone secretion and immunoregulation (Dhawan *et al*, 1996; Zastawny *et al*, 1994).

The DOP receptors are distributed in the forebrain at a higher level than in the hindbrain. They are mostly located in the olfactory bulb, the neocortex, the nucleus accumbens, amygdala, thalamus, hypothalamus and the dorsal horn of the spinal cord (Kitchen *et al*, 1997; Mansour *et al*, 1987). However, particularly the distribution of the DOP receptor shows a very wide range of density in central nervous system, as well as differential densities in different species (i.e. rat versus mouse). The functional roles of the DOP receptor are still unclear since there are many controversial studies. Apart from analgesia, there are suggestions that DOP receptors have a role in mood, behaviour, cardiovascular regulation and gastrointestinal motility (Dhawan *et al*, 1996).

Receptor Nomenclature ¹	Most common roles and functions	Most common location in the CNS ²	Endogenous Agonists ³	Selective Ligands ⁴
μ, mu, MOP, OP3	analgesia, intestinal transit, feeding, mood, hormone secretion, thermoregulation, cardiovascular function	thalamus, neocortex, amygdala, dorsal horn, inferior and superior colliculi	β-endorphin, enkephalins, endomorphin (no precursor identified)	morphine (A), DAMGO (A), β-FNA (N), DALDA(N)
δ, delta, DOP, OP1	analgesia, mood, gastrointestinal motility, behaviour, cardiovascular regulation	olfactory bulb, thalamus, neocortex, caudate putamen, nucleus accumbens, amygdala, dorsal horn	enkephalins, β-endorphin, dynorphin A(1-13),	Naltrindole (N), DPDPE (A), TIPP (N)
κ, kappa, KOP, OP2	analgesia in inflammation, diuresis, feeding, neuroprotection, neuroendocrine functions	cerebral cortex, nucleus accumbens, claustrum, hypothalamus	enkephalins, neoendorphin, dynorphin A(1-13),	KCN (A), bremazocine (A), norBNI (N)
ORL1/LC132, NOP, OP4	spinal analgesia, anxiety, mood, memory, feeding, locomotor activity	hippocampus, hypothalamus, amygdala, substantia nigra, dorsal horn, lateral septum	N/OFQ	UFP-101 (N), UFP-102 (A), Ro64-6198 (A)

Table 1.1. Classification and basic characteristics of opioid receptors, including endogenous and selective exogenous opioid ligands. *β-funaltrexamine (β-FNA), ketocyclazocine (KCN), [D-Ala², N-MePhe⁴, Gly-ol]-enkephalin (DAMGO), norbinaltorphimine (norBNI), (H-Tyr-D -Arg-Phe-Lys-NH₂ (DALDA), [D-Pen², D-Pen⁵]-enkephalin (DPDPE), nociceptin/orphanin-FQ (N/OFQ), tetrahydroisoquinoline-3-carboxylic acid (Tic), H-Tyr-Tic-Phe-Phe-OH (TIPP).* Keys: ¹Recommended and alternative nomenclature for opioid receptors as defined by NC-IUPHAR. ²For full information on receptor location in the CNS, see the NC-IUPHAR database on www.iuphar-db.org ³As published in IUPHAR receptor database. ⁴Denoted as (A) for agonist and (N) for antagonist.

The distribution of KOP receptors is in the cerebral cortex, nucleus accumbens, claustrum and hypothalamus (Kitchen *et al*, 1997; Mansour *et al*, 1987). In addition to analgesia, there is evidence that KOP receptors play a role in the regulation of diuresis, feeding, neuroendocrine and various immune system functions (Dhawan *et al*, 1996). NOP receptors are located in the anterior olfactory nucleus, lateral septum, ventral forebrain, hippocampus, hypothalamus, amygdala, substantia nigra, ventral tegmental area, locus coeruleus, brain stem nuclei and in the dorsal horn of spinal cord (Neal *et al*, 1999). In addition to the neuronal system and in contrast to other opioid receptors, the NOP receptor has also been shown to be expressed in the surface of human peripheral blood mononuclear cells (Williams *et al*, 2007). This varying distribution of NOP receptors suggests a multiple functional role which includes behaviour, reinforcement and reward, nociception, stress response and other various autonomic and immune functions (Cox *et al*, 1976; Lambert, 2008).

1.1.4. Receptor structure

The opioid receptors are all typical G-protein coupled receptors (GPCRs), stretching from an extracellular N-terminus to an intracellular C-terminus through seven transmembrane helical domains that create three intracellular and three extracellular loops. The opioid receptors adopt a cylindrical-like conformation at rest on the cell membrane, with the transmembrane domains orientated in such a way that they form a binding pocket, where ligands bind to the receptor (figure 1.4).

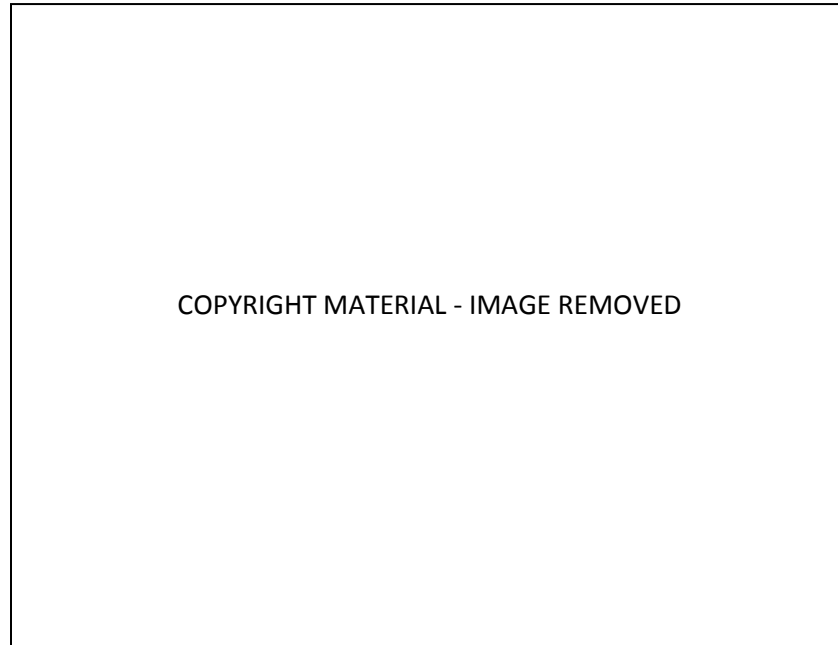


Figure 1.4. *Illustration of a MOP receptor model in an active state with agonist binding. The outer (A) and inner layer (B) of a cell's lipid bilayer determine the extracellular, intracellular and transmembrane domains of the receptor (C). The opioid ligand (D) docks in a pocket that is formed by the transmembrane and extracellular domains of the receptor and forms bonds with specific amino acids. Figure modified from (Fowler et al, 2004).*

Selectivity of each opioid ligand is explained by sequence differences among the opioid receptors at specific recognition points, the residues that play key role in formation of receptor-ligand bonding (Metzger *et al*, 1996). All four opioid receptors (MOP, DOP, KOP, NOP) are expressed through four distinct genes. Further information on the opioid genes is discussed later in this Chapter.

1.1.5. Opioid receptor signalling

1.1.5.1. General opioid receptor signalling pathway

Upon ligand binding to the receptor pocket, the receptor changes its conformation. This change of conformation increases its affinity for a nearby intramembrane G-protein, phosphorylating specific intracellular receptor residues by GPCR kinases (GRKs). G-proteins are cellular proteins that interact with the third intracellular loop and parts of the C-terminus of the receptor, comprising a family of different isoforms that have different roles (Carman & Benovic, 1998; Kenakin, 2009). Opioid receptors are associated with $G_{i/o}$ proteins, the role of which is discussed below

The G protein is a heterotrimeric protein composed of $G\alpha$, $G\beta$ and $G\gamma$ subunits. The $G\alpha$ subunit of a $G_{i/o}$ protein ($G\alpha_{i/o}$) is linked to a guanosine diphosphate (GDP), whereas the $G\beta$ and $G\gamma$ subunits are inter-associated as one subunit, the $G\beta\gamma$. Upon association of the G-protein with the receptor, the $G\alpha$ subunit exchanges GDP with guanosine triphosphate (GTP). The cell maintains a 10:1 ratio of cytosolic GTP:GDP and thus the exchange for GTP is ensured (Carman & Benovic, 1998; Kenakin, 2009). The activation of the G-protein induces the dissociation of the $G\alpha$ and the $G\beta\gamma$ subunits from the trimer, along with their dissociation from the receptor (figure 1.5).

COPYRIGHT MATERIAL - IMAGE REMOVED

Figure 1.5. *Representation of the G-protein cycle. Upon ligand binding, GDP is exchanged with GTP attached with the $G\alpha$ subunit, causing the dissociation of the $G\alpha$ and the $G\beta\gamma$ subunits and their release from the receptor. The subunits are then free to interact with their effectors. The intrinsic GTPase activity of the $G\alpha$ subunit causes the hydrolysis of the GTP to GDP and the release of a phosphate ion. The formation of GDP causes the dissociation of the $G\alpha$ subunit from its effector and increases its affinity for the $G\beta\gamma$ subunit, forming the trimeric $G\alpha\beta\gamma$ protein that associates back with the intracellular part of the receptor.*

The activated subunits modulate the activity of a number of proteins (effectors). The $G\alpha$ -GTP diffuses within the membrane and binds to a number of effectors, such as adenylyl cyclase (AC; inhibition; (Keith *et al*, 1996; Whistler & von Zastrow, 1998), K^+ channels (activation; (Cerver *et al*, 2004) and Ca^{++} channels (closure; (Borgland *et al*, 2003). AC

catalyses the conversion of cytosolic adenosine triphosphate (ctATP) to cyclic adenosine monophosphate (cAMP), acting as a second messenger within the cell. cAMP regulates a number of cellular processes through an activation-cascade of protein kinase A and gene transcription. The $G\beta\gamma$ subunit also plays a modulatory role triggering different signaling cascades by the activation of various proteins (i.e. phospholipase C, protein kinase C) (figure 1.6). However, although initially thought that $G\alpha$ and $G\beta\gamma$ have distinct signaling pathways, two prominent early studies in *Science* and *Nature* (Clapham & Neer, 1993; Tang & Gilman, 1991) have shown that not only do they share common effector proteins but also the activity of one can be modulated by the activity of the other, forming a complex mechanism that depends on a variety of factors such as the type of $G\alpha$ subunit, the type of receptor and the type of tissue.

The $G\alpha$ subunit possesses slow intrinsic GTPase activity for the $G\alpha$ -GTP bond to yield back the $G\alpha$ -GDP form. This is a protective cellular mechanism to avoid continuous activation of the opioid signalling pathway. The reformation of the $G\alpha$ -GDP triggers the re-association of all subunits and the initial conformation to the heterotrimeric form ($G\alpha\beta\gamma$). The rate of GTP hydrolysis is often mediated by the activity of allosteric modulating proteins called regulators of G-protein signalling (RGS).

COPYRIGHT MATERIAL - IMAGE REMOVED

Figure 1.6. *A simplified schematic overview of opioid receptor signaling induced by agonist binding. Solid arrows represent stimulation of effector proteins. Blunt-end lines represent inhibition of effector proteins. Dotted arrows indicate generation of second messenger signaling molecules. The $G\alpha$ subunit is also known to act on ion channels and modulate their activity (not shown here). Keys: AC; adenylyl cyclase, cAMP; cyclic adenosine monophosphate, PKA; protein kinase A, PLC; phospholipase C, DAG; diacylglycerol, IP_3 ; inositol triphosphate, PKC; protein kinase C. (Kuszk et al, 2009).*

Activated presynaptic opioid receptors in nerve terminals on non-GABAergic neurons (such as C- and A δ - fibers), directly inhibit the voltage-gated Ca^{2+} channels through the $G\alpha$ binding and the inhibition of protein kinase A activation. This inhibition of the Ca^{2+} channel causes blockage of inward Ca^{2+} and therefore the inhibition of the release of neurotransmitters by the nerve terminals (such as glutamate, substance-P and calcitonin gene-related peptides), which are responsible for propagating a “pain signal”. Activation also enhances an outward K^+ conductance. This inhibition of the pain neurotransmitters results in analgesia. Additionally, activation of presynaptic opioid receptors located in GABAergic neurons results in the inhibition of GABA release, allowing the release of dopamine from dopaminergic neurons and therefore the increase of dopamine in the nucleus accumbens, which is associated with the euphoric effect of opioids.

1.1.5.2. The role of $G\alpha$ subunit to analgesia

Pertussis toxin (PTX) modifies the structure of the $G\alpha_{i/o}$ subunit and this modification prevents the interaction of the G-protein with the receptor, rendering PTX an important tool to study $G_{i/o}$ -specific mechanisms (Fields & Casey, 1997; Ribeiro-Neto & Rodbell, 1989). Agonist-activation of MOP leads to activation of all members of pertussis toxin (PTX)-sensitive $G\alpha_{i/o}$ proteins (Chakrabarti *et al*, 1995). However, peptide and non-peptide agonists cause differential binding and activation of G-protein at the MOP receptor (Chaipatikul *et al*, 2003).

$G\alpha_i$ proteins are classified into $G\alpha_{i1}$, $G\alpha_{i2}$ and $G\alpha_{i3}$ proteins. $G\alpha_o$ is expressed at very high levels in brain and is considered to be an important protein for transducing opioid signals (Jiang *et al*, 2001). All $G\alpha_i$ subunits are able to mediate inhibition of AC, but G_{i3} is more effectively coupled in inwardly rectifying potassium channel activation, whereas $G\alpha_o$ in the inhibition of voltage-gated Ca^{2+} channels in neuronal cells (Jiang *et al*, 2001). However, $G\alpha_{i2}$ has been shown to couple more efficiently to adenylyl cyclase than other $G\alpha_i$ proteins and $G\alpha_o$ proteins. On the other hand, $G\alpha_o$ couples more effectively to inhibition of Ca^{2+} inward currents (Kenakin, 2003).

The significance of the specific- $G\alpha$ protein activation to analgesia has been investigated in a large number of studies. Antisense oligonucleotide knockdown of $G\alpha_{i2}$, but not other $G\alpha_{i/o}$ proteins, has been shown to significantly attenuate MOP-induced supraspinal antinociception in the mouse (Raffa *et al*, 1994). In addition, knockdown of different $G\alpha$ proteins differentially affects supraspinal antinociception by different MOP agonists (Sánchez-Blázquez *et al*, 2001). However, a study that used PTX-insensitive mutant $G\alpha_{i/o}$ subtypes coupled to MOP receptors, (Clark *et al*, 2006) did not observe any change in the rank order of relative agonist efficacy or potency of different MOP

agonists to receptors coupling to different $G\alpha_{i/o}$ subtypes, although reporting that agonist-activated MOP receptor couples to $G\alpha_{i3}$ more efficiently than to other $G\alpha_{i/o}$ subtypes. These results imply that any agonist-specific signalling may involve downstream signalling through a non-PTX sensitive G-protein mechanism rather than differential activation of $G\alpha_{i/o}$ subunits.

Nevertheless, a full agonist might activate all $G\alpha_{i/o}$ proteins expressed in a cell and the downstream pathways to which they are coupled, but a partial agonist may only be able to stimulate enough of the most preferred or abundant $G\alpha$ protein subtype and thus activate signalling through specific downstream pathways.

1.1.6. Receptor desensitization and internalization

Upon opioid ligand binding to the opioid receptors and the subsequent phosphorylation and activation of the G-protein, receptor desensitization occurs through its association with β -arrestins (figure 1.7). This association causes the internalization of the receptor into the cellular matrix through endocytosis by engulfment of the receptor via clathrin-coated cell membrane pits, mediated by β -arrestins and GRKs. Internalized receptors can be either incorporated into recycling endosomes which will then recycle back to the cell membrane resensitized, or will be hydrolysed by enzymes in lysosomes and thus feed the cellular amino acid engine. Additionally, there are differences among opioid receptors in terms of receptor trafficking upon ligand activation. MOP receptors are internalized and recycled to the cell membrane after dephosphorylation. DOP receptors are mostly guided to lysosomes after internalization instead of recycling to the cell surface, whereas KOP receptors do not readily internalise after ligand binding (Corbett *et al*, 2006).

Rapid endocytosis of opioid receptors is of particular interest because it is differentially regulated by individual peptide agonists and alkaloid drugs, both in cultured cells and native tissue (Keith *et al*, 1996; Koch *et al*, 1998; Von Zastrow *et al*, 1993; von Zastrow & Kobilka, 1994; Whistler & von Zastrow, 1998). Morphine has been shown to cause diminished internalization of the MOP receptor (Whistler & von Zastrow, 1998). Morphine therefore causes activation of G-protein but evades β -arrestin-mediated internalisation of the MOP receptor which remains phosphorylated on the cell membrane.

Most synthetic opioid peptides have been shown to stimulate the internalization of MOP receptors within minutes. However, MOP receptors fail to internalize even after prolonged activation with saturating concentrations of morphine, although morphine activates the same receptor-mediated signalling pathways as other ligands that induce MOP internalization (Keith *et al*, 1996). This observation has immediately attracted the attention of pharmacologists to try to explain the physiological meaning of internalization failure. As will be discussed later in this Chapter, it is believed that the failure of morphine to induce MOP receptor internalization plays a crucial role to its ability to induce analgesic tolerance.

COPYRIG COPYRIGHT MATERIAL - IMAGE REMOVED

Figure 1.7. *Mechanisms of membrane trafficking for opioid receptors. Upon agonist binding (1), the opioid receptor is phosphorylated by kinases (i.e. GRK) (2), binds to arrestin proteins (3), and undergoes internalization via endocytosis through clathrin-coated pits (4). Once internalized, the receptor is subjected to a sorting processes and is targeted either to endosomes in the recycling pathway (5) back to the membrane, or to lysosomes for degradation (6). Opioid receptors can be also synthesized in the endoplasmic reticulum (7), then transported to the trans-Golgi network (8) and become a mature receptor. Mature receptors are transported in large dense-core vesicles (9) as an intracellular pool of receptors, ready for membrane insertion. Modification from (Bie & Pan, 2007).*

1.1.7. Alternative splicing

As it has been discussed above, each type of opioid receptors is produced from a distinct gene. Nevertheless, different observations in the pharmacology of ligands that act on the same type of opioid receptor had triggered a discussion for the existence of putative opioid receptor subtypes. The supporters of this postulation have proposed ‘alternative splicing’ of the opioid receptor genes as a possible explanation behind these observations. This section will describe the mechanism of alternative splicing and discuss the studies that investigated opioid receptor gene splicing.

A gene comprises introns (non-transcriptional genomic sequence) and exons (transcriptional sequence), where mRNA is produced by excluding the introns and placing the exons in tandem (figure 1.8). Translation of the mRNA produces a functional protein. The MOP, DOP, and KOP mRNA include highly conserved regions, but also have differences in the exons translated for receptor production (Wei & Loh, 2011). MOP mRNA is composed of exons 1, 2, 3, and 4; DOP mRNA is composed of exons 1, 2, and 3, whereas KOP mRNA is composed of exons 2, 3, and 4. Alternative splicing occurs when, by various modes, the mRNAs produced from a single gene have differences in their exon composition and thus make up a different mRNA that will eventually produce a different (alternative) protein (Black, 2003).

Alternative splicing is considered a mechanism used by cells in order to enhance protein (i.e. receptor) diversity, by simply using a single gene-template. Abnormal regulation of alternative splicing is also implicated in disease (Matlin *et al*, 2005). This mode of producing different proteins from a common gene-product has been used in the opioid field in an attempt to explain the existence of putative subtypes (Tanowitz *et al*, 2008).

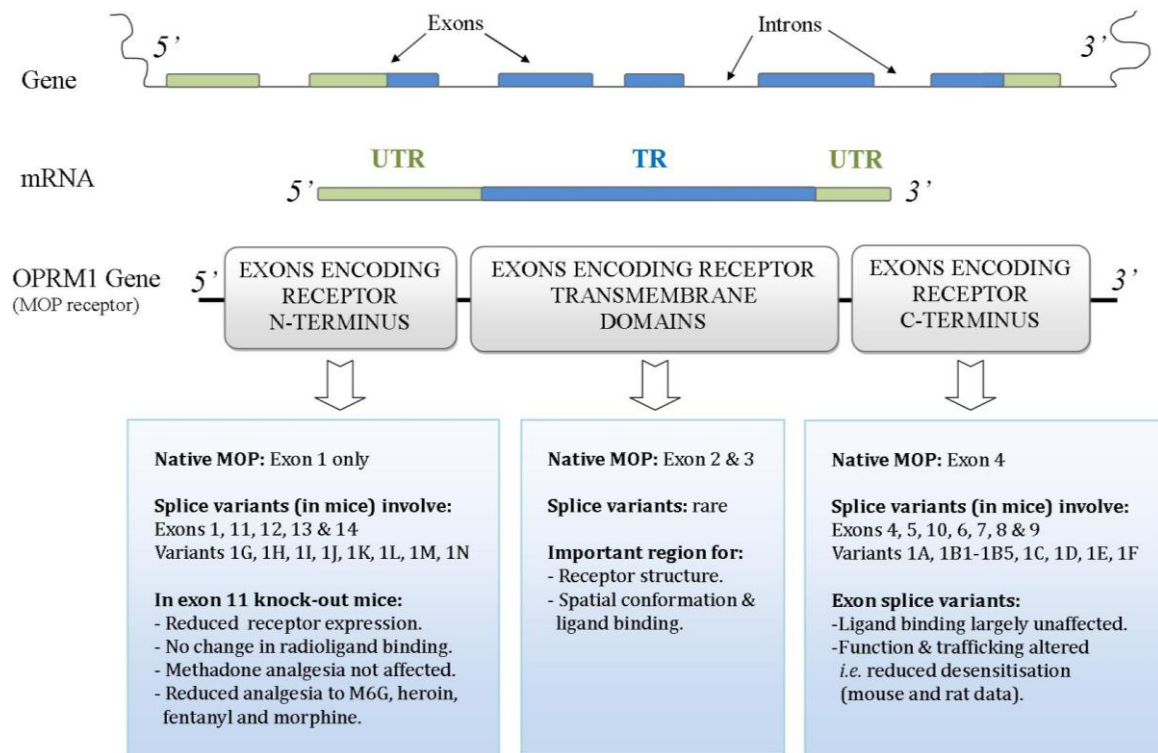


Figure 1.8. Schematic representation of the important MOP-receptor gene (*OPRM1*) splice variants. A gene contains a series of exons (seen as blocks) and introns (seen as gaps between exons). Transcription of the gene to a messenger RNA (mRNA) retains the sequence of individual exons and excludes the intermediate introns. Translation will process the mRNA to a functional protein (i.e. a receptor). The region of the mRNA that will or will not translate into a part of the protein is called the untranslated (UTR; shown as green) and translated region (TR; shown as blue) respectively. Image produced using Microsoft Office Publisher.

The first concrete data came from the MOP gene where Zimprich and colleagues (Zimprich *et al*, 1995) identified an additional splice variant of the rat MOP (then called rMOR1B) which produced a receptor truncated at the C-terminus. In the absence of C-terminal phosphorylation sites, this receptor was relatively resistant to desensitization and hence functionally different from the 'normal' MOP receptor. However, both variants bound naloxonazine (a MOP-specific antagonist) equally and the authors concluded that these receptors were not $\mu 1$ and $\mu 2$. In following studies, the MOP receptor gene (*OPRM1*) has been shown to produce a large number of splice variants

(Cadet *et al*, 2003; Pan, 2005; Pan *et al*, 2001; Pasternak, 2005; Xu *et al*, 2011) and it is beyond the scope of this thesis to cover all of these in detail. We have considered the OPRM1 gene in more detail, in terms of three very general regions: at the 5' end encoding the N-terminus in the "middle", encoding the trans-membrane regions of the receptor and at the 3' end encoding the C-terminus.

Considering first the N-terminus (*i.e.* targeted deletion of exon 11), this reduces opioid receptor density but does not affect ligand recognition at the expressed receptor. The analgesic response to M6G, heroin, fentanyl, and morphine, but not methadone, is reduced (Pan *et al*, 2009). Splice variants affecting the transmembrane portion of the receptor are rare and we have already described that C-terminally truncated variants show loss of function and reduced desensitisation (Zimprich *et al*, 1995). Cadet and colleagues proposed a correlation of an OPRM1 splice variant with the μ 3 (MOP3) putative subtype (Cadet *et al*, 2003). Compared with the OPRM1 mRNA, the variant contained a truncated mRNA 5' end (hence a truncated exon-1 and different receptor N-terminus), and a unique exon at the mRNA 3' end (hence longer receptor C-terminus), followed by a 202-nucleotide fragment of the OPRM1 untranslated region. When expressed in a heterologous system, the pharmacology of this variant was the same as that of the putative μ 3.

Interestingly, Schuller and colleagues showed that although morphine analgesia was completely abolished in exon-1 knockouts, diamorphine and M6G analgesia were still present (Schuller *et al*, 1999). These results strengthened the idea that variants of the MOP receptor lacking exon-1 are responsible for the residual activity of M6G and diamorphine. Antisense oligonucleotide targeting studies for exon-1 and -2 (*i.e.* own-

regulation of mRNA) did not show similar effects for morphine, but they blocked the analgesic effects of M6G (Pasternak, 2005). This is consistent with the suggestion that M6G and diamorphine may act through different receptor subtypes when compared with morphine (or bind with different affinities), or conversely, these receptors are splice variants. In addition to receptor variations in terms of density, function and desensitization profiles, regional differences should also be mentioned. Xu and colleagues showed that in mouse, there is a differential expression of the receptor variants among brain regions (Xu *et al*, 2011). However, this expression could be at low levels. These data may be in line with regional differences seen in opioid receptor binding and activation, and also degrees of opioid tolerance seen in different tissues as observed by Xu and others. Pasternak reports that some receptor variants differ greatly in distribution and localization with respect to the regular MOP receptor. For example, in the dorsal horn of the mouse spinal cord, there are cells expressing either MOP1 or MOP1C, but not both (Pasternak, 2005). Also, MOP1 is equally distributed pre- and post-synaptically, whereas MOP1C is distributed only presynaptically. Finally, MOP1C is always co-localized with calcitonin gene-related peptide (CGRP), whereas MOP1 is not. This example is characteristic for the distribution and localization of different splice variants and, although consistent with histological data, its biological significance is not entirely understood.

1.1.8. Dimerization of opioid receptors and molecular interactions

The mixed pharmacological profile observed for the putative opioid receptor subtypes (as discussed above), as well as data from different studies that suggested co-expression and co-localisation of opioid receptors in the same cell types, have led to studies that investigated receptor-receptor associations. One form of such associations is

dimerisation (involving two distinct receptors) or oligomerisation when the association involves more than two receptors. Dimerisation of receptors has been classified in two different forms: *Heterodimerisation* refers to the association of two different receptor types, whereas *homodimerisation* refers to the process that involves the same type of receptors. Additionally, two different receptor dimerization mechanisms have been proposed: *constitutive* dimerization (where dimers are constructed in the endoplasmic reticulum after RNA translation), and *ligand-induced* dimerization (where dimers are formed on the cell membrane in response to the presence of specific ligands) (Angers *et al*, 2002).

Data that support the interaction between two opioid receptors have been the focus of intense activity since the late 1990s, in particular opioid heterodimerization. This interest was partially triggered by the large number of possible combinations arising from the four main (or primary) opioid receptor types (MOP, DOP, KOP, and NOP), and also by initial studies that proposed distinct pharmacology and differences in signalling mechanisms (Cvejic & Devi, 1997; George *et al*, 2000; Jordan & Devi, 1999; McVey *et al*, 2001; Ramsay *et al*, 2002). Studies using immunoaffinity and immunoprecipitation assays have confirmed that opioid receptors not only dimerize in various combinations but mostly exist as receptor dimers and not monomers, in a variety of different tissues (Jordan & Devi, 1999). Other studies have confirmed that dimerization modulates receptor function and that different receptor dimers possess distinct pharmacological profiles (Jordan *et al*, 2001).

Jordan and Devi studied the DOP-KOP heterodimer and first proposed that heterodimerization modulates receptor function by presenting different pharmacological

characteristics of ligands binding to the DOP-KOP heterodimer compared to the DOP and KOP monomers (*i.e.* differences in binding affinities and potencies of agents, changes in receptor internalization ability of ligands). Opioid receptor dimers have been shown by some studies to be formed through constitutive dimerization (Milligan, 2005), although it is not yet clear if this form of dimerisation is a general rule of opioid dimerisation or if it depends on specific receptor types.

Although it has been shown that opioid receptors are coupled allosterically in a dimeric form without compromising their individual binding sites, it has been shown that the binding of a ligand to one receptor in the dimer-complex can cause a conformational change of that receptor which can affect the binding site of the other receptor in the dimer-complex (Portoghese, 2001). This effect may be described as *positive or negative co-operativity*. Portoghese proposes the existence of two recognition sites in an opioid receptor dimer, which modulate receptor activation and antagonism.

A number of studies have attempted to link the pharmacology observed in opioid receptor dimer studies, with the pharmacology seen from investigations regarding putative opioid receptor subtypes. Based on studies in the spinal cord of mice, Portoghese and Lunzer characterized the putative $\delta 1$ and $\kappa 2$ opioid receptor as a DOP-KOP heteromeric receptor (Portoghese & Lunzer, 2003). In addition, other studies suggest that the $\delta 2$ and $\kappa 1$ phenotypes might represent neighbouring associated DOP and KOP receptors (Levac *et al*, 2002). Knock-out studies by Simonin and colleagues have suggested that the putative $\kappa 2$ receptor may represent mixed populations of MOP, DOP, and KOP receptors (Simonin *et al*, 2001). Nielsen and colleagues also suggested

that the pharmacology seen with oxycodone may represent the binding and activation of an opioid receptor dimer, like DOP-KOP (Nielsen *et al*, 2007).

In the study of Hirose and colleagues on the inhibition of dopamine release via opioid receptor stimulation, it was suggested that stimulation of MOP receptors activates putative $\delta 1$ receptor subtypes which in turn activate putative $\delta 2$ sites in nucleus accumbens, a suggestion that attempts to explain the gradual rise of extracellular dopamine after MOP activation (Hirose *et al*, 2005). These data imply either cross-communication of MOP and DOP systems or a direct receptor interaction such as receptor dimerization.

There is also evidence for dimerization of the NOP receptor (described as $\kappa 3$ in some of these papers). Pan and colleagues demonstrated the presence of NOP–MOP dimers where some MOP ligands could displace [^3H]N/OFQ binding (Pan *et al*, 2002). Similar NOP–MOP dimers were described by Wang and colleagues in which MOP signalling (cAMP formation) was reduced, perhaps providing a cellular basis for the anti-opioid actions of NOP (Wang *et al*, 2005). In a very recent and elegant study, Evans and colleagues showed that NOP could dimerize with all opioid (MOP, DOP, KOP) receptors and that activation of NOP causes internalization of all receptor types and interestingly MOP and NOP co-localize and co-internalize with voltage-dependent calcium channels (Evans *et al*, 2010b).

However, some less clear data have also been generated when studying MOP-DOP dimers. Gomes and colleagues provided evidence that MOP-DOP dimers possess functional and ligand binding synergy (Gomes *et al*, 2000), whereas George and

colleagues showed a distinct binding profile of opioid ligands at MOP-DOP dimers (George *et al*, 2000). Van Rijn recently reviewed data for opioid receptor dimer trafficking, and some may be used to correlate with the properties seen of putative pharmacological subtypes (van Rijn *et al*, 2010). In another interesting recent study, Chakrabarti and colleagues reported *in vivo* data indicating that MOP-KOP dimers are vastly more prevalent in the spinal cord of females *vs* males and proestrous *vs* diestrous, suggesting that MOP-KOP dimers are a female-specific pain target (Chakrabarti *et al*, 2010).

There are opioid receptor-protein interactions, apart from dimerisation, that have been studied either in terms of receptor function or as a possible explanation for the putative opioid subtypes proposed, based on differences in coupling to effector systems. There is some evidence that opioid receptors are capable of coupling to Gi/o and Gs proteins (Chakrabarti *et al*, 2010; Chakrabarti *et al*, 2005; Connor & Christie, 1999; Crain & Shen, 1998) and we have shown that MOP, DOP, and KOP were capable of coupling to phospholipase C to increase the production of Ins(1,4,5)P₃ (Smart & Lambert, 1996; Smart *et al*, 1994). However, the pharmacology of these responses did not yield clues as to distinctly different receptor populations. There are differences in the way peptide and non-peptide MOP ligands induce receptor internalization, but these have not been reconciled against putative μ 1 or μ 2 sites (Whistler & von Zastrow, 1998). Receptor dimerization between opioid and non-opioid receptors has also shown a number of combinations, for example KOP and β 2-adrenoceptor (Ramsay *et al*, 2002) or DOP and α 1-adrenoceptor (Ramsay *et al*, 2004), and these may produce differences in pharmacological behaviour but are outside the scope of this thesis.

Another phenomenon that can alter opioid receptor function and could therefore account partially for the putative subtypes observed pharmacologically, is functional selectivity (or biased agonism) (Kenakin, 2007). This stems from the observations that ligands active at the same receptor are capable of producing different responses (i.e. the end response is biased depending on the ligand and signalling repertoire of the cell/tissue under consideration); there are compelling data in this context for the β -adrenoceptor (Evans *et al*, 2010a). Focusing on the opioid receptors, the seminal work of Whistler and von Zastrow showed that etorphine but not morphine desensitized the MOP receptor (a biased response) (Whistler & von Zastrow, 1998). Etorphine (and other ligands like fentanyl) produce high levels of phosphorylation and coupling to the arrestin pathway to produce desensitization; on the other hand, morphine appears to produce little MOP phosphorylation and couples to protein kinase C (PKC) to enhance ERK phosphorylation and hence desensitization (Chu *et al*, 2010). In an elegant study using MOP mutants that blocked phosphorylation, Zheng and colleagues recently demonstrated that etorphine (and fentanyl) now behaved like morphine (Zheng *et al*, 2011).

Similar agonist biased responses have been reported for the DOP receptor where SNC80 and ARM390 (DOP ligands with similar antinociceptive actions) produced different desensitization responses; SNC80 desensitized but ARM390 did not. Following chronic treatment, SNC80 reduced receptor density and ARM390 resulted in uncoupling of Ca^{2+} channels (Pradhan *et al*, 2010).

1.2. Opioid ligands

1.2.1. Endogenous ligands

There are a number of endogenous opioid peptides that derive from different genes and possess different binding selectivities to opioid receptors (see Table 1.1). Enkephalins derive from the the pro-enkephalin polypeptide, binding more selectively to DOP receptors. Endorphins, such as β -endorphin, derive from the pro-opiomelanocortin polypeptide and bind with higher affinity to MOP and DOP receptors than the KOP opioid receptors. Endomorphins such as endomorphin-1 (Tyr-Pro-Trp-Phe-NH₂) and endomorphin-2 (Tyr-Pro-Phe-Phe-NH₂) are tetrapeptides which act selectively at the MOP receptor. Dynorphins are derived from the pro-dynorphin polypeptide being highly selective for the KOP receptor. Nociceptin/orphaninFQ is a peptide that binds to the NOP receptor.

1.2.2. Exogenous opioid ligands and morphine

Opium poppy has been cultivated as early as 3400 BC in Mesopotamia and Far East Asia. A mixture of alkaloid extracts from the poppy seed is called opium. Opiates are naturally occurring alkaloids in opium, such as morphine and codeine. The receptors that were identified to interact with opiates were named opioid receptors, since the term “opioid drug” was used for any compound, natural or synthetic, that binds to these receptors.

Morphine is an optically active opioid; only the levorotatory isomer is antinociceptive (figure 1.9). It has a benzene ring with a phenolic hydroxyl group (position 3) and an alcohol hydroxyl group (position 6), along with a tertiary nitrogen atom. Morphine's

hydroxyl groups makes it easily convertible to other opioids (ethers and esters), such as codeine (O-methylated at position 3) and heroin (O-acetylated at position 3 and 6). The tertiary nitrogen is crucial to morphine analgesia since making it quaternary significantly decreases antinociception. Changes to the methyl group linked to the nitrogen, not only reduces analgesia but can create opioid antagonists such as nalorphine (Trescot *et al*, 2008).



Figure 1.9. Structure of morphine, indicating the phenolic hydroxyl group at position 3 and the alcohol hydroxyl group at position 6. Modified from (Boettcher *et al*, 2005)

Although the usual pharmacokinetic parameters (half-life, clearance, volume of distribution) of most opioids are well known, their pharmacodynamic properties and the properties of all their metabolic products have not been fully explored. Exogenous opioids are classified by the IUPHAR into four chemical classes according to their structural similarities (figure 1.10).

COPYRIGHT MATERIAL - IMAGE REMOVED

Figure 1.10. *Classification of different chemical classes of opioid drugs according to their molecular structure. Modification from (Trescot et al, 2008).*

- 1) Phenanthrenes are the largest ‘class’. They include opioids such as morphine, codeine, hydromorphone, oxycodone, levorphanol, hydrocodone, oxymorphone, buprenorphine, nalbuphine and butorphanol. The hydroxyl group at position 6 in some of these drugs (i.e. morphine and codeine) is associated with the nausea and hallucinatory effects, contrary to hydromorphone and oxycodone that lack this group and the associated effects.
- 2) Benzomorphans are a ‘class’ of opioids that until today has only pentazocine as its member, an opioid that acts as a full agonist to DOP receptors and as a partial agonist at MOP and KOP receptors. Pentazocine administration has been associated with a high degree of dysphoria.
- 3) Phenylpiperidines are the most chemically simple ‘class’ of all, with lower molecular weight drugs including fentanyl, alfentanil, sufentanil and meperidine. Fentanyl has a high affinity for the MOP receptor and is 80-100 times more potent than morphine.

- 4) Diphenylheptanes is a class that includes propoxyphene and methadone, the later used widely in cases of opioid-dependence based on its effects on opioid withdrawal symptoms and its long duration of action.

There are a number of opioids that do not fit into the above classes. These include opioids such as tramadol (a 4-phenyl-piperidine analogue of codeine) and tapentadol which acts on MOP receptors in addition to possessing other non-opioid activities. Similarly, there are novel synthetic opioid ligands that combine two pharmacophoric structures interlinked by a chemical linker (thus being bivalent opioids) or others that are synthetic peptides. Some of these are discussed further below.

1.2.3. Pain pathways and processing

Most of the time, the perception of nociceptive stimuli (pain) serves as a warning signal to possible tissue damage, although there are cases where excessive or persistent pain is part of a pathological condition (i.e. hyperalgesia and chronic pain). The study of pain pathways and the neurobiological mechanisms of pain processing have been the focus of intense research to explore pain relief strategies.

The two main nerve fibres that carry nociceptive input from the periphery to the spinal cord are the A δ and the C fibres. The differences in the structure of these fibres are responsible for the different perception of pain; A δ fibres are myelinated and have faster signal conduction velocities, thus being responsible for sharp pain, whereas unmyelinated C fibres have low signal velocities and are responsible for dull pain (Rang *et al*, 1999). Afferent fibres (from periphery to spinal cord) enter the spinal cord through the dorsal roots, ending in the gray matter of the cord (dorsal horn), delivering

excitatory neurotransmitters such as glutamate and substance P. The dorsal horn first receives sensory information from the periphery and its cells are the first processing level in the pain pathway.

Ascending fibres (from spinal cord to the CNS) in the spinothalamic tract, project from the dorsal horn and terminate in the thalamus, delivering the pain signal to the brain by further excitatory neurotransmission (Greenstein & Greenstein, 1999) (figure 1.11). However, some ascending fibres project to the upper spinal cord (medulla oblongata) where it affects consciousness and the cardiorespiratory responses to pain, whereas others project to the hypothalamus where they trigger endocrine responses.

Nevertheless, the thalamus is a very important relay station for pain processing, since it disseminates signals to other brain areas, such as the cortex where the perception of pain takes place. The limbic system also accepts pain information from the thalamus, acting as a regulation center for pain threshold and emotional responses to pain. The midbrain gray area (periaqueductal gray; PAG) plays a key role in the descending modulation of pain.



COPYRIGHT MATERIAL - IMAGE REMOVED

Figure 1.11. *Transmission of pain signals from the periphery to the brain through the activation of ascending fibres. The dorsal horn in the spinal cord (A) is the first processing level of the pain signal. The thalamus (C) is the dissemination centre, acting as a relay station that sends signals to various areas of the brain (D). Open-access figure from the electronic educational portal ChangePain (<http://www.changepain-modules.com>).*

The descending fibres (from CNS to the spinal cord) are responsible for transmitting processed signals from the brain to the effector organs (figure 1.12). Signals arriving at the PAG from the brain, modulate initial pain intensity through a negative feedback system, by releasing serotonin, noradrenaline and endorphins to inhibitory pathways that project to the dorsal horn. This activation of the inhibitory pathways takes place in the raphe nuclei or the locus coeruleus.

COPYRIGHT MATERIAL - IMAGE REMOVED

Figure 1.12. *Descending pain pathways and modulation of signal through various inhibitory systems. Periaquaeductal matter (2) plays a crucial role in signal modulation through the serotonergic inhibitory system (4), but not through the noradrenergic pathway (3). All inhibitory descending fibres synapse in the drorsal horn and affect the firing of ascending fibres (6) and motor reflexes (7). Open-access figure from the electronic educational portal ChangePain (<http://www.changepain-emodules.com>).*

At the synaptic level, opioids have presynaptic as well as postsynaptic activity (figure 1.13). Activation of presynaptic opioid receptors decreases Ca^{2+} influx either through reduction of intracellular cAMP or through a direct inhibition by the $\text{G}\alpha_i$ -protein and thus inhibits the release of neurotransmitters from the pain fibre (glutamate, substance P). Opioid binding to postsynaptic opioid receptors evokes hyperpolarization of the

neuronal membrane through opening of the K^+ ion channels, thus decreasing the possibility of a generation of an action potential.

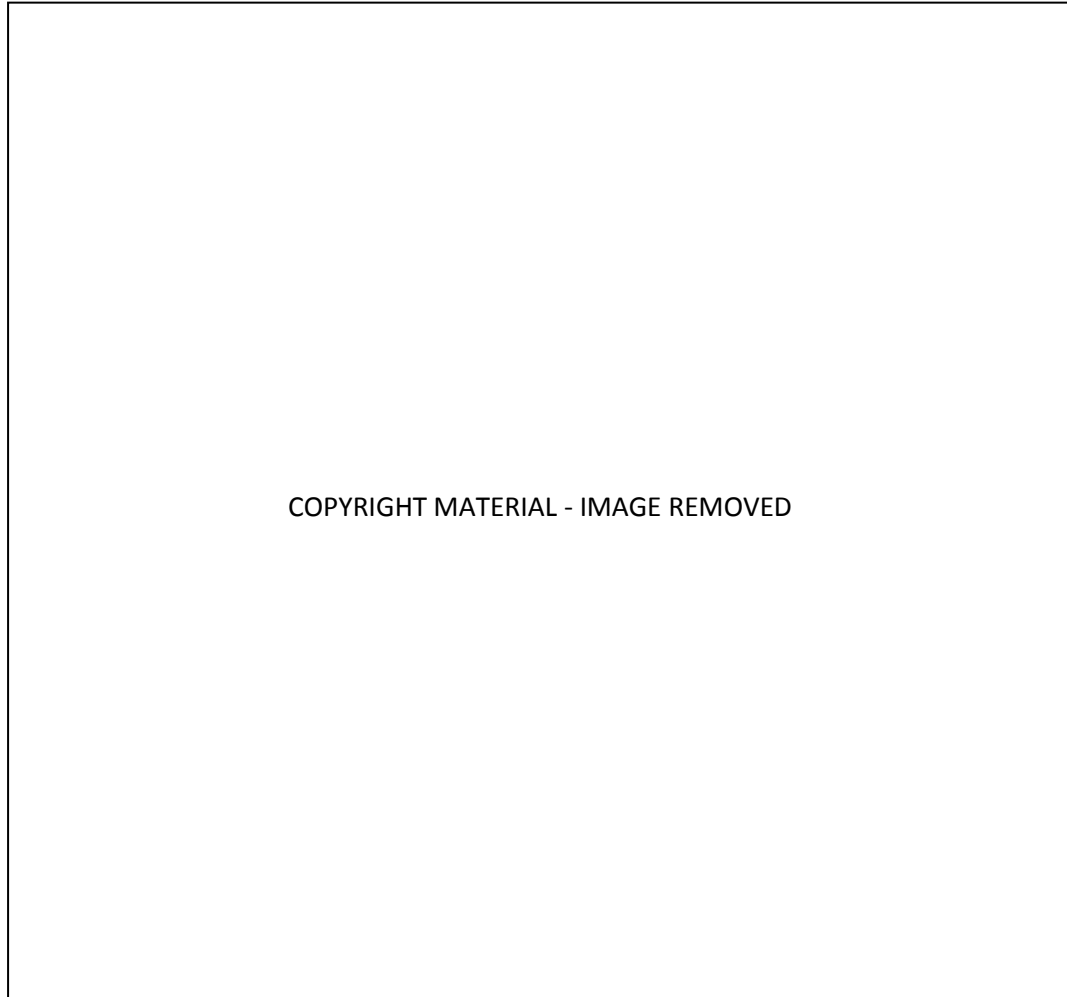


Figure 1.13. Graphical representation of MOP receptor (μ) activation by morphine and activation of its signalling pathways, presynaptically (leading to a decrease of Ca^{2+} influx) and postsynaptically (leading to an increase in efflux of K^+). Dotted arrows denote 'decreased' effect and blunted lines denote inhibition. AC; adenylyl cyclase, PKA1; protein kinase 1, NMDA; N-methyl-D-aspartate receptor. Open-access figure from the educational portal ChangePain (<http://www.changepain-emodules.com>).

1.2.4. Molecular basis of analgesic tolerance: morphine as an example

By the general term “opioid tolerance” we address analgesic opioid tolerance, rather than *i.e* respiratory opioid tolerance. Opioid tolerance manifests as the attenuation of analgesic efficacy caused after repeated opioid presence, such that constant doses of opioid administration are unable to sustain the same analgesic effect and therefore the dosing of opioid has to be increased in order to achieve the same degree of analgesia. (Bailey & Connor, 2005; Bailey *et al*, 2004; Corbett *et al*, 2006; Koch & Höllt, 2008).

At a cellular level, a number of distinct neural circuits control the cellular adaptations to chronic opioids, but whether different cellular adaptations are underscored by the same molecular mechanisms remained controversial. Understanding the molecular basis of opioid tolerance has been a very challenging task for many research groups in the last 20 years, as plenty of different factors are believed and have been shown to be involved. However, a series of independent studies in the last decade have produced strong evidence towards a molecular theory that involves receptor non-internalisation upon opioid binding as the platform for further studies (Koch & Höllt, 2008).

The ability of morphine to activate opioid receptors without promoting internalisation is believed to contribute to morphine’s opiate tolerance. Studies of knockout mice have established that morphine-induced analgesia and tolerance are both mediated by MOP receptors (Matthes *et al*, 1996; Sora *et al*, 1997). However, various opioid-related cellular adaptations and alterations at the second messenger level have also been identified by independent studies in different brain areas in response to opioid tolerance (Kieffer & Evans, 2002).

Cross-tolerance of opioids is an associated interesting and complex phenomenon, where chronic administration of an opioid that leads to the manifestation of tolerance shows tolerance to another opioid at the first administration. For example, in an interesting study in mice by Rossi and colleagues, they showed that morphine-tolerant animals exhibited cross-tolerance to codeine but not to morphine-6-glucuronide (M6G), diamorphine or methadone (Rossi *et al*, 1996). In another study in animals tolerant to i.v. morphine, Nielsen and colleagues showed that there is an absence of antinociceptive cross-tolerance to i.c.v. oxycodone (Nielsen *et al*, 2000). Morphine and etorphine (a semi-synthetic opioid that possesses 3000 times higher potency than morphine), although they differ significantly in their ability to promote both internalization of receptor and the development of tolerance *in vivo* (Duttaroy & Yoburn, 1995) are shown not to produce cross-tolerance (Lange *et al*, 1980). These data suggest that opioid tolerance involves shared mechanisms or ligand properties that result in receptor non-internalisation.

Significant differences in the subcellular localization of opioid receptors are also observed in cultured cells after chronic treatment with morphine compared with opioid peptide, suggesting that agonist-specific differences in receptor endocytosis may have long-term physiological consequences (Arden *et al*, 1995). Moreover, mice treated chronically with etorphine, which stimulates receptor endocytosis to an extent similar to opioid peptides (Keith *et al*, 1998; Keith *et al*, 1996), develop less physiological tolerance than do mice treated chronically with equi-effective doses of morphine (Duttaroy & Yoburn, 1995), further demonstrating that agonist selective internalization could play a key role in mediating the different physiological responses to opiate analgesics.

Differences between MOP ligands in mediating internalization may be due to agonist-dependent differences in the degree of phosphorylation of the MOP receptor, leading to differences in the ability to recruit β -arrestin1 and β -arrestin2 for internalization, which may be independent of G protein (Bohn *et al*, 2004). However, tolerance to opioids can also be attenuated by a number of compounds that do not have a direct interaction with opioid receptors, such as calcium channel blockers (Smith *et al*, 1999), intrathecal magnesium (McCarthy *et al*, 1998), NMDA antagonists (McCarthy *et al*, 1998), protein kinase C (PKC) inhibitors (Corbett *et al*, 2006), cholecystokinin antagonists (McCleane, 2003) and phosphodiesterase inhibitors (Ledeboer *et al*, 2007).

1.3. Cancer pain

1.3.1. Clinical description

Acute pain is a very common presenting complaint in primary and secondary care. Chronic pain, on the other hand, is a rather complex syndrome associated with a range of diseases and is particularly difficult to treat effectively. Chronic pain is one of the most common symptoms associated with cancer, with a prevalence of approximately 30–50% among patients who are undergoing active treatment for a solid tumour and 70–90% among those with advanced disease (Addington-Hall & McCarthy, 1995; Colvin & Lambert, 2008).

1.3.2. Current therapies and limitations

It is acknowledged that the pharmacological mainstay of cancer pain management is based on opioids. Following the steps of the WHO analgesic ladder, weak opioids such

as codeine and tramadol are used earlier in pain management, with more potent opioids such as oxycodone, buprenorphine, fentanyl and morphine to follow. Additionally, a major role is also thought to be played by non-analgesic adjuvant drugs, compounds that although may not have intrinsic analgesic activity they can modulate the disease processes causing pain and thus have an effect on certain types of pain (Forbes, 2008). These include anti-inflammatory drugs (i.e. corticosteroids), anxiolytics, antidepressants and antibiotics. When in conjunction with opioids, adjuvant analgesics are thought to enhance pain relief and reduce the amount of opioid used (Rana *et al*, 2011).

Although opioids remain the gold standard in cancer pain therapies, there is a trade-off between good analgesia and poor side-effect profile. Long-term clinical use of opioids (mainly MOP receptor agonists) can cause a wide range of side-effects such as respiratory depression, constipation, tolerance, and possibly dependence (Ossipov *et al*, 2004). As discussed above (section 1.2.4), tolerance leads to dose escalation with the potential to produce increased side-effects and thus a vicious cycle develops with a patient under pressure at the centre (figure 1.14).

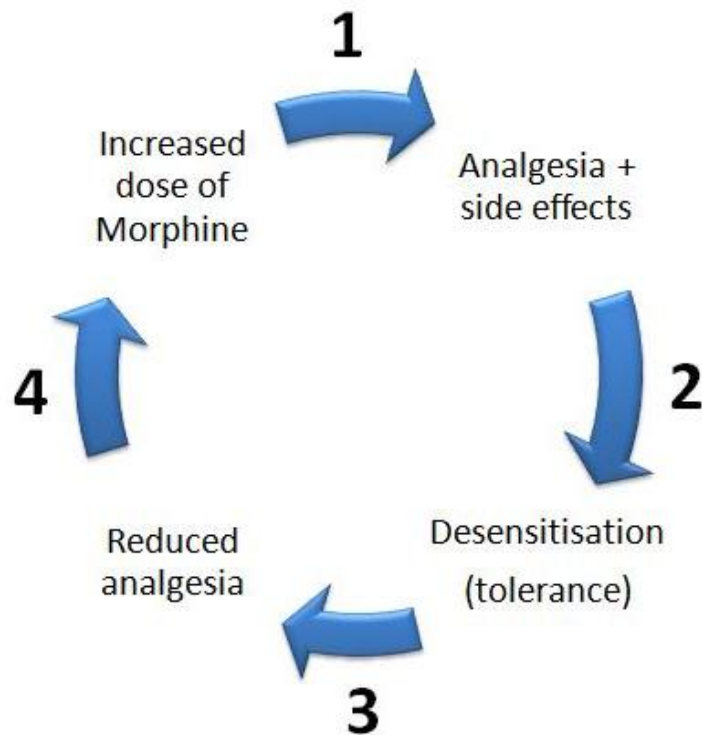


Figure 1.14. *Contribution of morphine analgesic tolerance to the increased manifestation of morphine-associated side-effects in patients receiving chronic administration of morphine. (1): The patient receives morphine to alleviate pain; (2): analgesic tolerance is produced after chronic administration; (3): tolerance leads to an experienced reduction in analgesia for the patient; (4): which in turn leads to an increase in the prescribed dose by the clinician. The escalation of morphine doses feeds again the same cycle of effects. Image produced using Microsoft Office Powerpoint.*

Selective KOP or DOP receptor agonists do not possess some of the morphine-like side-effects such as constipation, respiratory depression and addiction, but they have a side-effect profile of their own, characterised by diuresis, sedation and dysphoria, which are especially strong for KOP receptor ligands (Peng & Neumeyer, 2007).

1.3.3. Pain undertreatment

Despite the number of drugs that are available in the clinic, cancer pain undertreatment is well documented. Cancer pain is shown to be moderate to severe in 45% of patients and severe to excruciating in 27% of patients (Ripamonti *et al*, 1998). However, approximately 80-90% of cancer patients with advanced cancer (terminal stages), experience intense pain (Portenoy & Lesage, 1999). In a later study, data have shown specifically that 70% of head/neck cancer patients experience intense pain, as well 64% of cancer patients on average across all cancer types (van den Beuken-van Everdingen *et al*, 2007). Records show that 88% of cancer patients in the last year of their life are in pain and 47% of those treated for pain by their general practitioner said their treatment only partially controlled their pain (Addington-Hall & McCarthy, 1995; Colvin & Lambert, 2008). From this description of chronic cancer pain it is fair to state that, despite a wide range of potential therapeutic targets, the control of cancer pain is still poor.

The reason for cancer pain undertreatment is not always obvious and may depend on different factors, including the reported ineffective communication of pain intensity, the reluctance of clinicians to prescribe opioids, patient compliance due to the route of administration and other factors (Christo & Mazloomdoost, 2008). Additionally, there has also been documented an opioid-induced hyperalgesia, as a paradoxical response to opioids, which can also affect pain management and lead to pain undertreatment.

Nevertheless, although cancer pain undertreatment is believed to be multidimensional in terms of its causes, opioid tolerance and opioid prescribing is believed to contribute substantially to pain undertreatment. Due to the development of analgesic tolerance,

increased opioid doses can result in increased opioid side-effects. When tolerance is produced by the administration of a strong opioid such as morphine, clinicians are constrained to switch their patients to opioids that are less-effective in order to avoid further development of analgesic tolerance, an action which increases the possibility of pain undertreatment. Common opioid dosing errors among clinicians either due to failure to implement the WHO guidelines or due to insufficient knowledge and education on opioid prescribing, have been identified (Shaheen *et al*, 2010). However, some have questioned the effectiveness of the WHO analgesic ladder. These guidelines were introduced nearly twenty five years ago and although they included the administration of adjuvant drugs (i.e. for neuropathic pain or anxiety), or the combination of non-opioids (i.e. NSAIDs) with opioids, the undertreatment of cancer pain is well documented (Cohen *et al*, 2003). Many clinicians have identified a number of issues that the WHO analgesic ladder does not address and more specifically, there is an increasing criticism for the use of the second step of the WHO analgesic ladder, with the main argument being that it cannot be applied to all cases (i.e. cancer patients that experience severe pain from the early stages of the disease may require the early use of strong opioids) (Eisenberg *et al*, 2005).

From all the above, it is understandable that there is a strong need for morphine-like molecules with reduced side-effects, especially with reduced tolerance liability, reduced respiratory depression and reduced effect on gastrointestinal motility. It is beyond doubt that if there was an opioid analgesic in the clinical stage that would produce decreased tolerance and similar analgesic potential to morphine, there would be less cases of pain undertreatment reported in the clinic, certainly rendering opioid prescribing and management of opioid use less complicated.

1.4. The “multi-targeting” concept

1.4.1. Bivalent and bifunctional ligands

A pharmacophore is defined by the International Union of Pure and Applied Chemistry (IUPAC) as “an ensemble of steric and electronic features that is necessary to ensure the optimal supramolecular interactions with a specific biological target and to trigger (or block) its biological response”. Ligands that have two distinct binding properties can be found in the literature under two different names; bivalent and bifunctional. A bivalent ligand is a compound that possesses two distinct pharmacophores in its structure (Portoghese, 1989) (see figure 1.15).

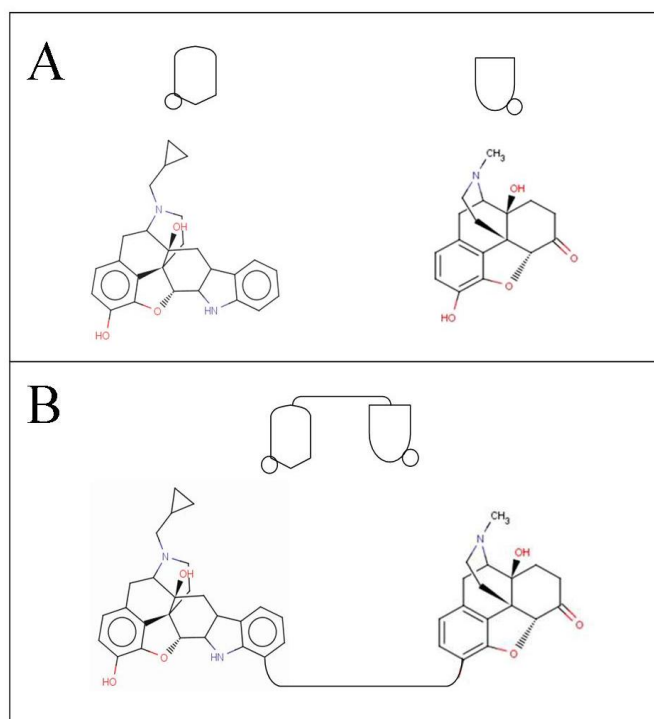


Figure 1.15. A schematic and chemical representation of two individual pharmacophoric units (**A**; structures are oxymorphone on the right and naltrindole on the left), that can be linked together (**B**) by an intermediate spacer (linker), in order to produce a molecule with two active sites (valences); a bivalent ligand. The chemical structures were produced using the SureChem software.

On the other hand, a bifunctional ligand is a non-selective compound that acts at two different targets (Li *et al*, 2007) and thus presents two distinct binding properties (figure 1.16). There are a number of structurally different bifunctional opioid ligands that have been developed and studied by different research groups, as reported in the literature. Table 1.2 presents the structure and binding affinities of some MOP-DOP opioid bifunctional ligands that have been reported in the literature.

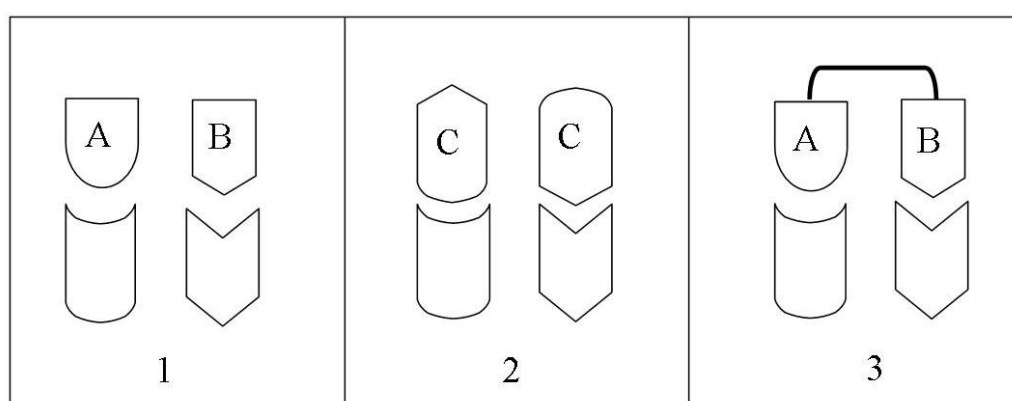


Figure 1.16. Possible mechanisms that can produce two biological effects through two different (and independent) receptors: **1)** drug A and drug B bind to their respective receptors when administered simultaneously, **2)** non-selective ligand C has a structure that promotes binding to both receptors and **3)** a bivalent ligand with two pharmacophores, A and B, binds to two receptors recognised by their active sites. In this simple schema, the two receptors are represented as individual monomers.

Two sub-categories of bivalent ligands also exist: homobivalent ligands, where both pharmacophores are of the same structure and heterobivalent ligands, where the two pharmacophores are different (Peng *et al*, 2007). It is possible that a bivalent ligand may have only one function if both of its pharmacophores are selective for the same receptor.

	<i>Non-selective ligands (bifunctional)</i>	Ki(μ) (nM)	Ki(δ) (nM)	Pharmacological Profile*
1	Butorphan	0.23	5.90	MOP ^A – DOP ^A – KOP ^A (Peng <i>et al</i> , 2007)
2	Naltrexone	0.23	38.0	MOP ^N – DOP ^N – KOP ^N (Peng <i>et al</i> , 2007)
3	Cyclorphan	0.06	1.90	MOP ^A – DOP ^A (Peng <i>et al</i> , 2007)
4	H-Dmt-Tic-Gly-NH-CH ₂ -Ph	0.16, $pEC_{50}^{\mu}=7.70^{**}$	0.03, $pA_2^{\delta}=9.25^{**}$	MOP ^A – DOP ^N (Balboni <i>et al</i> , 2002)
5	H-Dmt-Tic-Gly-NH-Ph	0.16, $pEC_{50}^{\mu}=8.59^{**}$	0.04, $pEC_{50}^{\delta}=8.52^{**}$	MOP ^A – DOP ^A (Balboni <i>et al</i> , 2002)
6	H-Dmt-Tic-NH-CH ₂ -Bid	0.50, $pEC_{50}^{\mu}=7.57^{**}$	0.03, $pEC_{50}^{\delta}=9.90^{**}$	MOP ^A – DOP ^A (Balboni <i>et al</i> , 2002)
7	H-Dmt-Tic-Gly-NH-CH ₂ -Bid	20.5, $pEC_{50}^{\mu}=6.45^{**}$	0.06, $pA_2^{\delta}=9.00^{**}$	MOP ^A – DOP ^N (Balboni <i>et al</i> , 2002)
8	H-Dmt-Tic-Phe-Phe-NH ₂	1.19	0.12	MOP ^A – DOP ^N (Schiller <i>et al</i> , 1999)
9	H-Tmt-Tic-Phe-Phe-NH ₂	4.08	0.39	MOP ^A – DOP ^N (Schiller <i>et al</i> , 1999)
10	H-Dmt-Tic Ψ [CH ₂ NH]-Phe-Phe-NH ₂	0.94	0.48	MOP ^A – DOP ^N (Schiller <i>et al</i> , 1999)
11	H-Tyr-Tic-Phe-Phe-NH ₂	78.8	3.00	MOP ^A – DOP ^N (Schiller <i>et al</i> , 1999)
12	H- Dmt-Pro-Trp-D-1-Nal-NH ₂	-	- , $pA_2^{\delta}=8.59^{**}$	MOP ^A – DOP ^N (Fichna <i>et al</i> , 2007)

Table 1.2. Binding affinity (K_i) and general pharmacological profile of various bifunctional (non-selective) ligands at the opioid receptors. Key: 2',6'-dimethyl-L-tyrosine (Dmt), tetrahydroisoquinoline-3-carboxylic acid (Tic), benzyimidazole (Bid), phenyl (Ph), phenylalanine (Phe), glycine (Gly), tyrosine (Tyr), glycine (Gly), alanine (Ala), tyrosine (Tyr), tryptophan (Trp), proline (Pro), 3-[1-naphthyl-D-Ala] (D-1-Nal). *The profile of bivalent ligands is denoted as μ (MOP), δ (DOP), κ (KOP), A (agonist) and N (antagonist).

In contrast, it may also be possible that a bifunctional ligand can have only one pharmacophore which is non-selective and thus acts on two different targets. For example, the non-selective opioid receptor agonist butorphan acts on KOP and MOP receptors and as it has only one pharmacophore, it is regarded as a bifunctional (non-selective) ligand. Similarly, the monovalent opioid-receptor ligands cyclorphan and pentazocine act as agonists at KOP receptors and antagonists at MOP receptors, so are also bifunctional (non-selective) ligands. Morphy and Rankovic have proposed a further chemical sub-classification depending on whether the pharmacophores are merged, conjugated, or overlapping (Morphy & Rankovic, 2005). Table 1.3 presents the structure of different bivalent ligands and their binding affinities to the three classical opioid receptor types. The terms ‘bivalent’ and ‘bifunctional’ are often used interchangeably in the literature and in this thesis we will use both terms in order to describe the properties of a number of different ligands according to the definitions given above.

1.4.2. MOP and DOP receptor interaction studies

Although the potent antinociceptive effect of morphine is attributed solely to its high selectivity for the MOP receptor, questions had been raised during the last decade about the contribution of the delta (DOP; δ) or kappa (KOP; κ) opioid receptors towards morphine tolerance.

	Pharmacophore 1	Linker	Pharmacophore 2	$K_i(\mu)$ (nM)	$K_i(\delta)$ (nM)	$K_i(\kappa)$ (nM)	Pharmacological profile**
Bivalent Ligands							
1	H-Tyr- <i>D</i> -Phe	NH-NH	<i>D</i> -Phe-Tyr-H	31.0	187	360	MOP ^A - DOP ^A (Lipkowski <i>et al</i> , 1982)
2	H-Tyr- <i>D</i> -Ala-Gly-Phe	NH-NH	Phe-Gly- <i>D</i> -Ala-Tyr-H	1.40	2.60		MOP ^A - DOP ^A (Lipkowski <i>et al</i> , 1999)
3	Butorphan	fumaryl ester	Butorphan	0.20	9.40	0.08	MOP ^A - KOP ^A (Mathews <i>et al</i> , 2005)
4	Butorphan	10-C linker	Butorphan	0.09	4.20	0.05	MOP ^A - KOP ^A (2003; Peng <i>et al</i> , 2007)
5	(-)-Butorphan	10-C linker	(+)-Butorphan	2.20	23.0	1.20	MOP ^A - KOP ^A (Neumeyer <i>et al</i> , 2003)
6	Dmt-Tic-OH	β -Ala	Butorphan	0.69	1.50	0.28	mixed-N (Neumeyer <i>et al</i> , 2006)
7	<i>N,N</i> -dimethyl-Dmt-Tic	Diaminoalkyl-pyrazinon	<i>N,N</i> -dimethyl-Dmt-Tic	1.68, pA_2 7.7*	0.29, pA_2 10.4*	-	MOP ^N - DOP ^N (Li <i>et al</i> , 2005)
8	<i>N,N</i> -dimethyl-Dmt-Tic	NH-(CH ₂) ₆ -NH	<i>N,N</i> -dimethyl-Dmt-Tic	2.21, pA_2 8.3*	0.06, pA_2 11.3*	-	MOP ^N - DOP ^N (Li <i>et al</i> , 2005)
9	Dmt	Aminoalkyl linker	Dmt	0.04	14.8	-	MOP ^A - DOP ^N (Okada <i>et al</i> , 2003)
10	Endomorphin-2	ethylenediamine	Dmt-Tic	1.03	1.45	-	MOP ^A - DOP ^N (Salvadori <i>et al</i> , 2007)
11	JD	(no linker)	Tic	3.73	301	0.32	MOP ^A - KOP ^N (Carroll <i>et al</i> , 2004)
Reference compounds							
12	Dermorphin	-	-	0.28	82.5	1.10	MOP ^A (Balboni <i>et al</i> , 2002)
13	Endomorphin-2	-	-	0.69	9233	5240	MOP ^A (Harrison <i>et al</i> , 1999)
14	Morphine	-	-	0.88	140	24	MOP ^A (Peng <i>et al</i> , 2006)
15	Deltorphan C	-	-	387	0.21	0.08	DOP ^A (Balboni <i>et al</i> , 2002)
16	Dynorphin A(1-13)	-	-	0.50	4.40	0.11	KOP ^A (Martinka <i>et al</i> , 1991)
17	Naloxone	-	-	0.79	76.0	0.25	mixed-N (Balboni <i>et al</i> , 2002)
18	Dmt-Tic-OH	-	-		0.022		DOP ^N (Li <i>et al</i> , 2005)
19	NTI	-	-	50	0.29, pA_2 7.95*	34.1	DOP ^N (Ananthan <i>et al</i> , 1998)

Table 1.3. Receptor binding (K_i ; (Cheng & Prusoff, 1973) and general pharmacological profile of various bivalent ligands, monovalent ligands and endogenous peptides at the μ , (MOP) δ (DOP) and κ (KOP) opioid receptors. Key: 2',6'-dimethyl-L-tyrosine (Dmt), naltrindole (NTI), tetrahydroisoquinoline-3-carboxylic acid (Tic), benzimidazole (Bid), phenyl (Ph), (3*R*)-7-hydroxy-*N*-((1*S*)-1-[(3*R*,4*R*)-4-3(hydroxyphenyl)-3,4-dimethyl-1-piperidin]methyl]-2-methylpropyl (JD), phenylalanine (Phe), glycine (Gly), alanine (Ala), tyrosine (Tyr), proline (Pro), Tyr-Pro-Phe-Phe-NH₂ (endomorphin-2,). * pA_2 is the logarithmic value for antagonist potency derived by Schild plot **The profile of bivalent ligands is denoted as M (MOP), D (DOP), K (KOP), A (agonist) and N (antagonist). i.e MDAN (MOP-agonist and DOP-antagonist).

Following the above observations, it has been shown in a number of animal studies that when DOP receptors are blocked or absent, at the same time when MOP receptors are activated, then analgesia with reduced tolerance and dependence results (Abdelhamid *et al*, 1991; Fundytus *et al*, 1995; Kest *et al*, 1996; Zhu *et al*, 1999) as shown collectively in Table 1.4.

In these studies, co-administration of morphine and a DOP receptor antagonist caused a marked increase in analgesia, with reduced tolerance and dependence. Similarly, DOP receptor knock-out and antisense oligodeoxynucleotide knock-down studies have all reported a marked reduction in tolerance and dependence. These studies indicate that the pharmacology of opioid receptors is far more complicated than originally thought, possibly through linked mechanisms where the binding of a ligand to one opioid receptor (i.e. DOP) can affect the behaviour of another (i.e. MOP). This cross-talk between two different opioid receptors has been the focus of studies for a number of years, either by investigating the type of interaction among opioid receptors (Alfaras-Melainis *et al*, 2009; van Rijn *et al*, 2010; Walwyn *et al*, 2009) or by investigating the pharmacology of ligands that bind to these receptors and the change in their conformation in various ways (Ballet *et al*, 2008; Berque-Bestel *et al*, 2008; Liu *et al*, 2004a).

Study	Model	Methodology	Findings
(Abdelhamid <i>et al</i> , 1991)	Mice	Acute: 100 mg/kg of morphine sulfate s.c Chronic: 75mg s.c implanted pellet	<ul style="list-style-type: none"> • Nt-pretreated animals showed reduction of analgesic tolerance and dependence
(Fundytus <i>et al</i> , 1995)	Mice	i.c.v. Nt, TIPP and TIPP[ψ]	<ul style="list-style-type: none"> • TIPP[ψ] attenuated morphine analgesic tolerance and withdrawal, but not Nt or TIPP
(Kest <i>et al</i> , 1996)	Mice	Antisense-oligonucleotide of DOR-1 i.c.v morphine 3 days	<ul style="list-style-type: none"> • Blocked morphine tolerance and acute dependence in antisense-treated animals
(Hepburn <i>et al</i> , 1997)	Rats	s.c morphine injection increments 5 days co-treatment with s.c 1 mg/kg Nt (-1h)	<ul style="list-style-type: none"> • Reduced analgesic tolerance in Nt-treated rats • Reduced withdrawal symptoms in Nt-treated rats • No effect on respiratory-tolerance of morphine
(Zhu <i>et al</i> , 1999)	Mice	Deletion of exon 2 in DOR-1 (knock-out)	<ul style="list-style-type: none"> • Reduced spinal DOP-analgesia • Peptide DOP agonists retained supraspinal analgesic potency, only partially antagonized by Nt • DOR-1 depleted mice did not develop morphine analgesic tolerance
(Nitsche <i>et al</i> , 2002)	Mice	Knock-out of preproenkephalin gene Knock-out of NMDA receptor i.c.v 5mg/kg morphine for 10 days	<ul style="list-style-type: none"> • Reduced morphine analgesic tolerance in both • Antagonist-induced opioid withdrawal in both

Table 1.4. *Studies reporting reduced development of morphine analgesic tolerance after the blocking or removal of the DOP receptor. Key: naltrindole (Nt), H-Tyr-Tic-Phe-Phe-OH (TIPP), H-Tyr-Tic psi [CH₂-NH]-Phe-Phe- OH (TIPP[ψ]) are all DOP receptor antagonists.*

More interestingly, in an elegant study by Hepburn and colleagues (Hepburn *et al*, 1997) it has been shown that although the administration of naltrindole (a selective DOP antagonist) to chronically morphine-treated rats resulted in the attenuation of the antinociceptive tolerance to morphine, as well as to reduced withdrawal effects, it did not prevent the development of tolerance to morphine-induced respiratory depression. This selective “effect” of naltrindole administration -to allow the development of a “protective” tolerance to morphine induced respiratory depression while at the same time reducing the antinociceptive tolerance - highlights the possibility that the mechanisms behind antinociceptive tolerance to morphine may implicate a MOP-DOP receptor interaction, whereas the mechanisms behind tolerance to respiratory depression does not (or at least not in the same way).

Moreover, Nitsche *et al* has reported that although knock-out mice for the endogenous ligand preproenkephalin did not develop analgesic tolerance to morphine, they still display physical dependence, implying that morphine tolerance is genetically distinct or manifests distinctly from mechanisms of dependence (Nitsche *et al*, 2002). Additionally, in the same study, a similar tolerance-deficit profile to morphine has been shown in NMDA receptor-deficient mice, underlying the possibility that common mechanisms of the development of morphine tolerance also exist between opioid and non-opioid receptors. These interesting interactions have also been confirmed in a different study by Sharif *et al* where intrathecal administration of metabotropic glutamate receptor-1 antisense oligonucleotides in rats resulted in an attenuation of morphine tolerance (Sharif *et al*, 2002).

1.4.3. Multiple receptor selectivity

The above studies underline the importance of developing an effective strategy for the simultaneous targeting of two different opioid receptors, with a particular focus on MOP and DOP receptors, not only for the exploration of various mechanisms contributing to tolerance, but also for providing a possible alternative to morphine in terms of increased analgesia with reduced or no tolerance at all. The effort to exploit the pharmacological advantages described above, could be applied by either using two selective drugs simultaneously or by using a single drug that can bind to both receptors of interest. For the latter case, we introduced the term “multiple receptor selectivity” in order to describe the activity of a ligand that is designed intentionally to bind selectively to more than one receptor (and thus having a different meaning from the generally-used term ‘*non-selective*’). This strategy could possibly prove clinically advantageous over the “double” administration, with regards to reduced drug-drug interactions and pharmacokinetic parameters.

Multiple receptor selective ligands have been the focus of an increasing number of studies in recent years. Rational drug design and structure-activity relationship studies have evaluated the pharmacology of various ligands that act simultaneously either on two different types of opioid receptors (Schiller, 2010; Toll *et al*, 2009) or an opioid receptor with an unrelated receptor (Agnes *et al*, 2008; Kulkarni *et al*, 2009; Yamamoto *et al*, 2010). Single drugs that display multiple receptor selectivity could therefore prove to be not only a very useful tool for the study of these cellular mechanisms, but also potentially effective towards reducing opioid tolerance, compared with morphine.

1.5. UFP-505

As part of an ongoing programme to design single MOP-agonist/DOP-antagonist drugs (Balboni *et al*, 2002; Balboni *et al*, 2010; Jinsmaa *et al*, 2008; Neumeyer *et al*, 2006; Salvadori *et al*, 2008; Salvadori *et al*, 2007) our collaborators in Italy have produced the pseudotripeptide *H-Dmt-Tic-Gly-NH-Bzl* (named UFP-505; University of Ferrara Peptide 505; (figure 1.17). UFP-505 was evolved from Dmt-Tic analogues that possessed a potent DOP-receptor antagonism and its mixed-opioid ligand profile is associated with the inclusion of a benzyloxy-methylene group of a carboxyl function in the Dmt-Tic pharmacophore, which permits the retention of DOP antagonism with appearance of MOP agonism. After early preliminary data in functional tests, UFP-505 was reported to be a potential ‘bifunctional’ compound that needs further characterization (these preliminary data are described in the Discussion – Chapter 8).

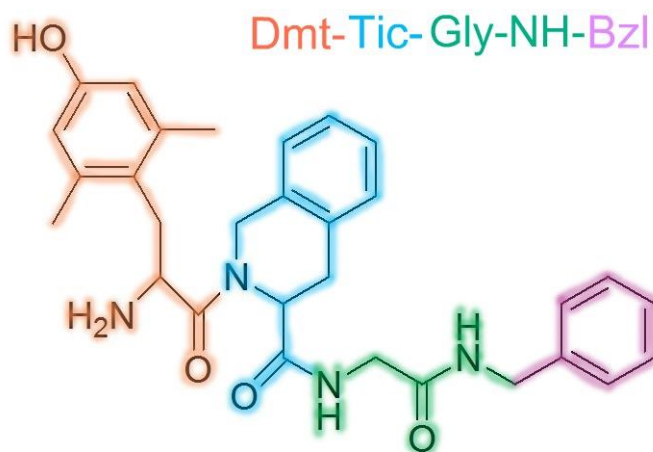


Figure 1.17. Chemical structure of *H-Dmt-Tic-Gly-NH-Bzl* (UFP-505), our prototype pseudotripeptide.

1.6. Aims of the thesis

The primary aim of this project was to characterize the pharmacology of UFP-505 in different model systems, in comparison with a number of reference ligands and other novel bifunctional opioids. Our hypothesis is that UFP-505 as a MOP-agonist/DOP-antagonist will produce analgesia with reduced tolerance and that its effect on receptor trafficking will differ from that of morphine in terms of induced internalization. Experiments to address this hypothesis:

1. To provide a basic and comprehensive *in vitro* pharmacological characterization of UFP-505, in CHO cell lines stably expressing different recombinant opioid receptors and in native neuronal tissue (*i.e.* binding affinity, activation of G-protein, inhibition of cAMP).
2. To examine the ability of UFP-505 to induce opioid receptor internalization and the effect of ligand concentration and time of incubation and to compare with morphine.
3. To investigate the acute antinociceptive properties of UFP-505 *in vivo* and provide further pharmacological information in comparison with morphine (*i.e.* equianalgesic dose, analgesic potency). To further study the ability of UFP-505 to induce analgesic tolerance after repeated administration (chronic) and provide comparisons with morphine.
4. Opioid administration has been shown to induce differentiated regulation of opioid receptor mRNA. To investigate the possible regulatory effects of UFP-505 and morphine on opioid receptor mRNA expression after acute and repeated administration *in vivo*, by examining the neuronal tissue of treated animals.
5. The simultaneous expression of MOP and DOP receptors has been shown *in vitro* to induce the formation of receptor heterodimers which may reveal

different pharmacological properties of ligands. To produce and characterize a novel double-expression recombinant system of MOP and DOP receptors in CHO cells and to investigate the basic pharmacological characteristics of UFP-505 and reference ligands in this novel cell line.

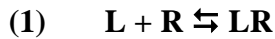
CHAPTER 2.

GENERAL METHODS

Chapter 2. General Methods

2.1. General theory of ligand binding

Receptor-ligand binding models follow the law of mass action in that at any given time there is a proportion of receptors that are ligand bound along with a proportion of receptors that are in a non-bound (free) state. The law is illustrated simply as (1):



(*L*; ligand, *R*; receptor, *LR*; receptor-ligand complex)

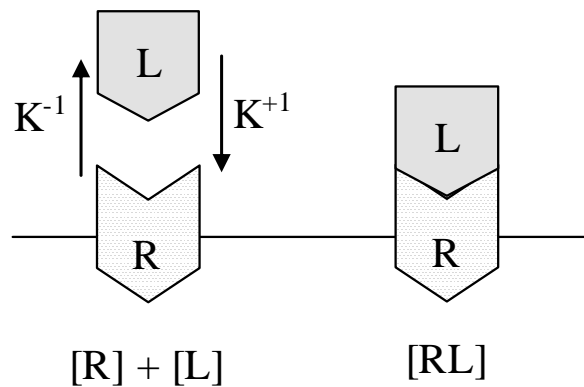


Figure 2.1. Illustration of the law of mass action, where $[R]$ is the receptor, $[L]$ the ligand, $[RL]$ the receptor-ligand complex, K^{+1} the rate of association constant and K^{-1} the rate of dissociation.

The rate of the formation of the receptor-ligand complex (association rate; K^{+1}) and the rate of the reverse (dissociation rate; K^{-1}) are expressed as constants, based on the physicochemical properties of the receptor and ligand (figure 2.1). These rates are dependent on various factors, such as the affinity of the ligand to the receptor. When equilibrium is reached, the equation (1) can be represented in terms of concentration (2):

$$(2) \quad [L] \cdot [R] \cdot K^{+1} = [LR] \cdot K^{-1} \Leftrightarrow [L] \cdot [R] / [LR] = K^{-1} / K^{+1} = K_d$$

(K_d ; equilibrium dissociation constant expressed in units of *M*)

The dissociation constant represents the concentration of the ligand which will bind to half of the total number of receptors at equilibrium. In logarithmic terms the K_d is converted to pK_d using the equation (3):

$$(3) \quad pK_d = -\log_{10} K_d$$

The law of mass action has limitations, as it assumes specific terms:

- All receptors are accessible to the ligand
- There is no intermediate binding between bound and free receptors
- Ligand is not depleted in the medium
- Ligand binding is reversible

2.2. Properties and handling of radioligands

2.2.1. Characteristics of radioligands

Tritium [^3H] and radioactive sulphur [^{35}S] are radioactive isotopes that can be incorporated into ligands (radioligands), in specific positions, without altering the structure and biological activity of the native ligand (i.e. [^3H]diprenorphine and the radioactive guanosine triphosphate $\text{GTP}\gamma[^{35}\text{S}]$). The radiation emitted by these radioligands is beta (β) radiation and has a low energy capacity and therefore low intrusion ability. Data from a receptor-radioligand binding assay represent the interaction of the ligand with its target and is therefore a reliable method for studying receptor-ligand binding.

Radioligands decay as their radioactive isotope decays in time. This decay is represented by the isotope's half-life ($t_{1/2}$), which is the time taken for half of the isotope to decay. Tritium's half-life is 12.43 years, whereas [^{35}S] has a half-life of 87 days.

The radioactivity of a radioligand is expressed as the "specific activity" (SA) and is measured as Curies per mmol (Ci mmol^{-1}). It is best to use radioligands with short half life quickly, as the energy released by the radioactive decay during a long term storage may affect the functionality of the pharmacophores of the ligand (even if they are stored at -20°C).

2.2.2. Efficiency of detection of radioactivity (β -counting)

Radioactivity is detected and measured by a scintillation β -counter, after mixture in scintillation liquid. Beta-particles emitted by the disintegration of the radioligand collide with fluor molecules in the scintillation fluid and produces photons in the form luminescence. The luminescence is captured by the counter and is expressed as counts per minute (cpm) and when corrected for quenching as disintegrations per minute (dpm). The counter reading is therefore a quantified expression of the radioactivity present in the sample measured, since 2.22×10^6 disintegrations per minute are detected in $1\mu\text{Ci}$ of radioactive material.

2.3. The role of non-specific binding

Ligands can bind to sites other than the binding pocket of the targeted receptor and this is known as non-specific binding (NSB). These interactions take place at sites distinct

from the receptor (i.e. a membrane macromolecule). In order to determine the receptor-specific binding, NSB must be quantified. An appropriate unlabelled ligand is used at a saturating concentration that will compete with the radiolabelled ligand for the receptor binding site (figure 2.2). The saturable concentration used is multiple excess of the K_d of the radioligand. The specific binding is calculated from the total binding and NSB using the formula (4):

$$(4) \quad \text{Total binding} - \text{NSB} = \text{specific binding}$$

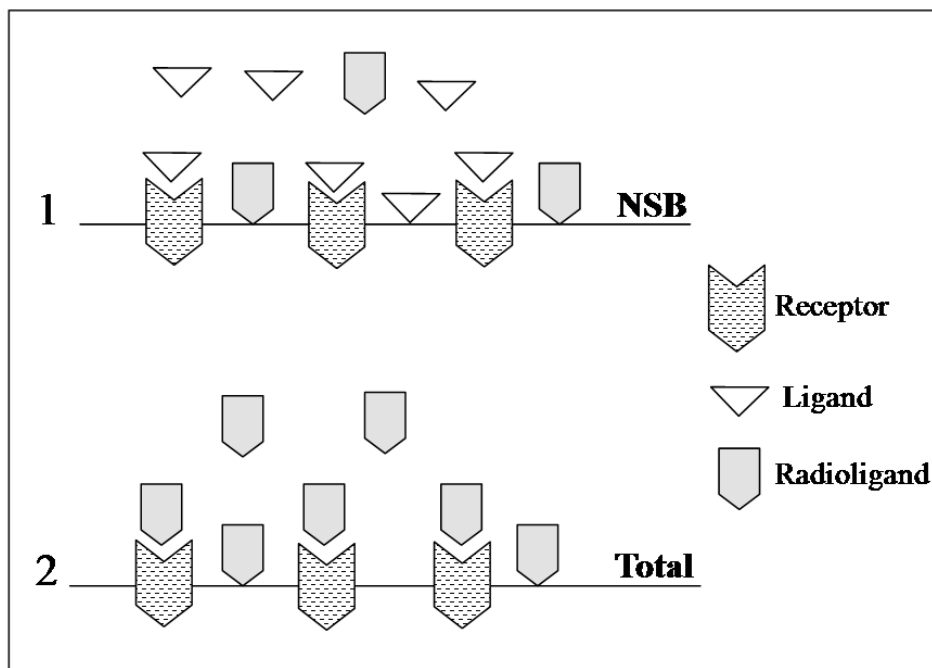


Figure 2.2. Illustration of the role of non-specific binding (NSB). Panel 1 depicts the non-specific binding of a saturable concentration of a non-labelled ligand when incubated with radioligand. Panel 2 depicts total radioligand binding. Substraction of NSB from the total yields the specific binding sites at the receptors (see formula 4).

2.4. Saturation binding assay

2.4.1. Theory

Saturation binding assay is a common experimental way used for determining two important values: a) the equilibrium dissociation constant or affinity (K_d) of the radioligand and b) maximal number of receptor binding sites (B_{max} ; expressed as receptor density). In the saturation assay, increasing concentrations of the radioligand in the assay are incubated with and without the presence of a saturable concentration of an NSB ligand. The competition of the NSB and the radioligand for the binding site of the receptor will produce binding that can be used to predict a hyperbolic curve dependent on the concentrations of [RL] and [L]. When 50% of the receptor sites are occupied at a specific radioligand concentration then this concentration represents the K_d of the radioligand. The same curve can predict the receptor density (B_{max}) at a point where further increase of the radioligand does not increase the [RL].

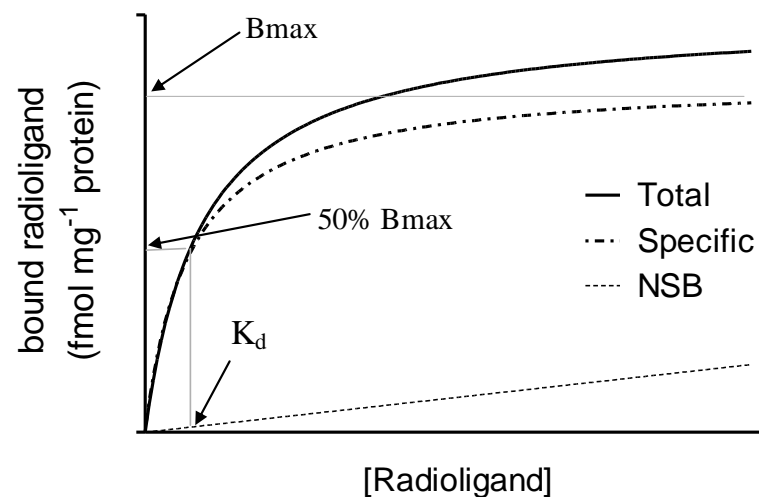


Figure 2.3. Hyperbolic curve of receptor binding sites (shown as bound radioligand) plotted against increasing radioligand concentration. B_{max} is the maximal receptor binding sites and K_d the dissociation constant of the radioligand. This is where 50% of the receptors are occupied.

Analysis of equilibrium binding experiments such as the saturation assay, assumes that binding is measured at equilibrium. A Langmuir isotherm (rectangular hyperbola) that represents $\text{fmol} \cdot \text{mg}^{-1}$ of protein *vs* radioligand concentration can be plotted to visualise specific binding (figure 2.3), arising from subtraction of the non-specific binding from the total. The equation of this analysis assumes only one population of receptors and is analysed using one-site binding models in the analysis package used (GraphPad Prism)

The rectangular hyperbola of specific binding is more commonly transformed to a semi-logarithmic plot (figure 2.4) ($\text{fmol} \cdot \text{mg}^{-1}$ protein versus $\log[\text{radioligand}]$), where the K_d can be determined as 50% of B_{max} .

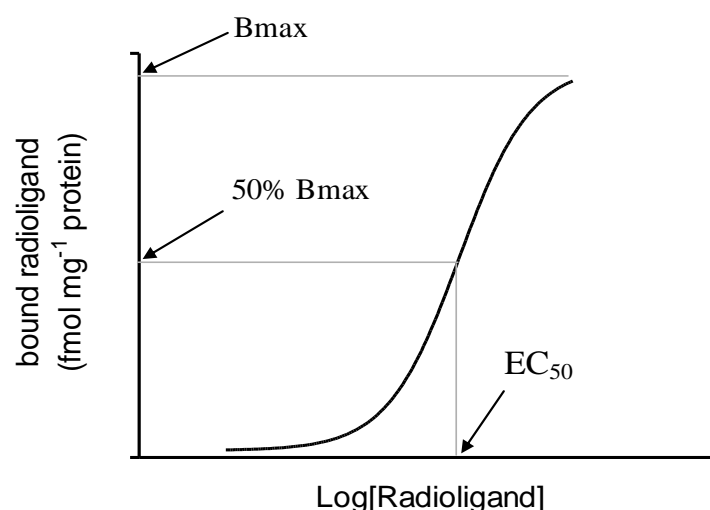


Figure 2.4. *Semi-logarithmic sigmoidal curve of receptor binding sites (shown as bound radioligand) plotted against log radioligand concentration.*

A requirement of the saturation binding assay is that less than ~10% of the added radioligand has to bind (at all radioligand concentrations tested) in order to prevent ligand depletion from the assay and therefore an appropriate amount of protein is determined.

2.4.2. Methodology

Membranes were prepared as described in (Kitayama *et al*, 2003) and this method was used in all *in vitro* experiments in this thesis (detailed description of membrane preparation in Appendix; Section A2). Appropriate amount of membrane protein (typically 70-100 µg) was incubated in 0.5 ml volumes of 50 mM Tris (pH 7.4 with KOH), 0.5% BSA, 10µM of a variety of peptidase inhibitors (amastatin, bestatin, captopril, phosphoramidon; as appropriate) and various concentrations of radioligand deprenorphine ([³H]-DPN) for hMOP, hDOP, hKOP and hMOP/hDOP; or tritiated UFP-101 ([³H-UFP-101) for hNOP, for 1h at room temperature. NSB was defined in the presence of 10 µM naloxone (for hMOP, hDOP, hKOP and hMOP/hDOP) or 1 µM unlabelled N/OFQ for hNOP. Reactions were terminated and bound/free radioactivity was separated by vacuum filtration through polyethylenimine (PEI; 0.5%)-soaked Whatman GF/B filters, using a Brandel harvester. Bound radioactivity was determined after 8h extraction in scintillation liquid, using liquid scintillation spectroscopy. Table 2.1 below shows a representative example of the components used in the assay solutions of a typical saturation binding experiment, in a total volume of 500µl each.

Solution type	Solution components			
	<i>Binding buffer</i>	<i>Radioligand</i>	<i>Membrane</i>	<i>NSB</i>
Total binding	300µl	100µl	100µl	-
Non-specific binding	200µl	100µl	100µl	100µl

Table 2.1. *Solution components and volumes used in a typical saturation binding assay using 500µl total volume for each solution. In saturation binding, total and non-specific binding was prepared for each radioligand concentration (typically 12).*

2.5. Displacement binding assay

2.5.1. Theory

Displacement binding assay is used to determine a ligand's binding affinity (the strength of interaction; pK_i) to the target receptor. In this assay, increasing concentrations of the non-labelled ligand are incubated in a series of samples with a constant concentration of a radioligand. The ligand's concentration determines the displaced amount of radioligand from the receptor. A semi-logarithmic sigmoidal curve is used to describe bound ligand (as percentage displacement of the radioligand) versus free ligand (in logarithmic scale) in order to calculate the EC_{50} of the ligand (figure 2.5).

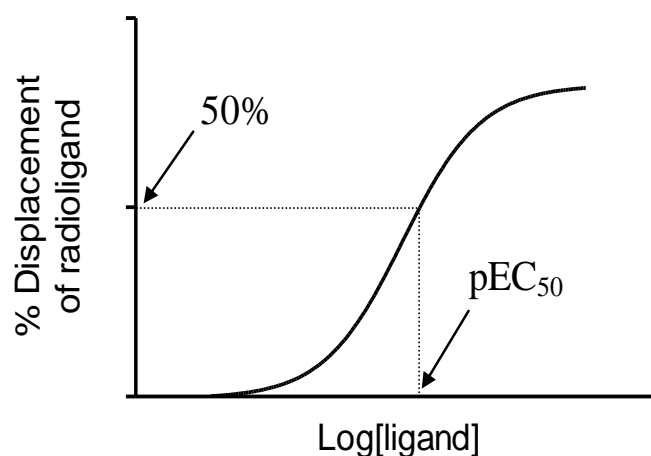


Figure 2.5. *Semi-logarithmic sigmoidal curve of percentage displacement of radioligand (bound ligand) plotted against log ligand concentration used. The concentration of the ligand that displaces 50% of the radioligand used is the EC_{50} , which is expressed as a pEC_{50} and is used to calculate binding affinity.*

The EC₅₀ is related to the affinity of the displacer but is confounded by the amount of radioligand used. More radioligand required more displacer to produce the same displacement so the curve effectively shifts to the right in proportion to radioligand concentration. The Cheng-Prusoff equation (Cheng & Prusoff, 1973) is used to correct the EC₅₀ obtained from these assays in order to estimate the ligand's affinity (5):

$$(5) \quad K_i = EC_{50}/1+\{([L]/K_d)\}$$

(K_i; binding affinity, [L]; concentration of radioligand, K_d; dissociation constant of radioligand)

The K_i can also be expressed in a logarithmic scale as the pK_i, when changing equation 5 into a logarithmic equation (6):

$$(6) \quad pK_i = \log[EC_{50}/(1+\{([L]/K_d)\})]$$

([L]; concentration of radioligand, K_d; dissociation constant of radioligand)

2.5.2. Methodology

One of the main differences in the methodology of this assay with that of a saturation binding assay, is the use of one concentration of radioligand across all tubes in the assay, with varying concentrations of the displacer. Membrane protein (70-100 µg) was incubated as in the saturation assay, using one concentration of radioligand (~1 nM ³H-DPN for hMOP, hDOP, hKOP and hMOP/hDOP cell lines or ~0.8 nM ³H-UFP-101 for hNOP) and varying concentrations of a displacer ligand (1 pM - 10 µM). Non-specific binding (NSB) was defined in the presence of 10 µM naloxone for hMOP, hDOP, hKOP and hMOP/hDOP or 1µM N/OFQ for the hNOP preparations. Assay incubation time, reaction termination and bound radioactivity were determined as in the saturation

assays. Table 2.2 below shows a representative example of the components used in the assay solutions of a typical displacement binding experiment, in a total volume of 500µl each.

Solution type	Solution components				
	<i>Binding buffer</i>	<i>Radioligand</i>	<i>Membrane</i>	<i>Drug</i>	<i>NSB</i>
Total binding	300µl	100µl	100µl	-	-
Non-specific binding	200µl	100µl	100µl	-	100µl
Displacer	200µl	100µl	100µl	100µl	-

Table 2.2. *Solution components and volumes used in a typical displacement binding assay using 500µl of total volume for each condition. In displacement binding there are typically 8 tubes prepared for the displacer.*

2.6. GTPγ³⁵S assay

2.6.1. Theory

The GTPγ³⁵S assay is a functional assay used to quantify the level of G-protein activation after receptor-ligand binding and is based on the exchange of Gα-bound GDP for GTP. When in the trimeric form the Gα subunit possesses high affinity for GDP. Upon receptor activation, the affinity of the Gα-subunit to GDP decreases and the Gα-bound GDP is replaced by GTP, allowing for the activation of Gα and the initiation of the signal cascade (Befort *et al*, 1996). The activated Gα subunit is an intrinsic GTPase and thus hydrolyzes the γ-phosphate bond of the bound GTP, releasing its phosphate group and transforming the purine nucleotide back to GDP. In the assay, cellular GTP is replaced by the synthetic GTPγ³⁵S, where its γ-thiophosphate bond cannot be hydrolyzed by the Gα subunit. Therefore, binding of the Gα-GTPγ³⁵S upon receptor

activation is measurable. However, GDP is required in the assay in order to reduce the basal binding of $\text{GTP}\gamma[^{35}\text{S}]$. The use of the non-hydrolysable radiolabeled $\text{GTP}\gamma[^{35}\text{S}]$ allows measurement of receptor activation at the earliest point in the signal transduction cascade, which is the GDP/GTP exchange (Milligan, 2003). Therefore the assay measures a functional consequence of receptor occupancy by a measurement that is subjected to low degrees of amplification or modulation, which occur further downstream.

Although the “receptor occupation theory” states that the agonist-mediated response is proportional to the number of occupied receptors, there are agonists that even in saturable concentrations cannot yield the system’s maximum response and therefore their ability to produce a response is capped by their “intrinsic activity” (Milligan, 2003). These ligands are called partial agonists. Figure 2.6 presents an example of dose-response curves of a full agonist and a partial agonist, illustrating the relationship between the EC_{50} and the percentage stimulation of the ligands.

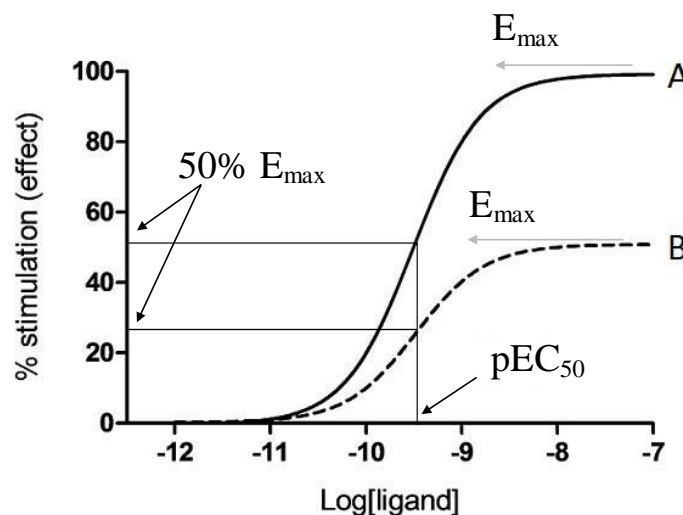


Figure 2.6. Representative dose-response curves of two ligands, A and B. The effect (presented as percentage stimulation of $\text{GTP}\gamma^{35}\text{S}$ binding from basal) is plotted against the concentration of the ligand on a logarithmic scale. The concentration of the ligand that produces 50% of its maximum effect (E_{\max}) is shown as the EC_{50} .

The term efficacy describes the ability of an agonist to promote a receptor conformation upon binding producing a cellular response; usually expressed in its maximum capacity by the E_{\max} value. Potency describes the molar concentration of an agonist that produces a given response; usually expressed by its EC_{50} .

2.6.2. Methodology

Membrane protein (50-80 μ g) was incubated in 0.5 ml volumes of 50 mM Tris, 0.2mM EGTA, 1 mM $MgCl_2 \cdot 6H_2O$ 100mM NaCl, 0.1% BSA, 0.15 mM bacitracin; pH 7.4 (with NaOH), for 1h at 30°C with gentle shaking, to which 10 μ M peptidase inhibitors (amastatin, bestatin, captopril, phosphoramidon), GDP (33 μ M) and ~150 pM $GTP\gamma[^{35}S]$ were added (Vergura *et al*, 2006). Ligands were included at various concentrations and combinations, depending on each experiment. Non-specific binding was determined in the presence of non-radiolabelled 10 μ M $GTP\gamma S$. Two samples were incubated with the absence of ligand; with and without NSB. These samples determine the total radioligand binding and the non-specific binding as described in the binding assay above. Reactions were terminated by vacuum filtration through dry Whatman GF/B filters, using a Brandel harvester. Bound radioactivity was determined as in the binding assays. Table 2.3 below shows a representative example of the components used in the assay solutions of a typical $GTP\gamma[^{35}S]$ experiment, in a total volume of 500 μ l each.

Solution type	Solution components							
	<i>AB</i>	<i>BSA</i>	<i>BAC</i>	<i>GDP</i>	<i>Dr</i>	<i>RL</i>	<i>M</i>	<i>NSB</i>
Total stimulation	240µl	20µl	20µl	20µl	-	100µl	100µl	-
Non-specific stimulation	220µl	20µl	20µl	20µl	-	100µl	100µl	20µl
Agonist	220µl	20µl	20µl	20µl	20µl	100µl	100µl	-

Table 2.3. *Solution components and the volumes used in a typical $GTP\gamma[^{35}S]$ assay using 500µl of total volume for each solution. In a $GTP\gamma[^{35}S]$ assay there are typically 8 tubes prepared for the agonist. Peptidase inhibitors are included in the membrane solution. Key: *AB*; assay buffer, *BSA*; bovine serum albumin, *BAC*; bacitracin, *GDP*; guanosine diphosphate, *Dr*; drug, *RL*; radioligand, *M*; membranes, *NSB*; non-specific binding.*

2.7. Cyclic adenosine monophosphate assay

2.7.1. General theory

The adenosine-3',5'cyclic monophosphate (cAMP) assay is a functional assay used to quantify downstream GPCR activation. Opioid receptors couple to G_i -proteins and therefore their activation leads to reduction of cAMP levels by inhibition of the catalytic activity of adenylyl cyclase (AC) to transform adenosine triphosphate (ATP) to cAMP (see figure 1.6 in Chapter 1). Hence, the assay measures a functional consequence of receptor activation by measuring the levels of the second messenger. cAMP is elevated by the AC activator, forskolin.

2.7.2. Assay theory

The assay utilises radiolabelled cAMP ($[^3H]cAMP$) and bovine binding protein (BP) from bovine adrenal gland in a protein-binding assay in order to determine the cAMP

concentration in the samples. Both cAMP and [^3H]cAMP bind competitively to the BP binding sites (protein kinase A), proportionally to their respective concentrations. There is an inverse relationship between the amount of unlabelled and labelled cAMP present in the assay, *i.e.* as the mass of cAMP present in the assay increases, it displaces more of the bound [^3H]cAMP and therefore there is decreased radioactivity in the measurement. Increasing amounts of unlabelled cAMP of known mass (0, 0.25, 0.5, 1, 2, 4, 6, 8 and 10pmol 50 μl^{-1}) are used as standards for the construction of a concentration-related displacement curve (Vergura *et al*, 2006). The displacement of [^3H]cAMP by the unknown quantity of the cAMP in the samples being measured, is compared against the standard curve (figure 2.7) and the concentration of the cAMP in the samples is calculated from the curve using Riasmart software associated with the β -counter (Packard Bell, Berkshire, UK).

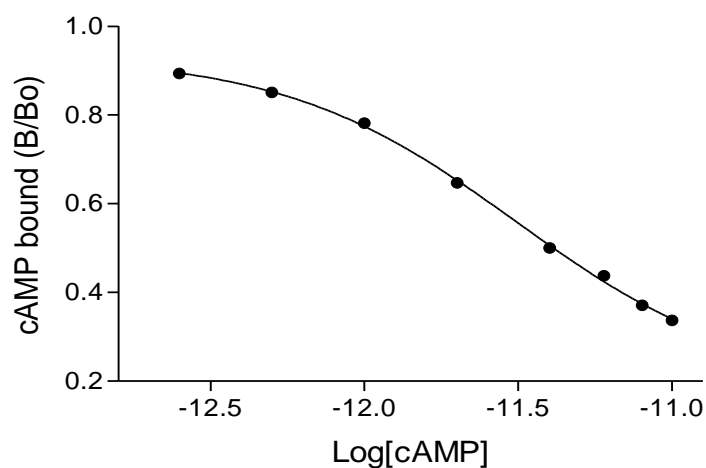


Figure 2.7. Representative cAMP standard curve as produced by the Riasmart software.

2.7.3. Methodology

Confluent cells were harvested with appropriate buffer (154mM NaCl, 10mM HEPES, 1.71mM EDTA, to pH 7.4 with NaOH) for 5 mins. After detachment, the cell suspension was centrifuged at 1500rpm for 2mins. The supernatant was discarded and the cell-pellet was resuspended in an appropriate volume of Krebs/HEPES buffer (143mM NaCl, 10mM HEPES, 12mM glucose, 4.7mM KCl, 1.2mM KH₂PO₄, 2.6mM CaCl₂, 1.2mM MgSO₄, to pH 7.4 with NaOH). Centrifugation was repeated three times. The pellet was finally resuspended at Krebs/BSA buffer (0.5% BSA) in an appropriate volume.

Whole cell suspensions were then incubated in 300µl of Krebs/BSA at 37°C for 15mins, in the presence of 1mM isobutylmethylxanthine (IBMX) and in the absence (for “basal”) or presence of 1µM forskolin (to activate adenylyl cyclase) and opioid ligand (10⁻⁵M) (table 2.4).

Solution	Buffer	Forskolin 1µM	Drug	IBMX 1mM	Cells
Basal	60 µl	-	-	40 µl	200 µl
Forskolin	40 µl	20 µl	-	40 µl	200 µl
Drug	20 µl	20 µl	20 µl	40 µl	200 µl

Table 2.4. Addition table of appropriate reagents in a cAMP assay. IBMX; isobutylmethylxanthine.

Reactions were terminated by the addition of 20µl HCl (10M). The pH was equilibrated with the addition of 20µl NaOH (10M) and 200µl Tris-HCl buffer (pH 7.4) prior to vortexing. Centrifugation at 16100g for 2mins was applied to the solutions prior to measurement of cAMP concentration in the supernatant using the binding protein (BP)

method described in 2.7.2. The assay was carried out at 4°C on ice. A low concentration of [³H]cAMP (100µl, ~0.5nM) and diluted BP (150µl, ~1/20) were added to each standard and sample, then equilibration was allowed to occur for minimum 4 hours at 4°C (table 2.5).

Solution	Buffer	NSB	Standards	SS	Radioligand	Binding protein
Total	50 µl	-		-	100 µl	150 µl
NSB	-	50 µl	-	-	100 µl	150 µl
Standards	-	-	50 µl	-	100 µl	150 µl
Sample	-	-	-	50 µl	100 µl	150 µl

Table 2.5. *Addition table of reagents in a cAMP assay. The ‘standards’ solutions included a known amount of cAMP for constructing a standard curve. Measurements of non-specific binding (NSB) were subtracted from that of the ‘total’ to determine specific binding. Total volume was 300µl. SS; supernatant sample.*

Bound and free radioactivity were separated by the addition of 250µl of charcoal mixture (250mg charcoal, 100mg BSA per 25ml solution, 50mM Tris-HCl and 4mM EDTA buffer at pH 7.4). Each tube was allowed to stand for 1min before centrifugation at 12000g in a Sarstedt microfuge at room temperature (°RT). The supernatant (200µl) was taken and mixed with 1ml of Optiphase Hi-Safe scintillation liquid and radioactivity was counted using liquid scintillation spectroscopy.

2.8. Receptor internalization studies

2.8.1. General theory

When receptor internalisation occurs upon ligand binding (as discussed in Section 1.1.6; Chapter 1), the total number of the receptors expressed on the cell surface decreases. This can be shown as a decreased B_{\max} in a saturation binding assay of a membrane preparation, after incubating the cells with a ligand for a given time. Whole cell studies are not particularly useful in these studies as receptors can recycle back to the cell surface within the incubation period.

2.8.2. Methodology

Cells (grown in large T175 flasks) were incubated with appropriate concentration of a given ligand in 20ml of fresh culture medium for 1 hour. Adherent cells were washed three times at 4°C with harvest buffer to remove any receptor-bound ligand, before harvesting. Membranes were prepared as in the binding assays, washing three times with buffer prior to three centrifugations at 1600g and three centrifugations at 14000g, with subsequent removal of supernatant and resuspension of the pellet, in order to ensure that all ligand is washed off. A saturation binding assay was then performed as described previously in Section 2.4.2; Chapter 2.

2.9. In Vivo nociception assays

2.9.1. Particulars of the study

The *in vivo* experiments were designed and performed in the laboratory of Dr Giovanni Vitale (Assistant Professor of Pharmacology, Section of Pharmacology, Department of Biomedical Sciences) at the University of Modena & Reggio Emilia (Via Campi 287, I-41125, Modena), Italy. The experimental design was planned under the consultation of Dr Giro Calo (Department of Experimental and Clinical Medicine, Section of Pharmacology, University of Ferrara, Italy).

2.9.2. Animal handling

Seventy male Wistar rats (Strain code 003, albino, 200-250g/rat) were obtained from Charles River Laboratories (Charles River Laboratories Italia S.r.l., Via Indipendenza 11, Calco (Lecco) 23885, Italy). All experimental procedures adopted for *in vivo* studies complied with the standards and ethical guidelines for the investigation of experimental pain in conscious animals of the European Communities Council directives (86/609/EEC), national regulations (D.L. 116/92) and ethical policies/regulations detailed by Drummond (2009). The animals were housed in groups of two-three under standard controlled conditions (22°C, 12 h light-dark cycle) with food and water *ad libitum* for at least 5 days before experiments began. Animal behavior was monitored prior, during and after each experiment in order to detect evident behavioral changes after drug administration. Animal weight was recorded and monitored throughout the study.

2.9.3. Catheterization of animals

A modification of the (Storkson *et al*, 1996) method of catheterization was applied at the lumbar region of the spinal cord (between the L5 and L6) for all animals (figure 2.8). All animals were weighed and were anaesthetized by a ketamine/xylazine cocktail (10 mg/kg ketamine hydrochloride/xylazine hydrochloride, by Sigma, USA). After removing the fur at the lumbar region, the lumbar part of the spinal cord was rendered kyphotic by raising the ventral iliac spines and a longitudinal incision was made. The needle could advance 2-4mm in the narrow space between L5 and L6, where the correct intrathecal localization was confirmed by a tail flick and/or a paw retraction by easy insertion of the catheter (polyethylene tube; 0.6mm diameter; PE-10) through the cannula. The catheter, which was 14cm in total, including the 4cm of the subarachnoid space, was passed through the subcutaneous space and exited behind the animals' neck so that it would minimize the animals' reach. Sterile saline (NaCl 9mg/ml, i.t.) was injected in a volume of 10µl in order to flush the catheter, avoiding blood clots in the site and to check for leaks. All rats were then sutured and left for two days to recover and full recovery was assessed by full motility and normal behavior of the animal.

COPYRIGHT MATERIAL - IMAGE REMOVED

Figure 2.8. *Modification of (Drummond, 2009) showing the i.t. catheter implantation in rats. (L5: lumbar 5 spine, L6: lumbar 6 spine, Cin: position of catheter when initially inserted, Cout: catheter exit position after subcutaneous pass.)*

Lidocaine (15µl, 20mg/ml, *i.t.*) followed by saline (10µl, *i.t.*) was administered after recovery to all animals in order to confirm the correct positioning of the catheter and the intrathecal application of the drug through the subsequent loss of motor control of the rear limbs within 15sec lasting for 20-30mins. Animals that did not pass the lidocaine test were excluded from the study. The rest of the animals were left to recover individually (one animal in each cage) for at least 24 hours after lidocaine administration before being used for experimentation.

2.9.4. Tail-flick assay

2.9.4.1. Theory

The tail-flick assay is an antinociceptive assay that mainly assesses spinal analgesia. The animal is placed on a level-surface apparatus with its tail protruding on top of a photoelectric radiant-heat cell. The application of thermal radiation to the tail of the

animal provokes the withdrawal of its tail by a brief vigorous movement. The apparatus' chronometer records the time between the initiation of the beam and tail retraction (test latency; TL) where the chronometer stops automatically. Lengthening of the reaction time is interpreted as an antinociceptive action. The exposure time to the radiant heat does not exceed 15sec (cut-off time), in order to avoid tail injury. By using the apparatus' rheostat, the intensity of the radiant heat emission can be controlled in such a way that one can empirically predetermine the tail-withdrawal latency time of naive (non-treated) rats (i.e. basal latency, most commonly between 2 and 5 secs). Figure 2.9 shows an example of an antinociceptive profile obtained by the tail-flick assay.

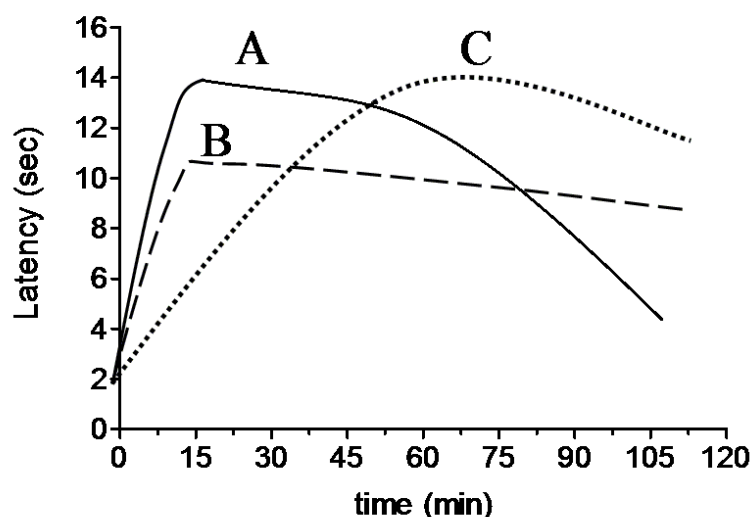


Figure 2.9. An example of the antinociceptive profile of three drugs (A, B and C) from a tail-flick assay. Before injection (at $t=0$ sec), animals show basal latency of 2secs. Drug A shows peak effect of 14 sec latency, at 15 mins after injection, with gradual decrease in antinociception over time. Drug B shows a peak effect of 11 sec, at 15 mins after injection, with more persistent antinociception over time than Drug A. Drug C is equianalgesic with Drug A (peak analgesia at 14 sec), but has a slower action since it reaches peak after 60 mins of injection.

2.9.4.2. *Experimental design.*

The study was divided in two major phases: acute and repetitive administration. The acute phase was further divided into two parts, A1 and A2, as shown in figure 2.10. Phase A1 was a preliminary phase for UFP-505 antinociceptive assessment, which was applied in order to determine the maximum dose of UFP-505 that would reach the cut-off time and assess the optimum analgesic dose to be used in the repetitive phase. Two doses of UFP-505 were used in Phase A1 (10 and 50nmol) and the analgesic profile was compared with saline. Phase A2 utilized three sub-maximum doses of UFP-505 (1, 3 and 10nmol) and one dose of morphine (10nmol) in order to determine the equipotent dose of UFP-505 to 10nmol morphine. The sub-chronic phase utilized the equipotent doses of UFP-505 and morphine determined in phase A2 in order to assess the analgesic profile of the two drugs during repetitive administration (5 days). Additionally, the analgesic profile after co-administration of naltrindole 10nmol and morphine 10nmol (N+M) was determined.

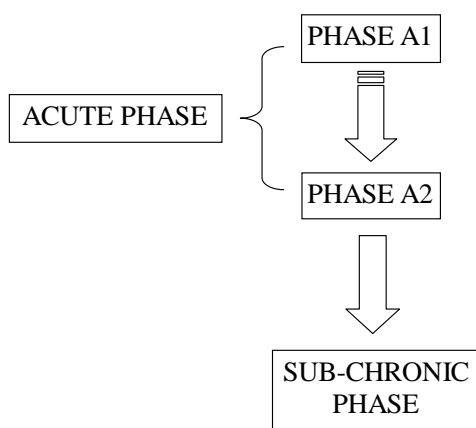


Figure 2.10. *Experimental design for the tail-flick tests. Phase A1 determined the dose of UFP-505 that produced maximal analgesia (reached cut-off time). Phase A2 determined the equianalgesic doses of UFP-505 and morphine. The sub-chronic phase (repetitive administration) determined the tolerance profile of UFP-505 and morphine using equianalgesic doses.*

Catheter disruption (usually by self-scratching) was a major issue in the study, causing the removal of the catheter from the rats. The animals that removed their catheter were excluded from the rest of the study. Figures and further information on the number of rats excluded from the acute and subchronic phases of the study due to the failure of the lidocaine-test or due to removal of the catheter are presented in the respective section of Results-Chapter 5.

2.9.4.3. Methodology for acute experiments

Animals were submitted to the tail-flick test as described above, prior to *i.t.* treatment in order to determine their basal latency (BL; at time T=0 min), and after *i.t.* treatment (for TL) at times T = 15, 30, 60, 90 and 120 mins, in order to assess their analgesic levels. The control animals was treated with sterile saline (20µl) whereas the drug-tested animals was treated with 10µl (*i.t.*) for concentration of the appropriate drug, followed by administration of sterile saline (10µl *i.t.*). Behavioural monitoring of all animals was applied as described above.

2.9.4.4. Methodology for repeated administration experiments

Animals were treated and submitted to the tail-flick test as in the acute experiments as described above. The length of the experiment was 5 days and analgesia was assessed by the tail-flick test at Day 1, Day 3 and Day 5, with the same format as described in the acute experiments. For the N+M group of animals, naltrindole was introduced 5 minutes prior to morphine. Animal treatment was performed at the same time of the day for each of the 5 days of the experiment. Behavioural monitoring of all animals was used as described above. The analgesic efficacy and analysis of data were evaluated as above in acute experiments.

2.9.5. Hot-plate assay

2.9.5.1. Theory

The hot-plate apparatus (Socrel DS-35, Ugo Basile, Comerio, VA, Italy) consists of an electrically-heated metallic surface which is kept at a constant temperature of $54 \pm 0.5^{\circ}\text{C}$, attached to a manual pedal-chronometer. The animal is placed on the metallic surface and protected from escaping by a clear plastic border surrounding the plate. The heated plate induces a nociceptive response to the animal and its pain-reflex behaviour is expressed by licking its paws or jumping. The investigator stops the chronometer upon the first observation of pain-reflex behaviour and records the time. The hot-plate assay is suitable for short periods of testing (up to 10 days), as it has been shown to display behavioural tolerance in long-term use (>10 days) and therefore a decrease in the latencies with reduced sensitivity to analgesic agents (Carter & Shieh, 2010).

2.9.5.2. Experimental design and methodology

In order to be able to compare any observed mRNA changes of opioid receptors between intrathecal and subcutaneous administration of morphine, a subchronic study (4 days) of subcutaneous morphine administration was performed. The analgesic profile and tolerance developed after the administration of morphine was recorded, and the neuronal tissue of the rats was used for RT-qPCR as discussed further below.

Six of the animals that were untreated in the tail-flick assays (due to failing the lidocaine test), were used in this experiment for subcutaneous (s.c) injection of morphine (5mg/kg twice daily for 4 days) along with six animals that were used as controls (treated with saline). All animals were weighed at the beginning of each day and the appropriate volume of solution of prepared drug was administered as according

to Sandrini *et al* (2007). The latencies for paw licking and/or jumping were recorded for each animal, prior to the first treatment (BL) and after the second treatment for each day (TL).

2.9.6. Tissue removal

The brain and spinal cord tissues of some of the animals used in the tail-flick and hot-plate assays were removed in order to be analyzed *in vitro* for opioid receptor mRNA expression by PCR and protein by radioligand binding. Due to the fact that the tissues had to be removed immediately after the completion of each part of the study and that the necessary time for each operation and the human resources available were limiting factors for this experiment, not all animals could be used for tissue removal. Five animals for each of the A2, sub-chronic phases and hot-plate assay were used for brain and spinal cord isolation after animal decapitation. The animals were kept on ice during the isolation of neuronal tissues, a process that was carried out at the minimum 1 hour after the end of each *in vivo* experiment and lasted for at least 40 minutes. For the brain tissue, after removal of the limbic parts of each brain tissue (including the *corpus callosum*, hypothalamus and thalamus), the rest of the tissue was divided into two pieces: frontal cortex and the rest of the cortex.

Tissues scheduled for PCR analysis were treated with RNAlater® solution (AM7020, Applied Biosystems, USA) an RNA-stabilization solution that readily permeates all fresh tissues and protects RNA from degradation or attack by RNAases. The solution-tissue complex was then stored at -20°C for two days and then at -80°C for three days. Tissues scheduled for radioligand binding were incubated directly at -80°C.

2.10. Production of a double-expression system

2.10.1. Theory

The question of how the activity of UFP-505 is affected by the simultaneous presence of MOP and DOP receptors, was addressed by producing a cell line that stably expressed both opioid receptors (CHO_{hMOP/hDOP}; noted hereafter as the ‘MOP/DOP cell-line’) and performing binding and internalization assays. A stable cell line was produced by transfecting a DNA plasmid vector that incorporated the human DOP receptor gene (OPRD1), into CHO cells that were stably expressing the human MOP receptor. In order to secure the right selection of cells after transfection, the incorporated plasmid included a hygromycin B resistance gene (pcDNA 3.1/Hygro(+)- OPRD1, whereas the CHO_{hMOP} (recipient) cells were already resistant to the antibiotic geneticin. RT-qPCR was performed using extracted RNA from the MOP/DOP cells in order to confirm the transcription levels of MOP and DOP receptor mRNA prior to binding experiments.

2.10.2. Concentration-death plot

The concentration-death plot determines the relationship between antibiotic concentration and the death of non-resistant cells. It is used to determine the optimum concentration of antibiotic selection pressure used in the stock medium of resistant cell lines in order to avoid reversion. A concentration-death plot for hygromycin B in geneticin-resistant CHO_{hMOP} cells was constructed according to (Liu *et al*, 2004b). Different concentrations (50-1000µg.ml⁻¹) of hygromycin B (Invitrogen Corporation, 5791 Van Allen Way, PO BOX 6482, Carlsbad, CA 92008, US) were added in random order to CHO_{hMOP} cells grown in a 12-well plate that was observed by two blinded observers under the light microscope for 14 days. The percentage of live cells was

estimated by the observers when compared with a control hygromycin-free well and the mean values were recorded. The concentration of hygromycin B that produced 100% cell death at 4 days was termed 'selection pressure' whereas the concentration that produced 100% cell death at 14 days was termed 'stock pressure'.

2.10.3. Stable transfection

A pcDNA3.1+/Hygro plasmid vector was supplied by Invitrogen (Invitrogen Corporation, 5791 Van Allen Way, PO BOX 6482, Carlsbad, CA 92008, US) and the human DOP gene (OPRD1) was supplied by S&T (Missouri University of Science and Technology, cDNA Resource Center, 105 Schrenk Hall, 400 West 11th St, Rolla, MO 65409-1120, US) (details of the map of the plasmid used and further information is presented in the Appendix A7 and A8). The two products were used by S&T to produce an OPRD1-pcDNA3.1+/Hygro plasmid vector. The new vector's concentration was estimated to be 518ng/μl using a NanoDrop®.

Two T25 flasks of CHO_{hMOP} cells were cultured to ~60% confluency (log-phase), prior to substitution of medium with serum-free antibiotic-free (SF-AF) medium to promote maximum transfection. A FuGene® HD transfection reagent kit was used in order to transfect the plasmid vector into CHO_{hMOP} cells. The kit uses a multi-component reagent that forms a complex with the cDNA and then transports the complex into the cells. Based on previous work, a transfection complex of 3:2 was prepared in 300μl SF-AF medium (table 2.6), according to the equation (7):

$$(7) \text{ [FuGene reagent } (\mu\text{l}): \text{DNA } (\mu\text{g})/100\mu\text{l}]}$$

The complex was allowed to settle at °RT for 15mins and was then added to the flask of cells (containing 10ml of appropriate medium) and distribution over the entire surface was ensured. The cells were incubated at 37°C for 24 hours to allow incorporation of the complex and expression of DOP receptors on the cell surface.

3:2 Transfection ratio complex	
OPRD1-pcDNA3.1+/Hygro	11.59µl
FuGene [®] HD Reagent	9µl
SF-AF Medium	279.41µl
Final volume	300µl

Table 2.6. *Components of the transfection complex used for the stable production of the novel CHO_{hMOP/hDOP} cell line. According to formula (9), 6µg of DNA (vector) and 9 µl of reagent are needed for a 300µl final volume. The 6µg of DNA were found in 11.59µl of the vector solution (518ng/µl concentration).*

2.10.4. Subcloning

Following incubation, the SF-AF medium in both cell flasks was substituted by the CHO selection medium supplemented with additional hygromycin-B *selection pressure*. Cells were incubated at 37°C for one week with frequent medium changes in order to clear the dead non-transfected cells. The polyclonal cells were allowed to grow and reach 100% confluency, then were trypsinised and resuspended in 10ml of stock medium. A haemocytometer was used, as per Freshney (Freshney, 2005), to estimate the concentration of cells (cells.µl⁻¹) and the concentration was then adjusted to 0.1cells.200µl⁻¹.

The cell suspension was dispensed to six 96-well plates by adding 200µl of suspension in each well. The plates were covered with a humid tissue, placed in a humidification box and incubated at 37°C for two weeks. During this time, the cell medium was

replaced with fresh every three days and wells were observed under the microscope every two days. Wells that were found to include one clear and spherical colony were the ones grown from a single cloned cell. These wells were marked and were allowed to reach confluency. Wells that included more than one colony, a non-spherical colony or an unequally-distributed colony were excluded. The selection pressure was then replaced by the *stock pressure* (named hereafter as a 'MOP/DOP stock medium'). A final number of 30 clones were grown into 6-well plates and were then used for a primary PCR screen in order to determine MOP and DOP receptor mRNA expression levels.

2.10.5. Reverse transcription PCR

2.10.5.1. General theory

Polymerase chain reaction (PCR) is a technique that allows measurement of very small amounts of DNA by amplification. Reverse transcription PCR (RT-PCR) is a variation of the PCR technique. Where traditional PCR is used to confirm the presence or absence of a gene, reverse transcription PCR allows relative gene expression quantification (RT-qPCR) through the reverse transcription of RNA to an identifiable DNA.

RT-PCR presupposes the extraction of total RNA (messenger, ribosomal and transfer RNA) and the degradation of any genomic DNA (gDNA) present. The resulted gDNA-free ('clean') total RNA sample is then reverse transcribed in order to create a copy DNA (cDNA) from the messenger RNA (mRNA) present in the 'clean' total RNA sample. The reverse transcription uses a negative control (lacking the transcriptase enzyme; RT⁻), whereas the samples tested contain the transcriptase enzyme (RT⁺). The PCR technique uses repeated thermal cycles to amplify the cDNA of a sample. Each

thermal cycle consists of three stages: the first stage ('denaturation') separates double-stranded DNA into single strands. In the second stage ('hybridisation'), the specific oligonucleotide primers, designed specifically for the DNA sequence studied, bind to the open strands of DNA. In the final stage ('extension'), the thermo-stable DNA polymerase enzyme is directed by the bound primers to produce complimentary strands to the single strands of DNA (from 5' to 3' end). Since both sense and anti-sense strands of DNA are complimented during each cycle, the amount of DNA is doubled in principle per cycle.

Real-time PCR is an extension to the reverse transcription where a measurement of the relative quantity of DNA is recorded at the end of each thermal cycle using a fluorometric probe (in these experiments, TaqMan™ probes, described below). An amplification curve is produced at the end of each experiment that reflects amplification of DNA in real-time as the cycles progress. A computer software (in this thesis the StepOne™ Software used) determines the cycle number at which a threshold quantity of fluorescence is reached and at which the amplified DNA becomes detectable (named cycle threshold; Ct), as shown in figure 2.11. The Ct value is inversely proportional to the starting quantity of cDNA, thus a low Ct value indicates a high starting quantity. The gene of interest (GOI) is quantified by normalising the Ct value to that of an endogenous control (EC) gene, producing the ΔC_t value, as shown by the formula (8):

$$(8) \quad \Delta C_t = C_{tGOI} - C_{tEC}$$

COPYRIGHT MATERIAL - IMAGE REMOVED

Figure 2.11. *An indicative example of PCR curves, showing the C_t values of two samples, A and B. If sample A is the endogenous control (EC) and sample B the gene of interest (GOI), then the ΔC_t value is the difference of the two C_t values (8 in this case). Sample B has less copies of cDNA than sample A.*

The choice of the EC is selected based on the fact that its expression does not change as a consequence of the experimental conditions (or disease for clinical samples). Fold-change of the GOI expression can be calculated by the formula (9), assuming 100% efficiency of the PCR reaction:

(9) **Fold change** = $2^{-\Delta C_t}$

2.10.5.2. TaqMan probes

The rationale behind the use of fluorometric probes in PCR relies on the addition of a DNA hybridisation probe to the reaction mixture which is specific to the target sequence to be amplified. The TaqMan probe possesses a fluorophore (FAM) and a quencher (TAMRA), which are bound in close proximity so that the fluorescence of the fluorophore is suppressed by the quencher. During the complementary strand extension,

the probe is hydrolysed by the nuclease activity of the *Taq* polymerase and thus the fluorophore and the quencher are separated, releasing fluorescence by the fluorophore, which is detected and measured (figure 2.12).

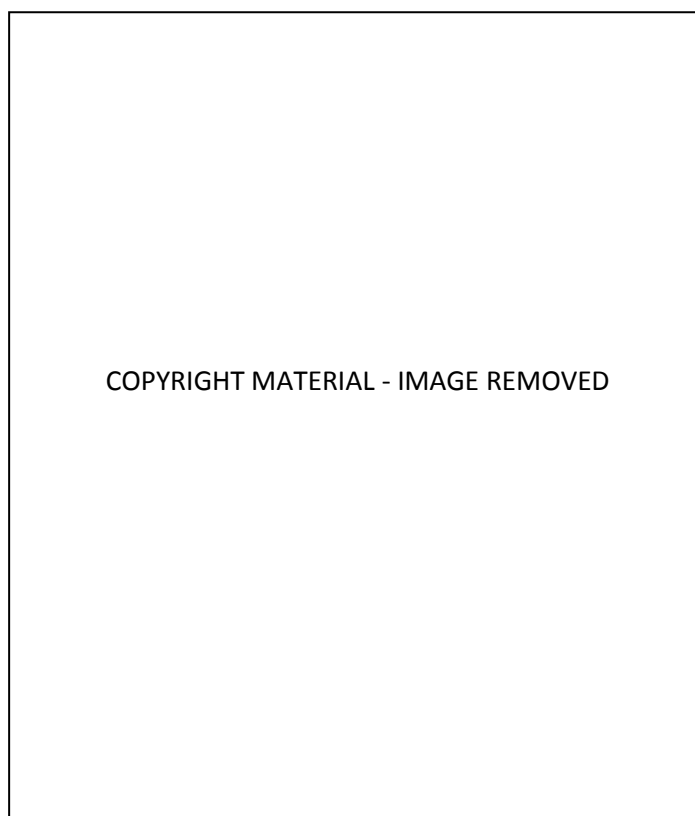


Figure 2.12. *An illustration of how the TaqMan probes work in PCR. The primers and the probe bind to the template DNA and fluorescence is suppressed due to the close proximity between the quencher and the probe. As Taq polymerase extends on the complementary strand in a 5' to 3' direction, it reaches the probe's fluorophore and cleaves it irreversibly (polymerase nuclease activity). Once cleaved, the fluorophore produces a fluorescent signal (yellow) which is detected. Taken from the access-free website <http://www.primerdesign.co.uk>.*

2.10.5.3. Cells-to-CT™

Cells-to-CT™ gene expression kit (Applied Biosystems) was used to extract total RNA from CHO_{hMOP/hDOP}, CHO_{hMOP} and CHO_{hDOP} cells cultured in 6-well plates. Cells were rinsed with 200µL of ice-cold PBS before being lysed with 50µL of 'lysis solution'

containing DNase I enzyme. Cells were incubated for 5 min at °RT during which the plasma membranes were lysed and gDNA was degraded by the enzyme. Inactivation of DNase I was achieved by adding 5µL of ‘stop solution’ to the lysates. Reverse transcription reaction mixtures were prepared as in table 2.7. The RT⁻ was used to evaluate the effectiveness of the DNase I treatment for the degradation of gDNA.

Component	Volume per reaction (RT ⁺)	Volume per reaction (RT ⁻)
2x RT buffer	25µl	25µl
RT enzyme mix	2.5µl	-
PCR-grade water	12.5µl	15µl
<i>Final volume</i>	<i>40µl</i>	<i>40µl</i>

Table 2.7. *Reaction components and volumes used for the reverse transcription assay*

The RT⁺ and RT⁻ reaction mixtures (total volume 40µL each) were incubated with 10µL of the DNAase-treated cell lysates in PCR-grade tubes according to the following thermocycler program (table 2.8). The cDNA produced from the reverse transcription was stored at -20°C until the RT-qPCR was performed.

	Stage	Temperature (°C)	Time (min)
1 st	ReverseTranscription	37	60
2 nd	Enzyme inactivation	95	5
3 rd	Hold	4	-

Table 2.8. *Thermocycler program for reverse transcription.*

2.10.5.4. Methodology for RT-qPCR

The TaqMan™ PCR kit was used in order to prepare the samples for the polymerase chain reaction using the Step-One® instrument (Applied Biosystems). Table 2.9 shows the components of the prepared mixtures. The master mix contained the necessary components for the reaction (DNA polymerase, dNTPs, dUTP and uracil-DNA glycosylase), whereas the assay mix contained the forward and reverse primers. All samples were incubated according to the thermal cycler program of the Step-One® instrument as shown in table 2.10.

Component	Volume (µl)
2x Master Mix	10
20x Assay mix for EC or GOI	1
Template cDNA	2
PCR-grade water	7

Table 2.9. Reaction mixture preparation for TaqMan™ PCR

Steps per cycle	Description	Temperature (°C)	Time (min)
1	Uracil-DNA glycosylase incubation	50	2
2	Polymerase activation and denaturation	95	10
3	Annealing/extension*	60	1

Table 2.10. Thermal cycler program for polymerase chain reaction *Fluorescence measured at the end of this stage

2.11. Statistical analysis methodology

Data representation (i.e. mean \pm SEM) and n values are shown in the figure legend of each graph. Details of statistical analysis are also shown in specific figure legends. All statistical analysis, curve fitting and linear or non-linear regression analyses were performed on GraphPad Prism v.5 (GraphPad Software Inc., San Diego, USA). Saturation and displacement curves were analysed using non-linear regression (fit) one-site binding (hyperbolae) or dose-response with variable slope (sigmoidal). pK_i values were obtained from displacement curves and values were determined using non-linear regression (corrected using the Cheng-Prusoff equation (formula 7) as described in section 2.5.1). pEC_{50} and E_{max} values in functional experiments were obtained from the sigmoidal curve with a variable slope.

Details and specific analysis are shown in appropriate figure and table legends (significance of $p < 0.05$). Normal distribution was assessed using a Kolmogorov-Smirnov test in GraphPad Prism.

CHAPTER 3.

***IN VITRO* PHARMACOLOGICAL**

CHARACTERIZATION OF UFP-505

Chapter 3. *In vitro* pharmacological characterization of UFP-505

3.1. Introduction

The pharmacology of opioid ligands may be studied using a number of different models, from cell lines expressing recombinant opioid receptors to whole organs and animals. *In vitro* study of opioid ligands using cell lines expressing opioid receptors can provide basic information about receptor binding affinity, potency and efficacy, as well as other data regarding functional consequences of opioid receptor activation. Using radioligand binding assays can provide information about the number of binding sites (B_{\max}) and a displacer's affinity for these sites (K_i). Biochemical functional assays can be employed to provide information about receptor activation, the relationship between occupancy and response and the range of functional characteristics like potency and efficacy. Figure 3.1 presents the overall methodological strategy followed in this thesis.

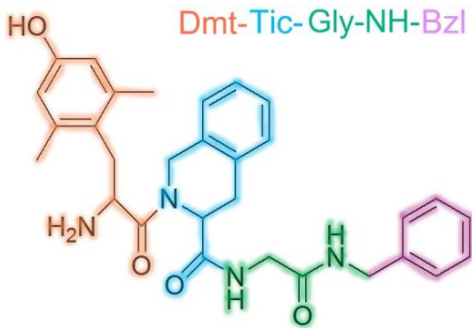
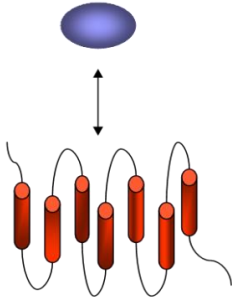
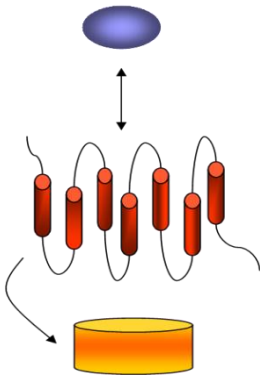
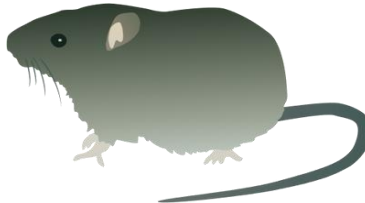
Methodological approach	<i>in vitro</i> upstream	<i>in vitro</i> downstream	<i>in vivo</i>
UFP-505	Drug-Receptor Binding	Receptor Activation	Animal Response
			
Characteristic Tested	Affinity for receptors	Potency and Efficacy	Potency and Efficacy
System Used	CHO _{hMOP/hDOP/hKOP/hNOP}	CHO _{hMOP/hDOP} Rat Cerebral Cortex Rat Spinal Cord	Wistar Rat
Assay	Displacement binding assay	GTPγ ³⁵ S assay cAMP assay	Tail-flick assay

Figure 3.1. Methodological strategy for the pharmacological characterization of UFP-505, upstream to downstream. A schematic representation of the chemical structure of the tripeptide UFP-505 (H-Dmt-Tic-Gly-NH-Bzl) and the pharmacodynamic approach taken (blue = drug, red = receptor; yellow = G-protein, green = tissue response). In the schematic Dmt: 2',6'-dimethyl-L-tyrosine, Tic: tetrahydroisoquinoline-3-carboxylic acid, Gly: glycine, Bzl: benzyl.

3.2. Aims

The aims of this chapter are to provide a basic *in vitro* characterisation of UFP-505 using CHO cells expressing recombinant opioid receptors (CHO_{hMOP}, CHO_{hDOP}, CHO_{hKOP}, CHO_{hNOP}) and to define its pharmacological properties. The receptor density of the cell lines used (B_{\max}) and the binding affinity of the respective radioligands (K_d) will be determined and used to estimate the binding affinity of UFP-505. The effects on G-protein activation and cAMP formation will be examined, in order to characterize ligand function and this will be compared with known reference ligands. This *in vitro* work will provide essential information regarding UFP-505 which will be used later for the *in vivo* characterization of the compound, as well as for the interpretation of subsequent work on opioid receptor internalization.

3.3. Saturation binding assays

The relationship between total, NSB and specific binding can be seen in the saturation binding isotherms in figure 3.2. The binding of ^3H -DPN and ^3H -UFP-101 to all CHO membranes was concentration-dependent and saturable, as shown in figures 3.2 and 3.3. The B_{\max} (fmol radioligand/mg protein) and pK_d values for ^3H -DPN or ^3H -UFP-101 at CHO_{hMOP}, CHO_{hDOP}, CHO_{hKOP} and CHO_{hNOP} cell membranes can be seen collectively in the inserted table of figure 3.3. Saturation assays were also performed on CHO_{hMOP} whole cells as part of the development of the methodology. The B_{\max} in these cells was not significantly different from the cell membrane preparations (figure 3.4).

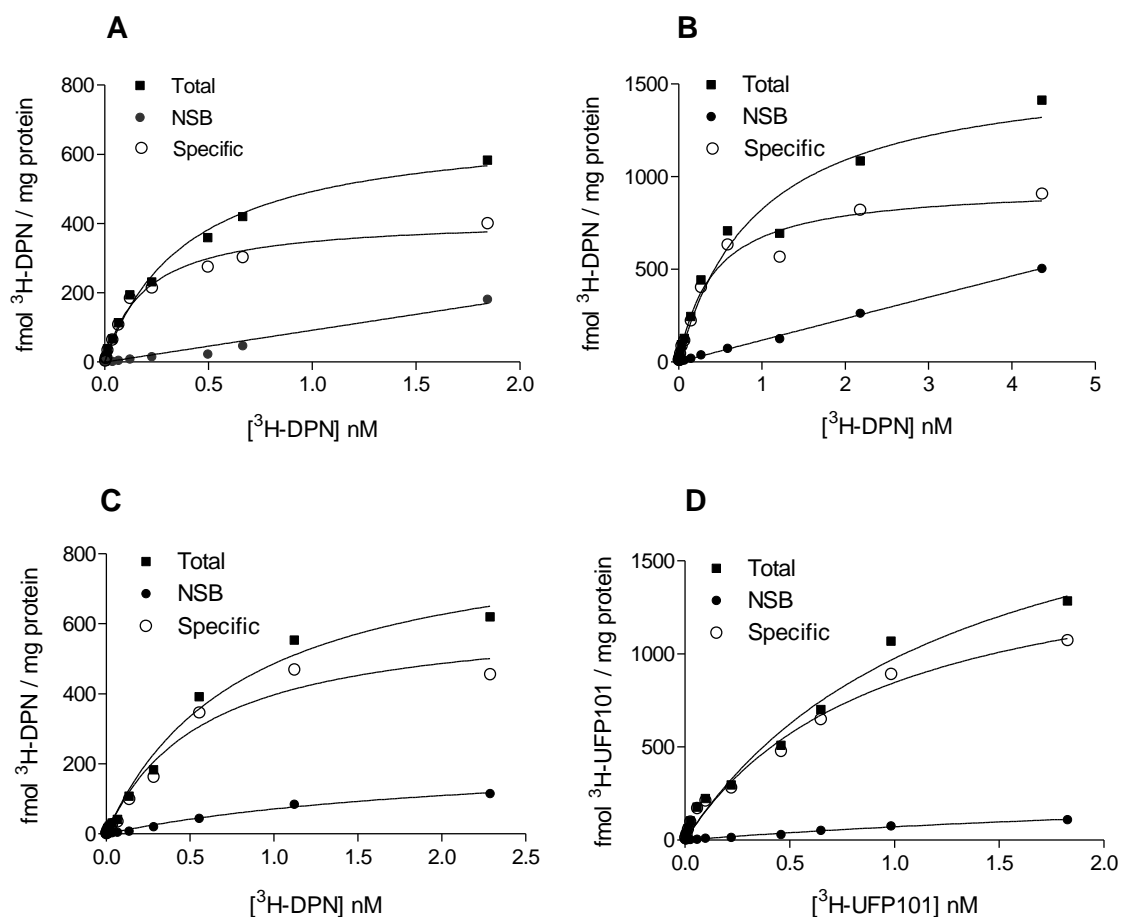
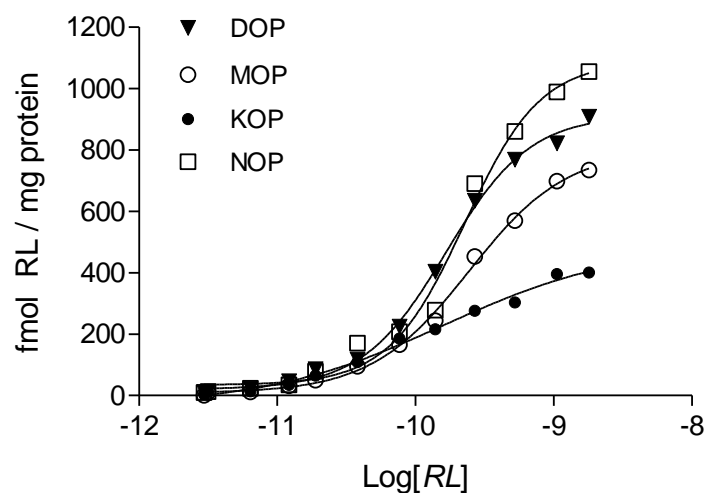


Figure 3.2. Saturation binding assays performed on (A) CHO_{hKOP}, (B) CHO_{hDOP}, (C) CHO_{hMOP} and (D) CHO_{hNOP} cell membranes, with increasing concentrations of tritiated diprenorphine (³H-DPN) or tritiated UFP-101 (³H-UFP101). Non-specific binding (NSB) was measured in the presence of 10 μM naloxone or N/OFQ. Single representative curves are presented here (from n=5). Radioligand binding affinity (pK_d) and receptor density (B_{max}; fmol/mg protein) values are summarized in the inserted table of figure 3.3.



	pK_d	B_{max}
¹ CHO _h MOP	9.52 ± 0.20	458 ± 110
¹ CHO _h DOP	9.29 ± 0.21	1038 ± 184
¹ CHO _h KOP	9.50 ± 0.12	321 ± 59
² CHO _h NOP	8.92 ± 0.24	1054 ± 142

Figure 3.3. Log-transformed specific binding isotherms were used to determine the maximum receptor binding capacity (fmol radioligand/mg protein; B_{max}) and equilibrium dissociation constant (pK_d) in the respective membranes. Single representative curves are presented here (mean \pm SEM from $n=5$). Radioligand (RL) binding affinity and receptor density values are summarized in the inserted table. Radioligands: ¹ [³H]-DPN, ² [³H]-UFP-101.

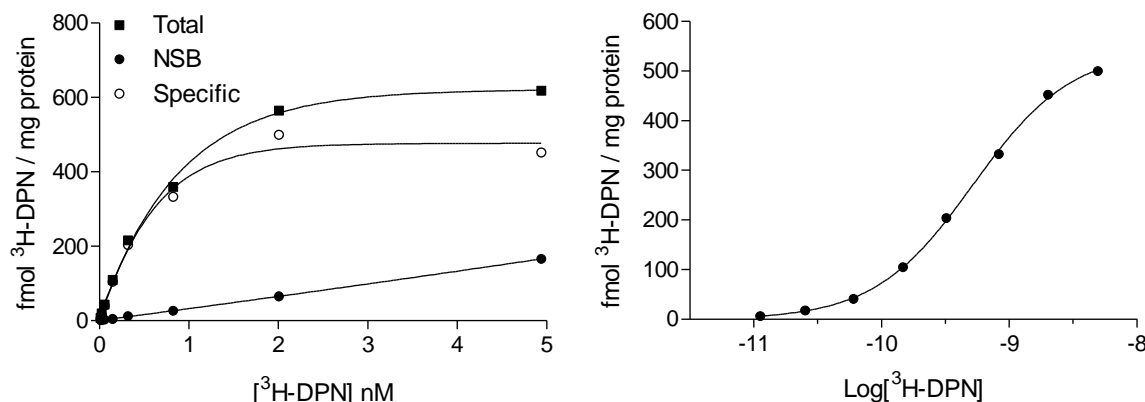
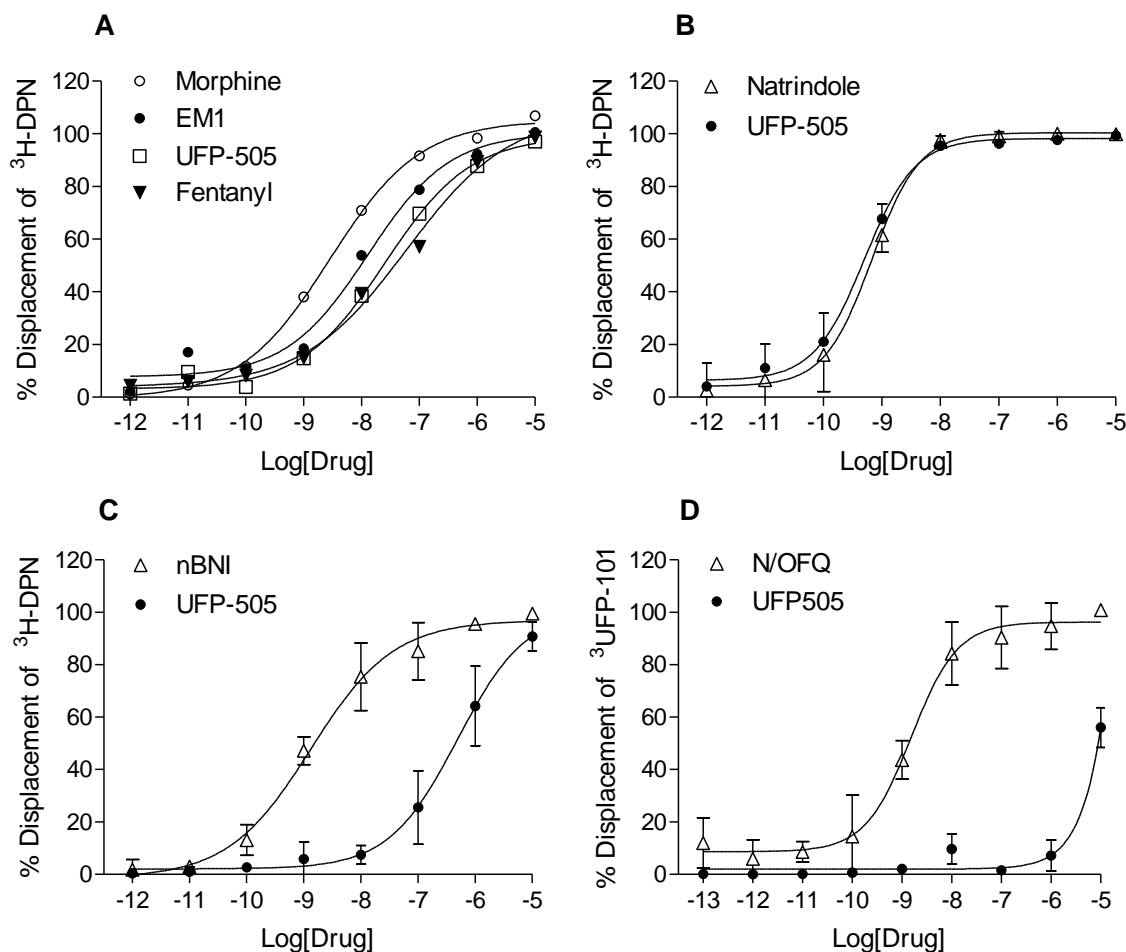


Figure 3.4. Representative curves of a single saturation assay (from $n=5$), performed on CHO_{hMOP} whole cells with increasing concentrations of tritiated diprenorphine (3H -DPN). Assay conditions and parameters of all experiments were kept similar to those performed on cell membranes (only the assay buffer was Krebs/HEPES) as shown in figures 3.2 and 3.3. The mean pK_d and B_{max} values were found 9.40 ± 0.1 and 610 ± 36 respectively, expressed as mean \pm SEM. The B_{max} and pK_d was not significantly different than the respective values produced from CHO_{hMOP} cell membranes of figure 3.3 ($p>0.05$ by an unpaired Student's t -test).

3.4. Displacement binding assays

The binding of 3H -DPN and 3H -UFP-101 was displaced in a concentration-dependent manner by the respective reference ligands (endomorphin-1; EM1, natrindole, norbinaltorphimine; nBNI and nociceptin/orphanin FQ; N/OFQ) as seen in figure 3.5. Estimated receptor binding affinity values (pK_i) for all ligands used are shown in the inserted table.



	pK _i	
	UFP-505	Reference ligands
CHO _{hMOP}	7.79 ± 0.18	¹ 8.09 ± 0.15
CHO _{hDOP}	9.82 ± 0.06	² 9.82 ± 0.13
CHO _{hKOP}	6.29 ± 0.10	³ 8.80 ± 0.23
CHO _{hNOP}	5.86 ± 0.14	⁴ 9.07 ± 0.10

Figure 3.5. Displacement of tritiated diprenorphine (^3H -DPN) and ^3H -UFP-101 by UFP-505 and reference ligands at (A) CHO_{hMOP}, (B) CHO_{hDOP}, (C) CHO_{hKOP} and (D) CHO_{hNOP} cell membranes. Receptor binding affinities of UFP-505 and reference ligands (pK_i) were calculated using the Cheng-Prusoff equation and summarized in the inserted table. Fentanyl and morphine binding curves at CHO_{hMOP} (A) are included for comparison and their pK_i were found as 7.35±0.33 and 8.55±0.14 respectively (error bars in the figure are omitted for clarity). Data are mean ± SEM for n=5. Reference ligands: ¹ endomorphin-1 (EM1), ² naltrindole, ³ nor-binaltrophimine (nBNI), ⁴ nociceptin/orphanin FQ (N/OFQ).

UFP-505 displaced ^3H -DPN binding to MOP and DOP receptors with pK_i values of 7.79 and 9.82 ($n=5$) respectively. The pK_i of UFP-505 for the MOP receptor was similar to that of the endogenous ligand EM1 (8.09). Fentanyl and morphine binding curves were included in CHO_{hMOP} experiments for comparison (pK_i ; fentanyl 7.35, morphine 8.55).

The rank order pK_i of the four MOP agonists was *morphine* > *EM1* > *UFP-505* > *fentanyl*. For the DOP receptor the UFP-505 affinity was the same as that of the highly selective antagonist natrindole (9.82). The affinity for KOP and NOP receptors was negligible (<6.3). The rank order pK_i of UFP-505 for the opioid receptors was DOP >> MOP >> KOP > NOP.

3.5. GTP γ ^{35}S assays

Data for G-protein activation were expressed as percentage stimulation of GTP γ ^{35}S binding from basal (un-stimulated). Both UFP-505 and endomorphin-1 stimulated the binding of GTP γ ^{35}S to membranes prepared from CHO_{hMOP} cells, with similar efficacy values (stimulation of UFP-505 and EM1 was 128% and 129.3% respectively) and potency values (pEC_{50} of UFP-505 and EM1 was 6.37 and 6.38 respectively), as seen in figure 3.6A. At the DOP receptor (figure 3.6B), UFP-505 was essentially inactive as an agonist (6.2% stimulation at the highest concentration), where the reference ligand and full DOP agonist, DPDPE, stimulated GTP γ ^{35}S binding by 31.3% with a potency of 8.34 ($n=3$). The responses of our DOP cells were always found lower than those of MOP and this is in general agreement with laboratory data.

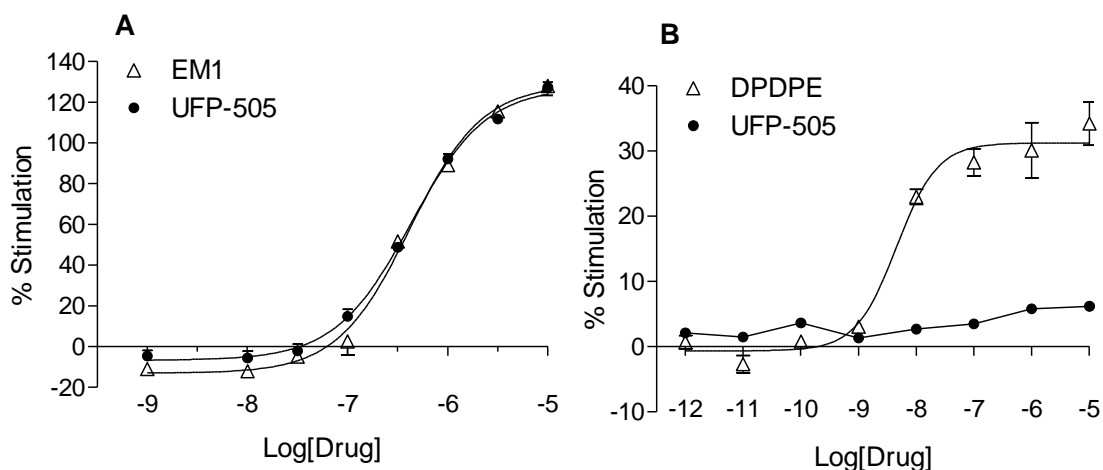


Figure 3.6. Effect of UFP-505 at MOP and DOP receptors. Ligand-mediated $GTP\gamma^{35}S$ binding was measured in membranes prepared from (A) CHO_{hMOP} and (B) CHO_{hDOP} cells. Data are presented as percentage stimulation of $GTP\gamma^{35}S$ binding from basal (unstimulated) and are represented as means \pm SEM of $n=3-5$ (data shown also in table 3.1). A Student's t -test revealed that the 6.2% stimulation shown at the 10 μ M UFP-505 (10^{-5} M) on CHO_{hDOP} membranes (panel B) was non-significant ($p>0.05$). EM1; endomorphin-1, DPDPE; [D-Pen²,D-Pen⁵]-enkephalin.

Based on previous work (McDonald *et al*, 2003) where increased receptor density results in differences in efficacy, the weak stimulation of DOP receptors by UFP-505 was probed further in a DOP cell line with higher receptor-density (denoted as $CHO_{hDOP/high}$ cell-line). $CHO_{hDOP/high}$ cells expressed an increased B_{max} of 1923 (compared to that of 1038 for CHO_{hDOP} , see inserted table in figure 3.3). Figure 3.7 presents the curves produced from a set of 5 independent experiments. The efficacy (E_{max}) and potency values (pEC_{50}) generated from figures 3.6 and 3.7 are shown collectively in table 3.1. There was a measurable agonist activity for UFP-505 in these high expressing cells. In addition, the response to DPDPE was not found significantly different (E_{max} CHO_{hDOP} 31.30 % and E_{max} $CHO_{hDOP/high}$ 49.50 %, $p>0.05$ by a t -test).

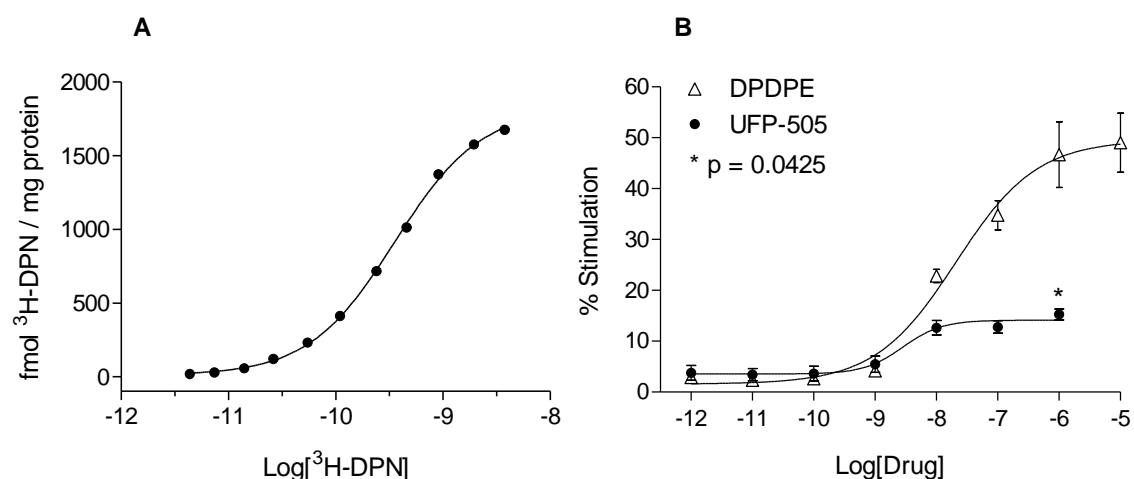


Figure 3.7. Panel A shows a representative curve of a single saturation experiment (from $n=3$) performed in CHO cells which expressed higher density of DOP receptors than those normally used ($CHO_{hDOP/high}$, B_{max} 1819 ± 33 , pK_d 9.49 ± 0.18). Panel B shows the effect of UFP-505 on G-protein stimulation at $CHO_{hDOP/high}$ cells, in similar conditions as to those in figure 3.6. Data are represented as means \pm SEM of $n=5$ (shown also in table 3.1). The 14.13% of stimulation shown for the top concentration of UFP-505 was found significant ($p<0.05$; t -test) compared to basal (unstimulated), indicating partial agonism for UFP-505.

	UFP-505		Reference ligands	
	pEC_{50}	E_{max} (%)	pEC_{50}	E_{max} (%)
CHO_{hMOP}	6.37 ± 0.04	128 ± 4.42	¹ 6.38 ± 0.06	¹ 129.3 ± 6.23
CHO_{hDOP}	-	6.20 ± 1.86	² 8.34 ± 0.13	² 31.30 ± 1.38
$CHO_{hDOP/high}$	8.54 ± 0.28	14.13 ± 0.95	² 7.68 ± 0.20	² 49.50 ± 3.51
$\alpha E_{max} CHO_{hDOP} = 19.80\%$				
$\alpha E_{max} CHO_{hDOP/high} = 28.50\%$				

Table 3.1. Efficacy (E_{max}) and potency values (pEC_{50}) for UFP-505 and reference ligands in the $GTP\gamma^{35}S$ binding assays (figure 3.6 and 3.7). E_{max} values are expressed as percentage stimulation of $GTP\gamma^{35}S$ binding from basal (un-stimulated) and are represented as are mean \pm SEM of $n=3-5$. $CHO_{hDOP/high}$ cells expressed higher DOP receptor density than CHO_{hDOP} cells, as seen in figure 3.3 and figure 3.7. αE_{max} percentages express the ratio of E_{max} -UFP-505/ E_{max} -reference ligand, for the same cell line. Keys: ¹ endomorphin-1 (EM1), ² [D-Pen²,D-Pen⁵]-enkephalin (DPDPE).

3.6. Antagonist affinity of UFP-505 in a $\text{GTP}\gamma^{35}\text{S}$ assay

The antagonist activity of a ligand (pK_b) can be calculated by analyzing the rightward shift of the concentration response curve of an agonist in a functional assay (i.e. $\text{GTP}\gamma^{35}\text{S}$ assay), after adding a fixed antagonist concentration. At CHO_{hDOP} cells, adding 10 nM of UFP-505 to DPDPE produced a parallel rightward shift in the concentration response curve (figure 3.8), yielding a pK_b value of 9.81. The pK_b value of UFP-505 was calculated using the formula $\text{pK}_b = -\log\{(\text{CR}-1)/[\text{UFP-505}]\}$, where CR is the ratio of the EC_{50} of DPDPE in the presence and absence of UFP-505. The pK_b value of UFP-505 is in agreement with the pK_i value determined in the ^3H -DPN binding assays (9.82; figure 3.5). However, this is not in agreement with the pEC_{50} in the $\text{CHO}_{\text{hDOP/high}}$ cells (8.54; table 3.1) since for a partial agonist the $\text{pK}_i = \text{pEC}_{50} = \text{pK}_b$. The low efficacy might have played a role in this observation.

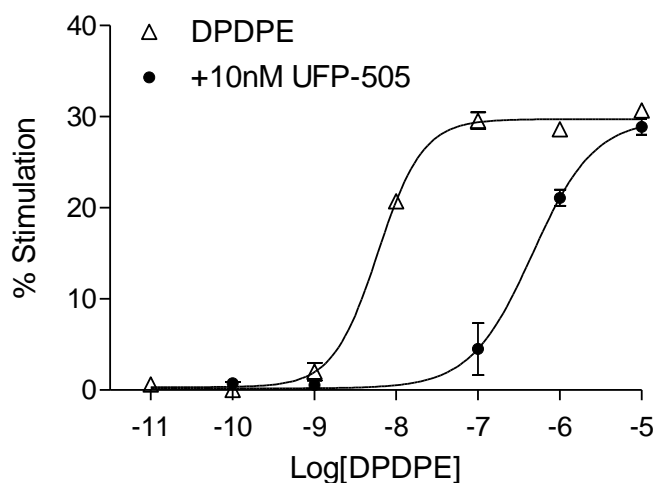
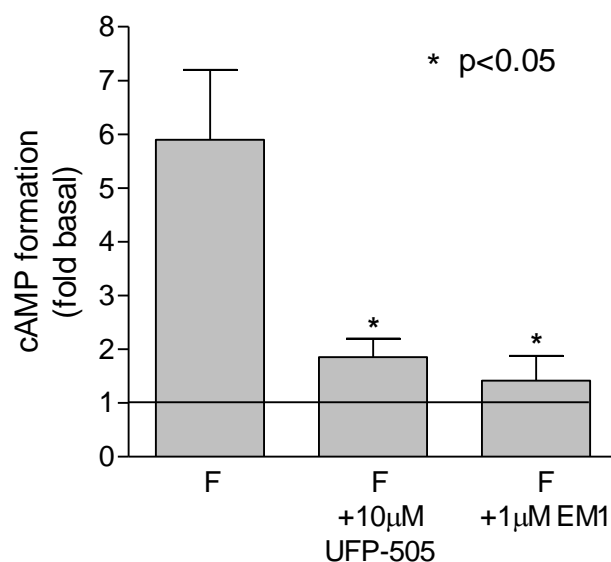


Figure 3.8. The effect of 10nM UFP-505 on DPDPE stimulation of G-protein activation at membranes from CHO_{hDOP} cells. The addition of UFP-505 shifts the agonist DPDPE (control) curve to the right (mean \pm SEM of 5 independent experiments). The pK_b of UFP-505 was found 9.81 ± 0.40 (mean \pm SEM). For comparison, the pK_b of naltrindole has been reported as 9.74 ± 0.04 (mean \pm SEM) in the literature (Feuerstein et al, 1996).

3.7. Inhibition of forskolin-stimulated cAMP formation

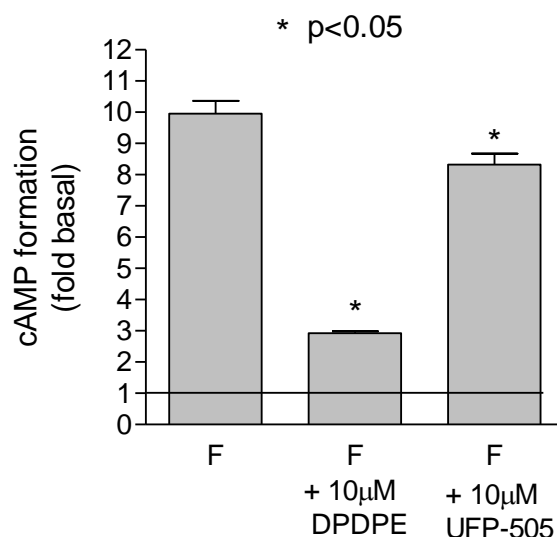
Ligand efficacy can be amplified by assessing functional activity ‘down-stream’ in the signal transduction cascade. We have utilised the adenylyl cyclase assay in this context. Forskolin activates adenylyl cyclase and increases intracellular levels of cAMP, inhibition of forskolin-stimulated cAMP formation by UFP-505 was studied in this assay. For CHO_{hMOP} cells, forskolin-stimulated cAMP inhibition was measured after the addition of 10µM UFP-505 and 1µM EM1 (figure 3.9). Forskolin stimulated cAMP formation which was inhibited by EM1 1µM (91.62%) and UFP-505 10µM (82.62%), as shown in table 3.2. There was no significant difference between these two ligands at saturating concentrations, indicating that UFP-505 behaves as a full agonist in this downstream amplified assay.

Measurements of cAMP formation in CHO_{hDOP} cells have shown that 10µM DPDPE inhibited forskolin-stimulated cAMP formation by 78.57%, as expected for a DOP full agonist (figure 3.10 and table 3.2). However, the addition of 10µM UFP-505 resulted in a small but significant inhibition of forskolin-stimulated cAMP (18.3%), suggesting that UFP-505 behaves as an ultra low efficacy DOP partial-agonist in this highly amplified assay (and agrees with the GTPγ³⁵S data).



	Forskolin	Forskolin + UFP-505	Forskolin + EM1
cAMP formation (fold basal)	5.89 ± 2.91	1.85 ± 0.76 *	1.41 ± 1.03 *

Figure 3.9. Effects of inhibition with UFP-505 and endomorphin-1 (EM1) on forskolin-stimulated (F) cAMP formation in CHO_{hMOP} cells. Data are presented as \pm SEM fold of basal stimulation ($n=5$). Percentage inhibition of cAMP is shown in table 3.2. *Significant ($p<0.05$) inhibition compared with forskolin-stimulated cAMP formation by repeated measurements in One-Way ANOVA with Bonferroni post-test. There was no significant difference between F+UFP-505 and F+EM1 stimulation.



	Forskolin	Forskolin + DPDPE	Forskolin + UFP-505
cAMP formation (fold basal)	9.96 ± 0.41	2.92 ± 0.06 *	8.32 ± 0.35 *

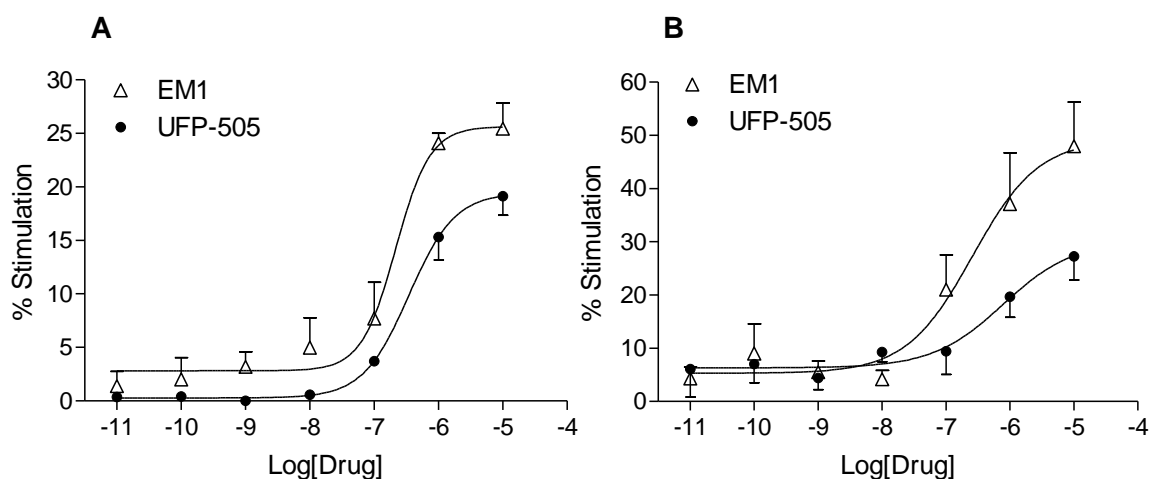
Figure 3.10. Effects of UFP-505 and DPDPE on forskolin-stimulated (F) cAMP formation in CHO_{hDOP} cells. Data are presented as ± SEM fold of basal stimulation (n=6). Percentage inhibition of cAMP is shown in table 3.2. *Significant (p<0.05) inhibition compared with forskolin-stimulated cAMP formation by repeated measurements in One-Way ANOVA with Bonferroni post-test.

	MOP		DOP	
	<i>F</i> + <i>EM1</i>	<i>F</i> + <i>UFP-505</i>	<i>F</i> + <i>DPDPE</i>	<i>F</i> + <i>UFP-505</i>
cAMP inhibition	91.62 %	82.62 %	78.57 %	18.30 %

Table 3.2. Percentages cAMP inhibition by UFP-505 and reference ligands based on forskolin-induced cAMP formation levels in CHO cells expressing MOP or DOP receptors. cAMP inhibition (reduction in cAMP levels) is opioid-receptor agonism. Percentages are translated from values in figures 3.9 and 3.10. All compounds were used at 10µM concentration and caused a significant inhibition compared to forskolin.

3.8. GTP γ ³⁵S assay in rat nervous tissue

In order to determine the efficacy and potency of UFP-505 in tissues expressing mixed opioid receptors at a variety of receptor densities, rat neuronal tissues (spinal cord and cerebral cortex) were used to perform a series of independent GTP γ ³⁵S assays. Figure 3.11 presents the curves produced in the rat spinal cord and frontal cortex. The pEC₅₀ and E_{max} values are shown in the inserted table. The pEC₅₀ and E_{max} of endomorphin-1 and UFP-505 were found to be similar for both tissues (no statistically significant difference). Data of the pharmacological *in vitro* characterization of UFP-505 presented in this section of the thesis are shown collectively in table 3.3.



	UFP-505		Endomorphin-1	
	<i>pEC</i> ₅₀	<i>E</i> _{max} (%)	<i>pEC</i> ₅₀	<i>E</i> _{max} (%)
Rat spinal cord	6.53 ± 0.15	19.46 ± 1.18	6.69 ± 0.21	25.60 ± 2.20
Rat cerebral cortex	6.11 ± 1.65	30.17 ± 9.88	6.59 ± 0.39	49.24 ± 9.07

Figure 3.11. Ligand-mediated GTP γ ³⁵S binding by UFP-505 and endomorphin-1 (EM1), measured in membranes prepared from (A) rat spinal cord and (B) rat cerebral cortex. Data are presented as percentage stimulation of GTP γ ³⁵S binding from basal (un-stimulated). Measured efficacy (*E*_{max}) and potency values (*pEC*₅₀) are shown in the inserted table (means ± SEM of *n*=3-4 independent experiments). Efficacy and potency values of UFP-505 showed no significant difference compared to the respective values of EM1 by paired student's *t*-test (*p*>0.05).

			UFP-505			Reference Ligands		
	pK_d	B_{max}	pK_i	pEC_{50}	E_{max} (%)	pK_i	pEC_{50}	E_{max} (%)
CHO_{hMOP}	¹ 9.52 ± 0.20	¹ 458 ± 110	7.79 ± 0.18	6.37 ± 0.04	128 ± 4.42	³ 8.09 ± 0.15	³ 6.38 ± 0.06	³ 129.3 ± 6.23
CHO_{hDOP}	¹ 9.29 ± 0.21	¹ 1038 ± 184	9.82 ± 0.06	-	6.20 ± 1.86	⁴ 9.82 ± 0.13	⁷ 8.34 ± 0.13	⁷ 31.30 ± 1.38
CHO_{hKOP}	¹ 9.50 ± 0.12	¹ 321 ± 59	6.29 ± 0.10	N	N	⁵ 8.80 ± 0.23	N	N
CHO_{hNOP}	² 8.92 ± 0.24	² 1054 ± 142	5.86 ± 0.14	N	N	⁶ 9.07 ± 0.10	N	N
CHO_{hMOP/whole cells}	¹ 9.40 ± 0.10	¹ 610 ± 36	N	N	N	N	N	N
CHO_{hDOP/high}	¹ 9.49 ± 0.18	¹ 1819 ± 33	N	8.54 ± 0.28	14.13 ± 0.95	N	7.68 ± 0.20	49.50 ± 3.51
Rat spinal cord			N	6.53 ± 0.11	19.50 ± 1.18	N	³ 6.69 ± 0.21	³ 25.6 ± 2.20
Rat cerebral cortex			N	6.11 ± 0.65	30.20 ± 9.88	N	³ 6.59 ± 0.39	³ 49.2 ± 9.10
gpI**			N	7.50 ± 0.01	N	N	⁸ 9.47 ± 0.03	N
mVD**			N	-	N	N	⁶ 8.07 ± 0.05	N
CHO_{hDOP} antagonism				pK_b 9.81 ± 0.19			pK_b ⁴ 9.74 ± 0.03 *	
mVD antagonism **				pA_2 9.15 ± 0.18			pK_b ⁹ 8.26 ± 0.07	
cAMP inhibition (MOP)				82.62%			⁴ 91.62%	
cAMP inhibition (DOP)				18.3%			⁷ 78.57%	

* (Feuerstein et al, 1996), ** S. Molinari, G. Calo and R. Guerrini, unpublished data

Table 3.3. Pharmacological profile of UFP-505 as presented in this thesis. Data are mean ± SEM. Agonist potency (pEC_{50}) is the negative logarithm of the agonist molar concentration that produces 50% of the maximal possible effect (E_{max}) of the agonist. Affinity (pK_i) is the negative logarithm of the agonist molar concentration that is required in order to bind 50% of the receptors present. Antagonist potency (pA_2 and pK_b) is the negative logarithm of the antagonist molar concentration that makes it necessary to double the agonist concentration in order to elicit the original response (pK_b ; when in the Schild equation the slope is assumed as unity). Dissociation constant of the radioligand is expressed as the negative logarithm of the molar concentration of the ligand in order to bind to 50% of the receptors. Receptor density (B_{max}) is expressed as the amount of protein per membrane unit (fmol/mg). gpI; guinea pig ileum, mVD; mouse vas deferens, N; not investigated. Reference ligands: ¹ [³H]-DPN, ² [³H]-UFP-101, ³ endomorphin-1, ⁴ naltrindole, ⁵ nor-binaltrophimine, ⁶ nociceptin/orphanin FQ, ⁷ [D-Pen², D-Pen⁵]-enkephalin, ⁸ dermorphin, ⁹ naloxone.

3.9. Discussion

The data show that UFP-505 has affinity for the MOP receptor comparable to the endogenous ligand endomorphin-1 and to agonists used in the clinic; morphine and fentanyl with a rank order: morphine>EM1>UFP-505>fentanyl (figure 3.5). UFP-505 displayed higher affinity at DOP receptor and was very weak at the KOP and NOP receptors.

In functional screens of GTP γ ³⁵S assays in CHO cells, UFP-505 was a full MOP agonist and failed to significantly stimulate the G-protein in CHO_{hDOP} cells (figure 3.6). In a study using CHO cells with 2x higher expression of DOP receptors than CHO_{hDOP} cells (CHO_{hDOP/high}), UFP-505 produced a weak stimulation and presented a partial-agonist profile (figure 3.7). Although the small increase in GTP γ ³⁵S binding seemed to vary with receptor density, it is in agreement with previously published values in the limited functional study of Balboni et al (Balboni *et al*, 2010) (UFP-505 E_{max} 6.8% \pm 1.8). Even though it is reassuring that the pK_b calculated at CHO_{hDOP} agrees with the pK_i estimated in radioligand displacement assays (figure 3.8), the stimulation in CHO_{hDOP/high} cells has raised concerns for a potentially masked residual agonist activity of UFP-505.

Subsequent functional screens downstream (cAMP assays) in CHO_{hMOP} and CHO_{hDOP} cells have confirmed that UFP-505 is a full agonist at the MOP receptor and shows a weak partial-agonist activity at the DOP receptor since it reduced forskolin-induced cAMP by 82.62% (figure 3.9) and 18.3% (figure 3.10) respectively. As discussed further below, there are additional data on UFP-505 by our collaborators that show an antagonist profile when tested *ex vivo* in rat tissues with abundant expressed DOP receptors. As a link between the simple and genetically pure CHO_{hMOP} and CHO_{hDOP}

preparations, we assessed functional activity ($\text{GTP}\gamma^{35}\text{S}$) in a relevant mixed opioid population; rat spinal cord and cerebrocortical membranes. We demonstrated efficacy lower than endomorphin-1, with higher E_{max} values of UFP-505 in the cortex than in cord (figure 3.11).

In this following section some *ex vivo* experiments performed by S. Molinari, G. Calo and R. Guerrini at the University of Ferrara in Italy are presented. Whilst the author of this thesis coordinated the analysis of the data, he did not perform these experiments and for these reasons these data are not included in the data section of this Chapter.

As an assessment of functional activity, we have produced additional data in the well characterized MOP rich guinea pig ileum (gpI) and the DOP rich mouse vas deferens (mVD) tissues, used as screening tools for UFP-505 (analytical methodology of the experiments shown in Appendix; Section A4). In the electrically stimulated gpI, we have shown that the selective MOP receptor agonist dermorphin inhibited the electrically induced twitches with a pEC_{50} of 9.47 (figure 3.12A). This effect was antagonized by the non-selective opioid antagonist naloxone (pEC_{50} 8.74, pK_b 8.64) and the MOP-selective antagonist CTOP (MOP antagonist pEC_{50} 8.07, pK_b 8.66). In the same preparation, UFP-505 inhibited the electrically-induced twitches in a similar manner, with a pEC_{50} of 7.50 (figure 3.12B). This effect was antagonized by naloxone (pK_b 8.80) and CTOP (pK_b 8.29). These data confirmed the full agonist behavior of UFP-505 in MOP-enriched native tissue.

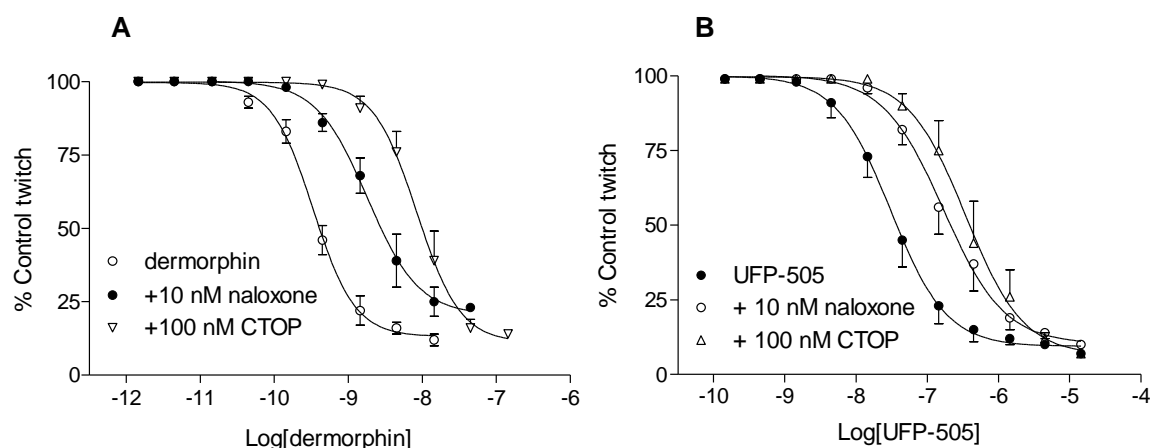


Figure 3.12. Effects of dermorphin and UFP-505 in the electrically stimulated guinea pig ileum (MOP receptor-rich), presented as percentage of control twitch in the absence and presence of 10nM naloxone and 100nM of the MOP-selective antagonist *D*-Phe-Cys-Tyr-D-Trp-Orn-Thr-Pen-Thr-NH₂ (CTOP). (A) The dermorphin curve was shifted to the right by naloxone and CTOP. (B) Similarly, the UFP-505 curve was shifted to the right by naloxone and CTOP. All Data are mean \pm SEM from at least 5 experiments.

Similarly, in the electrically-stimulated mouse vas deferens, DPDPE inhibited the electrically-induced twitches with a pEC_{50} value of 8.07, while addition of various concentrations of UFP-505 shifted the DPDPE curve to the right (figure 3.13A). In the same tissue, naloxone shifted the control DPDPE curve (pEC_{50} 8.23) to the right in a similar manner, with a pEC_{50} of 7.78 and a pK_b of 8.26 (figure 3.13B). The Schild analysis for UFP-505 produced an antagonist potency (pA_2) of 9.15 and a slope factor of 0.96 (± 0.04 , $r^2=0.992$) (figure 3.13C). These data showed a competitive antagonist profile for UFP-505 in a DOP-enriched native tissue. Additionally, the pEC_{50} for UFP-505 in gpI appears more potent than in CHO and rat tissues. This may result from the use of disrupted and well washed membranes in the receptor and $GTP\gamma^{35}S$ binding assays compared to the use of intact guinea pig tissue. This supposition might be correct based on the reasonably close agreement in the antagonist potency for this compound at

DOP (i.e., antagonist interaction should be unaffected by the presence/absence of any intracellular mediators). However, simple species differences might also be important.

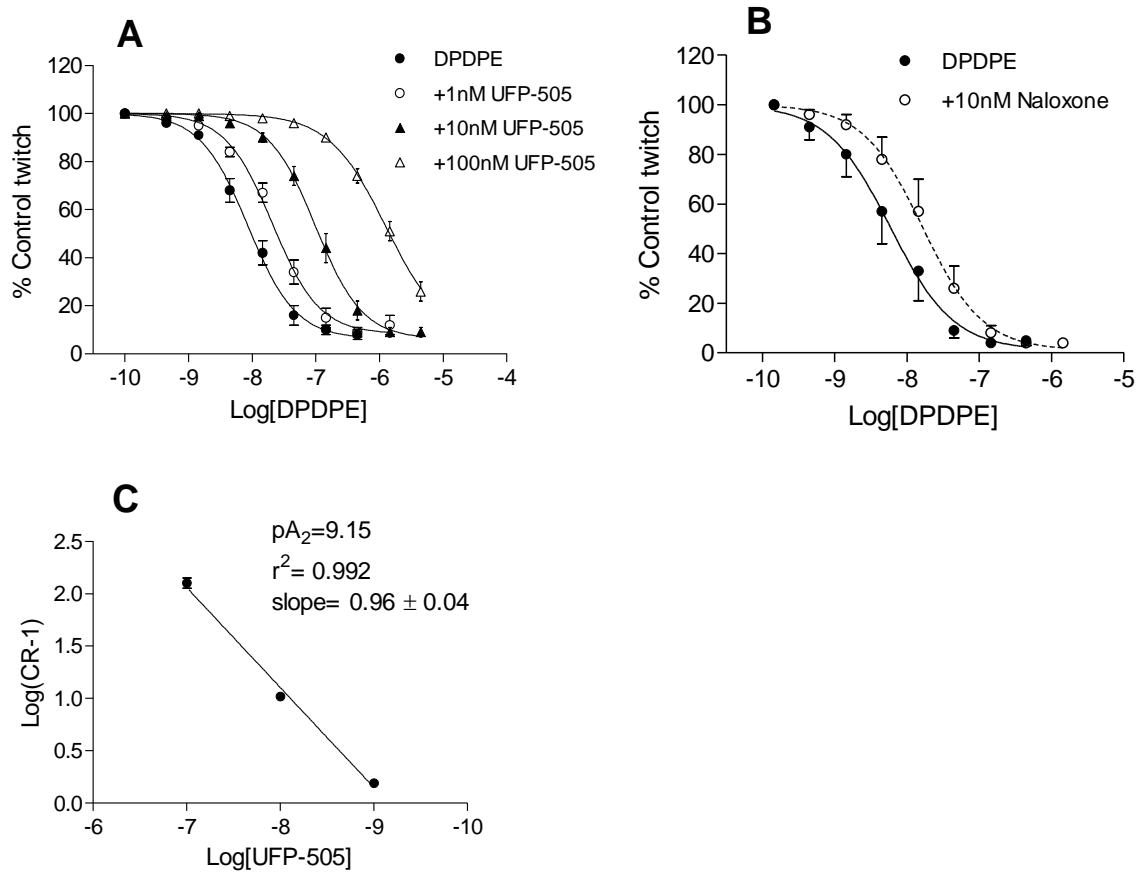


Figure 3.13. Effects of DPDPE in the electrically stimulated mouse vas deferens (DOP receptor-rich), in the absence and presence of increasing concentrations UFP-505 and 10nM naloxone. (A) The DPDPE curve is shifted in parallel to the right by increasing concentrations of UFP-505 (1, 10, 100 nM). (B) In a similar preparation, naloxone shifted the DPDPE curve to the right. Data for (A) and (B) are presented as percentage of control twitch. (C) Schild analysis of (A) produces a regression line with a slope of 0.96 ± 0.04 which represents competitive antagonism, whereas the extrapolation of the line when $y=0$ represents the antagonistic potency pA_2 (logarithmic) 9.15. All data were produced from at least 5 experiments for each preparation.

Collectively in these downstream functional assays, UFP-505 behaved as a MOP agonist (gpI) and a DOP antagonist (mVD). The antagonist affinity pA_2 was close to the pK_i and the pK_b determined for the human DOP receptor in a recombinant system (CHO_{hDOP}). From the above, it is doubtful that the partial agonism of UFP-505 seen in the high-expression recombinant model (CHO_{hDOP/high}) can occur at physiological conditions in a native tissue of the vas deferens, where the expression of opioid receptors is lower. To the best of the author's knowledge to date there are no studies that show partial agonism in a native system.

The data in this Chapter present a complete *in vitro* / *ex vivo* pharmacological characterization of UFP-505 in CHO cell lines stably expressing different recombinant opioid receptors and in native neuronal and contractile tissue. The results produced important information on the binding properties of UFP-505 and provide a platform for the following *in vitro* experiments that investigate the effect of UFP-505 binding on receptor internalization, presented in Chapter 4.

CHAPTER 4.
STUDIES OF OPIOID RECEPTOR INTERNALIZATION

Chapter 4. Studies of opioid receptor internalization

4.1. Introduction

Opioid receptor activation and trafficking has been extensively studied during the last twenty years. Opioid ligand binding to opioid receptors leads to the recruitment of specific kinases (GRKs) that phosphorylate the receptor. This phosphorylation increases the affinity of the receptor for β -arrestins and decreases the affinity of the receptor for its G-protein. The loss of ability of the receptor to connect to its effector system is termed 'receptor desensitization'. The activated and phosphorylated receptor is then internalized through endocytosis, assisted by the anchored β -arrestins (specifically β -arrestin-2). The internalized receptor can either return to the cell surface after dephosphorylation ('resensitization') or be degraded by enzymes ('down-regulation').

One of the main questions in opioid research has been the role of receptor internalization in analgesic tolerance. An initial hypothesis proposed that desensitization and internalization of opioid receptors directly contributed to analgesic tolerance (Chavkin & Goldstein, 1984). The observed reduction of agonist potency, manifested as a right-shift in the analgesic dose-response curve in tissue preparations of morphine-tolerant animals, was initially attributed to the reduction of the receptor reserve. A series of studies on β -arrestin-2 backed up this hypothesis. β -arrestin-2 knock-out mice showed high resistance to the development of morphine tolerance (Bohn *et al*, 2004; Bohn *et al*, 2000) after chronic treatment. Studies using small-interfering RNA (siRNA) to reduce β -arrestin-2 expression in animals also showed a reduction in tolerance to morphine after chronic exposure (Yang *et al*, 2011). A contradiction to this hypothesis was the fact that morphine was shown to induce only 10% MOP internalization in a

recombinant MOP expression system (Whistler *et al*, 1999). In the same study, morphine failed to induce detectable receptor phosphorylation above the constitutive level observed in cells incubated in the absence of agonist. So why/how does morphine induce tolerance if it fails to promote MOP internalization and phosphorylation?

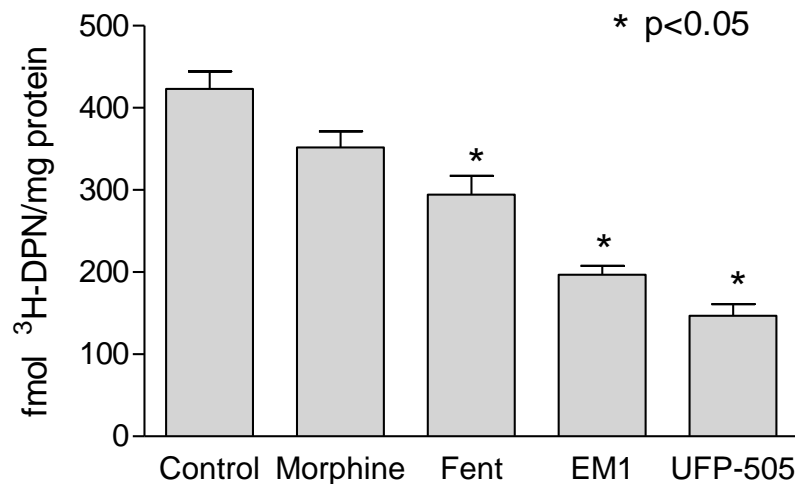
A different hypothesis for the role of receptor internalization has been postulated by the Whistler group: β -arrestin-mediated regulation of opioid receptors by endocytosis serves a protective role in reducing the development of drug tolerance (Whistler & von Zastrow, 1998). The initial hypothesis was based on the fact that receptor desensitization and internalization, with a subsequent enzymatic degradation, lead to receptor down-regulation that contributed to tolerance by decreasing the number of functional cell surface receptors. However, morphine-activated MOP receptors elude GRK phosphorylation, β -arrestin binding and desensitization, but failing to promote internalization (Qiu *et al*, 2003; Whistler & von Zastrow, 1998), in contrast to endogenous opioids and opioid drugs such as methadone (Keith *et al*, 1998). Thus it is unlikely that morphine tolerance is solely attributed to β -arrestin-mediated internalization and down-regulation of MOP receptors. Indeed, a number of early studies indicated that morphine failed to promote significant downregulation of MOP receptors even in analgesic tolerant animals (Lenoir *et al*, 1984; Simantov *et al*, 1984). The MOP agonist DAMGO was shown to promote MOP receptor internalization and pretreatment with a sub-analgesic dose reduces the development of morphine tolerance (He *et al*, 2002). Kim *et al*. demonstrated that if MOP endocytosis in response to morphine could be increased then it could reduce the development of tolerance in an animal model, suggesting that agonists that promote endocytosis of the MOP receptor might provide analgesics with reduced tolerance liability (Kim *et al*, 2008).

4.2. Aims

The aim of this chapter is to determine whether UFP-505 causes internalisation of MOP and DOP receptors expressed in CHO cells and how this particularly compares to morphine, as well as to other reference ligands.

4.3. UFP-505 induces internalization of recombinant MOP receptors expressed in CHO cells

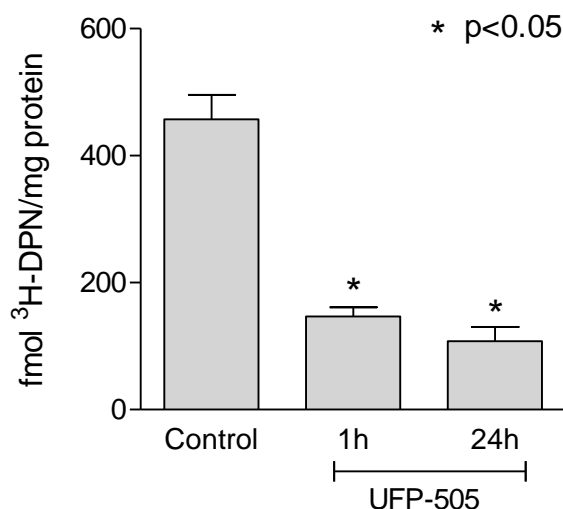
To examine if UFP-505 induces loss of cell surface receptors, pretreatment of CHO_{hMOP} cells with 10 μ M UFP-505 for 1h preceded the determination of the B_{max} by saturation binding assay with a saturating concentration of ³H-DPN. UFP-505 pretreatment produced a significant loss of MOP receptors (62.4%) as compared with non-treated cells (figure 4.1). In the same assay, pretreatment of CHO_{hMOP} cells with 10 μ M of EM1, fentanyl or morphine produced internalization of MOP receptors to differing levels. EM1 caused 49.6% receptor internalization, fentanyl produced 24.7%, whereas morphine did not produce any significant MOP receptor internalization.



CHO _{hMOP} pretreatment 1h	B _{max}	Internalization [†]
Control (untreated)	390.9 ± 26.9	-
10μM Morphine	351.8 ± 19.4	8 %
10μM Fentanyl	294.5 ± 22.8 *	24.7 %
10μM EM1	197.0 ± 10.6 *	49.6 %
10μM UFP-505	146.9 ± 14.1 *	62.4 %

Figure 4.1. MOP receptor density (B_{max} ; fmol $^3\text{H-DPN/mg protein}$) in $\text{CHO}_{h\text{MOP}}$ cells pretreated for 1h with various opioid ligands determined from binding assays with saturating radioligand concentration. Data are presented as mean \pm SEM from $n=5-7$. Receptor internalization (†) is presented as a percentage of control. The B_{max} values of all pretreated cells except morphine were significantly different from control (*; $p<0.05$), as shown by One-Way ANOVA with Bonferroni post test.

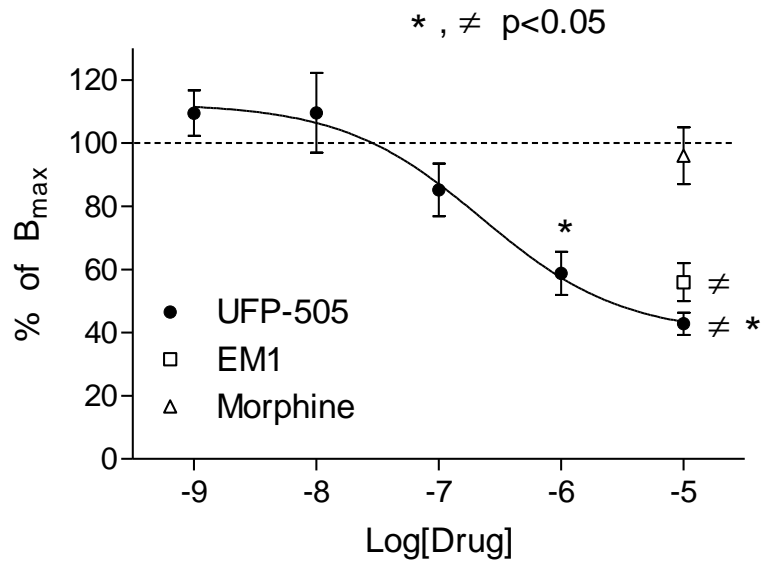
To determine whether the time of pretreatment of UFP-505 had an effect on the reduction of MOP receptors, binding assays with saturating radioligand concentration were performed after the pretreatment of $\text{CHO}_{h\text{MOP}}$ cells with 10μM UFP-505 for 1 hour and 24 hours (figure 4.2). Pretreatment of UFP-505 for 24 hours (76.47%) induced the internalization of MOP receptors in a similar manner as the pretreatment of UFP-505 for 1 hour (63.7%), this was not significantly different.



CHO_{hMOP}	B_{max}	Internalization [†]
Control (untreated)	457.3 ± 85.8	-
10µM UFP-505 1 hour	166.0 ± 15.1 *	63.70 %
10µM UFP-505 24 hours	107.6 ± 22.8 *	76.47 %

Figure 4.2. Receptor density (B_{max} , as fmol 3H -DPN/mg protein) of CHO_{hMOP} cells pretreated with 10µM UFP-505 for 1 hour and 24 hours produced from saturating concentration of radioligand. Data are presented as mean ± SEM from $n=5$. Receptor internalization (†) is presented as a percentage of control. B_{max} values of cells pretreated with UFP-505 1 hour and 24 hours were found significantly different ($p<0.05$) from the control, but not significantly different from each other, as shown by One-Way ANOVA analysis with Bonferroni post test.

The decrease in MOP receptor density induced by UFP-505 was concentration-dependent, as was shown after pretreatment of CHO_{hMOP} cells for 1 hour across different concentrations of UFP-505 (figure 4.3). UFP-505 induced a significant MOP receptor internalization at 10µM and 1µM compared to the control (untreated) B_{max} . The pEC_{50} of the internalization curve was 6.62. This is similar with the pEC_{50} produced from GTP $\gamma^{35}S$ binding (6.37) but was lower than the pK_i of UFP-505 (7.79).

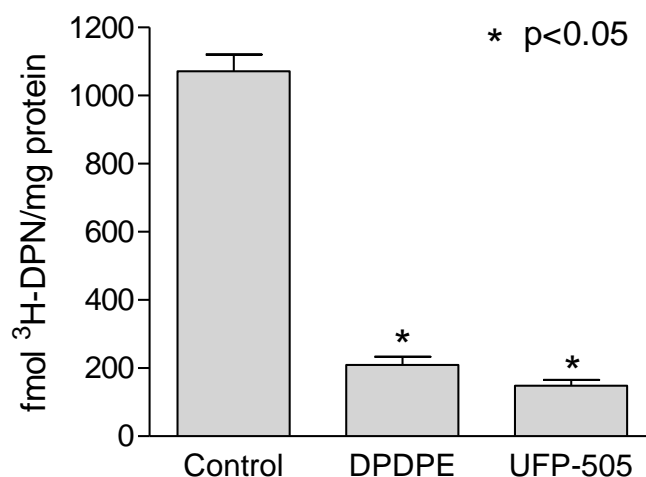


CHO _{hMOP} pretreatment 1h	Concentration (Log Molar)	B _{max} (% control)	Internalization (% control)
Control (untreated)	-	100	0
UFP-505	10μM (-5)	42.8 ± 3.5 * ≠	57.2 ± 3.5
UFP-505	1μM (-6)	58.8 ± 6.8 *	41.2 ± 6.8
UFP-505	100nM (-7)	85.2 ± 8.3	14.8 ± 8.3
UFP-505	10nM (-8)	109.6 ± 12.6	-9.6 ± 12.6
UFP-505	1nM (-9)	109.5 ± 7.2	-9.5 ± 7.2
EM1	10μM (-5)	56.0 ± 6.0 ≠	44.0 ± 6.0
Morphine	10μM (-5)	94.0 ± 6.0	6.0 ± 6.0

Figure 4.3. Internalization of MOP receptors after pretreatment of CHO_{hMOP} cells for 1 hour, with different concentrations of UFP-505, 10μM endomorphin-1 and 10μM morphine. UFP-505 internalizes the MOP receptor in a concentration-dependent manner. Data are presented as percentage mean ± SEM for n=5 and are normalized to a control (untreated) B_{max} (set to 100%). The pEC₅₀ of the internalization curve was found to be 6.62 ± 0.17. An analysis of variance (One-Way ANOVA with Bonferroni post test) revealed significant difference in the B_{max} at 1μM and 10μM UFP-505 when compared to that of control (*; p<0.05). Also, the 10μM UFP-505 and EM1 treated cells showed significant difference in their B_{max} (≠; p<0.05) when compared with that of 10μM morphine.

4.4. UFP-505 also induces internalization of recombinant DOP receptors expressed in CHO cells

As was discussed in Chapter 1 (1.1.6), receptor internalization has been linked to receptor activation and phosphorylation as part of the receptor trafficking mechanism. As shown in Chapter 3, although UFP-505 behaves as a DOP antagonist in native tissue (rat cortex and spinal cord) and recombinant systems (CHO_{hDOP}), it displays a very weak intrinsic activity in high receptor density models (i.e. $\text{CHO}_{\text{hDOP/high}}$). To examine whether UFP-505 induces loss of cell surface DOP receptors in a system where it behaves as a low efficacy partial agonist, CHO_{hDOP} cells were pretreated with 10 μM UFP- 505 for 1h prior to determining the B_{max} . Interestingly, UFP-505 10 μM induced extensive internalization of the DOP receptor in a similar manner to 10 μM of the DOP full agonist DPDPE (figure 4.4).



CHO_{hDOP}	B_{max}	Internalization [†]
Control (untreated)	1072 ± 49.28	-
10μM DPDPE 1 hour	209.7 ± 24.10 *	80.44 %
10μM UFP-505 1 hour	148.1 ± 17.62 *	86.19 %

Figure 4.4. Receptor density (B_{max} , as fmol $^3\text{H-DPN/mg protein}$) of CHO_{hDOP} cells pretreated with 10μM UFP-505 or 10μM DPDPE for 1 hour from binding assays with saturating concentration of radioligand. Data are presented as mean ± SEM from $n=5$. Receptor internalization ([†]) is presented as a percentage of control. The B_{max} values of pretreated cells with UFP-505 and DPDPE were found to be significantly different compared to the control (*; $p<0.05$) by analysis of variance (One-Way ANOVA with Bonferroni post test) and showed no significant difference between each other ($p>0.05$).

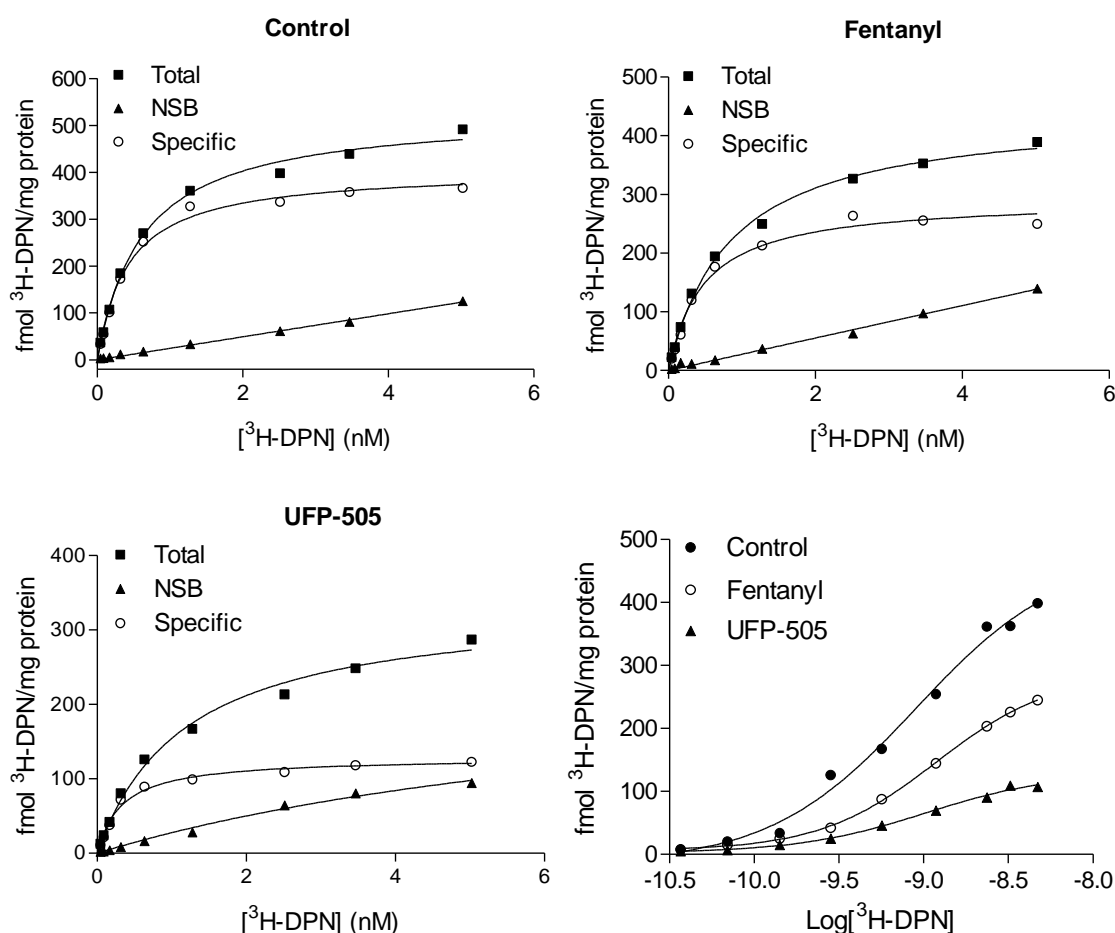
4.5. Full saturation curves after pretreatment of CHO_{hMOP} and CHO_{hDOP} cells with 10μM UFP-505 for 1 hour

The extensive internalization of DOP receptors seen by UFP-505 was unexpected. As the ligand possesses very weak intrinsic activity we suspected some internalization. An initial concern was that the reduction seen in receptor density after UFP-505 pretreatment could be due to incomplete wash off of the desensitising challenge. In order to exclude this possibility, full $^3\text{H-DPN}$ saturation curves were produced from

CHO_{hMOP} and CHO_{hDOP} cells pretreated with 10 μ M UFP-505 after wash off and the pK_d calculated. If the desensitizing UFP-505 challenge was still present in the assay, it would be reflected to a change in the pK_d of the saturation isotherm (as a rightward shift).

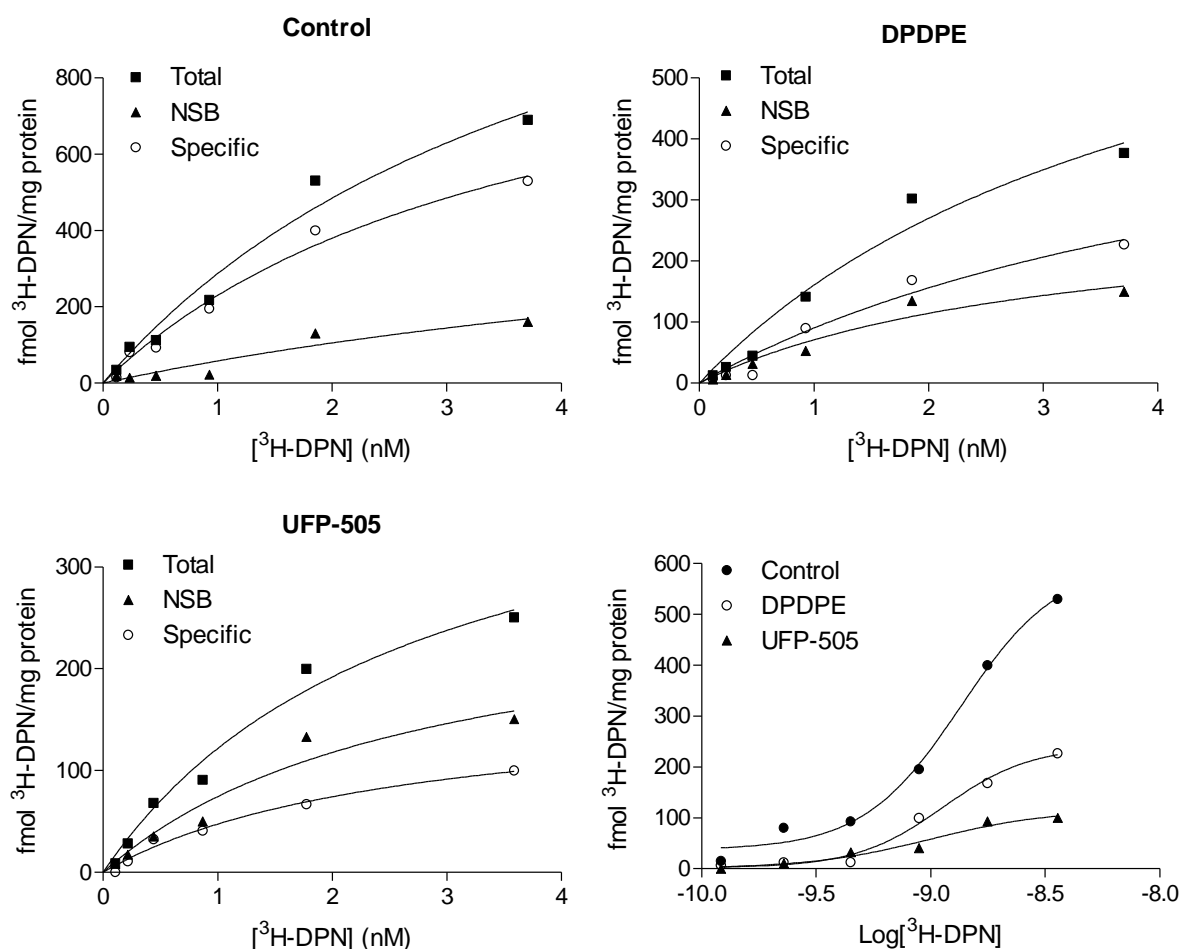
Figure 4.5 shows representative saturation curves from a series of five independent experiments performed in CHO_{hMOP} cells after pretreatment with 10 μ M UFP-505 and 10 μ M fentanyl. The pK_d of the curves produced from all pretreatment groups were not different from the control indicating that the reduced radioligand binding interpreted as a reduction in the B_{max} is attributed solely to the internalization of MOP receptors and not to the presence of residual UFP-505 in the assay.

Similarly, figure 4.6 shows representative saturation curves from a series of five independent experiments performed in CHO_{hDOP} cells after pretreatment with 10 μ M UFP-505 and 10 μ M DPDPE. The pK_d of the curves produced from all pretreatment groups did not differ from the control. The same consistency in pK_d, as seen as in the CHO_{hMOP} cells, indicates that the reduction in the B_{max} is attributed to the internalization of DOP receptors and not to the presence of residual UFP-505 in the assay.



(n=5) CHO _{hMOP}	B _{max}	³ H-DPN pK _d
Control (untreated)	378.5 ± 62.9	9.14 ± 0.09
10μM fentanyl	246.8 ± 29.2 ^α	9.14 ± 0.10
10μM UFP-505	120.0 ± 12.3 ^{α, β}	9.03 ± 0.07

Figure 4.5. Internalization of MOP receptors as a reduction in the B_{max} (fmol ³H-DPN/mg protein) in full saturation binding curves of CHO_{hMOP} cells pretreated with 10μM fentanyl or 10μM UFP-505. Representative hyperbola and sigmoidal saturation curves shown from $n=5$ experiments (data presented as mean ± SEM in the inserted table). The B_{max} value of drug-treated cells was significantly lower (α ; $p<0.05$) compared to the control by an analysis of variance (One-Way ANOVA with Bonferroni post test), whereas the B_{max} of the UFP-505 treated cells was shown to be significantly lower to that of the fentanyl treated cells (β ; $p<0.05$). The same analysis has shown no significant differences in the pK_d between all groups.



(n=5) CHO_{hDOP}	B_{max}	$^3\text{H-DPN } pK_d$
Control (untreated)	655 ± 145.7	9.05 ± 0.08
10 μM DPDPE	223.7 ± 60.1 *	8.90 ± 0.04
10 μM UFP-505	105.1 ± 15.4 *	9.05 ± 0.03

Figure 4.6. Internalization of DOP receptors as a reduction in the B_{max} (fmol ^3H -DPN/mg protein) in full saturation binding curves of CHO_{hDOP} cells pretreated with 10 μM DPDPE or 10 μM UFP-505. Representative hyperbola and sigmoidal saturation curves shown from $n=5$ experiments (data presented as mean \pm SEM in the inserted table). The B_{max} values of both drug-treated cells were significantly lower (*; $p < 0.05$) compared to the control by an analysis of variance (One-Way ANOVA with Bonferroni post test), whereas the B_{max} of UFP-505 treated cells was shown not to be significantly different compared to that of DPDPE-treated cells. The same analysis has shown no significant differences in the pK_d between all groups.

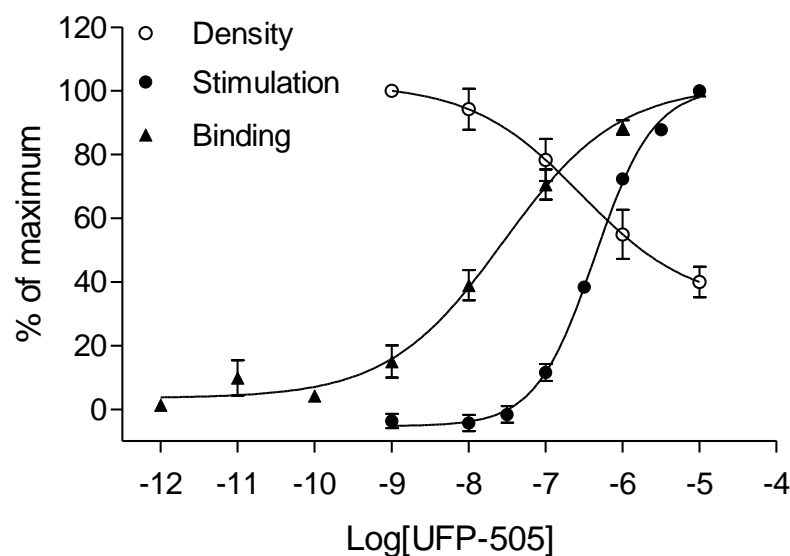
4.6. Discussion

The data presented here show that UFP-505 causes internalization of the human MOP and DOP receptors in CHO cells with the degree of internalization at the latter being a little unexpected. After 1h pretreatment, UFP-505 induced MOP receptor internalization at 62.4% (figure 4.1), which was higher than endomorphin-1 (49.6%) and fentanyl (24.7%). In the same preparation, morphine failed to induce significant internalization of the MOP receptor. These data are in agreement with data in the literature showing induction of MOP receptor internalization by endomorphin-1 (McConalogue *et al*, 1999; Song & Marvizón, 2003) and failure by morphine (Groer *et al*, 2007; Kim *et al*, 2008; McPherson *et al*, 2010; Whistler *et al*, 1999).

The 24h pretreatment of cells with UFP-505 did not increase MOP receptor internalization when compared to the 1h pretreatment (figure 4.2). Although most studies in the literature that have looked at opioid receptor internalization have used individual varying times of agonist treatment (i.e. 10min, 30min, 1h), to the best of the author's knowledge there are no studies so far that looked at the effect of incubation time on receptor internalization (i.e. using two or more incubation times). As discussed in the Chapter 1, receptor internalization is often linked with receptor recycling to the cell surface or receptor degradation by enzymes. However, the exact fate of the internalized receptors in this experiment or the time-scale of these cellular mechanisms are unknown and therefore the lack of difference between the 1h and 24h incubation could mean that the receptors internalized after 1h incubation do not recycle back to the surface. However, it is also possible that during the 24h of drug incubation some receptors may have internalized, recycled back to the surface and internalized again, which could also explain the similarity in receptor density for both incubation times.

In this Chapter it is also shown here that the internalization of the MOP receptor by UFP-505 is concentration-dependent (figure 4.3), causing significant internalization compared to control at 1 μ M and 10 μ M, but not for 1, 10 and 100nM. UFP-505 at 10 μ M induced 57.2% receptor internalization, whereas 10 μ M morphine induced only 6%. Also, the lack of difference between the pEC₅₀ values of the UFP-505 curves produced from the GTP γ ³⁵S assays (table 3.1, Chapter 3) and receptor internalization (figure 4.3) suggests that there is no amplification between receptor trafficking and G-protein activation.

Figure 4.7 illustrates collectively the relationship between changes in MOP receptor density, receptor binding and stimulation of GTP γ ³⁵S (taken from figures 3.5, 3.6 and 4.3). Data were normalized to the maximum observed. A leftward shift from the binding curve would be indicative of amplification, but this is not the case. Differences in the buffers or reagents used in these three different assays could possibly explain this absence of amplification.



Graph curve	Observation	Value (in CHO _{hMOP})
Density	Receptor internalization	pEC ₅₀ 6.62 ± 0.17
Stimulation	G-protein stimulation	pEC ₅₀ 6.37 ± 0.04
Binding	Radioligand displacement	pK _i 7.79 ± 0.18

Figure 4.7. Concentration-response relationship for internalization, $GTP\gamma^{35}S$ and displacement binding assays in CHO_{hMOP} cells, normalized to their maximum (taken from figures 3.5, 3.6 and 4.3). The figure illustrates that there is no amplification (shown as an absence of a leftward shift from the binding curve).

DOP receptor internalization by 10 μ M UFP-505 was profound (86%) and was not significantly different to that caused by 10 μ M DPDPE (80%). The possibility that UFP-505 was not washed off properly from the assay prior to the estimation of B_{max}, (thus causing reduction in B_{max}), was excluded for both MOP and DOP receptors by the full saturation data produced (figures 4.5 and 4.6), where the pK_d of 3H -DPN was shown not to be different from the control, both in CHO_{hMOP} and in CHO_{hDOP} cells.

Also, it has been previously shown that UFP-505 behaves as a DOP antagonist *ex vivo* (figure 3.13) and as a DOP weak partial agonist in the high density recombinant model (CHO_{hDOP/high}; figure 3.7), in addition to its weak ability to inhibit cAMP formation in CHO_{hDOP} cells (figure 3.10). Although the mechanisms of DOP receptor internalization have been studied and presented in the literature (Eisinger & Schulz, 2005; Zhang *et al*, 2005) and the ability of DPDPE to internalize the DOP receptor is also documented (Bradbury *et al*, 2009), the functional properties of UFP-505 at the DOP receptor cannot fully explain its ability to promote substantial DOP receptor internalization to a similar extent as that of a full DOP agonist such as DPDPE (since the internalization study used the CHO_{hDOP} cells and not the CHO_{hDOP/high} cells). Bradbury and colleagues (Bradbury *et al*, 2009) were able to demonstrate DOP receptor phosphorylation and internalization by DPDPE, even after pretreatment with pertussis toxin, which has the ability to prevent G-protein coupling to the receptor. They have therefore proposed the existence of an alternative, G-protein-independent, internalization pathway. If this pathway really exists and even possibly co-exists with the G-protein dependent internalization mechanism, then this could explain the ability of a high-affinity/low efficacy ligand at the DOP receptor such as UFP-505 to promote profound DOP receptor internalization.

The inability of morphine to internalize the MOP receptor in transfected cells has been well documented in the literature, as previously described, and although there are some contradictory hypotheses made for the role of MOP receptor internalization in analgesic tolerance (which are discussed in Chapter 8 – General Discussion), the data in this thesis show that UFP-505 behaves differently to morphine in terms of its ability to affect MOP receptor trafficking. This is the first reported study that shows internalization of two distinct opioid receptors (MOP and DOP) by a single bifunctional

opioid ligand (UFP-505), as well as a substantial internalization of an opioid receptor (DOP) by a ligand that behaves as a weak partial agonist in the assay studied. These data form the basis for further internalization studies with UFP-505 in a double-expression recombinant system (MOP & DOP), as well as in native neuronal tissue, which will be presented and discussed in the following chapters.

Before further examination of the way that UFP-505 affects receptor trafficking when different types of opioid receptors are present, it is important to investigate the potential antinociceptive effect of UFP-505 *in vivo* in order to establish a link between its molecular properties and its biological effect.

CHAPTER 5.

***IN VIVO* CHARACTERIZATION OF UFP-505 IN RATS**

Chapter 5. *In vivo* characterization of UFP-505 in rats

5.1. Introduction

A number of studies have shown that when inhibiting or depleting the DOP receptor with simultaneous activation of the MOP receptor, the resulting analgesia is accompanied with reduced analgesic tolerance (Abdelhamid *et al*, 1991; Fundytus *et al*, 1995; Hepburn *et al*, 1997; Kest *et al*, 1996; McNaull *et al*, 2007; Nitsche *et al*, 2002; Zhu *et al*, 1999). Combining MOP agonism and DOP antagonism in a single compound may produce additional benefits *in vivo* when compared to individual administration of two drugs, in terms of pharmacokinetic/pharmacodynamic effects.

In Chapter 3, it was shown that UFP-505 is a bifunctional opioid ligand, exhibiting full MOP receptor agonism and DOP receptor weak partial agonism. However, no previous animal work has been carried out with UFP-505 and this is the first attempt to gather *in vivo* data that will be useful for further studying this novel bifunctional opioid and bifunctional opioids as a class. Preliminary work in mice (Rizzi and Calo, unpublished data) has shown evidence of low bioavailability for UFP-505. For this reason, these studies have been conducted using solely intrathecal (i.t.) injections as the administration method of UFP-505 and reference ligands.

5.2. Aims

The aim of this chapter was to determine the effects of intrathecal (i.t.) UFP-505 in Wistar albino rats. More specifically, the objectives of this chapter were: 1) to determine the levels of analgesia from acute administration of UFP-505 and the analgesic tolerance profile of UFP-505 after subchronic i.t. administration in a tail-flick

assay and 2) to determine the analgesic tolerance of subchronic s.c. morphine in a hot-plate assay.

5.3. Acute intrathecal administration of UFP-505 produces analgesia: acute administration.

In order to obtain a preliminary analgesic profile of i.t. UFP-505 and determine the effective concentrations to be used in later experiments, the effect of acute i.t. administration of 10 nmol and 50 nmol i.t. UFP-505 was studied in a tail-flick assay and latency periods were recorded at different time intervals until 120 minutes after drug administration.

UFP-505 10 nmol i.t. reached the cut-off time at 30 min until 90 minutes after administration and retained a high degree of analgesia until 120 minutes (figure 5.1). UFP-505 50nmol i.t. reached the cut-off time of 15 seconds throughout the study (not shown in figure 5.1; see figure 5.2). This experiment indicated that the concentration of 10 nmol UFP-505 was most appropriate for use in later experiments.

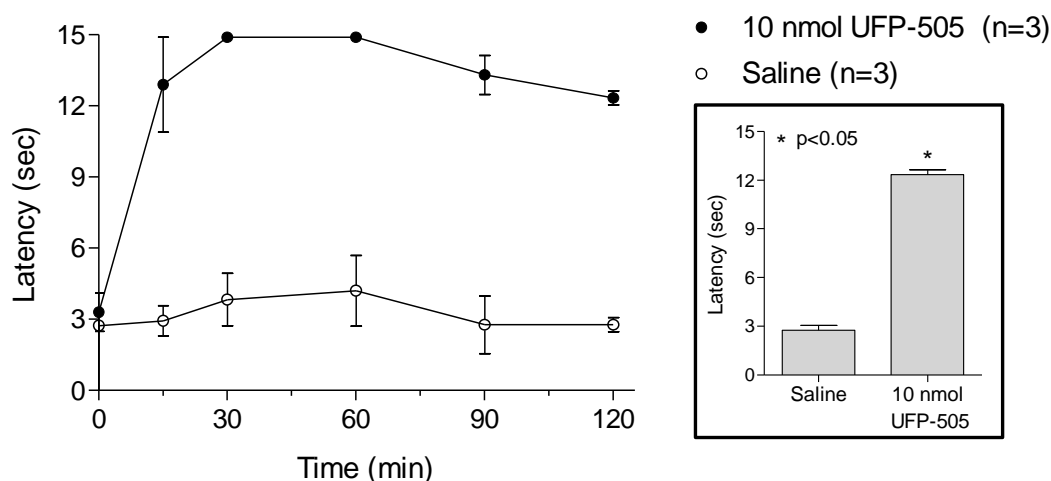


Figure 5.1. Analgesic profile of intrathecal UFP-505 10 nmol (i.t.) in rats using a tail-flick assay (left panel) compared to saline treated animals (control). The latency recorded prior to the administration of drugs (time=0 minutes) was the animal's basal analgesic latency. The latency of tail withdrawal at 120 minutes after injection with UFP-505 10 nmol showed a mean time of 12.33 sec which was significantly different that the control (unpaired Student's *t*-test; $p < 0.05$). Data presented as mean \pm SEM from 3 animals per group. In this experiment 50nmol UFP-505 was also included but is not shown as the cut-off (15sec) was recorded at all time points.

After identifying an analgesic effect of UFP-505 10 nmol, a dose response curve to i.t. UFP-505 was constructed in order to determine the dose that was equipotent to 10nmol morphine. The establishment of equipotent doses will be used in the subchronic experiments in order to compare the analgesic tolerance profiles of the two compounds.

UFP-505 1 and 3 nmol (i.t.) did not exhibit analgesia, as seen in figure 5.2 (non-significant compared to saline by One-Way ANOVA with Bonferroni post test). Morphine 10 nmol (i.t.) produced a similar analgesic profile to UFP-505 10 nmol (i.t.), which was not significantly different from 15 minutes until 90 minutes after injection. However, morphine analgesia was reduced when recorded at 120 minutes after injection (significantly lower than UFP-505 10 nmol by the same statistical analysis as above).

The equipotency of UFP-505 and morphine 10 nmol was assessed by the analgesic effect of the two compounds immediately after injection (*first recorded time; 15 minutes*). These concentrations were used in the subchronic experiments that followed to compare their analgesic tolerance profile.

An analysis of the time-latency curve (AUC) derived from figure 5.2, revealed that the overall analgesic profile of acute morphine 10nmol was not significantly different (figure 5.3A) when compared with UFP-505 10nmol and 50nmol, although they were all significantly different from control (One-Way ANOVA with Bonferroni post test). In addition to this, the analgesic profiles of UFP-505 1, and 3 nmol were not significantly different from control (by same statistical analysis). Dose-response curves of the latency at 120min and the overall analgesic profile (AUC) are shown in figure 5.3B, and the EC₅₀ values calculated for each curve were found to be very similar (6.27 and 6.38 nmol respectively).

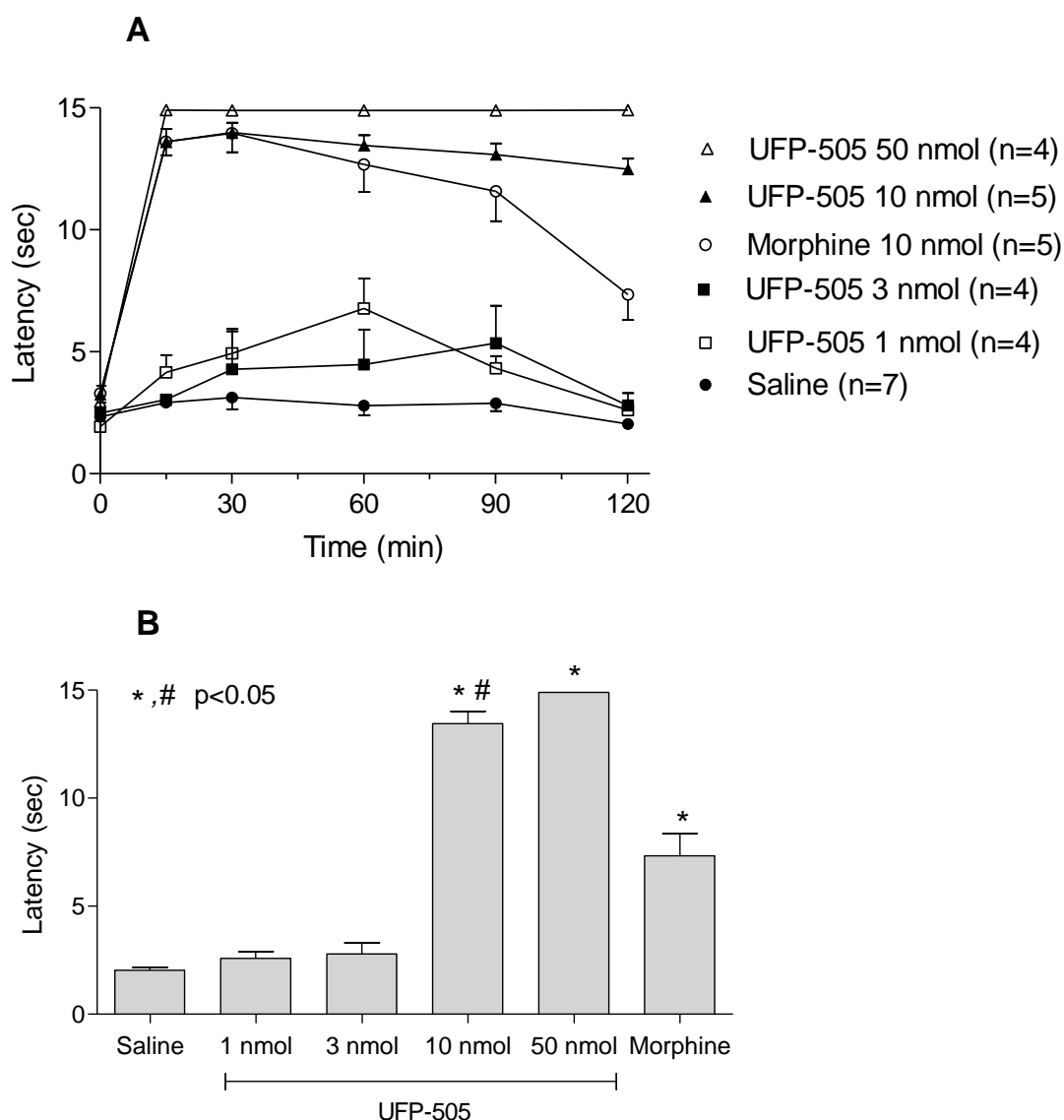


Figure 5.2. (A) Analgesic profile of acute intrathecal UFP-505 (10, 3, 1 nmol) and morphine 10 nmol administration in rats in a tail-flick assay. The data from UFP-505 50nmol were used from separate experiment for comparison. (B) The latency recorded after 120 minutes of injection for 10 nmol and 50 nmol UFP-505 as well as for 10 nmol morphine were significantly higher than control (*; $p < 0.05$), whereas UFP-505 10 nmol was significantly different from morphine 10 nmol (#; $p < 0.005$) as determined by One-Way ANOVA with Bonferroni post test. Data presented as mean \pm SEM from n=4-7 animals.

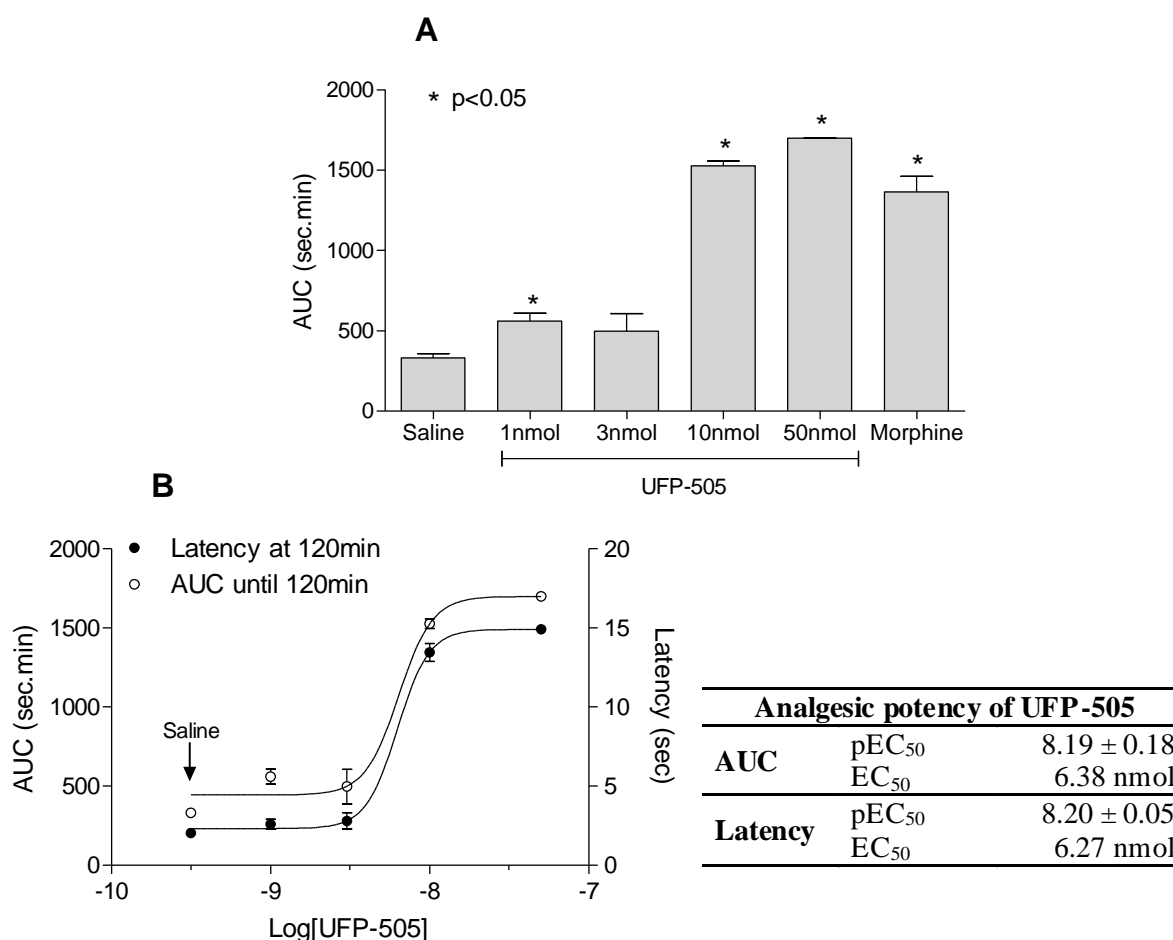


Figure 5.3. (A) Area under the curve (AUC; sec/min) estimated from the curves in figure 5.2A after acute administration of saline, 10 nmol morphine and UFP-505 (1, 3, 10 and 50 nmol). Morphine, UFP-505 (1, 10 nmol and 50 nmol) showed significant difference (*; $p < 0.05$, One-Way ANOVA with Bonferroni post test) compared to saline treated animals, whereas there was no significant difference between morphine 10 nmol and UFP-505 10 nmol. (B) The effect of different doses of UFP-505 from figure 5.2A, expressed as dose-response curves for latency after 120min (closed circles) and AUC (open circles). The analgesic potency of UFP-505 from these curves is shown in the inserted table, expressed as EC₅₀ and pEC₅₀. Data presented as mean ± SEM from $n = 4-7$ animals.

5.4. Subchronic intrathecal administration of UFP-505 10 nmol does not produce tolerance when compared to morphine 10 nmol.

Subchronic treatment (5 days; once per day) with UFP-505 10 nmol and morphine 10 nmol was examined in the tail-flick assay, in order to determine analgesic tolerance. I.t. administration of naltrindole 10 nmol (DOP antagonist) followed by morphine 10 nmol was also used as an additional treatment group. Analgesia was recorded at day 1, 3 and 5. Figure 5.4 shows the analgesic profile produced at day 1. The naltrindole/morphine group exhibited a similar analgesic profile to that of UFP-505 10nmol and morphine 10nmol, as seen by a non-significant difference of AUC analysis by One-Way ANOVA with Bonferroni post test (figure 5.4B).

Figure 5.5 shows the latencies at the first (15min) and the last (120min) recording of analgesic levels at Day 1 of the subchronic study. Although after 15 minutes all treated groups exhibited analgesia that was not-significantly different between each other, at 120 minutes the latency of the UFP-505 and the naltrindole+morphine groups were found significantly higher than those of morphine (#; $p < 0.05$ by One-Way ANOVA with Bonferroni post test).

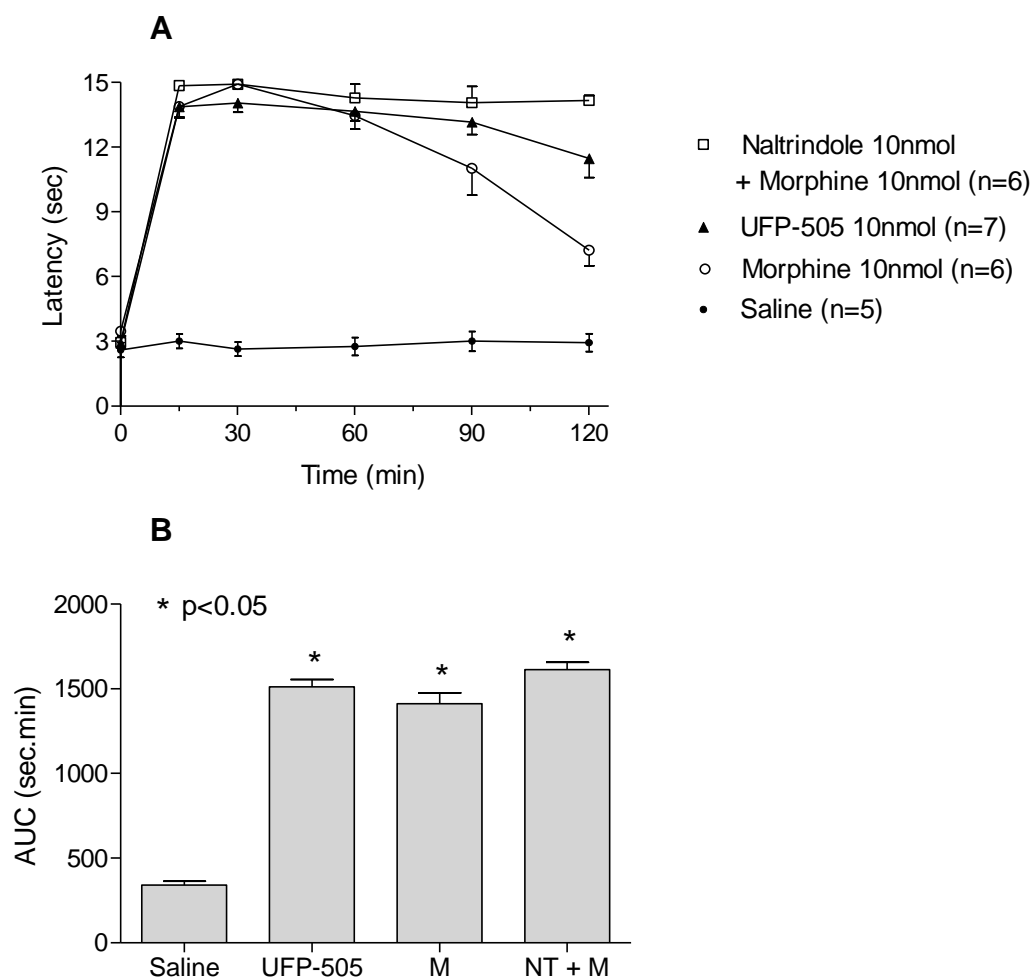


Figure 5.4. (A) Analgesic profile at day 1 of subchronic treatment with UFP-505, morphine (M) and naltrindole (NT) + morphine in rats in a tail-flick assay. (B) Area under the curve (AUC; sec/min) from curves in A. All treated groups showed significant difference in their analgesic profiles compared to saline treated animals (*; $p < 0.05$ by One-Way ANOVA with Bonferroni post test), and there were no significant differences between UFP-505 and the other two treatment groups. Data presented as mean \pm SEM from $n=5-7$ animals per group.

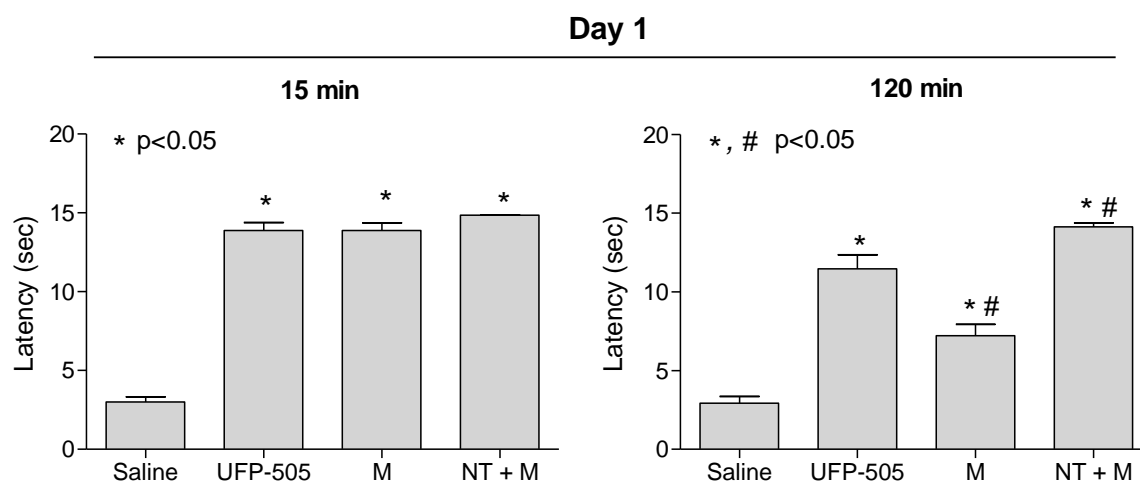


Figure 5.5. Latencies (sec; tail-flick) of treated animals from figure 5.4, as recorded after 15 minutes (left) and 120 minutes (right) after intrathecal administration at day 1 of the subchronic treatment course. For both time intervals, all treated groups showed significant analgesia compared to control (saline) animals, (*; $p < 0.05$ by One-Way ANOVA with Bonferroni post test). At 15 minutes after injection there was no significant difference in latencies between the groups. However, after 120 minutes, the morphine group showed significantly lower latencies than UFP-505 treated animals and the naltrindole + morphine group showed significantly higher latencies than UFP-505 (#; $p < 0.05$ by One-Way ANOVA with Bonferroni post test). Data presented as mean \pm SEM from $n = 5-7$ animals per group.

At Day 3 of the subchronic study the analgesic profile of UFP-505 remained unchanged throughout the assay, exhibiting high levels of antinociception (figure 5.6). In contrast, both the morphine and the naltrindole+morphine groups showed reduced analgesia from the early phases of the assay (15min). The analgesia produced as assessed by AUC analysis (figure 5.6B) showed that UFP-505 exhibited significantly higher analgesia compared to that of the morphine and the naltrindole+morphine groups (#; $p < 0.05$ by One-Way ANOVA with Bonferroni post test). As mentioned in Chapter 2 - General

Methods and will be further analyzed in the discussion below, the n numbers in the subchronic experiment were gradually reducing due to catheter removal.

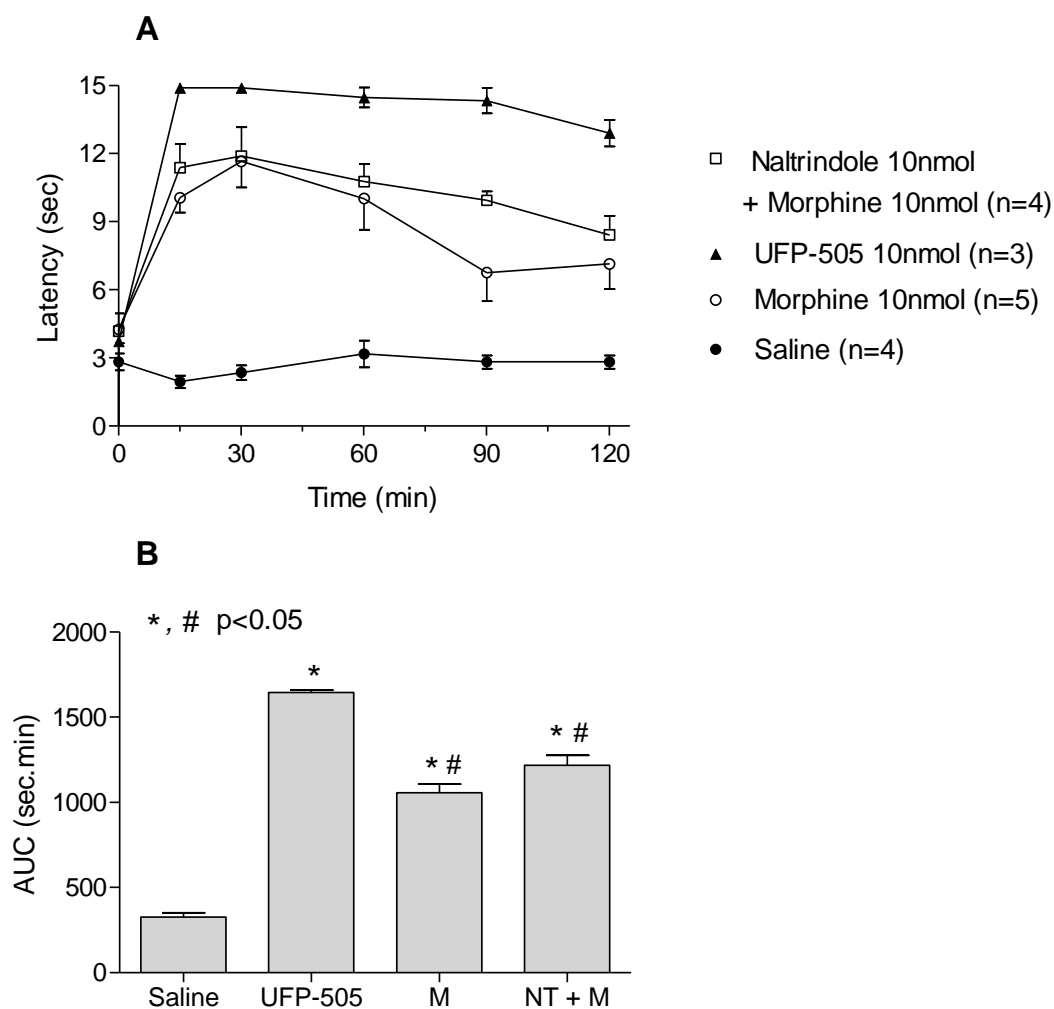


Figure 5.6. (A) Analgesic profile at day 3 of the subchronic treatment of UFP-505, morphine (M) and naltrindole (NT) + morphine in rats in a tail-flick assay. (B) Area under the curve (AUC; sec/min) from curves in A. All treated groups showed significant difference in their analgesic profiles compared to saline treated animals (*; $p < 0.05$ by One-Way ANOVA with Bonferroni post test). Additionally, the morphine and the naltrindole + morphine groups had significantly lower analgesia (#; $p < 0.05$ by One-Way ANOVA with Bonferroni post test) than the UFP-505 treated animals. Data presented as mean \pm SEM from $n=3-5$ animals per group.

Figure 5.7 presents the latencies at the first (15min) and the last (120min) recording of analgesia at Day 3 of the subchronic study. Firstly, 15 minutes after injection all treated groups exhibited higher analgesia when compared to saline, and UFP-505 exhibited higher analgesia when compared to the other two groups (#; $p<0.05$ by One-Way ANOVA with Bonferroni post test). Secondly, 120 minutes after injection, UFP-505 latency remained higher than both of the other groups (#; $p<0.05$ by the same statistical test), and the response of morphine treated animals reached statistical significance when compared to saline treated animals. Naltrindole inclusion facilitated morphine analgesia at this time.

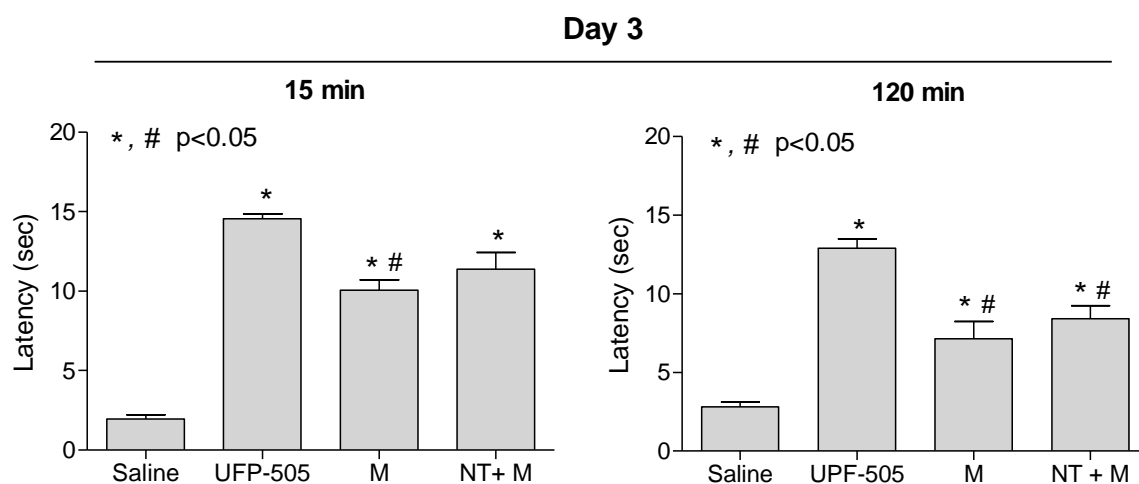


Figure 5.7. Latencies (sec; tail-flick) of treated animals from figure 5.6 recorded after 15 minutes (left) and 120 minutes (right) following intrathecal administration at day 3 of the subchronic treatment course. At both time intervals, all treated groups showed significant analgesia compared to saline animals (*; $p<0.05$ by One-Way ANOVA with Bonferroni post test). Additionally, at 15 minutes after injection, morphine-treated animals showed decreased latencies compared to UFP-505 (#; $p<0.05$ by One-Way ANOVA with Bonferroni post test) which was not observed with naltrindole+morphine treated animals. At 120 minutes after injection, UFP-505 was significantly higher than saline, morphine and naltrindole+morphine groups (#; $p<0.05$ by One-Way ANOVA with Bonferroni post test). Data presented as mean \pm SEM from $n=3-5$ animals per group in a single experiment.

At Day 5 (figure 5.8), the major problem of animal loss from the experiments due to the loss of catheters, as seen by the lower n numbers, rendered it impossible to statistically analyze the data further. The one UFP-505 treated animal showed higher analgesic profile than that of the morphine treated and the naltrindole+morphine animals (n=2) showed higher analgesia than saline animals (n=3) (AUC; no statistical analysis). Figure 5.9 shows the latency recordings at Day 5 of the subchronic study, at 15min and 120min after injection.

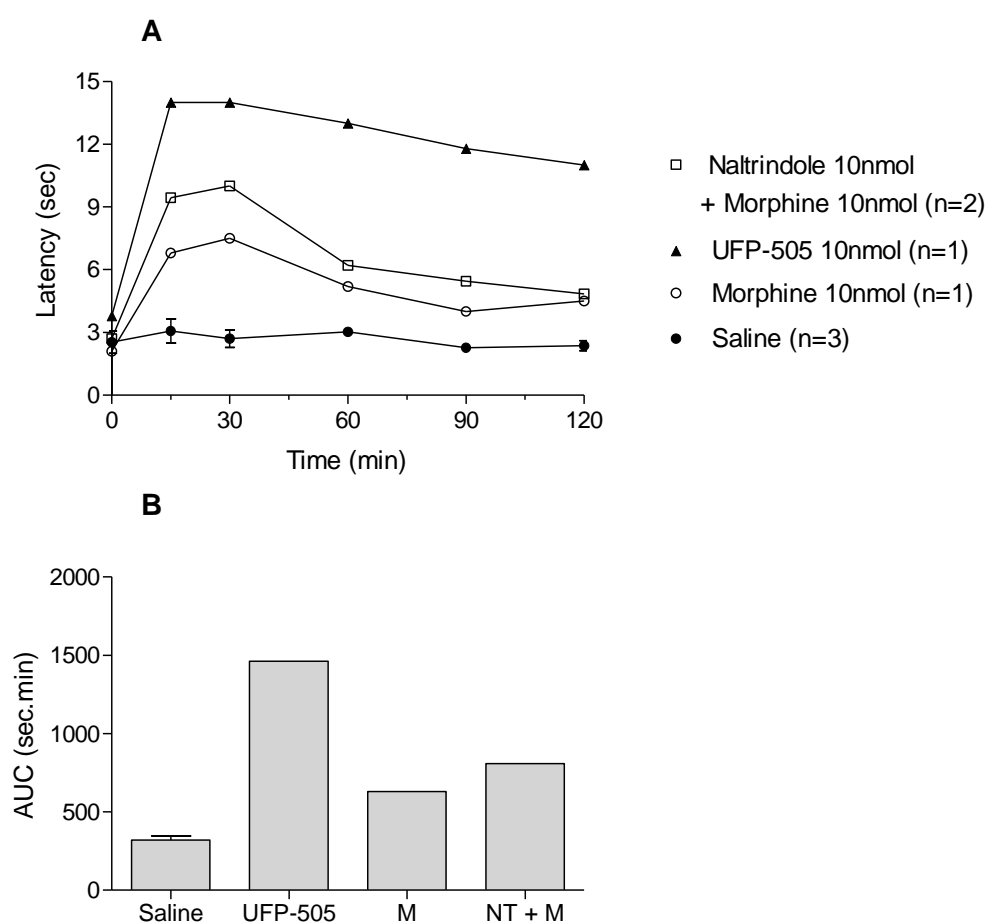


Figure 5.8. (A) Analgesic profile at day 5 of subchronic treatment with UFP-505, morphine (M) and naltrindole (NT) + morphine in rats in a tail-flick assay. (B) Area under the curve (AUC) from the curves in (A). There was a low number of animals left in the treated-groups due to the removal of the catheter and therefore statistical analysis was not possible. Naltrindole+morphine data are presented as mean of n=2 and saline data are presented as mean \pm SEM from n=3.

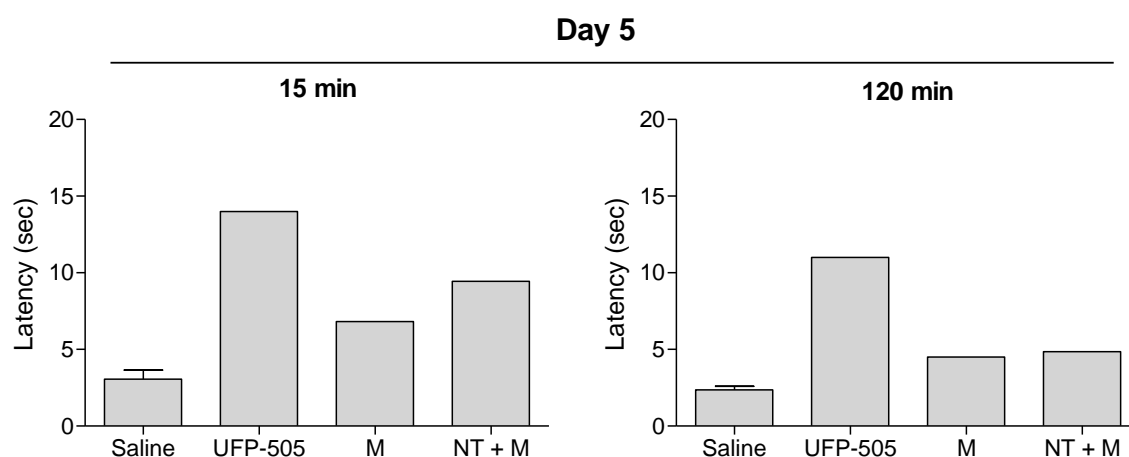


Figure 5.9. Latencies (sec; tail-flick) of treated animals from figure 5.8, as recorded after 15 minutes (left) and 120 minutes (right) of intrathecal administration at day 5 of the subchronic treatment course. The saline data are presented as mean \pm SEM from $n=3$ and the naltrindole + morphine data are presented as a mean of $n=2$ animals.

The first latencies taken in these in vivo experiments were after 15min from the administration of agents and thus these recordings were used as an indicator of the initiation of the antinociceptive response. A reduction in the recorded responses at 15min during the study is interpreted here as analgesic tolerance. Figure 5.10 presents a graph of collective data from figures 5.5, 5.7 and 5.9., with recordings at 15min after administration of all treatment groups from day 1, 3 and 5. The UFP-505 and morphine groups at day 5 had only 1 animal and therefore were not included in the statistical analysis but were included in the figure for illustration purposes.

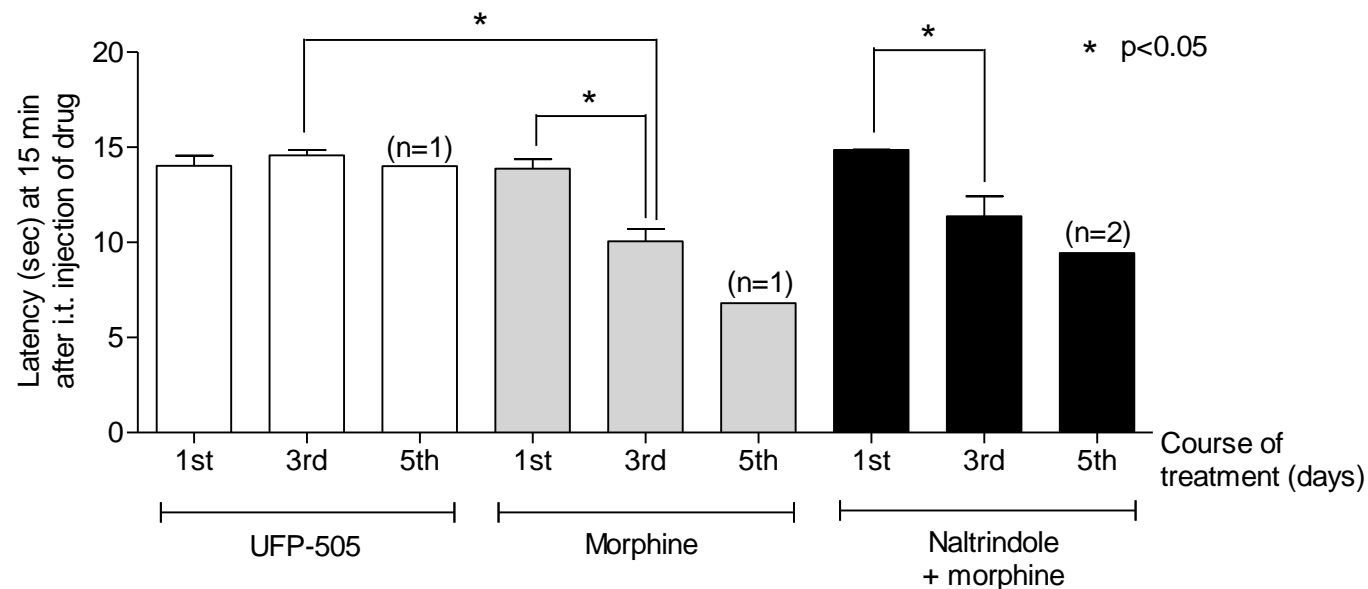


Figure 5.10. Collective latency (at 15mins) data from subchronically treated animals (Days 1, 3 and 5) after i.t. injection (Extracted from data in figures 5.5, 5.7 and 5.9.) Drop in latencies during the course of treatment within each group is interpreted as tolerance. Data are presented as mean \pm SEM from $n=3-7$ for day 1 and 3 (see respective figures). The latencies at day 5 included a low number of animals and were included in the figure for illustration purposes. UFP-505 did not show tolerance at day 3, as indicated by a non-significant reduction in latencies compared to day 1 (day 1 vs day 3 UFP-505; One-Way ANOVA with Bonferroni post test). Similarly, both morphine and naltrindole+morphine groups have shown tolerance at day 3, as indicated by a significant reduction in the latencies of these groups compared to day 1 (day 1 vs day 3; * $p<0.05$; One-Way ANOVA with Bonferroni post test). There were no significant differences in latencies between different treatment groups for day 1. For day 3, UFP-505 antinociception was significantly higher than morphine, but not significantly higher than naltrindole+morphine.

Morphine and naltrindole+morphine treated animals exhibited a reduction in their analgesic responses (latency) after administration for three consecutive days (10nmol each drug once daily), as shown by comparing day 1 and 3 ($p < 0.05$ by One-Way ANOVA with Bonferroni post test), indicating tolerance. In contrast, UFP-505 did not show a significant difference in the analgesic response after repeated administration for three days (day 1 vs day 3). However, comparison between different treatment groups has shown that at day 3 there was a significant difference in analgesia between UFP-505 and morphine ($p < 0.05$ by One-Way ANOVA with Bonferroni post test), but non-significant between UFP-505 and naltrindole+morphine.

5.5. Subchronic subcutaneous administration of morphine 5mg/kg produces tolerance in a hot-plate assay

In order to be able to compare any observed mRNA changes of opioid receptors between intrathecal and subcutaneous administration of morphine, subchronic (4 days) subcutaneous (s.c.) treatment with morphine (5mg/kg; twice a day for four days) was first examined in a hot-plate assay and then the neural tissues were removed for determining the opioid receptor mRNA levels. The data in this section present the antinociceptive profile of morphine treated animals, with the mRNA data presented in Chapter 6.

Figure 5.11 shows the analgesic profile of s.c morphine during the four-day treatment with recordings taken 30 minutes after injection. Morphine exhibited strong analgesia at day 1 (significance compared to saline; $p < 0.05$), which was later reduced gradually until the end of the study (day 4). Tolerance, indicated by a significant reduction in latency, was seen at day 3 (figure 5.6A; # $p < 0.05$), whereas on the last day of the experiment

there was no significant analgesia compared to the saline-treated animals. The total analgesia produced in the course of the study showed a significant difference compared to the saline-treated animals (figure 5.6B).

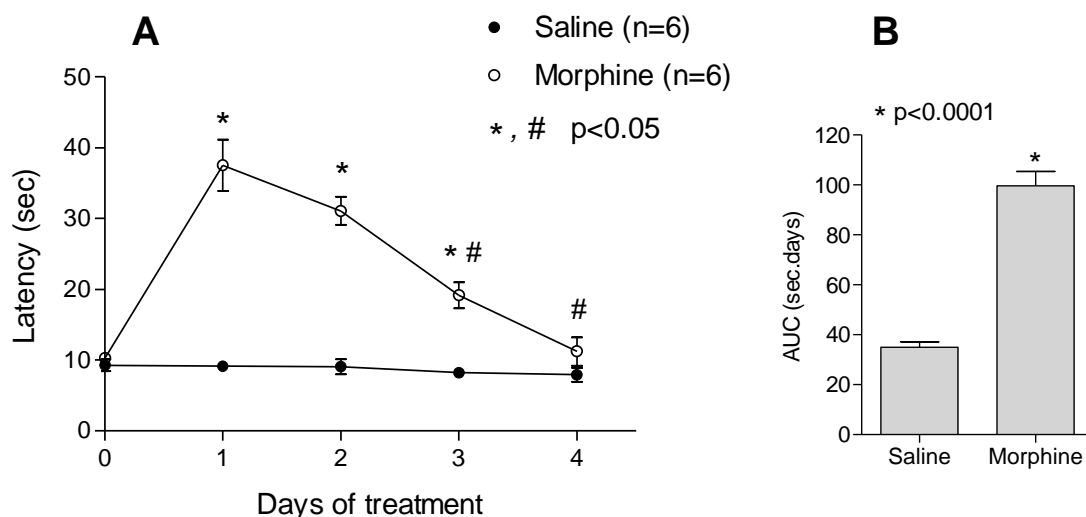


Figure 5.11. (A) Latencies (sec; hot-plate assay) of morphine treated animals (5mg/kg for 4 days; twice a day s.c). Significant difference from control was recorded every day but day 4 (*; $p < 0.05$), while on day 3 and 4 there was a significant difference in latency compared with day 1 (#; $p < 0.05$); (One-Way ANOVA with Bonferroni post test). (B) Area under the curve (AUC; sec.days) from A, showing significant difference in morphine-treated animals compared to saline (*; $p < 0.0001$) by unpaired Student's *t*-test. Data are presented as mean \pm SEM from $n = 6$ animals.

5.6. Discussion

The data presented in this chapter indicate that, in the tail-flick antinociception assay acute treatment with intrathecal UFP-505 produces antinociception comparable to that of intrathecal morphine. In addition to this, and in contrast to morphine, when intrathecal UFP-505 is administered daily for five days, not only is its analgesic effect

largely unaffected, but it does not appear to show the development of tolerance (at least after three days of treatment as the 5th day data is from only one remaining animal).

One major issue encountered in the subchronic study was animal withdrawal due to catheter removal. Although a number of preparative measures were taken to limit this issue (i.e. catheter exit at the back of the animal where the animal would have limited access, stitching of the catheter tube subcutaneously, protective cap around the catheter outside the body etc) and a number of alternative techniques that were tested prior to the study (i.e. gluing of the catheter to clean skin during anaesthesia), these were unable to prevent animals from eventually removing the catheter.

Although there was an apparent increase in itching for morphine treated animals (an expected side-effect of morphine administration; data not recorded by behavioural testing), it is unlikely that the removal of the catheter by the animals was a result of this side-effect as the catheter was deliberately positioned at the back of the animal's neck to minimize reach. Besides, catheter removal was also observed prior to opioid administration, illustrating that this was a methodological issue. Figure 5.12 shows the change in the numbers of animals throughout the study, due to failure of the lidocaine-test or catheter removal.

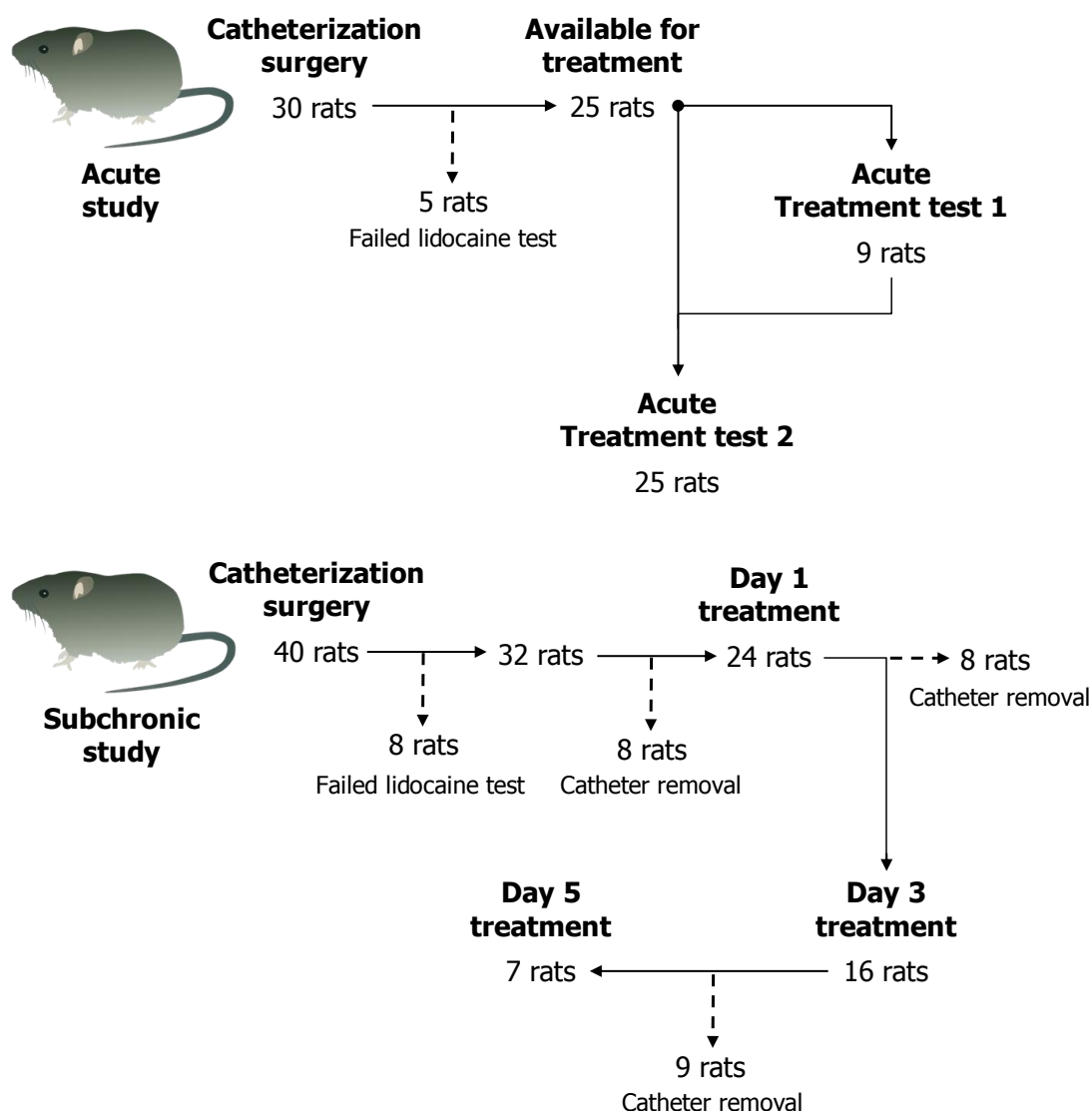


Figure 5.12. Allocation of animals in the acute and subchronic studies, showing the number of available animals in every part and the reasons for exclusion. For the acute study, 30 animals underwent catheterization surgery and 5 animals were excluded after the lidocaine test (evidence of incorrect positioning of the catheter). For the subchronic study, 40 animals underwent catheterization surgery and 8 rats were excluded after the lidocaine test. 25 rats lost their catheter during the course of the subchronic study, reducing dramatically the available rats at Day 5.

As this was the first *in vivo* study with UFP-505, the essential information needed was 1) to assess the analgesic profile of various doses of UFP-505 and 2) to find the equianalgesic dose of UFP-505 and morphine in order to be used in the subsequent subchronic tests. Acute i.t. injection of UFP-505 at 50nmol (per animal) produced analgesia that immediately reached the latency cut-off limit used in the assay (figure 5.2).

The analgesic peak of UFP-505 10nmol (15min; figure 5.2A) was the same as that of morphine 10nmol (indicating equipotency), and the analgesic profile of 10nmol UFP-505 (figure 5.3A) was not-significantly different from that of 10nmol morphine (indicating equiefficacy). From the respective dose-response curves (AUC and latency; figure 5.3B), the EC₅₀ of UFP-505 was estimated around 7nmol (6.55 and 7.52nmol respectively; inserted table figure 5.3B). The equianalgesic doses of 10nmol (per animal) for UFP-505 and morphine were used as the appropriate doses for comparison in the subchronic study.

The five-day subchronic study aimed to assess the analgesic tolerance. In addition to UFP-505 and morphine (10nmol), the co-administration of a selective DOP receptor antagonist (naltrindole; 10nmol) and morphine (10nmol) was used to assess its ability to reduce analgesic tolerance; as previously described in a number of studies (Abdelhamid *et al*, 1991; Fundytus *et al*, 1995; Hepburn *et al*, 1997). Naltrindole was used at 10nmol based on previous reported binding data in rat brain tissue (Fang *et al*, 1994; McNaull *et al*, 2007), as it is believed that this dose is sufficient to block all the DOP receptors in the spinal cord.

At day 1 of the subchronic study, the analgesic profiles of all treated groups (UFP-505, morphine and naltrindole+morphine; 10nmol each) showed non-significant differences, as estimated by their AUC (figure 5.4). However, the latencies recorded at 120min after injection have shown that UFP-505 produced significantly higher analgesia than morphine but this was not different compared to naltrindole+morphine (figure 5.5). Additionally, morphine latency 120 minutes after injection was reduced compared to 15 minutes, a reduction that was not seen in the case of UFP-505. This drop in morphine analgesia after 120 minutes of administration is in agreement with published data (Prado, 2003) and could be attributed either to: 1) a reduction in morphine concentration (i.e. metabolism, distribution to other compartments), 2) to a reduction in morphine targets or 3) to both. However, there was significantly higher analgesia recorded in the naltrindole+morphine group after 120 minutes of administration, compared to that of morphine (figure 5.5), implying that the addition of the DOP-selective antagonist reduces the drop seen with morphine alone. This comparison suggests that there is a DOP-related mechanism that can attenuate the reduction of analgesia seen 2 hours after morphine administration and this is consistent with data from Hepburn (Hepburn *et al*, 1997) and McNaul (McNaul *et al*, 2007).

At day 3 of the subchronic study, the analgesic profile of UFP-505 was significantly higher not only from that of morphine, but also from that of naltrindole+morphine treatment group (figure 5.6), whereas the recorded latencies at 120min after injection showed significantly higher values for UFP-505 compared to the other two groups (figure 5.7). The drop in analgesia at 2 hours after injection for the naltrindole + morphine treated animals, suggests that the influence of the DOP receptor antagonist to the effect of morphine deteriorates but is still present at day 3.

At day 5 of the subchronic study (figure 5.8), although the number of available animals left was low (due to catheter removal), UFP-505 retained an analgesic response (n=1) and at 120 minutes after injection of agents (figure 5.9) there was a decrease in analgesia for morphine (n=1) and naltrindole+morphine (n=2).

Looking at the comparison of all treated groups at 15min latencies for all days of treatment (figure 5.10), we conclude three major points: 1) UFP-505 presents persisting antinociception at day 3, without the manifestation of analgesic tolerance, 2) morphine and naltrindole+morphine groups show manifestation of analgesic tolerance at day 3, expressed as a significant reduction in tail-withdrawal latencies, 3) the drop in analgesia in naltrindole+morphine group at day 3 is not large enough to show significant difference of latencies compared to UFP-505 at the same day, whereas the respective drop in morphine group produces significant reduction in antinociception compared to UFP-505. These points underline the differences in the latencies of treated groups after 15mins of drug administration in the subchronic experiment.

Tolerance to morphine is also seen after s.c administration of 10nmol over a course of 4 days in the hot-plate assay (figure 5.11), as seen at day 3 and indicated by a significant drop of latency compared to day 1. These data will be used in Chapter 6 of this thesis in order to study changes in receptor regulation.

The data in this section represent the first *in vivo* data on the analgesic effects of UFP-505. Significantly a novel bifunctional opioid ligand is capable of producing analgesia with reduced tolerance when administered subchronically and therefore further (and/or longer) *in vivo* studies should be conducted in order to investigate the long-term

analgesic profile of UFP-505. However, bioavailability and the practicalities of i.t. administration should not be understated.

Neuronal tissue of the treated animals (UFP-505 and reference compounds) was removed in order to examine any changes in receptor density and opioid receptor mRNA levels, which is discussed in the next Chapter.

CHAPTER 6.

***IN VITRO* STUDIES OF NEURONAL TISSUES EXTRACTED
FROM RATS TREATED WITH UFP-505
AND REFERENCE LIGANDS.**

Chapter 6. *In vitro* studies of neuronal tissues extracted from rats treated with UFP-505 and reference ligands.

6.1. Introduction

Opioid receptor trafficking (internalization and recycling to the cell surface) as well as opioid-receptor mRNA regulation, are thought to be part of a mechanism that is involved to the development of analgesic tolerance. Opioid receptor internalization in lysosomal vesicles may lead to either receptor recycling to the cell surface (as part of the resensitization process) or to enzymatic degradation. It is believed that opioid-receptor mRNA regulation is part of a cellular response mechanism towards changes in cell-surface opioid receptor density, which can be ligand-dependent and ligand-specific. The exact biochemical process responsible for this is currently unknown. By studying the differences in cellular effects (such as receptor internalization and mRNA regulation) between morphine and ligands that do not produce tolerance, it will be possible to provide insights into the role of these effects in the mechanism of tolerance.

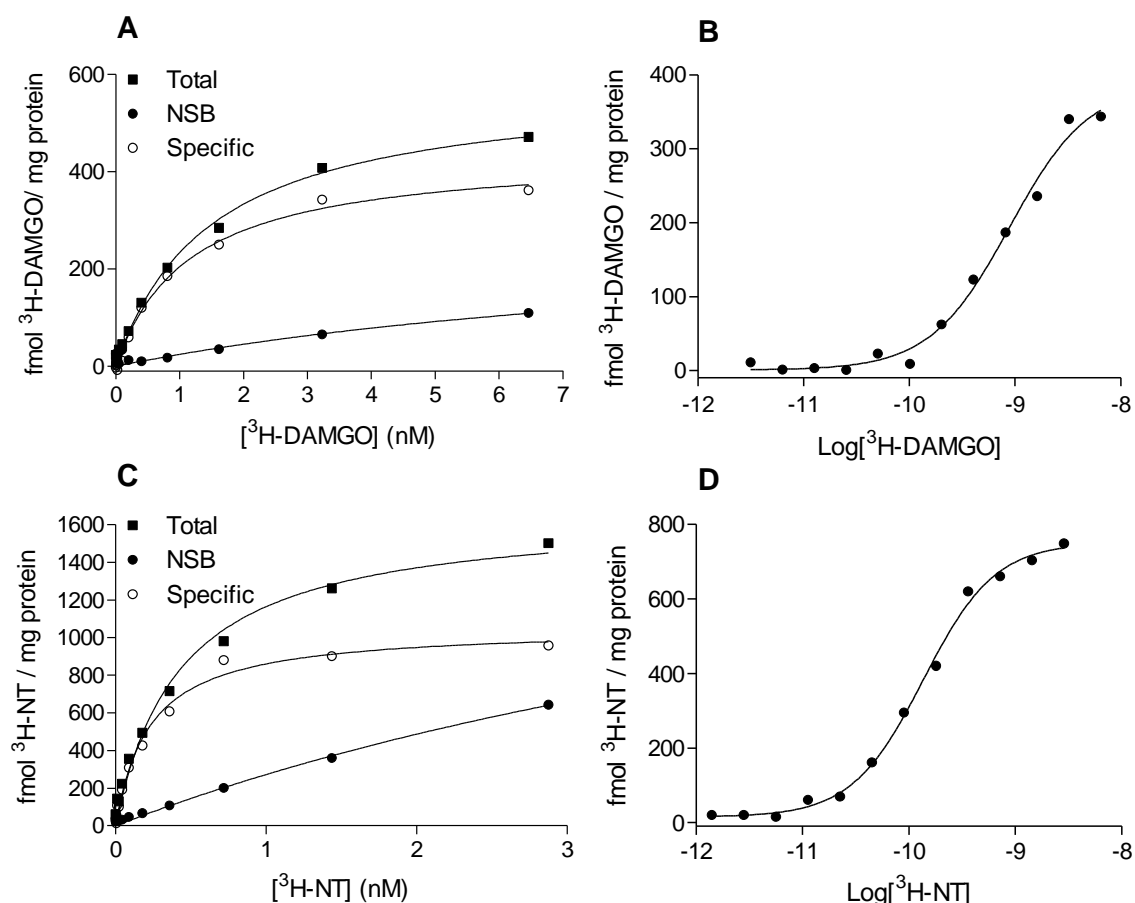
6.2. Aims

The spinal cord, the frontal cortex and the rest of the cortex from a number of treated animals from the *in vivo* study discussed in Chapter 5 were removed and studied *in vitro* as discussed in this Chapter. The aim of this study was to examine the effects of drug administration on cell-surface opioid receptor density and on opioid-receptor mRNA expression.

6.3. Loss of cell-surface opioid receptors in the spinal cord and the frontal cortex in rats treated acutely with intrathecal UFP-505 or morphine

Tritiated DAMGO (^3H -DAMGO) and tritiated naltrindole (^3H -NT) were used in order to specifically label the MOP and DOP receptors respectively in rat neuronal tissue. The radioligands were used in initial confirmatory saturation assays, in membranes prepared from CHO_{hMOP} and CHO_{hDOP} cells (figure 6.1) prior to use in rat tissues. The process of isolation of neuronal tissues (cortex and spinal cord) was carried out at least 1 hour after the end of each *in vivo* experiment and lasted for at least 40 minutes. These tissues were stored at -80°C for 1 week. Membranes were then prepared from the frontal cortex and spinal cord of the acutely treated (10nmol UFP-505 and 10nmol morphine; i.t.) and saline-treated rats which were used in the *in vivo* study (Chapter 5). A series of independent saturation binding assays were performed by applying saturating concentrations of ^3H -DAMGO and ^3H -NT (table 6.1).

Administration of morphine did not induce any changes in receptor density in the frontal cortex for both MOP and DOP receptors. In contrast, treatment with UFP-505 induced significant loss of cell-surface MOP and DOP receptors in this rat tissue, compared to morphine-treated and untreated membranes (internalization MOP: 36.5%, DOP: 48.8%). Additionally, for the spinal cord samples, the effect of UFP-505 and morphine on cell-surface receptor numbers was similar (internalization MOP: 44.7%, DOP: 43.1%). A significant reduction in density of both receptors was observed in the UFP-505 treated samples compared to the expression of the respective receptors in the morphine and untreated samples. The ineffectiveness of morphine to internalize the MOP receptor agrees with previous studies and also with work in this thesis (Chapter 4).



Radioligand	Cells	RL p <i>K</i> _d	RL K _d	B _{max}
³ H-DAMGO	CHO _{hMOP}	9.05 ± 0.07	0.89 nM	388 ± 28
³ H-NT	CHO _{hDOP}	9.87 ± 0.03	0.14 nM	751 ± 15

Figure 6.1. Representative curves of saturation assays (from $n=3$), performed on (A, B) CHO_{hMOP} and (C, D) CHO_{hDOP} cell membranes using increasing concentrations of tritiated DAMGO (³H-DAMGO) and tritiated naltrindole (³H-NT) respectively. Non-specific binding (NSB) was measured in the presence of 10 μM naloxone. The maximum receptor density for each receptor type (B_{max}; expressed as fmol radioligand/mg protein) and the equilibrium dissociation constant (p*K*_d) of the radioligands used are summarized in the inserted table.

B_{max} of MOP and DOP receptors in neuronal tissue samples from acutely treated rats						
	Frontal cortex			Spinal cord		
	<i>Saline</i>	<i>Morphine</i>	<i>UFP-505</i>	<i>Saline</i>	<i>Morphine</i>	<i>UFP-505</i>
MOP	73.85 ± 5.50	71.64 ± 3.51	46.91 ± 1.66 *	23.08 ± 1.94	21.44 ± 0.99	12.76 ± 2.40 *
DOP	91.68 ± 8.71	101.4 ± 7.99	40.24 ± 1.31 *	33.12 ± 3.21	32.54 ± 3.85	18.86 ± 2.08 *

Table 6.1 Cell-surface receptor density for MOP and DOP receptors (B_{max} ; fmol radioligand / mg protein) from binding experiments of saturating concentration of radioligand in extensively washed membranes prepared from the frontal cortex and spinal cord tissue, taken from rats treated acutely with either 10nmol UFP-505 or 10nmol morphine, (Chapter 5). Saturation assays were performed using ^3H -DAMGO ($\approx 6.7\text{nM}$) and ^3H -NT ($\approx 3.3\text{nM}$) respectively. Only the UFP-505 treated animals showed significant reduction in MOP (36.48% cortex, 44.71% cord) and DOP (48.80% cortex, 43.06% cord) B_{max} in both tissues, compared to saline (* $p < 0.05$ One-Way ANOVA with Bonferroni post test). Data are expressed as means \pm SEM for $n=3-4$.

6.4. Changes in opioid-receptor mRNA expression in neuronal tissue taken from acutely and chronically opioid treated rats

The spinal cord, frontal cortex and the rest of the cortex were removed from 3-5 rats from each treated group of the *in vivo* study (acute and chronic) and the tissue from *n* animals was pooled and processed as a batch to determine opioid receptor mRNA expression by RT-qPCR. mRNA levels were expressed as ΔC_t (cycle threshold) values (i.e. difference between the C_t value of the gene of interest and the C_t value of the housekeeper GAPDH) and are shown in table 6.2 (acute treatment) and table 6.3 (chronic treatment). Significant effects on mRNA regulation ($p < 0.05$, One-Way ANOVA repeated measurements) are indicated with an up-arrow (\uparrow) for upregulation (lower ΔC_t) and a down-arrow (\downarrow) for downregulation (higher ΔC_t) compared with control.

For acutely morphine-treated animals (table 6.2), variable changes in opioid receptor mRNA levels were observed for all opioid receptors across all tissues examined. Morphine and UFP-505 treated animals showed significant upregulation of the MOP receptor in the spinal cord, but only morphine-treated animals showed significant upregulation of the DOP receptor. In the same tissue, NOP receptor mRNA levels were down regulated in both treatment groups. In the frontal cortex, only the KOP receptor mRNA levels were shown to upregulate in morphine-treated animals. In the rest of the cortex, only the DOP receptor mRNA levels were shown to significantly down regulate in both treatment groups.

Opioid receptor mRNA levels (ΔC_t values) in neuronal tissue from treated rats (i.t.) acutely				
	MOP	KOP	DOP	NOP
Spinal cord				
Morphine	<u>8.08 ± 0.13</u> ↑	10.89 ± 0.07	<u>9.14 ± 0.07</u> ↑	<u>12.34 ± 0.05</u> ↓
UFP-505	<u>8.54 ± 0.32</u> ↑	11.13 ± 0.12	9.55 ± 0.50 ‡	<u>12.27 ± 0.17</u> ↓
Saline	9.64 ± 0.15	10.87 ± 0.06	11.01 ± 0.24	9.80 ± 0.17
Forntal cortex				
Morphine	9.16 ± 0.04	<u>11.73 ± 0.48</u> ↑	10.82 ± 0.22	10.22 ± 0.11
UFP-505	9.73 ± 0.46	11.81 ± 1.13 ‡	11.13 ± 0.04	10.12 ± 0.15
Saline	10.77 ± 0.44	14.05 ± 0.04	11.10 ± 0.18	11.47 ± 0.15
Rest of the cortex				
Morphine	10.24 ± 0.11	12.44 ± 0.31	<u>11.93 ± 0.09</u> ↓	9.38 ± 0.05
UFP-505	10.23 ± 0.01	12.29 ± 0.01	<u>12.70 ± 0.01</u> ↓	9.34 ± 0.01
Saline	9.75 ± 0.18	11.09 ± 0.07	10.36 ± 0.16	9.42 ± 0.13

Table 6.2. Opioid receptor mRNA expressed as ΔC_t values for the gene of interest (mean \pm SEM; n=3-5) using GAPDH as a housekeeper, in neuronal tissue of acutely-treated rats (10nmol UFP-505, 10nmol morphine and saline-treated; i.t.). Data were produced by RT-qPCR from tissue lysates (harvested membranes from tissues). Reduction in the ΔC_t indicates upregulation (↑) of receptor mRNA, whereas increase in the ΔC_t indicates downregulation (↓). Significant changes were analyzed and detected within each tissue/receptor subgroup by One-Way ANOVA with Bonferroni post test ($p < 0.05$) compared to that group's control value, and are highlighted by underlining. (‡) Values were found not different compared to the group's control, but their p value was very close to 0.05.

Investigation of mRNA levels of neuronal tissues from subchronically-treated animals was also performed from neuronal tissues removed at day 3 of the subchronic course, and the results are presented in table 6.3. No significant changes in mRNA levels were detected for all opioid receptors studied, in all tissues examined, across all groups.

Opioid receptor mRNA levels (ΔC_t values) in neuronal tissue from treated rats (i.t.) for 3 days				
	MOP	KOP	DOP	NOP
Spinal cord				
Morphine + Naltrindole	8.72 \pm 0.14	14.11 \pm 0.44	11.17 \pm 1.15	10.15 \pm 1.30
Morphine	8.38 \pm 0.45	13.81 \pm 0.13	11.09 \pm 1.44	9.85 \pm 1.60
UFP-505	8.61 \pm 0.40	13.94 \pm 0.55	11.23 \pm 1.51	9.87 \pm 1.44
Saline	8.64 \pm 0.40	13.84 \pm 0.20	11.39 \pm 1.53	10.05 \pm 1.80
Forntal cortex				
Morphine + Naltrindole	9.72 \pm 0.09	15.37 \pm 1.70	10.34 \pm 1.49	10.49 \pm 1.53
Morphine	9.92 \pm 0.02	15.89 \pm 0.96	10.01 \pm 1.57	10.26 \pm 1.56
UFP-505	9.54 \pm 0.47	14.96 \pm 0.45	10.05 \pm 1.60	10.57 \pm 1.43
Saline	9.35 \pm 1.00	14.77 \pm 0.71	10.20 \pm 1.40	10.54 \pm 1.57
Rest of the cortex				
Morphine + Naltrindole	10.67 \pm 0.15	15.30 \pm 0.72	10.60 \pm 1.58	10.57 \pm 1.44
Morphine	10.54 \pm 0.06	15.71 \pm 0.19	10.34 \pm 1.72	10.17 \pm 1.42
UFP-505	9.18 \pm 0.93	14.13 \pm 1.00	10.38 \pm 1.56	10.22 \pm 1.57
Saline	10.51 \pm 0.31	15.49 \pm 1.01	10.56 \pm 1.46	10.86 \pm 1.78

Table 6.3. Opioid receptor mRNA levels expressed as ΔC_t values for the gene of interest (mean \pm SEM; $n=3-5$) using GAPDH as a housekeeper, in neuronal tissue of chronically-treated rats (10nmol UFP-505, 10nmol morphine, 10nmol morphine + 10nmol naltrindole or saline-treated; i.t. once daily) at day 3 of treatment. Data were produced by RT-qPCR from tissue lysates. No significant changes were detected within each tissue/receptor subgroup by One-Way ANOVA ($p>0.05$) compared to that group's saline (control) value.

Neuronal tissues taken from the chronic subcutaneously morphine-treated rats (s.c 5mg/kg twice daily for 4 days), removed at the end of the study, were used to investigate changes in all opioid receptor mRNA levels, and compared to saline-treated animals by RT-qPCR (table 6.4). Only the KOP receptor mRNA levels in the cerebral cortex (both the frontal and the rest groups) were shown to be significantly down-regulated in morphine-treated animals.

Opioid receptor mRNA levels (ΔC_t values) in neuronal tissues From treated rats (s.c) for 4 days				
	MOP	KOP	DOP	NOP
Spinal cord				
Morphine	9.25 \pm 0.10	10.82 \pm 0.15	11.41 \pm 0.41	9.82 \pm 0.06
Saline	9.64 \pm 0.15	10.87 \pm 0.06	11.01 \pm 0.24	9.80 \pm 0.17
Frontal cortex				
Morphine	11.09 \pm 0.25	<u>15.42 \pm 0.42</u> ↓	10.88 \pm 0.13	11.39 \pm 0.12
Saline	10.77 \pm 0.44	14.05 \pm 0.04	11.10 \pm 0.18	11.47 \pm 0.15
Rest of the cortex				
Morphine	10.07 \pm 0.18	<u>12.04 \pm 0.24</u> ↓	10.46 \pm 0.22	9.24 \pm 0.14
Saline	9.75 \pm 0.19	11.09 \pm 0.07	10.36 \pm 0.16	9.42 \pm 0.13

Table 6.4. Opioid receptor mRNA levels expressed as ΔC_t values for the gene of interest (mean \pm SEM; n=3-5) using GAPDH as a housekeeper, in neuronal tissue of chronically-treated rats (morphine 5mg/kg twice daily for 4 days or saline-treated; s.c.). Data were produced by RT-qPCR from tissue lysates. Morphine-treated animals showed complete analgesic tolerance at day 4 when their tissues were removed (Chapter 5, figure 5.11). Significant increase in the ΔC_t values indicates significant downregulation (↓) of receptor mRNA (Unpaired Student's t-test; $p < 0.05$) compared to the control group.

6.5. Discussion

It is widely accepted that internalization of an opioid receptor upon ligand binding is ligand-specific and that this behaviour plays a role in the mechanism responsible for the development of analgesic tolerance (Arden *et al*, 1995; Burford *et al*, 1998; Groer *et al*, 2007; Lee *et al*, 2002; Pradhan *et al*, 2010). Additionally, it is known that the fate of an internalized receptor can be branched to either recycling to the cell surface after dephosphorylation, or dismantled to amino acids (degradation) by lysosomal enzymes (Qiu *et al*, 2003; van Rijn & Whistler, 2008; van Rijn *et al*, 2010). Also, part of the signaling cascade triggered by receptor binding, involves regulation of the transcription of different genes, including the opioid receptors (Patel *et al*, 2002). The questions that arise therefore are the following: 1) Is there any difference in the mRNA levels of opioid receptors after the administration of opioids? 2) Are there any changes in receptor protein after administration? 3) Is there any connection of analgesic tolerance to changes in opioid receptor mRNA levels? 4) Does the route of administration play a role in differences in mRNA expression?

In chapter 4 it was demonstrated in CHO cells that UPP-505 causes the internalization of the MOP (figure 4.1) and the DOP (figure 4.4) receptors, as well as the inability of morphine to internalize the former. In chapter 5 it was shown that acute intrathecal administration of UFP-505 produces a similar analgesic response to morphine (figure 5.3), in addition to the fact that repeated administration of UFP-505 does not produce tolerance in contrast to morphine (figure 5.10). In this chapter, neuronal tissues extracted from animals treated with UFP-505 and reference compounds *in vivo* were used to determine receptor internalization and opioid receptor mRNA levels.

The tritiated MOP-selective ligand DAMGO (^3H -DAMGO) and the tritiated DOP-selective ligand naltrindole (^3H -NT) were used in saturation assays in order to assess the B_{max} of MOP and DOP receptors respectively in the frontal cortex and spinal cord from the acutely treated rats that were used in the *in vivo* experiments producing figure 5.6 (Chapter 5). Both tissues from animals treated with UFP-505, but not morphine, have shown a significant reduction in their surface MOP and DOP receptors (table 6.1) when compared with saline-treated animals. These data agree with previous *in vitro* data in CHO cells presented in this thesis (Chapter 4). It is worth noting that UFP-505 acutely-treated animals have shown higher percentages of DOP receptor internalization than MOP, as was shown in the CHO cells.

Regarding the internalization data presented in this Chapter, an important point to stress is that the agents used were administered intrathecally and therefore it is interesting that there is a significant effect of opioid receptor internalization observed in the frontal cortex. One possible explanation for this phenomenon can be the diffusion of the drug to various supraspinal compartments which could allow it to reach the cortex, since the total time from the administration of the drug to the tissue extraction was approximately 3.5 hours. Another important point to stress is that the effect of UFP-505 in the mobilization of the DOP receptor remains prominent in both tissues as in the *in vitro* studies (Chapter 4). Finally, these data highlight that the inability of morphine to internalize the MOP or DOP receptors is in agreement with the *in vitro* data in CHO cells presented in Chapter 4, although morphine produced substantial analgesia in these animals as shown in Chapter 5. Our results agree with observations by Patel *et al* showing that morphine administration did not produce any change in MOP receptor density in mouse spinal cord (Patel *et al*, 2002).

Table 6.2 presents all the changes in mRNA levels produced from the acute intrathecal administration of UFP-505 10nmol and morphine 10nmol in native neuronal tissue. Four observations must be highlighted in this data set: 1) the mRNA changes observed, induced by an agent were different across the different tissues and receptors examined for the same agent. For example, in morphine-treated rats the DOP receptor mRNA upregulates in the spinal cord but downregulates in the rest of the cortex. The literature does not report similar findings. 2) The spinal cord was found to show the most changes in receptor mRNA levels. This may be explained partially based on the administration method of the drugs used (i.t.) and/or the drugs' pharmacokinetic properties that affect their distribution to the tissues examined. Also, it is unknown if the differences in receptor expression in these tissues have an effect on gene regulation upon receptor activation. 3) The receptor mRNA levels of KOP and NOP presented significant changes in different tissues, although the compounds used to treat the animals do not possess affinity for these receptors. This effect may be a direct effect of ligand binding (i.e. through receptor opioid dimerization) or an indirect effect of ligand binding (i.e. the activated transcription factors that arise from the MOP receptor signaling pathway may modulate the transcription of another receptor gene).

With regards to data in the literature on induced changes in opioid receptor mRNA levels, there are differential reports and contradictory data published. Patel et al have shown in mouse spinal cord that etorphine and morphine cause downregulation and upregulation of the MOP mRNA respectively and they attribute this different behaviour to the differential regulation of trafficking proteins (i.e. dynamin-2 and GRK-2) induced by these agents (Patel *et al*, 2002). Our results in morphine-treated animals showing upregulation of MOP receptor mRNA in the spinal cord agree with Patel's observations.

Yu et al has also reported differences in regulation of MOP mRNA levels by different MOP agonists, using *in vitro* experiments in recombinant cell lines (Yu *et al*, 2003). They showed that morphine treatment for 24 hours (10 μ M) significantly decreased MOP mRNA levels, whereas endomorphin-1 and -2 had the opposite effect. Additionally, Cecchi et al have shown that an acute administration of morphine (i.p.) in rats did not yield any significant differences in MOP receptor mRNA levels in the CNS (locus coeruleus, ventral periaqueductal gray, nucleus raphe magnus and nucleus reticularis paragigantocellularis) compared to untreated animals (Cecchi *et al*, 2008). These results agree with our observation that MOP receptor mRNA levels were unchanged in some tissues in morphine-treated animals (*i.e.* cortex).

In order to investigate if the observed alterations in mRNA expression persist in subchronically-treated animals, similar analysis was applied in tissues extracted from animals after repeated administration of the same agents (table 6.3). After 3 days of intrathecal administration, there were no significant changes observed in the mRNA of all opioid receptors, in every tissue examined across all different treatment groups. A possible explanation for the fact that although MOP and DOP receptor mRNA was upregulated after acute treatment but they were not-significantly different from control after 3 days of treatment, is that the receptor mRNA produced was transcribed to protein and transported to the cell membrane, as an auxiliary cellular mechanism to receptor recycling after internalization. Nevertheless, it was not possible to examine receptor density in tissue from subchronic treated animals as there was insufficient tissue available.

Finally, an examination of the mRNA of opioid receptors from neuronal tissues extracted from tolerant rats after 4 days of subcutaneous administration with morphine (table 6.4), has revealed a similar picture to the intrathecal-treated tolerant rats, with the only exception being that of the KOP receptor mRNA in the cortex which significantly down regulates in morphine-treated animals. At day 4 of the study, the systemic administration of morphine was not different with respect to MOP mRNA levels when compared with the i.t administration. Teodorov et al has shown in both acute and 5-day s.c morphine treated rats that there was a significant decrease in the expression of MOP mRNA in the periaqueductal gray (Teodorov *et al*, 2006).

Our data show no changes in the MOP receptor mRNA in the cortex or spinal cord and this adds to the different observations mentioned earlier for opioid receptor mRNA levels in different tissues. Li et al (Li *et al*, 2010) have also recently investigated changes in KOP receptor mRNA expressed in various CNS areas (thalamus, hypothalamus, hippocampus, locus coeruleus, periaqueductal gray, spinal cord and dorsal root ganglia) of morphine-tolerant rats after 7-day s.c morphine. They reported that only in the locus coeruleus and spinal cord that expression of KOP receptor mRNA was significantly increased, whereas in the dorsal root ganglia it was significantly decreased. Our data show no changes of KOP receptor mRNA in the spinal cord in s.c morphine-tolerant rats, but a decrease in expression in the cortex.

Collectively, the data in this chapter show for the first time that UFP-505 triggers the internalization of the MOP and the DOP receptors in the frontal cortex and spinal cord of animals treated with one intrathecal dose of 10nmol, whereas morphine does not have any effect in receptor density *in vivo*. Changes in opioid mRNA expression in

neuronal tissue of the treated animals are complex, differential and we cannot exclude the possibility that these may be non-specific changes.

CHAPTER 7.

ESTABLISHMENT OF AND STUDIES WITH A NOVEL

CHO_hMOP/hDOP CO-EXPRESSION SYSTEM

Chapter 7. Establishment of and studies with a novel CHO_{hMOP/hDOP} co-expression system

7.1. Introduction

Opioid ligand pharmacology may be studied using a number of different models. In previous chapters we have used recombinant systems expressing one type of opioid receptor (i.e. CHO_{hMOP}, CHO_{hDOP}) in order to study the pharmacological properties of UFP-505. However, a bifunctional MOP/DOP ligand such as UFP-505 may behave differently when both opioid receptors for which it has appreciable affinity are present simultaneously. Studying the internalization properties of UFP-505 for MOP and DOP receptors *in vivo* provided important data of its effect in receptor trafficking in a system where both receptors are present, but it is unknown if other opioid or non-opioid receptors that were also present had any effect in these observations. For this reason, it is important to determine the binding affinity of UFP-505 and its effect on receptor internalization in a model where only MOP and DOP receptors are expressed.

7.2. Aims

The aims of this section are to produce and characterise a CHO cell line stably expressing recombinant MOP and DOP receptors (noted as CHO_{hMOP/hDOP}) and to use this cell line to study UFP-505 pharmacology. In particular:

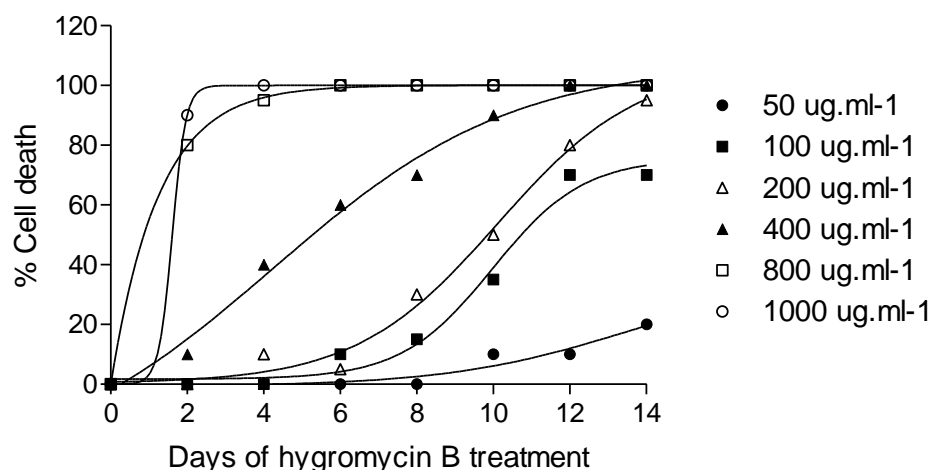
1. to produce and maintain a stable CHO_{hMOP/hDOP} cell line using CHO_{hMOP} as the ‘starting cell type’ into which hDOP is transfected,
2. to determine the receptor density of MOP and DOP receptors,
3. to determine the binding affinity of UFP-505,

4. to investigate the degree of internalisation of MOP and DOP receptors upon UFP-505 binding.

The results of this study will provide important comparison for UFP-505 data with CHO_{hMOP} and CHO_{hDOP} cell lines and will reflect the effect of co-expression of MOP and DOP receptors to this bifunctional ligand's properties and model in a very simple/controlled way the *in vivo* situation.

7.3. The concentration-death plot

A concentration-death plot of cells that do not possess resistance to a particular antimicrobial agent will determine the concentration of this agent to be used after the transfection of the cells with the resistance plasmid, in order to apply "selection". Treatment of CHO_{hMOP} cells with different concentrations of hygromycin B produced death curves seen in figure 7.1. Adding 800 µg.ml⁻¹ of hygromycin B produced near to 100% cell death after 4 days of treatment (termed 'selection pressure'), whereas 200 µg.ml⁻¹ of hygromycin B has produced near to 100% cell death after 14 days (termed 'stock pressure'). The former was used as an antimicrobial pressure for the polyclonal CHO_{hMOP/hDOP} cell stock, and the later was used for the selected monoclonal CHO_{hMOP/hDOP} cell stock.



[HygroB] µg.ml ⁻¹	Alive CHO _{hMOP} cells (%)						
	Day 2	Day 4	Day 6	Day 8	Day 10	Day 12	Day 14
50	100	100	100	100	90	90	80
100	100	100	90	85	65	30	30
200 †	100	90	95	70	50	30	05
400	70	60	30	10	0	0	0
800 ‡	50	10	0	0	0	0	0
1000	20	0	0	0	0	0	0

Figure 7.1. Graph: Death curves of CHO_{hMOP} cells for different concentrations of hygromycin B. Data are represented as percentage of cell death and are produced from results seen in the table. **Table:** Percentages of live CHO_{hMOP} cells as recorded under the light microscope by two blinded investigators (mean %). Different concentrations of hygromycin B ([HygroB]) were used for 14-day treatment period. The 200 µg.ml⁻¹ hygromycin B is named 'stock pressure' (†), whereas the 800 µg.ml⁻¹ concentration is named 'selection pressure' (§), producing 100% cell death after 14 days and 4 days respectively.

7.4. Selection of an appropriate monoclonal CHO_{hMOP/hDOP} cell batch

The mRNA levels of MOP and DOP receptors in every monoclonal CHO_{hMOP/hDOP} cell that survived the selection pressure of gentamicin and hygromycin B (named as 'cell batches') were measured by RT-qPCR with data expressed as ΔC_t values, for the gene of interest (GOI) relative to GAPDH (the housekeeper). The ΔC_t for MOP and DOP

genes are noted as $\Delta C_t^{\text{MOP-GAPDH}}$ and $\Delta C_t^{\text{DOP-GAPDH}}$. Figure 7.2 presents a representative amplification plot produced from analysis of the RT-qPCR data. From a total of 30 clones isolated, three batches were selected for further pharmacological analysis (batch № 10, 17 and 25) based on their $\Delta C_t^{\text{DOP-GAPDH}}$ values (low, medium and high). Table 7.1 presents the ΔC_t values for DOP and MOP genes for the selected batches, as well as the respective values from the CHO_{hDOP} and CHO_{hMOP} cells as a reference.

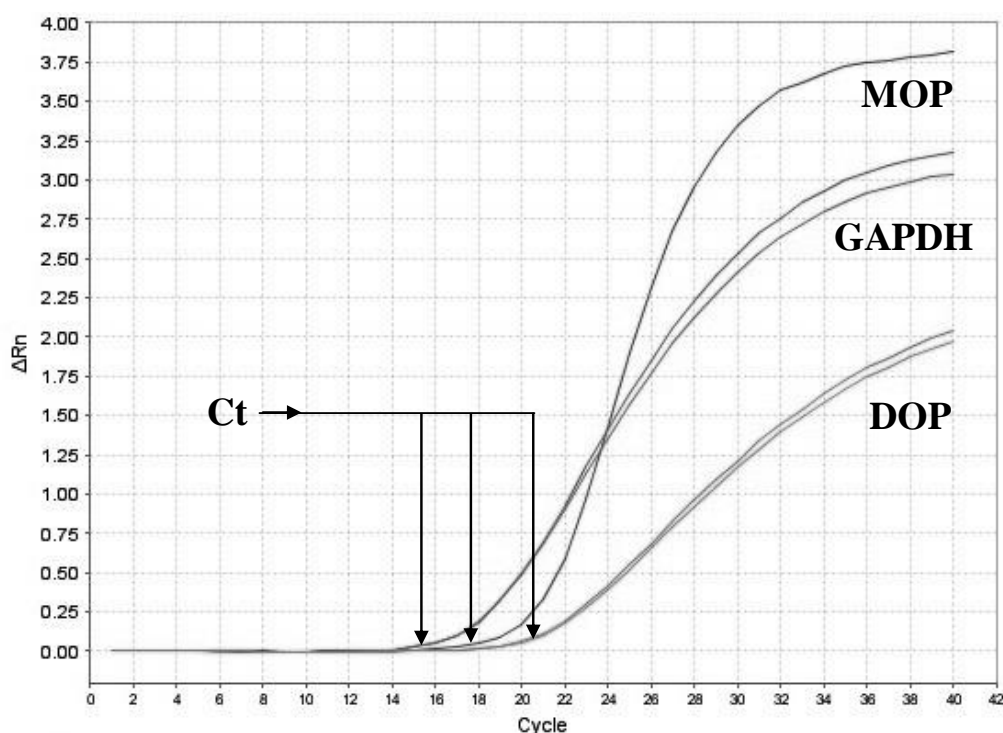


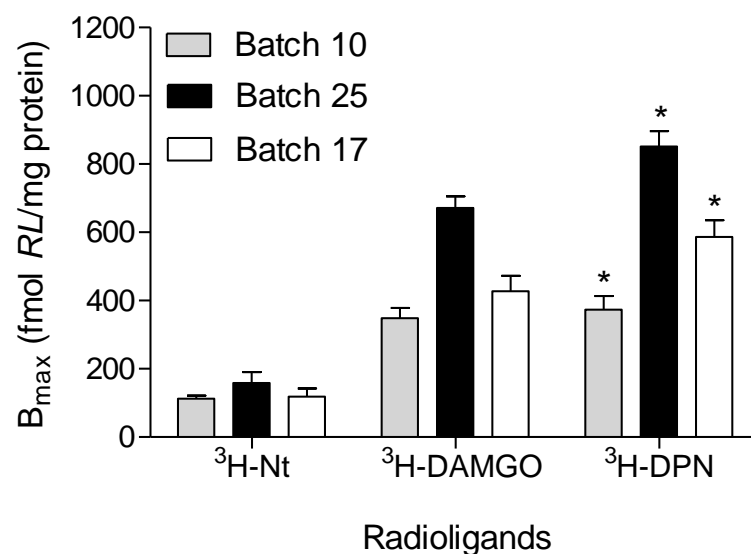
Figure 7.2. A representative amplification plot (CHO_{hMOP/hDOP} cell batch 17) from RT-qPCR. ΔRn corresponds to the increment of fluorescent signal at each time point. The ΔRn threshold (the level of fluorescence chosen on the basis of the baseline variability) is automatically adjusted by the software for each sample so that it is in the region of exponential amplification across all plots produced. The cycle number where the signal is detected above the threshold level is used to define the threshold cycle value (C_t) for each sample. The C_t for DOP and GAPDH was calculated as a mean of two samples. C_t MOP: 18.57, C_t GAPDH: 14.73, C_t DOP: 21.95. The higher the C_t value, the lower the amount of RNA detected in the sample.

CHO_{hMOP/hDOP} batch №	$\Delta C_t^{MOP - GAPDH}$	$\Delta C_t^{DOP - GAPDH}$
1	3.13	14.53
2	3.28	16.97
3	4.79	16.80
4	1.15	2.38
5	1.44	6.20
6	1.25	0.78
7	2.43	7.49
8	0.47	2.81
9	4.26	19.50
10	3.62	-0.81
11	5.75	2.52
12	3.58	17.03
13	5.60	1.94
14	2.76	3.61
15	3.24	3.77
16	2.12	14.46
17	3.22	3.83
18	3.24	3.53
19	7.56	3.25
20	1.72	8.05
21	5.75	4.74
22	3.56	8.70
23	2.52	8.18
24	2.13	8.17
25	4.39	8.66
26	3.42	5.24
27	5.74	5.22
28	3.45	17.73
29	5.45	2.37
30	2.20	16.07
Controls	$\Delta C_t^{MOP - GAPDH}$	$\Delta C_t^{DOP - GAPDH}$
CHO _{hMOP}	1.53	17.19 ^a
CHO _{hDOP}	19.15 ^b	2.30

Table 7.1. ΔC_t values ($C_t^{GOI} - C_t^{GAPDH}$) for all isolated batches of CHO_{hMOP/hDOP} cells (GOI: gene of interest), as produced from their respective amplification plots by analysis of RT-qPCR data. The higher the ΔC_t value, the lower the amount of RNA of the GOI detected in the sample. The respective ΔC_t values determined in CHO_{hMOP} and CHO_{hDOP} cells were used for comparison. Keys: (a) In CHO_{hMOP} the C_t^{DOP} was near its highest values ≈ 35 (max cycles 40), (b) In CHO_{hDOP} the C_t^{MOP} was near its highest values ≈ 36 (max cycles 40).

The three chosen monoclonal batches of CHO_{hMOP/hDOP} cells were used to determine the B_{max} for the MOP and DOP receptor protein, by performing saturation binding assays. Tritiated naltrindole (³H-Nt) and DAMGO (³H-DAMGO) were used as a DOP-selective and MOP-selective radioligands respectively, along with the non-selective ³H-DPN. The CHO_{hMOP/hDOP} batch 25 showed the highest density for both MOP and DOP receptors (figure 7.3) and was therefore selected as the most appropriate to be used in following studies. For the remainder of this work this batch of cells will be simply referred to as 'CHO_{hMOP/hDOP}' cell line.

The pK_d for ³H-DPN was calculated from full saturation curves produced from CHO_{hMOP/hDOP}, as shown in figure 7.4. The pK_d value for ³H-DPN (9.51) was found to be the same as that determined in CHO_{hMOP} cells and this may be a result of greater MOP expression.



Radioligands used	Receptors studied	B _{max} of CHO _{hMOP/hDOP} batches of cells		
		Batch 10	Batch 17	Batch 25
³ H-Nt	DOP	112.9 ± 8.8	118.7 ± 24.1	158.8 ± 31.8
³ H-DAMGO	MOP	328.6 ± 29.7	427.9 ± 44.7	671.9 ± 33.5
³ H-DPN	DOP + MOP	373.3 ± 40.4	586.4 ± 48.9	851.1 ± 45.3 *
Additive Prediction	MOP + DOP	441	547	831
Ratio	MOP : DOP	2.9	3.6	4.2

Figure 7.3. Determination of receptor density (B_{max}) for MOP and DOP receptors in three different batches of the monoclonal CHO_{hMOP/hDOP} cell line by saturation binding assays (saturating concentrations of radioligands used; data as mean \pm SEM for $n=3$ in duplicates). Cells from batch №25 expressed significantly higher (*; $p<0.05$) MOP+DOP receptors when compared to the other two batches using the respective radioligand (One-Way ANOVA with Bonferroni post test). Measured ³H-DPN B_{max} and predicted additive expression were similar. ³H-Nt; tritiated naltrindole, ³H-DPN; tritiated diprenorphine, ³H-DAMGO

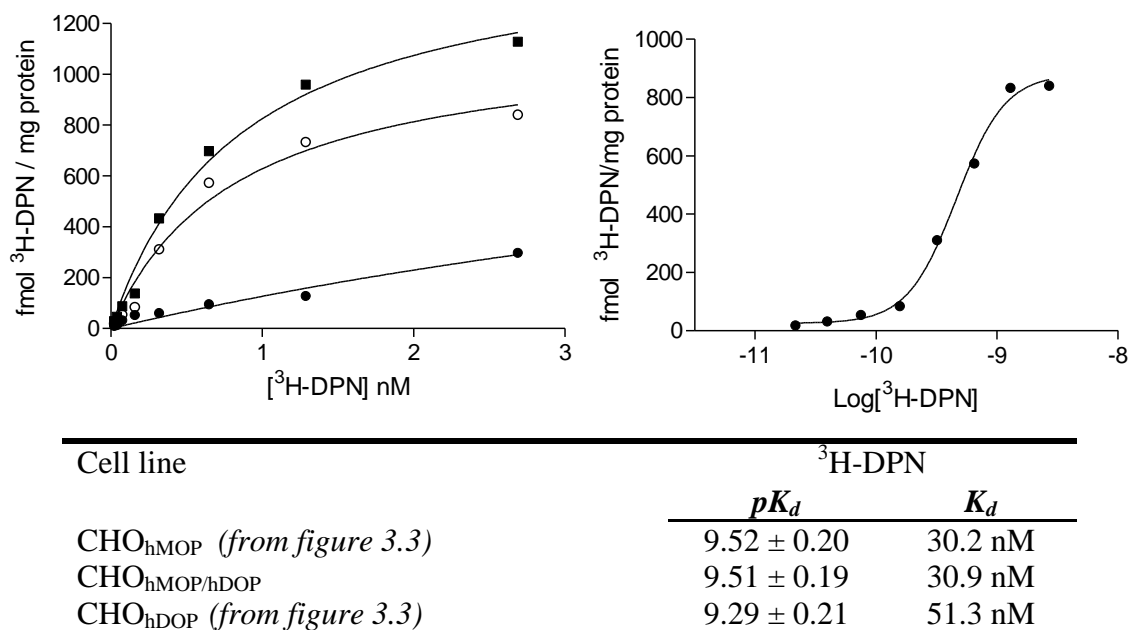


Figure 7.4. Representative saturation binding curves (hyperbola and sigmoidal) performed on CHO_{hMOP/hDOP} cells (previously known as batch 25) with increasing concentrations of tritiated diprenorphine (³H-DPN). Non-specific binding (NSB) was measured in the presence of 10μM Naloxone. Single representative curves are presented here from total n=3. The radioligand binding affinity value (pK_d, K_d; inserted table) was calculated and compared to values from CHO_{hMOP} and CHO_{hDOP} cells as presented in an earlier chapter.

7.5. Displacement binding assay of various ligands in CHO_{hMOP/hDOP} cells

The binding of ³H-DPN was displaced in a concentration-dependent manner by UFP-505 and three reference ligands; endomorphin-1 (EM1), naltrindole and morphine. Figure 7.5 shows the displacement curves produced and the respective binding affinities calculated using the ³H-DPN pK_d determined previously (9.51).

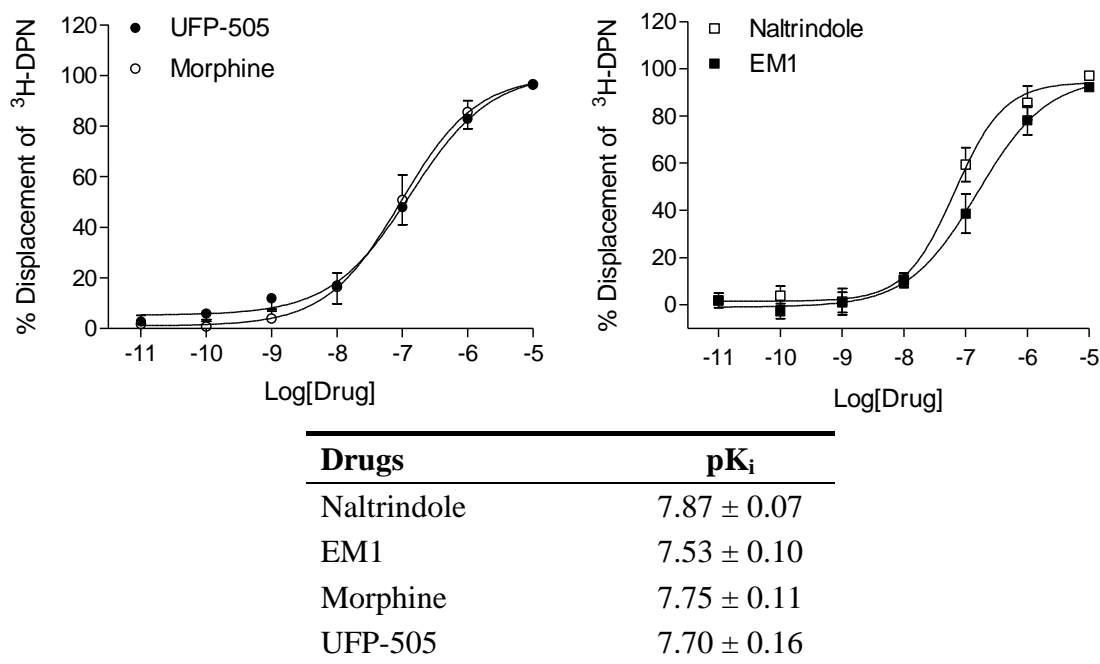
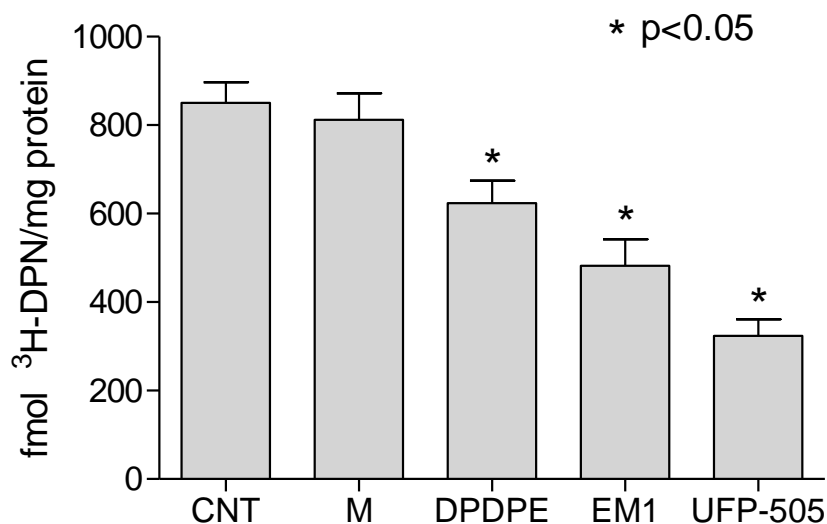


Figure 7.5. Displacement of tritiated diprenorphine (^3H -DPN) by UFP-505 and reference ligands (naltrindole, morphine and endomorphin-1; EM1) at $\text{CHO}_{\text{hMOP/hDOP}}$ cell membranes. Receptor binding affinities (pK_i) of UFP-505 and the reference ligands were calculated using the Cheng-Prusoff equation and summarized in the inserted table. Data are mean \pm SEM for $n=5$.

7.6. Receptor internalization in $\text{CHO}_{\text{hMOP/hDOP}}$ cells

Since the binding affinity of UFP-505 to the receptor population in $\text{CHO}_{\text{hMOP/hDOP}}$ cells was found to be similar to that of morphine and endomorphin-1, it was interesting to see whether there is a difference in the behaviour of these ligands in terms of their capacity to induce receptor internalization. The capacity of UFP-505 to induce receptor internalization in segregated MOP and DOP populations (CHO_{hMOP} and CHO_{hDOP} cells) was presented in Chapter 4. Figure 7.6 presents the B_{max} values of cells after pre-treatment with various ligands for 1 hour and a reduction in B_{max} was interpreted as receptor internalization (compared to control). UFP-505 induces 61.92% receptor

internalization, significantly higher than morphine which did not induce significant internalization compared to control.



<i>CHO_{hMOP/hDOP}</i> pretreatment 1h	B _{max}	Internalization †
Control (CNT)	850.5 ± 46.2	-
10μM Morphine (M)	812.4 ± 59.4	4.48 %
10μM DPDPE	627.1 ± 54.1 *	26.62 %
10μM EM1	482.0 ± 60.1 *	43.33 %
10μM UFP-505	323.9 ± 37.2 *	61.92 %

Figure 7.6. Receptor density (B_{max} , fmol $^3\text{H-DPN/mg}$ protein) and percentage internalization of receptors in $\text{CHO}_{h\text{MOP/hDOP}}$ cells pretreated for 1h with various opioid ligands as produced from saturation binding assays (saturating concentration of radioligand used). Data are presented as mean \pm SEM from $n=3$. Only the mean B_{max} of cells pretreated with morphine was found non-significantly different than that of control as analyzed by One-Way ANOVA with Bonferroni post test (*; significance $p<0.05$). Receptor internalization (†) is presented as a percentage of control.

7.7. Discussion

The stable transfection of CHO_{hMOP} cells with a plasmid that included the human DOP gene produced a high number of clones, from which 30 were isolated. Although the fact of survival of these clones under mixed antibiotic pressure (gentamicin and hygromycin B) clearly indicated the presence of resistance to both antibiotics and therefore a likely expression of the gene of interest, the degree of receptor expression varies greatly among clones. The amount of an RNA product transcribed from a gene correlates with the amount of protein translated but is not an absolute indicator. RT-qPCR analysis provided a fast initial screening method in order to select the best clone to use in the pharmacological studies that followed.

Although the expression of RNA from the MOP gene should be similar in all clones (since they all derived from the same CHO_{hMOP} transfection), there was some variation. Regarding the expression of RNA from the DOP gene, three batches were chosen based on their high, medium and low ΔC_t values compared to the others. Batch 10 showed the higher expression of RNA for the DOP gene (ΔC_t 0.80), followed by batch 17 (ΔC_t 3.84) and batch 25 (ΔC_t 8.66) (table 7.1). However, the pharmacological analysis that followed for these batches (amount of receptor protein expressed by saturation binding assay) has produced a slightly different picture (figure 7.3). All three batches showed a similar expression of the DOP receptor ($^3\text{H-Nt}$ B_{\max} 112.9, 118.7 and 158.8 for batch 10, 17 and 25 respectively), whereas the variation of the MOP receptor expression was greater ($^3\text{H-DAMGO}$ B_{\max} 328.6, 427.9 and 671.9 for batch 10, 17 and 25 respectively). Nevertheless, the overall B_{\max} values produced with $^3\text{H-DPN}$ binding (non-selective) were additive as expected, with batch 25 showing the highest expression of opioid receptors (B_{\max} 851.1) and as such this was used for further pharmacological

experiments. These data also underscore the need to interpret PCR data alone with caution.

The binding affinity of ^3H -DPN (pK_d 9.51) was found to be closer to that produced in CHO_{hMOP} cells (pK_d 9.52), than to CHO_{hDOP} cells (pK_d 9.29) (figure 7.4). This may be due to the fact that the expression of MOP receptors in $\text{CHO}_{\text{hMOP/hDOP}}$ cells is nearly four times higher than DOP receptors.

UFP-505, along with two MOP-selective ligands (morphine and endomorphin-1) and one DOP-selective ligand (naltrindole), fully displaced ^3H -DPN in competitive binding assays performed in $\text{CHO}_{\text{hMOP/hDOP}}$ cells (figure 7.5). The binding affinities of the selective ligands (pK_i) in the 'double-expression' cell line were found lower than those in the respective single-expression CHO cells, as shown collectively in table 7.2. In contrast, the binding affinity of UFP-505 in $\text{CHO}_{\text{hMOP/hDOP}}$ cells was found similar to that in CHO_{hMOP} cells. These data indicate that the co-expression of MOP and DOP receptors produces changes in the binding affinity of the selective ligands to the mixed receptor population.

Binding affinities (pK_i) of ligands to opioid receptors in different cell lines			
Ligand	CHO_{hMOP}⁽¹⁾	CHO_{hDOP}⁽¹⁾	CHO_{hMOP/hDOP}⁽²⁾
UFP-505	7.79 ± 0.18	9.82 ± 0.06	7.70 ± 0.16
Morphine	8.55 ± 0.14	-	7.75 ± 0.11
Endomorphin-1	8.09 ± 0.15	-	7.53 ± 0.10
Naltrindole	-	9.82 ± 0.13	7.87 ± 0.07

Table 7.2. Binding affinities (pK_i) for various ligands, tested in single-expression (CHO_{hMOP} and CHO_{hDOP}) and a double-expression system (CHO_{hMOP/hDOP}). Data were taken from figure 3.5 (1) and figure 7.5 (2). In CHO_{hMOP/hDOP} cells naltrindole shows a two-log decrease, morphine shows a one-log decrease and endomorphin-1 shows a half-log decrease, compared to the single-expressing cell lines.

The decreased affinity of the selective ligands in the double-expression system was completely expected. However, this explanation should apply to UFP-505 where the pK_i of UFP-505 determined in the CHO_{hMOP/hDOP} cells should be between the one determined for CHO_{hMOP} (7.79) and that in CHO_{hDOP} (9.82). Nevertheless, this expectation assumes that the expression of the MOP and DOP receptors in the ‘double-expression’ system is similar, which is not the case as previously shown in figure 7.3 (MOP is four times higher-expressed than DOP). This is probably why the pK_i of UFP-505 in CHO_{hMOP/hDOP} cells is similar to that determined in CHO_{hMOP} cells.

It has been previously shown that UFP-505 induces internalization of the MOP and the DOP receptors in single-expression systems and that morphine fails to induce internalization of the MOP receptor (Chapter 4). Additionally, it has been shown that in neuronal tissue from rats that developed analgesic tolerance after a three-day administration of morphine (i.t) there was no difference in their B_{max} compared to control (Chapter 6, table 6.1), in contrast to UFP-505 treated animals that showed

reduction in B_{\max} after three-day administration (i.t). Data in this chapter provided a link between single-expression recombinant systems and native tissue by studying the internalization of opioid receptors (MOP and DOP) in a double-expression system. Table 7.3 presents collective data of receptor internalization from different cell lines and tissue for the ligands tested. Morphine failed to induce significant internalization compared to control, both in the recombinant systems and in neuronal tissues of tolerant rats. In contrast, UFP-505 induced significant internalization of MOP and DOP in all recombinant systems and in the neuronal tissue of non-tolerant rats. However, the percentage internalization induced in the latter was much lower compared to the recombinant systems and this may be due to lower levels of expression in the native tissues or due to other differences in methodology between these two systems (i.e. drug incubation time, dose).

Collectively, these data indicate that UFP-505 induces significant internalization of both MOP and DOP receptors in a recombinant system, which is consistent with its capacity to induce MOP and DOP receptor internalization *in vivo*.

Internalization (%) induced by various ligands					
System	Receptor studied	Ligands tested			
		<i>Morphine</i>	<i>UFP-505</i>	<i>DPDPE</i>	<i>EMI</i>
CHO _{hMOP} ⁽¹⁾	MOP	8.0	62.4 *	-	49.6 *
CHO _{hDOP} ⁽²⁾	DOP	-	86.2 *	80.4 *	-
CHO _{hMOP/hDOP} ⁽³⁾	MOP & DOP	4.5	61.9 *	26.6 *	43.3 *
Rat Frontal cortex ⁽⁴⁾	MOP	3.0	36.5 *	-	-
	DOP	-13.3	48.8 *	-	-
Rat Spinal cord ⁽⁴⁾	MOP	7.10	44.7 *	-	-
	DOP	1.7	43.1 *	-	-

Table 7.3. Ligand induced internalization (% reduction of B_{max} compared with control) by various ligands tested in single-expression systems (CHO_{hMOP} and CHO_{hDOP}), a double-expression system (CHO_{hMOP/hDOP}) and neuronal tissue of treated animals (frontal cortex and spinal cord). Ligands induced internalization after either one hour incubation of 10 μ M (**1**, **2** and **3**) or intrathecal administration of 10nmol for three days to Wistar rats (**4**). *Significant differences from control ($p < 0.05$). Morphine fails to induce internalization of opioid receptors in all systems tested, in contrast to UFP-505 which induced significant internalization of both MOP and DOP receptors in all systems tested.

CHAPTER 8.
GENERAL DISCUSSION

Chapter 8. General Discussion

Despite many years of drug development, the mainstay of treatment for the majority of patients with cancer pain is agents such as morphine acting at the MOP (μ ; mu) receptor. Indeed, morphine is still considered by clinicians as the gold standard against which new molecules are compared. The evidence shows that the presentation of cancer pain varies widely and that it is still undertreated. There are several factors that lead to this undertreatment, including poor assessment of pain intensity, reluctance of many clinicians to prescribe opioids, patient compliance due to route of administration and, in many cases, opioid related side effects. Although chronic administration of morphine to cancer patients can produce a number of side effects (i.e. respiratory depression and arrest, constipation, nausea, vomiting and pruritis), analgesic tolerance is regarded by clinicians as the most difficult to address. This is because tolerance leads to increasing dose requirements and therefore inevitably, to more side effects because of this increase (see figure 1.14; Chapter 1). A major problem has been the lack of drugs that would be equally effective as morphine but without developing analgesic tolerance. This lack of effective non-tolerant analgesics in the clinic reflects the relative lack of basic knowledge on the the molecular and cellular mechanisms responsible for the development of opioid tolerance and how they are regulated.

The inability of the MOP receptor to internalize after activation by morphine has been directly linked with the development of analgesic tolerance (Berger & Whistler, 2010; Kim *et al*, 2008), although there are a number of additional (signaling) mechanisms that are found to contribute to this (Liu & Prather, 2001; Raehal & Bohn, 2011). On the other hand, blockade of DOP receptors with an antagonist (Abdelhamid *et al*, 1991;

Fundytus *et al*, 1995), antisense DOP knockdown (Kest *et al*, 1996) and knockout of the DOP receptor (Nitsche *et al*, 2002; Zhu *et al*, 1999) reduces morphine tolerance and this coincides with the co-localisation and co-expression of MOP and DOP (Cheng *et al*, 1997; Wang *et al*, 2010) and the existence of MOP/DOP dimers (George *et al*, 2000; Gomes *et al*, 2000; Law *et al*, 2005; Liu *et al*, 2009). Unfortunately, to date there are no DOP antagonists available for clinical use and therefore there is a growing interest in the development of bifunctional opioids (MOP agonists/DOP antagonists) in order to investigate whether they show reduced tolerance. This *in vitro-in vivo* project has examined the pharmacology of the novel bifunctional pseudopeptide prototype UFP-505 (H-Dmt-Tic-Gly-NH-Bzl).

8.1. Summary of main findings

Figure 8.1 summarizes the overall findings of this thesis by presenting the key aims and results.

In **Chapter 3**, the B_{\max} of CHO cells expressing recombinant opioid receptors was determined using the radiolabeled non-selective opioid antagonist diprenorphine (^3H -DPN), and the dissociation constant (K_d) of the radioligand was calculated. The binding affinities of UFP-505 and selective reference ligands to opioid receptors were determined by displacement binding assays. UFP-505 was shown to have an affinity for

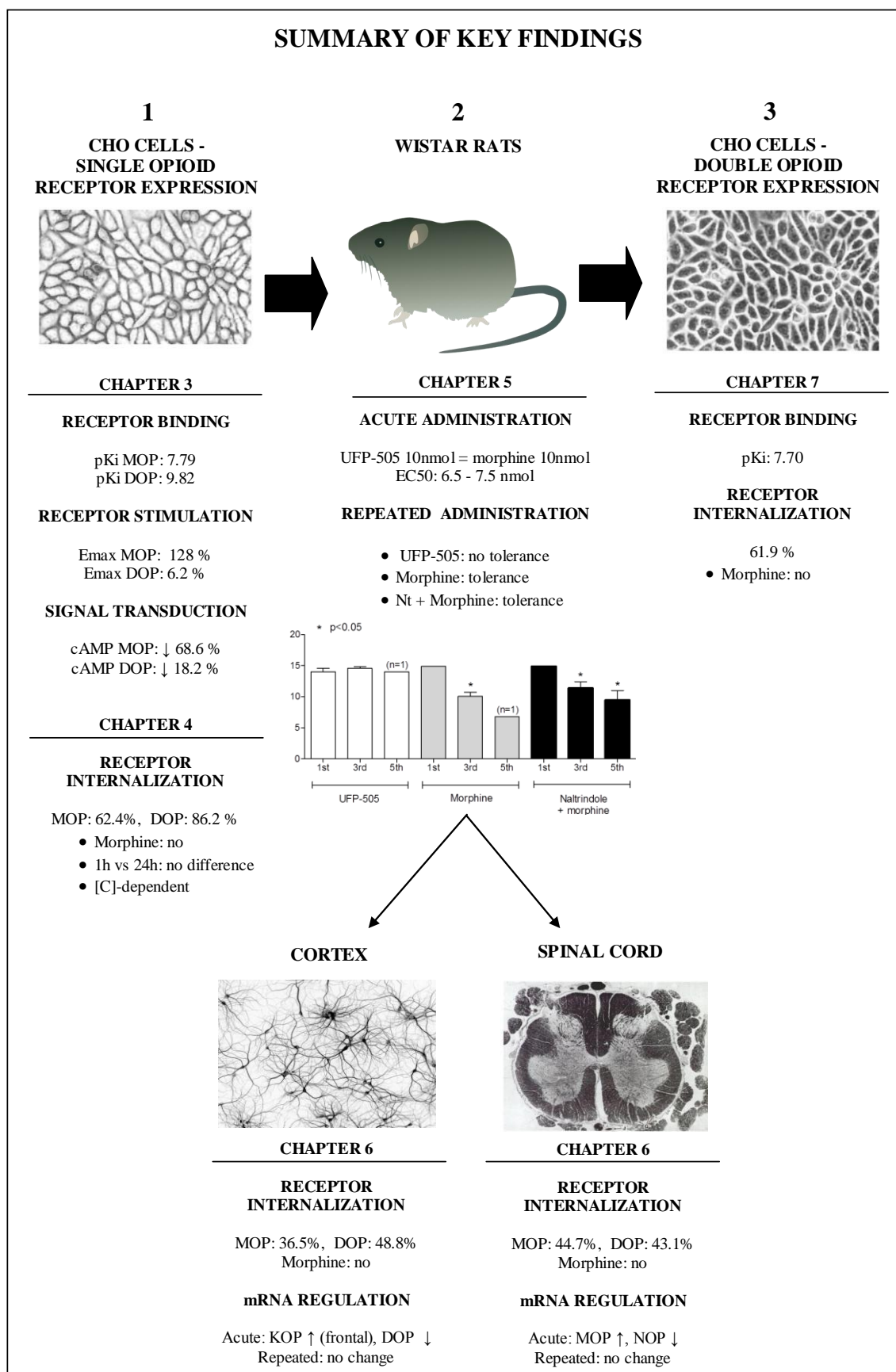


Figure 8.1. Illustration of the key findings of the thesis, showing the sequence of the models used (1, 2 and 3) and the chapters where each finding is presented analytically.

MOP and DOP receptors similar to the selective reference ligands used (endomorphin-1 and naltrindole respectively), whereas it did not exhibit substantial affinity for the KOP and NOP receptors. The effect of UFP-505 binding to MOP and DOP receptors was studied in functional assays investigating G-protein activation (GTP γ ³⁵S assay) and second-messenger formation (cAMP assay). UFP-505 binding to MOP produced a stimulation of G-protein activation and inhibition of cAMP formation comparable to that of endomorphin-1. At the DOP receptor, UFP-505 produced a non-significant stimulation and a weak, but significant, inhibition of cAMP formation about 4 times lower than that produced by the potent specific DOP agonist DPDPE. UFP-505 was further characterized by binding and functional assays in higher-expression recombinant systems as well as in rat spinal cord and rat spinal cortex tissues. UFP-505 was characterized as a MOP receptor agonist and a DOP receptor weak partial agonist in the models studied.

The effects of UFP-505 on opioid receptor internalization were studied in **Chapter 4**, with reference to morphine and other ligands. UFP-505 produced a higher degree of MOP receptor internalization in CHO_{hMOP} cells compared to fentanyl and endomorphin-1, whereas morphine failed to cause significant internalization. The MOP internalization caused by UFP-505 was shown to be independent of the incubation time (no significant difference of 1 hour vs 24 hours) and concentration-dependent. Additionally, UFP-505 caused DOP receptor internalization in CHO_{hDOP} cells similar to that caused by DPDPE. Further investigation ruled out the possibility that the reduction in B_{max} observed could be attributed to insufficient removal of the radioligand from the system prior to the assay, as was shown by an unchanged binding affinity of ³H-DPN following extensive washing.

Chapter 5 presented *in vivo* data of UFP-505 administration to Wistar rats and investigated the effects of subchronic administration of UFP-505 and morphine, in terms of analgesic efficacy and development of tolerance. The acute intrathecal administration of 10 nmol UFP-505 was shown to be equianalgesic to 10 nmol morphine by a tail-flick antinociception assay. Administration of a range of different doses of UFP-505 produced an EC₅₀ close to 7 nmol, as determined by analysis of the analgesic levels after two hours of administration and by analysis of overall analgesia (area under curve). Morphine produces tolerance (expressed by gradual reduction of antinociception) but UFP-505 maintains high levels of analgesia after three days. The co-administration of naltrindole and morphine alleviated the reduction of antinociception levels compared to morphine alone. Additionally, investigation of analgesia in rats after repeated administration of subcutaneous morphine has shown tolerance after three days. The data presented in this chapter are the first ever *in vivo* data of UFP-505 and provide evidence of reduced tolerance after repeated administration of a bifunctional ligand.

In **Chapter 6**, neuronal tissue extracted from animals used in the *in vivo* study (cortex and spinal cord) was used to study opioid receptor internalization and regulation of opioid receptor mRNA. Tissue from acutely-treated animals showed that a single dose of intrathecal UFP-505 induced significant MOP and DOP receptor internalization in both the cortex and the spinal cord, whereas morphine failed to induce receptor internalization in both tissues. In spinal cord samples from acutely-treated animals, a single dose of morphine or UFP-505 caused the upregulation of the mRNA of MOP and DOP receptors, along with downregulation of the NOP receptor mRNA. However, in the cortex there were varying effects, with an upregulation of the KOP receptor in the

frontal cortex and the downregulation of the DOP receptor in the rest of the cortex. In contrast, tissue samples from repeatedly-treated animals with morphine, UFP-505 or naltrindole+morphine (extracted after three days of administration), have shown no change in the mRNA levels of all opioid receptors, a result that was consistent with data from the analysis of tissues from the subcutaneously-treated animals for four days with morphine. These data indicate that UFP-505 and morphine have differential effects in terms of receptor internalization after acute intrathecal administration in neuronal tissue, but have similar effects in terms of regulation of opioid receptor mRNA. Additionally, it was shown that the effects of ligands on receptor mRNA levels can vary in different tissues as shown by frontal cortex and spinal cord data.

Finally, **Chapter 7** presented data of opioid receptor binding and opioid receptor internalization of UFP-505 and reference ligands in a novel recombinant double-expression system (CHO_{hMOP/hDOP}), which was generated by transfection of CHO_{hMOP} cells with a plasmid containing the human DOP receptor gene. This model provided a system where the pharmacology of the ligands could be studied in isolation from KOP and NOP receptors, but with the simultaneous presence of MOP and DOP (in contrast to the single-expression system and the *in vivo* study). In this model it was shown that all ligands studied (morphine, UFP-505, EM1 and naltrindole) exhibited similar binding affinities, showing differences from half-log to two-logs compared to those exhibited in the single-expression systems. Investigating internalization in the double-expression system, UFP-505, EM1 and DPDPE induced significant internalization of opioid receptors, whereas morphine was ineffective. These data show that the co-expression of the two opioid receptors causes a reduction in the high binding affinities of ligands that are selective for one receptor. Additionally, the data in this chapter show that UFP-505

and morphine in the double-expression system behave the same as in the single-expression system in terms of induction of receptor internalization.

8.2. Putting the thesis findings into context with existing literature

8.2.1. Other UFP-505 data

UFP-505 is a prototype bifunctional pseudopeptide, developed by the spinout company University of Ferrara Peptides as part of a project that produced a number of compounds which were chemically related, using the pharmacophore Dmt-Tic as a reference since it was used chemically as a starting point in the synthesis. In 2002, Balboni and colleagues published the first preliminary *in vitro* data for UFP-505 as part of a group of Dmt-Tic analogue compounds (Balboni *et al*, 2002).

Table 8.1 shows collective data for UFP-505 from the literature with reference to data presented in this thesis. In the Balboni paper, UFP-505 (compound 6) was tested in a rat brain receptor assay and produced binding affinities (K_i) of 0.031 nM for the DOP and 0.16 nM for the MOP receptor. Additionally, UFP-505 produced a pA_2 of 9.25 in

UFP-505 pharmacological data		
Characteristic	Thesis	Literature
K_i MOP	16.2 nM (CHO _{hMOP})	0.16 nM (rat brain assay) ¹ 2.20 nM (CHO _{hMOP}) ² 26 nM (C6 _{rMOP} rat glioma) ³
K_i DOP	0.15 nM (CHO _{hDOP})	0.03 nM (rat brain assay) ¹ 0.26 nM (CHO _{hDOP}) ² 0.20 nM (C6 _{rDOP} rat glioma) ³
K_i KOP	512.89 nM (CHO _{hKOP})	128 nM (CHO _{hKOP}) ³
E_{max} MOP	128% (CHO _{hMOP})	84% (CHO _{hMOP}) ^{2, a} <10% (C6 _{rMOP} rat glioma) ^{3, b}
E_{max} DOP	6.2% (CHO _{hDOP})	6.8% (CHO _{hDOP}) ^{2, a} <10% (C6 _{rDOP} rat glioma) ^{3, b}
EC₅₀ MOP	426 nM (CHO _{hMOP})	19 nM (CHO _{hMOP}) ²
EC₅₀ DOP	<i>n/a</i> (CHO _{hDOP})	<i>n/a</i> (CHO _{hDOP}) ²
MOP cAMP inhibition (% of max)	82.62% at 10nM (CHO _{hMOP})	30% (C6 _{rMOP} rat glioma) ³
DOP cAMP inhibition (% decrease)	18.3% at 10 nM (CHO _{hDOP})	28% (C6 _{rDOP} rat glioma) ³
IC₅₀ DOP	-	1.3 nM (GTP ³⁵ γS assay; CHO _{hDOP}) ² 0.7 nM (cAMP assay; C6 _{rDOP} rat glioma) ³
IC₅₀ MOP	-	<i>n/i</i> (GTP ³⁵ γS assay; CHO _{hMOP}) ² 45 nM (cAMP assay; C6 _{rMOP} rat glioma) ³
pA₂ <i>ex vivo</i>	-	9.25 (MVD) ¹ 9.15 (MVD) ⁴
EC₅₀ <i>ex vivo</i>	-	2.69 nM (GPI) ¹ 31.62 nM (GPI) ⁴

Table 8.1. UFP-505 pharmacological data as published in the literature, in comparison with data in this thesis. Keys: *n/s*; non-significant, *n/a*; not active, *n/i*; not inhibitory, ^a percentage stimulation of GTPγ³⁵S binding from basal (un-stimulated), ^b percentage of maximal GTPγ³⁵S binding obtained with 10μM of ligand compared to a 10μM of DAMGO, ¹ Balboni et al 2002, ² Balboni et al 2010, ³ Purington et al 2011, ⁴ Molinari, Guerrini and Calo unpublished data presented in Chapter 3 (section 3.10) of this thesis. Balboni 2010 and Purington 2011 coincide with the conduct of the experimental phase of this thesis.

the electrically-stimulated MVD preparation, and an EC₅₀ of 2.69 nM in the electrically-stimulated GPI. In Chapter 3 (section 3.10) we discussed some *ex vivo* data produced by S. Molinari, G. Calo and R. Guerrini at the University of Ferrara in Italy. The UFP-505 pA₂ (9.15) in MVD agrees with the Balboni data shown above, although the EC₅₀ (31.62 nM) in GPI was found higher.

In a second paper published by Balboni et al in 2010 (Balboni *et al*, 2010), the authors presented the first preliminary data of UFP-505 (compound 1) at human opioid receptors expressed in CHO cells, by displacement of ³H-DAMGO and ³H-naltrindole in MOP and DOP respectively. UFP-505 pK_i values from CHO cells were similar to those presented in this thesis, although using different radioligands (table 8.1). Nevertheless, comparing Balboni's 2002 and 2010 data using rat brain and human receptors in CHO cells respectively, the values differ markedly, which further underscores the importance of the system used when comparing data for the same compound.

In a GTPγ³⁵S assay Balboni et al (2010) demonstrated that UFP-505 exhibited an E_{max} of 84% and an EC₅₀ of 19 nM for the MOP receptor, which is lower than the data in this thesis. For the DOP receptor in the same paper, they showed an I_{max} of 95% and an IC₅₀ of 1.3 nM (by GTPγ³⁵S assay in the presence of a DOP agonist; 10 nM SNC80). Additionally, in DOP cells Balboni et al showed a UFP-505 E_{max} of 6.8%, which is in agreement with the 6.2% presented in this thesis (table 8.1)

Recently, Purington and colleagues (Purington *et al*, 2011), presented data for another novel bifunctional (MOP/DOP) opioid ligand (KSK-103) and used UFP-505 as a comparator, in a C6 rat glioma cell model (for MOP and DOP studies) and CHO_{hKOP}

cells (for KOP studies). For UFP-505 binding, they showed a K_i of 26 nM, 0.2 nM and 128 nM for the MOP, DOP and KOP receptors respectively, by 0.2nM ^3H -DPN displacement (table 8.1). Although the affinities at the MOP and KOP receptors were found to be lower than the data in this thesis, the UFP-505 affinity for the DOP receptor agrees with our data. For the activation of the G-protein, the Purington paper also presented a “*non-significant stimulation of G-protein*” for UFP-505 for all receptors, which disagrees with both Balboni papers, as well as with data in this thesis. In cAMP assays, Purington et al presented a 30% maximum inhibition and a 28% decrease of forskolin-stimulated cAMP in cells expressing the MOP and DOP receptor respectively, concluding that UFP-505 is ‘a partial MOP-agonist/partial DOP-agonist’. These data are in contrast to this thesis that shows 82.62% and 18.3% respective values (MOP and DOP) for inhibition of forskolin-stimulated cAMP production, and not any statistical difference from the EM1 value (91.62%).

From the above, it is interesting that most of Purington *et al* data disagree with previous publications and with data in this thesis. In an attempt to explain this inconsistency, there are two major points to underline for the Purington paper: Firstly, the authors did not present any data for the opioid receptor density of the cell-lines used. As know from previous publications (McDonald *et al*, 2003) and from data shown in this thesis (figure 3.7, Chapter 3), receptor density may play a key-role when interpreting functional data and therefore providing the receptor density of the system used is important. Secondly and most importantly, there is a concern for using the recombinant C6 rat glioma cell-line (used frequently in literature for studying opioid-induced neural proliferation) as an appropriate model for studying opioid receptor pharmacology. Very early studies identified the expression of enkephalin precursor in these cells, observing that activation

of adenylate cyclase by forskolin elevated the preproenkephalin mRNA abundance in these cells (Yoshikawa & Sabol, 1986). Later studies have reported a low but significant expression of all classical opioid receptors in C6 glioma cells, although it was observed that specific binding of ligands to the expressed MOP receptors required treatment of these cells with the tricyclic compound desipramine (Bohn *et al*, 1998). All the above information questions the suitability of this cell model for the study of opioid pharmacology and may partially explain the differences with the Purington *et al* data.

8.2.2. Data in the literature for other bifunctional compounds

Bifunctional compounds have long been studied in opioid pharmacology, with a range of different strategies employed in chemical modifications of existing ligands to yield mixed receptor activity, or the addition of two pharmacophores through an intermediate linker (spacer) to produce a bivalent compound (Ding *et al*, 2012; Portoghese, 1989). Tables 8.2 and 8.3 show some examples of reported bifunctional and bivalent ligands in the literature.

The first peptide ligand with mixed MOP-agonist/DOP-antagonist activity was reported by the Schiller group (Schmidt *et al*, 1994). Based on the reported reduced tolerance after the co-administration of a DOP antagonist and a MOP agonist there has been a wider effort to develop novel bifunctional ligands with a MOP-agonist/DOP-antagonist activity. The Schiller group linked a DOP antagonist (H-Tyr-TicΨ[CH₂-NH]Cha-Phe-OH) with a selective MOP agonist (H-Dmt-D-Arg-Phe-Lys-NH₂) to produce a bivalent ligand with a high binding affinity to MOP and DOP receptors (Weltrowska *et al*, 2004). The group has produced a number of different analogues and reported a range of binding affinities *in vitro*, all within the nanomolar region (Ding *et al*, 2012). Neumeyer

et al reported a mixed ligand consisting of a butorphan analogue (a MOP/KOP agonist) and the Dmt-Tic pharmacophore (Neumeyer *et al*, 2006), whereas Salvadori and colleagues (Salvadori *et al*, 2007) have produced a bifunctional opioid ligand derived from endomorphin-2 and Dmt-Tic. Most of these studies had focused on the chemistry of these ligands rather than their biological effect and apart from the reported binding affinities the majority of these studies did not provide further *in vitro* or *in vivo* characterization. However, Purington et al have recently reported a novel MOP/DOP bifunctional tetrapeptide (KSK-103), providing data of its binding and functional properties (Purington *et al*, 2011). KSK-103 has been reported to show equal binding affinities for MOP and DOP receptors (2.4 nM and 2.3 nM respectively), which is higher than UFP-505 for the MOP and lower for the DOP (16nM and 0.15nM respectively, as shown in table 8.1). KSK-103 stimulated the activation of G-protein associated with the MOP receptor with the same efficacy as morphine but with increased potency (EC_{50} 4.7nM) which was markedly higher than UFP-505 (426nM). In addition, KSK-103 inhibited cAMP production by 77% at the MOP receptor, which is similar to UFP-505. KSK-103 did not activate the G-protein associated with the DOP receptor (K_b 4.4nM) and did not significantly inhibit cAMP formation (K_b 12nM and 9% inhibition) which implies DOP antagonism by KSK-103.

<i>Bifunctional ligands</i>	<i>Ki(μ) (nM)</i>	<i>Ki(δ) (nM)</i>	<i>Pharmacological Profile*</i>
Butorphan	0.23	5.90	MOP ^A – DOP ^A – KOP ^A (Mathews <i>et al.</i> , 2005)
Naltrexone	0.23	38.0	MOP ^N – DOP ^N – KOP ^N (Peng <i>et al.</i> , 2007)
Cyclorphan	0.06	1.90	MOP ^A – DOP ^A (Peng <i>et al.</i> , 2007)
H-Dmt-Tic-Gly-NH-CH ₂ -Ph	0.16, <i>pEC</i> ₅₀ μ=7.70	0.03, <i>pA</i> ₂ δ = 9.25	MOP ^A – DOP ^N (Balboni <i>et al.</i> , 2002)
H-Dmt-Tic-Gly-NH-Ph	0.16, <i>pEC</i> ₅₀ μ=8.59	0.04, <i>pEC</i> ₅₀ δ=8.52	MOP ^A – DOP ^A (Balboni <i>et al.</i> , 2002)
H-Dmt-Tic-NH-CH ₂ -Bid	0.50, <i>pEC</i> ₅₀ μ=7.57	0.03, <i>pEC</i> ₅₀ δ=9.90	MOP ^A – DOP ^A (Balboni <i>et al.</i> , 2002)
H-Dmt-Tic-Gly-NH-CH ₂ -Bid	20.5, <i>pEC</i> ₅₀ μ =6.45	0.06, <i>pA</i> ₂ δ =9.00	MOP ^A – DOP ^N (Balboni <i>et al.</i> , 2002)
H-Dmt-Tic-Phe-Phe-NH ₂	1.19	0.12	MOP ^A – DOP ^N (Schiller <i>et al.</i> , 1999)
H-Tmt-Tic-Phe-Phe-NH ₂	4.08	0.39	MOP ^A – DOP ^N (Schiller <i>et al.</i> , 1999)
H-Dmt-TicΨ[CH ₂ NH]-Phe-Phe-NH ₂	0.94	0.48	MOP ^A – DOP ^N (Schiller <i>et al.</i> , 1999)
H-Tyr-Tic-Phe-Phe-NH ₂	78.8	3.00	MOP ^A – DOP ^N (Schiller <i>et al.</i> , 1999)
H- Dmt-Pro-Trp-D-1-Nal-NH ₂		<i>pA</i> ₂ δ =8.59	MOP ^A – DOP ^N (Fichna <i>et al.</i> , 2007)

Table 8.2 (identical to Table 1.2, p47). Receptor binding (*K_i* (Cheng & Prusoff, 1973)) and general pharmacological profile of various bifunctional (non-selective) ligands at opioid receptors. Table shows data for the μ, (MOP) and δ (DOP) receptors. Keys: 2',6'-dimethyl-L-tyrosine (Dmt), tetrahydroisoquinoline-3-carboxylic acid (Tic), benzyimidazole (Bid), phenyl (Ph), phenylalanine (Phe), glycine (Gly), tyrosine (Tyr), glycine (Gly), alanine (Ala), tyrosine (Tyr), tryptophan (Trp), proline (Pro), 3-[1-naphthyl-D-Ala] (D-1-Nal). *The profile of bivalent ligands is denoted as μ (MOP), δ (DOP), κ (KOP), A (agonist) and N (antagonist).

Pharmacophore 1	Linker	Pharmacophore 2	K _i (MOP) (nM)	K _i (DOP) (nM)	K _i (KOP) (nM)	Pharmacological profile *
Bivalent Ligands						
H-Tyr- <i>D</i> -Phe	NH-NH	<i>D</i> -Phe-Tyr-H	31.0	187	360	MOP ^A - DOP ^A (Lipkowski <i>et al</i> , 1982)
H-Tyr- <i>D</i> -Ala-Gly-Phe	NH-NH	Phe-Gly- <i>D</i> -Ala-Tyr-H	1.40	2.60		MOP ^A - DOP ^A (Lipkowski <i>et al</i> , 1999)
Butorphan	fumaryl ester	Butorphan	0.20	9.40	0.08	MOP ^A - KOP ^A (Mathews <i>et al</i> , 2005)
Butorphan	10-C linker	Butorphan	0.09	4.20	0.05	MOP ^A - KOP ^A (Peng <i>et al</i> , 2007)
(-)-Butorphan	10-C linker	(+)-Butorphan	2.20	23.0	1.20	MOP ^A - KOP ^A (Neumeyer <i>et al</i> , 2003)
Dmt-Tic-OH	β-Ala	Butorphan	0.69	1.50	0.28	mixed-N (Neumeyer <i>et al</i> , 2006)
<i>N,N</i> -dimethyl-Dmt-Tic	Diaminoalkyl-pyrazinon	<i>N,N</i> -dimethyl-Dmt-Tic	1.68, <i>pA</i> ₂ 7.7	0.29, <i>pA</i> ₂ 10.4		MOP ^N - DOP ^N (Li <i>et al</i> , 2005)
<i>N,N</i> -dimethyl-Dmt-Tic	NH-(CH ₂) ₆ -NH	<i>N,N</i> -dimethyl-Dmt-Tic	2.21, <i>pA</i> ₂ 8.3	0.06, <i>pA</i> ₂ 11.3		MOP ^N - DOP ^N (Li <i>et al</i> , 2005)
Dmt	Aminoalkyl linker	Dmt	0.04	14.8		MOP ^A - DOP ^N (Okada <i>et al</i> , 2003)
Endomorphin-2	ethylenediamine	Dmt-Tic	1.03	1.45		MOP ^A - DOP ^N (Salvadori <i>et al</i> , 2007)
JD	(no linker)	Tic	3.73	301	0.32	MOP ^A - KOP ^N (Carroll <i>et al</i> , 2004)
Reference compounds						
Dermorphin	-	-	0.28	82.5	1.10	MOP ^A (Balboni <i>et al</i> , 2002)
Endomorphin-2	-	-	0.69	9233	5240	MOP ^A (Harrison <i>et al</i> , 1999)
Morphine	-	-	0.88	140	24	MOP ^A (Peng <i>et al</i> , 2006)
Deltorphan C	-	-	387	0.21	0.08	DOP ^A (Balboni <i>et al</i> , 2002)
Dynorphin A(1-13)	-	-	0.50	4.40	0.11	KOP ^A (Martinka <i>et al</i> , 1991)
Naloxone	-	-	0.79	76.0	0.25	mixed-N (Balboni <i>et al</i> , 2002; Peng <i>et al</i> , 2007)
Dmt-Tic-OH	-	-		0.022		DOP ^N (Li <i>et al</i> , 2005)
NTI	-	-	50	0.29, <i>pA</i> ₂ 7.95	34.1	DOP ^N (Ananthan <i>et al</i> , 1998)

Table 8.3 (identical to Table 1.3, p49). Receptor binding (*K_i* (Cheng & Prusoff, 1973)) and general pharmacological profile of various bivalent ligands, monovalent ligands and endogenous peptides at the μ, (MOP) δ (DOP) and κ (KOP) opioid receptors. Key: 2',6'-dimethyl-L-tyrosine (Dmt), naltrindole (NTI), tetrahydroisoquinoline-3-carboxylic acid (Tic), benzimidazole (Bid), phenyl (Ph), (3*R*)-7-hydroxy-*N*-((1*S*)-1-[(3*R*,4*R*)-4-3(hydroxyphenyl)-3,4-dimethyl-1-piperidin]methyl}-2-methylpropyl (JD), phenylalanine (Phe), glycine (Gly), alanine (Ala), tyrosine (Tyr), proline (Pro), Tyr-Pro-Phe-Phe-NH₂ (endomorphin-2,). *The profile of bivalent ligands is denoted as M (MOP), D (DOP), K (KOP), A (agonist) and N (antagonist). i.e MDAN (MOP-agonist and DOP-antagonist).

8.2.3. Receptor internalization and analgesic tolerance

In an effort to place the findings of this thesis into context, one has to acknowledge the current most popular theory on the role of receptor internalization in analgesic tolerance and Berger et al (Berger & Whistler, 2010) provides an analysis of this theory in four cellular ‘stages’ of opioid receptor function (shown in figure 8.2): 1) receptor activation leads to receptor phosphorylation and dissociation of the receptor from its G-protein. At this stage the receptor interacts with many proteins (GRKs, arrestins, etc) and is regarded as ‘desensitized’ (i.e. receptor occupancy does not lead to further activation), which is a cellular mechanism of defence against prolonged activation, 2) receptor is internalized by endocytosis through an arrestin-dependent or an arrestin-independent mechanism, in order to be dephosphorylated and thus to be ready for G-protein association (resensitization). Different receptors can have a different fate (i.e. degradation by lysosomal enzymes), 3) the receptor recycles back to the cell surface by association with various ‘guide’ proteins. Disruption of any of these steps by any opioid can lead to physiological side-effects apart from analgesia (i.e. tolerance, hyperalgesia, etc).

COPYRIGHT MATERIAL - IMAGE REMOVED

Figure 8.2. *Opioid receptor (OP) trafficking upon binding and activation of an opioid ligand (A). Receptor desensitization, endocytosis (i.e. internalization) and recycling are part of a cellular mechanism that prevents prolonged receptor activation. This thesis has provided evidence for UFP-505 receptor binding (α), activation (β , γ) and internalization (δ). The figure was modified from (Berger & Whistler, 2010).*

It is widely accepted that the inability of morphine to induce MOP receptor internalization plays a key-role in tolerance. Indeed, data in this thesis provide evidence that morphine fails to induce MOP or DOP receptor internalization, *in vitro* or *in vivo* after acute administration, along with analgesic tolerance after repeated administration. The literature provides strong evidence for various agents (i.e. methadone, oxycodone, fentanyl) that produce analgesia accompanied by induction of MOP internalization, and that they also have reduced propensity to produce analgesic tolerance (Alvarez *et al*, 2002; Arttamangkul *et al*, 2006; Dang *et al*, 2011; Enquist *et al*, 2011; Koch & Höllt, 2008; Martini & Whistler, 2007; Narita *et al*, 2006; Silva-Moreno *et al*, 2012; Whistler, 2012; Zuo, 2005). These observations agree with the data of UFP-505-induced receptor

internalization (*in vitro* and *in vivo*) and its aversion for the induction of tolerance *in vivo*.

In a recent paper (Kim *et al*, 2008), Whistler and colleagues tested a novel mutant MOP receptor that underwent morphine-induced endocytosis in a knock-in mouse model and reported substantially reduced antinociceptive tolerance and physical dependence (43% reduction in antinociception compared to pre-treatment scores, expressed as % MPE; maximum possible effect ¹). By transforming the data in figure 5.4 and 5.6 of this thesis to % MPE (calculations showed in Appendix; Section A5) it is shown that, after 3 days of repeated intrathecal administration, UFP-505 did not show any reduction in analgesia compared to a 37% reduction in analgesia in morphine-treated rats.

It is known that most DOP agonists can internalize the DOP receptor upon activation and in most cases the internalization results in full receptor degradation by lysosomal enzymes. In a study looking at the *in vitro* pharmacology of UFP-512 (a DOP agonist with a very similar structure to UFP-505 and the same DOP-acting pharmacophore; Dmt-Tic) it was found that UFP-512 can desensitize, internalize and successfully recycle human DOP receptors in a human neuroblastoma cell line (Aguila *et al*, 2007). In this thesis, UFP-505 has been shown to cause the internalization of the DOP receptor *in vitro* and *in vivo*, probably because of its residual DOP agonism. It is possible that the effect of UFP-505 in DOP receptor internalization may play a key role in its sustained analgesia and reduced tolerance profile discussed above.

¹ % MPE = [(postdrug latency – baseline latency)/(cutoff time – baseline latency)] × 100

Additionally, the role of DOP receptor in MOP-induced analgesia has been investigated in a very interesting study by Cahill and colleagues (Cahill *et al*, 2001). They showed that treatment of cultured cortical neurons for 48 hours with morphine lead to an increase in DOP receptors on the cell surface, which augmented DOP-induced analgesia *in vivo*. Based on Western blot analysis, Cahill et al suggested that the increase in receptors was caused by translocation of receptor reserves and not upregulation via mRNA synthesis. As reported in this thesis, morphine induced upregulation of DOP mRNA in the spinal cord of acutely-treated animals, which was not seen in tissues of repeatedly-treated animals. This agrees with Cahill et al since an incubation time of 48h *in vitro* may be a simulation of the cellular responses in subchronic treatment *in vivo* where we were unable to detect changes in opioid receptor mRNA levels. The mechanism that Cahill et al propose is MOP-mediated, as it was blocked by a selective MOP antagonist. These data could suggest that the UFP-505-induced DOP internalization shown *in vivo* may be both due to its residual DOP agonism (as shown *in vitro* in CHO_{hDOP} cells in this thesis) and its ability to activate the MOP receptor (as shown *in vitro* in CHO_{hMOP/hDOP} cells and native tissue in this thesis).

8.2.4. *In vivo* studies of analgesic tolerance with bifunctional ligands

There are a large number of studies that have investigated the development of analgesic tolerance after co-administration of various opioid ligands. Although there are a large number of novel bifunctional opioid compounds that have been reported to have high affinity for opioid receptors or increased potency *in vitro*, only a few of them have been tested for their analgesic activity *in vivo*, or their capacity to produce tolerance. Schiller and colleagues reported the first *in vivo* data of a mixed opioid compound in rats, DIPP(Ψ)NH₂, which had affinity for all three classical opioid receptors (0.4 nM at MOP

and DOP, 3.9 nM at KOP). The compound produced a potent analgesic effect and reduced tolerance, although the development of tolerance was not completely avoided (Schiller *et al*, 1999). In an interesting study by Roy and colleagues, knock-in mice with a mutant MOP receptor that conferred MOP agonism to the non-selective opioid antagonist naltrexone, showed analgesia with no tolerance to morphine or naltrexone (Roy *et al*, 2005). The authors based this result to the simultaneous activation of the mutant receptor as well as the block of the DOP receptor. A similar activity was observed *in vivo* with UFP-505 as presented in this thesis, with sustained analgesia after 2 hours of i.t. administration and reduced tolerance after 3 days of administration. In the same study by Roy *et al*, the authors suggested that inhibition of the DOP receptor must occur at the time of MOP activation to prevent development of tolerance. This suggestion could partially explain why the co-administration of naltrindole and morphine in the repeated-administration experiments presented in the thesis did not result in the complete prevention of tolerance (naltrindole was administered 10 mins prior to morphine).

The Portuguese group extensively studied the pharmacology of synthetic bivalent opioid ligands. In an *in vivo* study with mice (Daniels *et al*, 2005), the authors used i.c.v administration of a range of MDAN ligands (MOP-agonists/DOP-antagonists), that had linkers of varying length between pharmacophores. They observed that only the ligands with a space of 19 atoms or greater between pharmacophores showed reduced tolerance and dependence in chronically-treated animals, suggesting that these ligands act on MOP-DOP heterodimers and when they have an optimum distance can produce reduced analgesic tolerance. In contrast, although UFP-505 is a much smaller molecule than MDAN-19 (number shows spacer length in atoms), it is shown in this thesis that it

possesses a lower capacity for tolerance than morphine. This contradiction between the Daniels et al conclusion and the UFP-505 data on the importance of ligand length in terms of reduced tolerance, was further expanded by Ding et al (Ding *et al*, 2012) where bivalent MOP-agonist/DOP-antagonist compounds of varying lengths have been tested *in vitro* for their binding affinities. Ding et al showed decreasing MOP and DOP receptor binding affinities with increasing ligand length and concluded that any change in the length of a ligand analogue from its parent compound would result in a major change in its intrinsic efficacy.

What is very interesting is that, apart from reduced morphine tolerance reported in the literature when blocking or depleting the DOP receptor, there are a number of studies that report similar results with mixed MOP/DOP agonist ligands, which can be interesting in terms of the weak DOP partial activity shown *in vitro* for UFP-505. Lowery et al (Lowery *et al*, 2011) has tested a mixed MOP/DOP agonist in mice (MMP-2200), showing a strong antinociceptive capacity with reduced tolerance after repeated administration for 3 days. In another study by Yamazaki et al (Yamazaki *et al*, 2001), biphalin (a mixed MOP/DOP agonist) produced antinociceptive effects comparable to morphine after systemic injection and was shown to produce less tolerance and dependence than morphine after chronic use. These data are very similar to the *in vivo* data in this thesis.

Taken collectively, data for UFP-505 from this thesis and from other studies, indicate that a) UFP-505 behaves as a DOP weak partial agonist *in vitro* and a DOP antagonist *ex vivo* (stimulated MVD preparations in figure 3.13, Chapter 3), b) causes MOP and DOP receptor internalization *in vitro* and *in vivo* and c) causes prolonged analgesia with

reduced tolerance. As such UFP-505 may have a unique set of pharmacological properties that can advantageous compared to an absolute MOP-agonist/DOP-antagonist.

8.3. Unexpected and contentious issues arising from this thesis

8.3.1. Residual DOP agonism for UFP-505

As shown in this thesis, UFP-505 did not stimulate the G-protein activation of DOP receptors in CHO_{hDOP} cells (figure 3.6). However, in a higher expression system (CHO_{hDOP/high}), the efficacy of UFP-505 is amplified to significant percentage of maximum receptor stimulation (E_{\max} ~14%; figure 3.7). Residual agonism at the DOP receptor was confirmed by providing evidence downstream using a cAMP assay in CHO_{hDOP} cells, showing a significant inhibition of cAMP formation of ~18% (figure 3.10). By definition, these data lead to the conclusion that UFP-505 is an ultra-low efficacy DOP partial agonist (in addition to a MOP agonist). This conclusion was further supported by receptor internalization data, showing a UFP-505-induced DOP internalization (an amplified downstream event) in CHO_{hDOP} cells (figure 4.4 and 4.6), as well as *in vivo* internalization of the DOP receptor in neuronal tissues of UFP-505 treated rats (table 6.1). Nevertheless, additional *ex vivo* data for UFP-505 by our collaborators, in electrically-stimulated MVD preparations, have shown that UFP-505 behaves as a DOP antagonist, shifting the DPDPE curve to the right in a similar way to naloxone, producing a pA_2 of 9.15 and a slope of 0.96 (figure 3.13). These data show that although UFP-505 can trigger the DOP receptor signaling pathway and initiate DOP trafficking (cAMP inhibition & DOP internalization), its substantially lower efficacy at the DOP receptor translates to an antagonistic behaviour at this receptor,

which can be observed *ex vivo* and which may be similarly observed *in vivo*. It is unknown what the role of a possible expressed MOP-DOP receptor dimers play in the effects of UFP-505 *in vivo*, although this may be particularly important given the bifunctionality of this ligand.

Similar findings were reported in a study with an oxymorphindole analogue compound that exhibited potent MOP agonism and partial DOP agonism (Grundt *et al*, 2003). The authors suggested that its high potency/low efficacy at the DOP receptor would translate to DOP antagonist behaviour *in vivo*, such that it will mimic the properties of a MOP-agonist/DOP-antagonist compound. Foremost, a possible advantage of the weak DOP activity in a bifunctional ligand like UFP-505, compared to a strict MOP-agonist/DOP-antagonist, could be the fact that it can induce significant DOP receptor internalization, which could enhance its capacity to induce MOP receptor internalization through receptor dimerization thus contributing to the reduced tolerance seen *in vivo*.

8.3.2. Reduction of morphine analgesia at 2 hours after acute administration: acute tolerance or metabolism?

The initial *in vivo* experiment in rats presented in this thesis was the acute intrathecal administration of various concentrations of UFP-505 and 10 nmol morphine in a tail-flick assay (figure 5.2). The data have shown that, two hours after drug administration, rats that have been treated with morphine exhibited a significant reduction in analgesic levels. The question that arises is: does this reduction reflect pharmacokinetic changes *in vivo* or does it reflect acute tolerance? The answer to this question will have an impact to the interpretation of the sustained analgesic levels of UFP-505 at 2 hours after administration and therefore our understanding of this observation is important.

Some investigators study acute analgesic tolerance by administering an acute dose of a drug and then performing a dose-response experiment with the same drug. In those experiments, acute tolerance is reflected by a “right-shift” to the dose-response curve and an increase in ED₅₀ (Dighe *et al*, 2009; Fairbanks & Wilcox, 1997). However, with the support of pharmacokinetic data, a significant reduction in analgesia at the same time when the concentration of the drug in the system is unaltered would also reflect acute tolerance. In a very early study of acute tolerance in rats, Kissin *et al* reported that a single morphine s.c injection (6 mg/kg) leads to a 79% decrease in analgesia 90 minutes after injection when compared with that at 30 minutes, although the concentration of morphine in the brain (measured by radioimmunoassay with ¹²⁵I-morphine) was not reduced significantly (Kissin *et al*, 1991). The authors concluded that these results suggest acute tolerance which is “pharmacodynamic in nature”. This may support the hypothesis that the reduced morphine antinociception shown in this thesis for treated rats after a single dose at 120mins after i.t. injection is more likely to result from analgesic tolerance rather than morphine pharmacokinetics.

However, the data in this thesis are not sufficient to safely conclude that the reduction in analgesia observed at 120mins after morphine i.t administration is definitely due to acute tolerance, metabolism or both. Further pharmacological or pharmacokinetic experiments for both morphine and UFP-505 are needed in order to interpret the observation of reduced morphine antinociception and the sustained UFP-505 antinociception in these experiments.

8.3.3. Tolerance after repeated administration of naltrindole and morphine

As discussed in Chapter 5, a number of previous studies have reported that administration of a DOP antagonist with morphine produces analgesia with substantially reduced tolerance. The concept of producing a MOP-agonist/DOP-antagonist bifunctional ligand was based on these reports. The *in vivo* repeated administration experiments discussed in Chapter 5 incorporated a naltrindole + morphine group as a reference. Analysis of these data (figure 5.10) showed that the animals in this group exhibited analgesic tolerance similar to morphine, expressed as a significant reduction in analgesic responses at 15min after injection on day 3 of the subchronic experiment compared to day 1. However, the latency scores of the UFP-505 treated animals were non-significantly different than those of naltrindole+morphine group, whereas they were significantly higher than the morphine treated group (figure 5.10). This analysis shows that the addition of naltrindole to morphine has not prevented tolerance, but has constrained the reduction in antinociception at day 3 compared to morphine alone.

The inability to avoid the development of tolerance with the addition of naltrindole to morphine shown here may be the result of methodological nature (10 nmol naltrindole was administered about 5 minutes prior to the administration of 10 nmol morphine): In the Roy et al study (Roy *et al*, 2005), the authors showed attenuated tolerance in mice given a morphine pellet (s.c.; 75 mg for 3 days) and a simultaneous infusion of naltrindole (10 mg/kg/day; 3 days). They suggested that inhibition of DOP receptors must occur at the time of MOP activation to *prevent* the development of tolerance, based on the assumption that administering naltrindole to morphine-tolerant animals could not reverse the effect. However, their methodology included the application of the

infusion pump 2 hours prior to the application of the morphine pellet. It is possible that the protocol adopted in this thesis (5 minutes of naltrindole administration prior to morphine administration) did not give enough time for satisfactory DOP blockade. On the other hand, the dose of naltrindole used in this thesis was lower than that used by Roy et al. Even in the original study by Abdelhamid et al (Abdelhamid *et al*, 1991), the authors used “multiple administration of naltrindole before and during implantation with morphine base pellets” which resulted in inhibition of the development of morphine tolerance.

8.3.4. Downregulation of NOP mRNA after acute administration of morphine or UFP-505

Upregulation of the MOP and DOP receptor mRNA in neuronal tissue of acutely treated animals by UFP-505 or morphine (table 6.2) may be explained in terms of either the existence of MOP-DOP dimers (since binding of morphine results in upregulation of DOP receptor) or the cross-talk of the signaling pathways of these particular receptors such that desensitization or internalization of one receptor may affect the desensitization or internalization of the other. However, the data presented in this thesis surprisingly show extensive downregulation of the NOP receptor mRNA in these treated animals. Since UFP-505 and morphine do not bind substantially to the NOP receptor, NOP mRNA down regulation implies that is a MOP mediated effect. As previously discussed in Chapter 1 of this thesis for the putative opioid receptors, there are a number of studies that demonstrated evidence of the presence of MOP-NOP dimers and cross-talk in signalling pathways (Evans *et al*, 2010a; Pan *et al*, 2002; Wang *et al*, 2005). Wang et al showed that the activation of NOP-MOP dimers induces cross-desensitization of MOP and impairs the potency of DAMGO to inhibit cAMP and to

stimulate MAP kinase phosphorylation. Evans et al suggest that NOP can dimerize with all ‘classical’ opioid receptors and activation of NOP causes their internalization. Thus, there is substantial evidence for an interaction between MOP and NOP. But the question that arises is why the regulation of the NOP receptor is opposite to that of the other two and what that means in terms of the relationship of these receptors. Although it seems that the “anti-opioid” activity of the NOP receptor agrees with the observation of the reversed mRNA regulation, there is insufficient evidence in the literature to explain this behaviour since there are limited data for the effect of MOP activation on NOP receptor signaling.

As shown by Spampinato *et al* and Hashimoto *et al*, the NOP receptor is able to be internalized and recycled when activated by a number of NOP ligands (Hashimoto *et al*, 2002; Spampinato *et al*, 2007). However, in primary-cultured rat brain cells Takayama and Ueda have shown that morphine induces upregulation of the prepro-N/OFQ gene (a precursor of the endogenous NOP ligand) (Takayama & Ueda, 2005). This effect (observed in astrocytes, but not in neurons or microglia) was abolished by naloxone. In addition, Cannarsa et al showed that kainate (an analogue of kainic acid that mimics the effects of glutamate) downregulates NOP mRNA levels and is associated with increased N/OFQ release in the rat hippocampus (Cannarsa *et al*, 2008). Therefore, combining the above observations there is a possible hypothesis that morphine induces downregulation of NOP through the upregulation of N/OFQ or prepro-N/OFQ, and that the morphine-induced antidepressant effects may result partially from downregulation of the NOP receptor. Supporting this hypothesis, Green and Devine showed recently that stress induced an upregulation of the NOP receptor in rats, which provides a platform for

further studies to investigate the link between antidepressant actions and NOP downregulation (Green & Devine, 2009).

8.3.5. Relationship between mRNA levels and receptor expression in CHO_{hMOP/hDOP} cells

The RT-qPCR results presented in the thesis for the three selected batches of the novel CHO_{hMOP/hDOP} novel cell line (batch 10, 17 and 25) have shown that batch 25 produced the higher ΔC_t for the DOP receptor from the others, and a medium ΔC_t for the MOP receptor (table 7.1).

The RT-qPCR data showed a rank order of 10>17>25 for the expression of DOP, and an order of 10>25>17 for the MOP receptor. Surprisingly, pharmacological data for the three selected batches presented in this thesis (figure 7.3) have produced a different ranking order for receptor expression (B_{max}), both for MOP and DOP receptors: 25>17>10. These data indicate that batch 25 has both higher MOP and DOP receptor density, which is opposite to the RT-qPCR that suggested batch 10 as the highest expression of both receptors. Since the pharmacological tools use the direct interaction of the receptor and its ligand, we used batch 25 as the cell line for further experimentation. Nevertheless, this contradiction between molecular and pharmacological data is unexplained. A first interpretation of this contradiction could be that the transfected plasmid in the CHO_{hMOP/hDOP} cell produces receptor mRNA that either does not translate into receptor or not all produced receptors make it to the cell surface. Also, a few passages of a freshly-produced cell line may lead to changes in receptor density (i.e. between the PCR screening and the binding experiments). Whilst

further experiments are required to address this particular question the finding does not affect the pharmacological studies of the expressed protein.

8.3.6. Binding affinity of ligands in CHO_{hMOP/hDOP} Cells

There was an initial concern about the lower affinity of UFP-505 to MOP receptors compared to morphine, as was observed in CHO_{hMOP} cells, but that concern ended when similar potencies of UFP-505 and morphine were observed *in vitro* and *in vivo*. However, the observation that the binding affinity of morphine, EM1 and naltrindole were found lower in CHO_{hMOP/hDOP} cells compared to CHO_{hMOP} or CHO_{hDOP} cells was unexpected as UFP-505 did not show a marked difference in binding affinity (figure 7.7).

There are some remarks that need to be made prior to explaining this observation: Firstly, UFP-505 is the only bifunctional ligand from those tested, acting on both receptors. Morphine and naltrindole (highly selective) showed the greatest difference in pK_i (one- and two-logs reduction respectively), whereas EM1 showed a half-log reduction. Secondly, the greatest difference (reduction) in binding affinity was observed with naltrindole, which agrees with the fact that the density of the DOP receptor was found to be lower than MOP in the CHO_{hMOP/hDOP} cells. Thirdly, the radioligand used (³H-DPN) showed a value of pK_d closely to that shown in CHO_{hMOP} cells (possibly because of higher expression of MOP in the double-expression cells; figure 7.4). These remarks suggest that as DOP is co-expressed with MOP, the overall affinities of the compounds tested (to MOP and DOP receptors) should be lower than those observed for their selective receptor. The differences in receptor density combined with the above suggestions, may possibly explain why naltrindole shows the highest reduction in its

binding affinity in CHO_{hMOP/hDOP} cells and why the binding affinities of most ligands in the double-expression cell line differ compared to the single-expression cells.

Another possible explanation of the differences in pK_i values, is the potential formation of MOP-DOP dimers in double-expression cells. Dimerization of MOP and DOP receptors suggests changes in the conformation of the individual receptors (Filizola *et al*, 1999; Liu *et al*, 2009; Surratt & Adams, 2005), such that ligands may exhibit different binding affinities to the MOP-DOP dimers as well as different functional properties (Levac *et al*, 2002). Jordan and Devi first observed that selective ligands for the KOP and DOP receptors show markedly different binding affinities when tested in cells expressing both receptors (Jordan & Devi, 1999). George *et al* also presented different binding affinities of a large variety of opioid ligands when tested in CHO cells co-expressing MOP and DOP receptors, including morphine, DPDPE and DAMGO (George *et al*, 2000). Waldhoer *et al* presented *in vitro* and *in vivo* data of the first opioid ligand that shows selectivity for the KOP-DOP opioid receptor dimer (Waldhoer *et al*, 2005).

The simplest explanation for our observation is that both the above interpretations (co-existence of different receptor populations and/or formation of dimers) can occur simultaneously, since the co-existence of individual opioid receptor populations with opioid receptor dimers has been proposed (Gomes *et al*, 2002; Jordan *et al*, 2000; Wang *et al*, 2005).

8.4. Limitations of study and suggestions for further experiments

8.4.1. *In vivo* characterization

One major issue that has been encountered in the study was the reduction of animal numbers in the repeated administration part of the *in vivo* experiments. Catheter removal has not been overcome despite various attempts by a number of alternative methods and has eventually led to a significant reduction in the number of animals remaining at day 5. The gradual loss of animals has compromised the statistical analysis of the data for day 5. Additionally, the reduced numbers of animals in the repeated administration part of the study meant that the tissue available for *in vitro* analysis was also limited.

A possible solution to this issue could have been the application of osmotic pumps that control the rate and dose of drug administration. These pumps are placed subcutaneously during surgery and therefore the animals are unable to remove them. If this solution could be applied successfully, then the increased numbers of animals available could also facilitate further *in vivo* experiments looking at drug dependence or withdrawal effects of the compounds used. Insufficient funds and restricted time were the main two parameters that discouraged the application of this solution during this study.

8.4.2. Double-expression recombinant system

As discussed in Chapter 8, receptor density had an affect not only a ligand potency (as shown in CHO_{hDOP/high} cells for UFP-505) but also to the binding properties of ligands (shown by the pK_i or pK_d changes in CHO_{hMOP/hDOP} cells). The novel double-expression cell line created here, probably due to the transfection of CHO_{hMOP} cells with a hDOPgene-plasmid, had a 1:5 receptor expression ratio of DOP:MOP receptors. Theoretically, this ratio could bias the UFP-505 properties seen in the CHO_{hMOP/hDOP} cells towards properties that are closer to those seen in a CHO_{hMOP} cell line. Additionally, the receptor expression ratio of DOP:MOP at the spinal cord and cortex of the animals studied in this thesis were found 1:1.5 and 1:1.3 respectively. In order to study this a cell line with equal expression should be made but the transfection/expression process is not easy to control.

The study of receptor internalization in the novel CHO_{hMOP/hDOP} cell line provided a useful model for studying the effects of ligands in a system where only MOP and DOP receptors were present (figure 7.6). However, the receptor internalization experiments performed in this thesis used the non-selective ³H-DPN as a radioligand, presenting the overall receptor internalization of MOP and DOP. What this experiment did not provide in terms of information, is the ratio of MOP:DOP receptors internalized, which is an important factor in determining the effect of UFP-505 upon its individual receptor targets. Although the overall B_{max} observed in CHO_{hMOP/hDOP} cells after UFP-505 incubation was in agreement with the individual percentages of receptor internalization seen in the single-expression systems used (see Appendix; Section A6 for rationale and calculations), the use of ³H-Nt and ³H-DAMGO in these experiments would convey additional information about the nature of the receptor internalization observed in the

³H-DPN experiments. Similarly, there are a number of additional experiments that could be performed in the double-expression cell line and provide additional important data, as discussed in the next section.

Another aspect of receptor trafficking that the receptor internalization experiments did not address is receptor recycling to the cell surface. As discussed in Chapter 8, receptor recycling after activation and internalization is a vital part in the properties of an opioid ligand in terms of its ability to induce analgesic tolerance *in vivo*. Due to the fact that the internalized receptors can be either destroyed by lysosomal enzymes or resensitized and recycled on the cell surface, these different pathways could possibly be involved in analgesic tolerance induced by a particular ligand. Determining the degree of receptor recycling after UFP-505 binding could provide a valuable addition to the *in vitro* data of this thesis as well as support for the differences in tolerance between UFP-505 and morphine.

8.5. Importance of the thesis findings

Since the early '90s there have been an increasing number of studies that investigated various ways to reduce tolerance to morphine, mainly by investigating the interaction of MOP and DOP receptor trafficking and signaling pathways. A major milestone has been set by studies that provided evidence of reduced tolerance by blocking or removing the DOP receptor while activating the MOP receptor. These studies have promoted further research on bivalent and bifunctional compounds that incorporate both activities. One such compound is UFP-505, for which the *in vitro* and *in vivo* pharmacological characterization has been the main aim of this thesis. There are a few compounds that

have been studied in the literature in terms of their basic *in vitro* pharmacology and their ability to induce tolerance *in vivo*, although these studies did not offer a complete pharmacological and antinociception profile of these ligands (including mRNA changes and receptor internalization). This thesis describes an experimental continuum of basic pharmacology, receptor internalization, analgesia, tolerance and gene regulation by UFP-505, intending to build a complete picture of the properties of this ligand.

The major contribution of this thesis is that it provides strong evidence for a single bifunctional MOP/DOP compound producing sustained analgesia without analgesic tolerance and causing marked internalization of both receptors, results that promote this compound as a prototype for further development. Most importantly, previously reported studies have shown these desired effects by blocking or removing the DOP receptor thus assuming that blocking/removing the signaling pathway of the DOP receptor has a key role towards a reduced analgesic tolerance after morphine administration (which acts solely at MOP). However, this thesis provides evidence of a compound (UFP-505) that produces marked analgesia comparable to morphine but not analgesic tolerance, although it is a low-efficacy DOP agonist, inducing significant internalization of the DOP receptor. Additionally, the thesis provides evidence that morphine evokes the upregulation of mRNA for MOP and DOP receptors after one dose, although it does not have a significant binding affinity to the DOP receptor. Collectively, the data in this thesis in combination with previous studies, provide evidence that the DOP signaling pathway and the DOP receptor trafficking do not contribute towards the development of morphine tolerance directly, but they play an indirect role possibly through the interaction of the two receptors on the cell surface.

This thesis raises an important question: should the focus of the research community on MOP-agonists/DOP-antagonists now also be expanded to MOP-agonists/DOP-low efficacy agonists, and if yes, which type of compound is most efficient? This question is very important not only because until now the DOP-low efficacy bifunctional ligands were excluded for further *in vivo* experiments, but also because the DOP internalization may be a key mechanism for reducing the analgesic tolerance produced by morphine.

8.6. **Future work**

Some ideas to extend the work in this thesis are described below:

1. **Receptor internalization:** Are the receptors that do not internalize, functional? What is the effect of the receptor reserve on receptor internalization upon UFP-505 binding? Why does UFP-505 produce extensive DOP-receptor internalization when it has only very weak DOP agonist activity?
2. **NOP receptor regulation:** Why does morphine and UFP-505 have an effect on NOP receptor mRNA and does this have any physiological consequences? Does a NOP-antagonist or NOP-agonist have an effect on UFP-505 analgesia?
3. **Receptor dimers:** What is the trafficking effect of UFP-505 on MOP-DOP receptor dimers and does the receptor dimerization affect UFP-505 and morphine activity? What is the evidence of MOP-DOP receptor dimers in the novel double-expression cell line produced?
4. ***In vivo*:** What is the *in vivo* effect of the co-administration of UFP-505 and morphine? Is there an analgesic synergy and what is its effect on morphine tolerance?

APPENDIX

A1. Sources of materials

Department of Pharmaceutical Sciences at the University of Ferrara: UFP-505, dermorphin, nociceptin/Orphanin FQ (N/OFQ), endomorphin-1

Institute of Biochemistry, Szeged, Hungary: tritiated UFP-101 (22.6 Ci mmol⁻¹)

TOCRIS Bioscience, Bristol, UK: naloxone, norbinaltorphimine, [D-Pen²,D-Pen⁵]-enkephalin, CTOP, morphine, fentanyl

Sigma-Aldrich Co., St. Louis, USA: BSA, EDTA, PEI, amastatin, bestatin, Tris-HCL, carbacol, cAMP, IBMX, DMSO, folin's reagent, EGTA, GTP γ S

Fisher chemicals, Leicestershire, UK: sodium chloride, potassium chloride, magnesium sulphate, all the rest laboratory chemicals, Optiphase scintillation liquid, ScintisafeGel, all plasticware.

Perkin Elmer: Tritiated diprenorphine (50.9 Ci mmol⁻¹), tritiated naltrindole (25 Ci mmol⁻¹), tritiated DAMGO (50.9 Ci mmol⁻¹)

Amersham Pharmacia Biotech, Buckinghamshire, UK: GTP γ ³⁵S (1250 Ci mmol⁻¹), HEPES

Invitrogen, GIBCO, Paisley, UK: HAMS-F12 1x, DMEM/F12(Ham)1:1, minimum essential tissue culture media, penicillin, streptomycin, fungizone, fetal bovine serum, trypsin, geneticin, hygromycin B

Roche Applied Sciences, Indianapolis, USA: Eugene transfection reagent

Applied Biosystems, USA: all PCR material used

Charles River Laboratories Italia S.r.l., Calco, Italy: Male Wistar rats

Science and Technology (S&T), Missouri University, USA: pcDNA3.1, plasmid, pcDNA3.1+Hygro plasmid

A2. Cell culture and membrane preparation

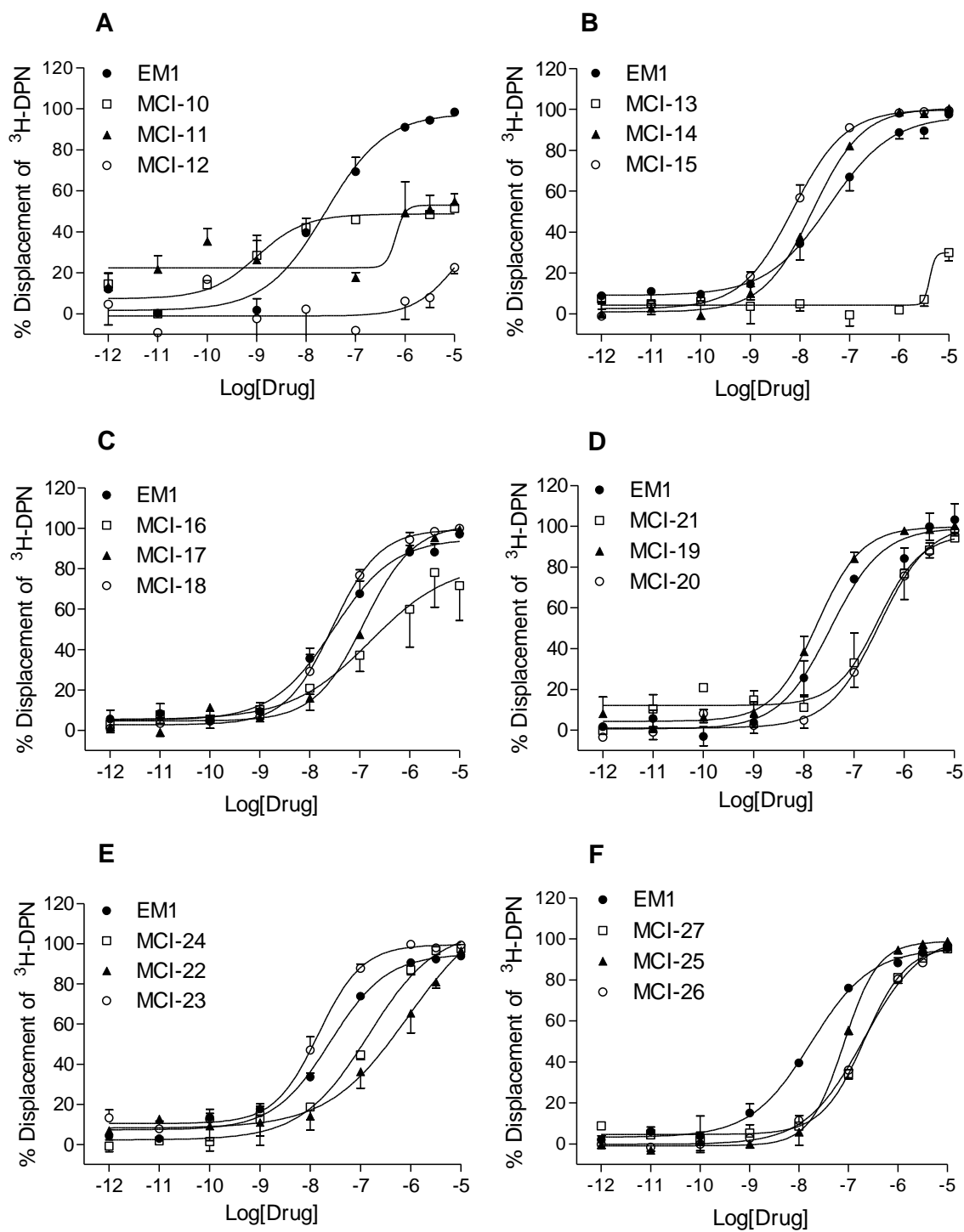
CHO cells were grown in an appropriate medium [F12(Ham)1X for the hMOP, hDOP, and hKOP cells and DMEM/F12(Ham)1:1 for the hNOP cells] containing 10% fetal bovine serum, 100 IU·ml⁻¹ penicillin, 100 mg·ml⁻¹ streptomycin, and 2.5 mg·ml⁻¹ fungizone, as described in (Kitayama *et al*, 2003). All media contained L-glutamine. Stock cultures were additionally supplemented with 200 mg·ml⁻¹ G418 (a selection agent used with hMOP, hDOP, and hKOP cells) and with additional 200 mg·ml⁻¹ hygromycin B (an additional selection agent) for the hNOP cell. Cell cultures were kept at 37°C in 5% CO₂/humidified air and subcultured as required using trypsin/EDTA.

When confluent, cells were harvested by incubation in 10 ml of harvest buffer, containing 0.9% Saline, 0.02% EDTA, 10mM HEPES, pH of 7.4, for 5 minutes at 37°C. The resulting suspension was centrifuged at 1600g for 2 minutes at 20°C. The membrane pellet was resuspended in appropriate buffer, homogenised and centrifuged at 14000g for 10 minutes at 4°C, this process was repeated twice more. Membranes were prepared and used fresh each day.

A3. Displacement binding curves for MCI compounds in CHO_{hMOP} cells

MCI compounds (designed and produced by the University of Ferrara Peptides) are a series of opioid ligands that are suspected of bifunctionality based on their chemical structure. The binding affinity (pK_i) of a number of MCI compounds for the MOP receptor in CHO_{hMOP} cells was estimated and is presented here.

Thirty two MCI compounds were tested and were screened compared to EM1 (control). Most MCI compounds displaced ³H-DPN binding in CHO_{hMOP} cells in a concentration-dependent manner (figure A), which when corrected for the amount of radioligand used, yielded the pK_i values shown in table A. Seven MCI ligands (10, 10A, 10B, 11, 12, 13 and 33) did not fully displace ³H-DPN indicating weak binding to the MOP receptor. The highest affinity MCI ligand for the MOP receptor was MCI-10. A number of MCI ligands have shown binding affinity similar to that of EM1 (14, 15, 18, 19, 23, 29B, 14A, 14B). The structure of these compounds may be subject to patent and so are not disclosed.



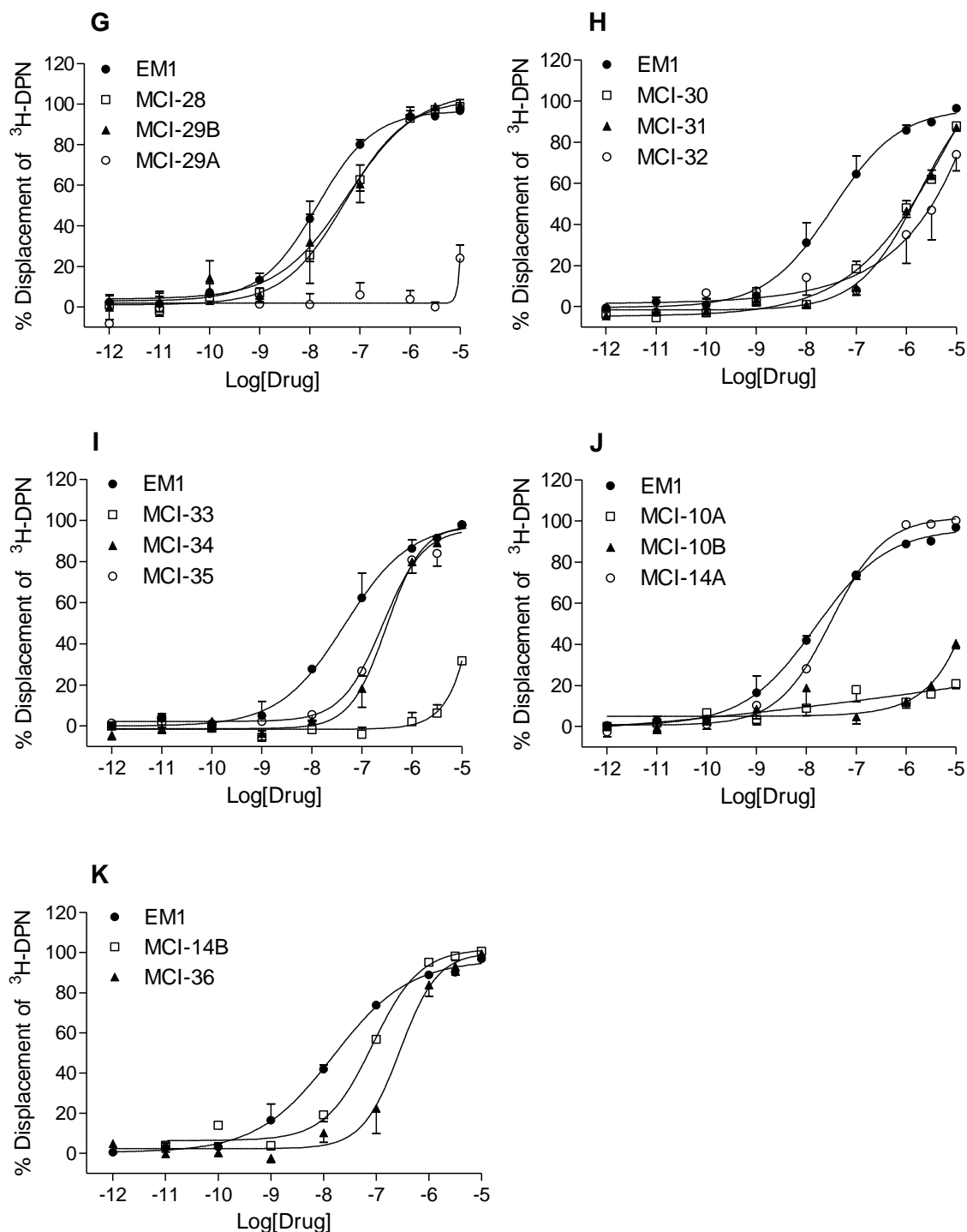


Figure A. Displacement binding assay of 32 MCI compounds and the reference ligand endomorphin-1 (EM1) in CHO_{hMOP} cell membranes. Non-specific binding was defined in the presence of 10 μ M naloxone. All studies were performed at room temperature using a fixed concentration of ³H-DPN. Data are mean \pm SEM for $n=3-5$ and were performed in groups of four (A-J) or three (K). Receptor binding affinity (pK_i) was calculated using the Cheng-Prusoff equation and are summarized in table A below.

MCI compound	Pk _i	MCI compound	Pk _i
EM1	8.29 ± 0.06	EM1	8.29 ± 0.06
10	9.19 ± 0.09	26	7.27 ± 0.10
11	5.81 ± 0.17	27	7.26 ± 0.04
12	ND	28	7.89 ± 0.15
13	ND	29A	ND
14	8.29 ± 0.07	29B	8.08 ± 0.23
15	8.63 ± 0.15	30	6.62 ± 0.04
16	7.56 ± 0.18	31	6.48 ± 0.02
17	7.46 ± 0.04	32	6.29 ± 0.48
18	8.18 ± 0.10	33	ND
19	8.36 ± 0.13	34	7.08 ± 0.18
20	7.24 ± 0.45	35	7.15 ± 0.03
21	7.18 ± 0.25	10A	ND
22	6.02 ± 0.83	10B	ND
23	8.42 ± 0.09	14A	8.10 ± 0.01
24	6.92 ± 0.59	14B	7.95 ± 0.23
25	7.62 ± 0.01	36	7.12 ± 0.12

Table A. Estimated receptor binding affinity values (pK_i) of 3H -DPN binding for MCI ligands in CHO_{hMOP} cell membranes. The control ligand used was endomorphin-1 (EM1). Graphical representation of the data is shown in figure A. Data are mean \pm SEM of $n=3-5$ for all MCIs and $n=31$ for EM1.

A4. Methodology for the electrically-stimulated isolated tissue

This is the methodology used in the *ex vivo* experiments presented in the discussion section of Chapter 1 (figures 3.12 and 3.13), as produced by Molinari, Calo and Guerrini. Tissues (GPI and MVD) were suspended in 5 ml organ baths containing heated Krebs solution oxygenated with 95% O₂ and 5% CO₂, at 33 °C for the mouse vas deferens and 37 °C for the guinea pig ileum. Tissues were stimulated through two platinum ring electrodes with supramaximal rectangular pulses of 1 msec duration and 0.05 Hz frequency. A resting tension of 0.3g and 1g were applied to the mouse vas deferens and guinea pig ileum respectively. The electrically evoked contractions (twitches) were measured isotonicly by means of Basile strain gauge transducers

(Basile 7006, UgoBasile s.r.l., Varese, Italy) and recorded with a PC-based acquisition system (Power Lab, 4/25, ADInstruments, Australia). Following an equilibration period of 60 min, the contractions induced by electrical field stimulation were stable. For the guinea pig ileum, dermorphin and UFP-505 were included at various concentrations and combinations, with or without the presence of the non-selective opioid receptor antagonist naloxone or the MOP-selective antagonist *D*-Phe-Cys-Tyr-*D*-Trp-Orn-Thr-Pen-Thr-NH₂ (CTOP), as described in the respective figure legend. For the mouse vas deferens, DPDPE was used at various concentrations and combinations, with or without the presence of different concentrations of UFP-505, as described in the respective figure legend.

A5. Conversion of tail-withdrawal latencies to % of Maximum Possible Effect

As discussed in Chapter 8 (section 8.2.3), we have converted the recorded latencies of animals repeatedly treated with UFP-505 or morphine to % maximum possible effect (% MPE), in order to compare our data with data in the literature. Here we present the calculations used for this conversion. The formula of MPE used is the following:

$$\% \text{ MPE} = [(\text{postdrug latency} - \text{baseline latency}) / (\text{cut-off time} - \text{baseline latency})] \times 100$$

Day 1, UFP-505 recordings at 15min:

$$[14.03\text{sec} - 3\text{sec}] / (15\text{sec} - 3\text{sec}) \times 100 = 11.3/12 \times 100 = 94.16\% \text{ MPE}$$

Day 1, morphine recordings at 15min:

$$[14.90\text{sec} - 3\text{sec}] / (15\text{sec} - 3\text{sec}) \times 100 = 11.9/12 \times 100 = 99.16\%$$

Day 3, UFP-505 recordings at 15min:

$$[14.57\text{sec} - 1.95\text{sec}] / (15\text{sec} - 1.95\text{sec}) \times 100 = 12.95/13.05 \times 100 = 99.23\%$$

Day 3, morphine recordings at 15min:

$$[10.06\text{sec} - 1.95\text{sec}] / (15\text{sec} - 1.95\text{sec}) \times 100 = 8.11/13.05 \times 100 = 62.15\%$$

A6. Receptor internalization in CHO_{hMOP/hDOP} cell line: is this consistent with single-expression internalization data?

As shown collectively in Chapter 7 table 7.3, UFP-505 produces 62.4% receptor internalization in CHO_{hMOP} cells and 86.2% in CHO_{hDOP} cells. The CHO_{hMOP/hDOP} cell line has shown a receptor density for MOP and DOP of 672 and 159 fmol.mg⁻¹ respectively, using ³H-DAMGO and ³H-Nt binding.

If we apply the capacity of UFP-505 to internalize the MOP and DOP receptors individually to the double-expression system, then:

- a) 62.4% of 671 fmol.mg⁻¹ of the MOP receptors should internalize ≈ 419 fmol.mg⁻¹
- b) 86.2% of 158.8 fmol.mg⁻¹ of the DOP receptors should internalize ≈ 137 fmol.mg⁻¹

Theoretically, UFP-505 should induce a total of $419 + 137 = 556$ fmol.mg⁻¹ of MOP and DOP receptors internalized. As shown by ³H-DPN binding, CHO_{hMOP/hDOP} cells presented a total B_{max} of 851 fmol.mg⁻¹ and UFP-505 induced 62% receptor internalization, thus $62\% \text{ of } 851 = 528$ fmol.mg⁻¹ of receptors internalized.

Therefore, the theoretical value of 556 fmol.mg⁻¹ is very close to the actual internalization percentage determined; 528 fmol.mg⁻¹.

A7. Plasmid information for the production of CHO_{hMOP/hDOP} cell line

In order to produce a CHO_{hMOP/hDOP} cell line we transfected an appropriate plasmid that incorporated the human DOP receptor gene into CHO_{hMOP} cells. However, there was no such plasmid available in the market and thus we obtained a gene receptor-free plasmid with hygromycin B resistance (pcDNA 3.1/Hygro(+)) and a human DOP receptor gene (OPRD1), both from Invitrogen Inc. We then provided these products to S&T at the University of Missouri, where they cloned the two products to produce a plasmid with hygromycin B resistance with a human DOP receptor gene (pc DNA 3.1/Hygro(+)-OPRD1). Here we provide additional information on the plasmid used. The pcDNA 3.1/Hygro (+) vector contains the human CMV immediate promoter that allows high-level constitutive expression of the gene of interest in mammalian cells (figure B). After this promoter, there are available sites of cleavage for various restriction enzymes which can be used in order to insert a gene of interest. Our plasmid used the BamHI (5') and XhoI (3') restriction sites to insert the OPRD1 gene.

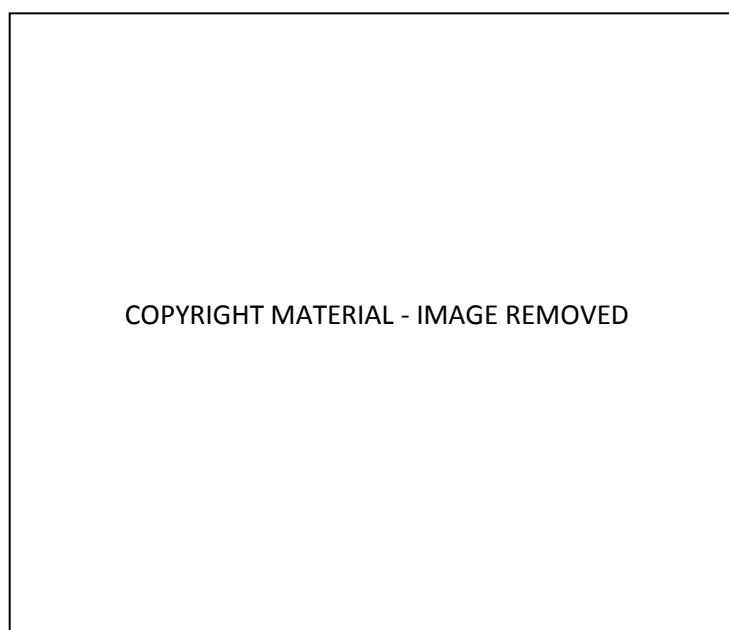


Figure B. The structure of the pcDNA3.1/Hygro(+) plasmid that was used for inserting the DOP receptor gene (OPRD1) and transfect the CHO_{hMOP} cells. The figure was modified from the Invitrogen website (<http://www.invitrogen.com>).

A8. Attempts to produce a pcDNA3.1/Hygro(+)-OPRD1 plasmid in the lab

Prior to using S&T for pcDNA3.1/Hygro(+)-OPRD1 plasmid preparation, we attempted to clone the plasmid in our lab. The procedure included a maxi prep of pcDNA3.1/Hygro(+) plasmid-incorporated DNA from E.Coli, a genetic manipulation of the plasmid by restriction enzymes in order to open the plasmid and incorporate the gene of interest, a transformation of the produced plasmid in E.Coli, an antibiotic selection of appropriate survived cells, a maxi prep of the produced plasmid-incorporated DNA, an enzymic cleavage test of the plasmid for identification of the correct cloned product, an isolation of the product by gel-electrophoresis and a determination of its composition by sequencing. Various different problems were confronted during this procedure. The experiment lasted approximately 6 months and ended in use of S&T.

In this section we will present some of the results from the above developmental work and will discuss the problems encountered. Most of this work took place to the laboratory of Dr Dave Lodwick at the Department of Cardiovascular Sciences at the University of Leicester, with the guidance and support of the laboratory manager Mrs Sonja Khemiri.

A8.1. Restriction enzyme digestion of plasmids

The OPRD1 gene (encoding the human DOP receptor) was supplied in a pcDNA3.1(+)-OPRD1 plasmid. Its transfer to a pcDNA3.1/Hygro(+) plasmid supposed that the gene should be placed using a “cut and paste” approach. After careful study of the plasmids’ composition and availability of appropriate restriction sites, digestion of both products (target plasmid and gene plasmid) was performed using the restriction enzymes *HindIII*

(5') and *XhoI* (3') by incubating all reagents at 37°C overnight. Because the enzymes used were diluted in different buffers, separate digestions had to be performed with an intermediate purification step (QIAGEN purification kit). The linearized target plasmid was dephosphorylated by incubating with alkaline phosphatase at 37°C for 30mins.

After plasmid digestion and dephosphorylation, the individual products (target plasmid and OPRD1 gene) were isolated by 1% agarose gel electrophoresis (0.5µg/ml ethidium bromide, 100V/400mA, 60min run). The gel was visualized in a UV box where the appropriate bands were identified using an appropriate DNA Molecular Weight Marker_X (0.07-12.2 kbp; OPRD1 1200bp, vector 5600bp) and were cut from the gel (figure C).

A8.2. DNA purification and ligation of products

The products (target plasmid and gene) were run through Ultrafree spin tubes (Millipore) that bind DNA. The product was eluted and run through a QIAquick PCR purification spin column (QIAGEN) in order to concentrate the DNA into a small working volume. The two final DNA solutions were quantified using a NanoDrop quantifier. The products were used in appropriate volumes of a molar ratio of 1:5 (vector: gene insert) and allowed to ligate by incubating them at °RT overnight with a T4 ligase enzyme.

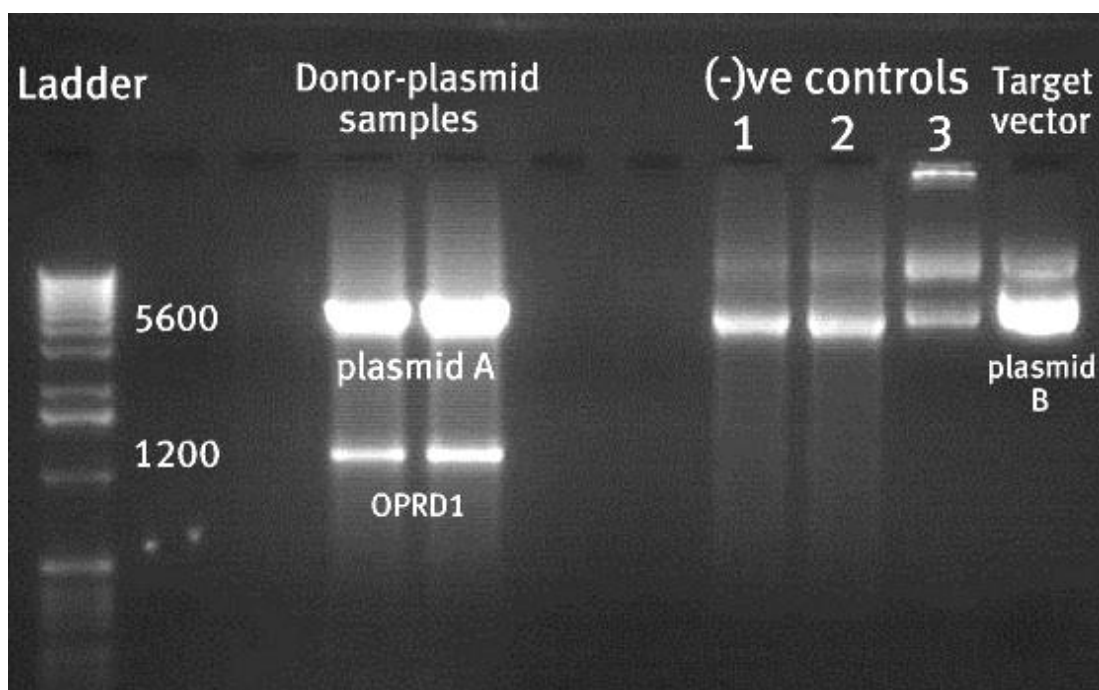


Figure C. Agarose gel-electrophoresis of different samples. The DNA marker (ladder) was used for determining the size of the band on the gel, numbers expressing base pairs. The donor-plasmid (*pcDNA3.1(+)-OPRD1*) was digested by restriction enzymes into its components; the gene of interest (*OPRD1*) and the rest of the plasmid (*plasmid A*). The target vector (*pcDNA3.1/Hygro(+)*) plasmid control was also treated with the same enzymes (*plasmid B*). A number of negative controls were also used in the same experiment; donor-plasmids without the presence of enzymes (1 and 2), and donor-plasmid prior to dephosphorylation (3). The empty wells in the gel were used as a protective distance to avoid possible ‘spill-overs’ while loading the gel or running the gel.

A8.3. Bacterial transformation, gene identification and purification

Bacterial transformation is a process where the target DNA is taken up by bacteria (*E.Coli*) by incubating them in appropriate medium at 37°C overnight. The mixed solution is added on an agar plate containing Amoxicillin, which the plasmid bears a resistance gene for. The DNA is replicated by growing the bacteria in the agar medium and then extracting the product by DNA isolation. Selection of the appropriate colonies

from the agar plate was based on the type of E.Coli used (XL-Blue), which allowed non-recombinant colonies (bacteria with either uncut vector or re-circularized cut vector) to turn a faint blue color on the agar plate, while colonies successfully incorporating the plasmids containing the cloned insert remained white. A number of white colonies were picked up and grown in appropriate medium in sufficient quantities. DNA was isolated from the individual colonies using a QIAGEN purification kit. A restriction enzyme test was used in order confirm the presence of the gene of interest in the target plasmid, by using two restriction enzymes that recognized a site within the OPRD1's sequence (figure D). A maxi prep was followed (QIAGEN Maxi kit) in order to isolate and purify the target DNA plasmid (pcDNA3.1/Hygro(+)) from the bacterial DNA. An appropriate amount of DNA was sent for sequencing and identification (The Protein Nucleic Acid Chemistry Laboratory, University of Leicester).

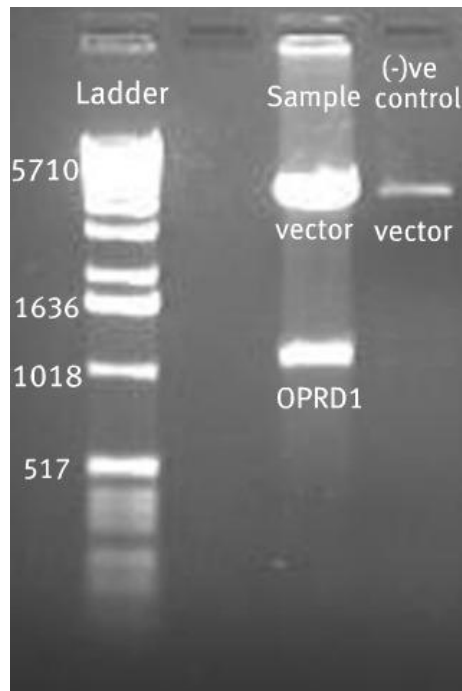


Figure D. Agarose gel after gel-electrophoresis of a DNA sample isolated from a transformation product. Two restriction enzymes cut a band of 1200bp (OPRD1) recognizing a site within the sequence of the gene of interest. The DNA marker was used for determining the size of the bands (ladder), numbers expressing base pairs. A negative (-ve) sample that did not have the required OPRD1 sequence (and therefore stayed un-cut) was used for comparison.

A8.4. Limitations and setbacks encountered

A major issue was the limited amount of DNA of target vector and OPRD1 gene available. Due to the different restriction enzymes used to cut both DNA templates (supplied by different companies and thus diluted in different type of buffers), subsequent steps of enzyme digestion and purification had to be applied to complete the digestion of the templates. These steps resulted in a further decrease of the amount of working DNA, which decreased the efficiency of the bacterial transformation.

Subsequent issues have arisen regarding the efficiency of the blue-marker of the XL-Blue cells, since many white colonies that were selected did not show to carry the

plasmid as shown by enzyme digestion and gel-electrophoresis. From the 59 white colonies that were initially selected, only 9 gave a positive OPRD1 band (example in figure D). For an unknown reasons, the maxi prep undertaken from these 9 positive colonies could not isolate efficiently the target plasmid (by eluting the bind column with warm distilled water), although a number of other alternatives were also used. There were only 3 samples of DNA that could be eluted successfully, none of which produced 100% positive identification of an OPRD1 gene after DNA sequencing. These may relate to academic modification of a commercially (and possibly modified) product.

A9. Publications arising from this thesis

A9.1. Full Papers

1. **Dietis, N**, Niwa H, Tose R, McDonald, Vitale, G, Calo, G, Guerrini, R, Rowbotham, JD, Lambert, DG (2012) Reduced tolerance to the bifunctional opioid ligand H-Dmt-Tic-Gly-NH-Bzl (UFP-505); *in vivo* and *in vitro* characterisation. For submission to Pain.
2. **Dietis, N**, McDonald, J, Molinari, S, Calo, G, Guerrini, R, Rowbotham, JD, Lambert, DG (2012) Pharmacological characterisation of the bifunctional opioid ligand H-Dmt-Tic-Gly-NH-Bzl (UFP-505). *Br J Anaesth* **108**(2): 262-70.

A9.2. Reviews

1. **Dietis, N**, Rowbotham, JD, Lambert DG (2011) Controlling cancer pain: Is morphine the best we can do? *Trends in Anaesthesia and Critical Care* **1**(5): 227-9
2. **Dietis, N**, Rowbotham, JD, Lambert, DG (2011) Opioid receptor subtypes: fact or fiction? *Br. J. Anaesth* **107**(1): 8-18.

3. **Dietis, N**, Guerrini, R, Calo, G, Salvadori, S, Rowbotham, JD, Lambert, DG (2009) Simultaneous targeting of multiple opioid receptors. A strategy to improve side effect profile. *Br J Anaesth* **103**(1): 38-49

A9.3. Abstracts

- Anaesthetic Research Society meeting, hosted by the Liverpool Medical Institution, Liverpool, Jul 2011:

Dietis, N, Ruggieri, V, Filaferro, M, Novi, C, Guerrini, R, Calo, G, Rowbotham, JD, Vitale, G, Lambert, GD (2011) Antinociceptive effects of the bifunctional opioid UFP505 in rats. *Br J Anaesth* **107**(5): 838P
- Anaesthetic Research Society meeting, hosted by the University of Nottingham, Nottingham, Jul 2010:

Tose, R, **Dietis, N**, McDonald, J, Guerrini, R, Calo, G, Salvadori, S, Rowbotham, JD, Lambert, DG (2010) Characterization of the bifunctional opioid UFP505. *Br J Anaesth* **105**(5): 728-9P

A9.4. Presentations

- Postgraduate Seminar Day, Department of Cardiovascular Sciences, University of Leicester, 2010:

Dietis. N. Bifunctional opioids: clean or dirty?
- Festival of Postgraduate Research, University of Leicester, 2010:

Dietis. N. A new HOPE for cancer pain relief
- Vitae Midlands Hub Regional Festival of Postgraduate Research, Nottingham, 2010:

Dietis, N. The “Holy Grail” of cancer pain research

- Signalling-group meetings, Department of Cardiovascular Sciences, University of Leicester:
 1. **Dietis, N.** *In vivo* work with the bifunctional opioid UFP-505 (2011)
 2. **Dietis, N.** Pharmacological characterization of UFP-505 (2010)
 3. **Dietis, N.** Outline and strategy of the PhD project (2009)

- HOPE Against Cancer meetings, Leicester:
 1. **Dietis, N.** Collective data from the PhD project: where are we now (2011)
 2. **Dietis, N.** A new HOPE for cancer pain relief (2010)
 3. **Dietis, N.** An outline of the PhD project (2009)

A10. Awards relating to this PhD thesis

Schachter Award (2010): Awarded by the British Pharmacological Society as a financial support towards visiting the University of Modena for the *in vivo* characterization of UFP-505

i-Qube Award (2010): Awarded at the Festival of Postgraduate Research at the University of Leicester for presenting current data for UFP-505.

Bain Memorial Bursary Fund Award (2009): Awarded by the British Pharmacological Society as a financial support towards participating at the 9th Congress of the European Association of Pharmacology and Therapeutics in Edinburgh and the workshop for opioids in cancer pain.

REFERENCES

- Abdelhamid EE, Sultana M, Portoghese PS, Takemori AE (1991) Selective blockage of delta opioid receptors prevents the development of morphine tolerance and dependence in mice. *J Pharmacol Exp Ther* **258**(1): 299-303
- Addington-Hall J, McCarthy M (1995) Dying from cancer: results of a national population-based investigation. *Palliat Med* **9**(4): 295-305
- Agnes RS, Ying J, Kövér KE, Lee YS, Davis P, Ma SW, Badghisi H, Porreca F, Lai J, Hruby VJ (2008) Structure-activity relationships of bifunctional cyclic disulfide peptides based on overlapping pharmacophores at opioid and cholecystokinin receptors. *Peptides* **29**(8): 1413-23
- Aguila B, Coulbault L, Boulouard M, Léveillé F, Davis A, Tóth G, Borsodi A, Balboni G, Salvadori S, Jauzac P, Allouche S (2007) In vitro and in vivo pharmacological profile of UFP-512, a novel selective delta-opioid receptor agonist; correlations between desensitization and tolerance. *Br J Pharmacol* **152**(8): 1312-24
- Alfaras-Melainis K, Gomes I, Rozenfeld R, Zachariou V, Devi L (2009) Modulation of opioid receptor function by protein-protein interactions. *Front Biosci* **14**: 3594-607
- Alvarez VA, Arttamangkul S, Dang V, Salem A, Whistler JL, Von Zastrow M, Grandy DK, Williams JT (2002) mu-Opioid receptors: Ligand-dependent activation of potassium conductance, desensitization, and internalization. *J Neurosci* **22**(13): 5769-76
- Ananthan S, Johnson CA, Carter RL, Clayton SD, Rice KC, Xu H, Davis P, Porreca F, Rothman RB (1998) Synthesis, opioid receptor binding, and bioassay of naltrindole analogues substituted in the indolic benzene moiety. *J Med Chem* **41**(15): 2872-81
- Angers S, Salahpour A, Bouvier M (2002) Dimerization: an emerging concept for G protein-coupled receptor ontogeny and function. *Annu Rev Pharmacol Toxicol* **42**: 409-35
- Arden JR, Segredo V, Wang Z, Lameh J, Sadée W (1995) Phosphorylation and agonist-specific intracellular trafficking of an epitope-tagged mu-opioid receptor expressed in HEK 293 cells. *J Neurochem* **65**(4): 1636-45
- Arttamangkul S, Torrecilla M, Kobayashi K, Okano H, Williams JT (2006) Separation of mu-opioid receptor desensitization and internalization: endogenous receptors in primary neuronal cultures. *J Neurosci* **26**(15): 4118-25
- Bailey CP, Connor M (2005) Opioids: cellular mechanisms of tolerance and physical dependence. *Curr Opin Pharmacol* **5**(1): 60-8
- Bailey CP, Kelly E, Henderson G (2004) Protein kinase C activation enhances morphine-induced rapid desensitization of mu-opioid receptors in mature rat locus ceruleus neurons. *Mol Pharmacol* **66**(6): 1592-8
- Balboni G, Guerrini R, Salvadori S, Bianchi C, Rizzi D, Bryant SD, Lazarus LH (2002) Evaluation of the Dmt-Tic pharmacophore: conversion of a potent delta-opioid receptor antagonist into a potent delta agonist and ligands with mixed properties. *J Med Chem* **45**(3): 713-20

- Balboni G, Salvadori S, Trapella C, Knapp BI, Bidlack JM, Lazarus LH, Peng X, Neumeyer JL (2010) Evolution of the Bifunctional Lead μ Agonist / δ Antagonist Containing the Dmt-Tic Opioid Pharmacophore. *ACS Chem Neurosci* **1**(2): 155-164
- Ballet S, Pietsch M, Abell AD (2008) Multiple ligands in opioid research. *Protein Pept Lett* **15**(7): 668-82
- Beckett AH, Casy AF (1954) Synthetic analgesics: stereochemical considerations. *J Pharm Pharmacol* **6**(12): 986-1001
- Befort K, Tabbara L, Kieffer BL (1996) [35S]GTP gamma S binding: a tool to evaluate functional activity of a cloned opioid receptor transiently expressed in COS cells. *Neurochem Res* **21**(11): 1301-7
- Berger AC, Whistler JL (2010) How to design an opioid drug that causes reduced tolerance and dependence. *Ann Neurol* **67**(5): 559-69
- Berque-Bestel I, Lezoualc'h F, Jockers R (2008) Bivalent ligands as specific pharmacological tools for G protein-coupled receptor dimers. *Curr Drug Discov Technol* **5**(4): 312-8
- Besse D, Lombard MC, Zajac JM, Roques BP, Besson JM (1990) Pre- and postsynaptic distribution of mu, delta and kappa opioid receptors in the superficial layers of the cervical dorsal horn of the rat spinal cord. *Brain Res* **521**(1-2): 15-22
- Bie B, Pan ZZ (2007) Trafficking of central opioid receptors and descending pain inhibition. *Mol Pain* **3**: 37
- Black DL (2003) Mechanisms of alternative pre-messenger RNA splicing. *Annu Rev Biochem* **72**: 291-336
- Boettcher C, Fellermeier M, Dräger B, Zenk MH (2005) How human neuroblastoma cells make morphine. *Proc Natl Acad Sci U S A* **102**(24): 8495-500
- Bohn LM, Belcheva MM, Coscia CJ (1998) Evidence for kappa- and mu-opioid receptor expression in C6 glioma cells. *J Neurochem* **70**(5): 1819-25
- Bohn LM, Gainetdinov RR, Caron MG (2004) G protein-coupled receptor kinase/beta-arrestin systems and drugs of abuse: psychostimulant and opiate studies in knockout mice. *Neuromolecular Med* **5**(1): 41-50
- Bohn LM, Gainetdinov RR, Lin FT, Lefkowitz RJ, Caron MG (2000) Mu-opioid receptor desensitization by beta-arrestin-2 determines morphine tolerance but not dependence. *Nature* **408**(6813): 720-3
- Borgland SL, Connor M, Osborne PB, Furness JB, Christie MJ (2003) Opioid agonists have different efficacy profiles for G protein activation, rapid desensitization, and endocytosis of mu-opioid receptors. *J Biol Chem* **278**(21): 18776-84
- Bradbury FA, Zelnik JC, Traynor JR (2009) G protein independent phosphorylation and internalization of the delta-opioid receptor. *J Neurochem* **109**(5): 1526-35
- Bunzow JR, Saez C, Mortrud M, Bouvier C, Williams JT, Low M, Grandy DK (1994) Molecular cloning and tissue distribution of a putative member of the rat opioid receptor gene family that is not a mu, delta or kappa opioid receptor type. *FEBS Lett* **347**(2-3): 284-8

- Burford NT, Tolbert LM, Sadee W (1998) Specific G protein activation and mu-opioid receptor internalization caused by morphine, DAMGO and endomorphin I. *Eur J Pharmacol* **342**(1): 123-6
- Burmeister MA, Ansonoff MA, Pintar JE, Kapusta DR (2008) Nociceptin/orphanin FQ (N/OFQ)-evoked bradycardia, hypotension, and diuresis are absent in N/OFQ peptide (NOP) receptor knockout mice. *J Pharmacol Exp Ther* **326**(3): 897-904
- Cadet P, Mantione KJ, Stefano GB (2003) Molecular identification and functional expression of mu 3, a novel alternatively spliced variant of the human mu opiate receptor gene. *J Immunol* **170**(10): 5118-23
- Cahill CM, Morinville A, Lee MC, Vincent JP, Collier B, Beaudet A (2001) Prolonged morphine treatment targets delta opioid receptors to neuronal plasma membranes and enhances delta-mediated antinociception. *J Neurosci* **21**(19): 7598-607
- Cannarsa R, Landuzzi D, Cavina C, Candeletti S, Romualdi P (2008) Kainic acid down-regulates NOP receptor density and gene expression in human neuroblastoma SH-SY5Y cells. *J Mol Neurosci* **35**(2): 171-7
- Carman CV, Benovic JL (1998) G-protein-coupled receptors: turn-ons and turn-offs. *Curr Opin Neurobiol* **8**(3): 335-44
- Carroll I, Thomas JB, Dykstra LA, Granger AL, Allen RM, Howard JL, Pollard GT, Aceto MD, Harris LS (2004) Pharmacological properties of JD1c: a novel kappa-opioid receptor antagonist. *Eur J Pharmacol* **501**(1-3): 111-9
- Carter M, Shieh J (2010) **Animal Behaviour**. In *Guide to Research Techniques in Neuroscience*, pp 51-52. **Burlington, MA**: Academic Press
- Cecchi M, Capriles N, Watson SJ, Akil H (2008) Differential responses to morphine-induced analgesia in the tail-flick test. *Behav Brain Res* **194**(2): 146-51
- Celver J, Xu M, Jin W, Lowe J, Chavkin C (2004) Distinct domains of the mu-opioid receptor control uncoupling and internalization. *Mol Pharmacol* **65**(3): 528-37
- Chaipatikul V, Loh HH, Law PY (2003) Ligand-selective activation of mu-opioid receptor: demonstrated with deletion and single amino acid mutations of third intracellular loop domain. *J Pharmacol Exp Ther* **305**(3): 909-18
- Chakrabarti S, Liu NJ, Gintzler AR (2010) Formation of mu-/kappa-opioid receptor heterodimer is sex-dependent and mediates female-specific opioid analgesia. *Proc Natl Acad Sci U S A* **107**(46): 20115-9
- Chakrabarti S, Prather PL, Yu L, Law PY, Loh HH (1995) Expression of the mu-opioid receptor in CHO cells: ability of mu-opioid ligands to promote alpha-azidoanilido[32P]GTP labeling of multiple G protein alpha subunits. *J Neurochem* **64**(6): 2534-43
- Chakrabarti S, Regec A, Gintzler AR (2005) Biochemical demonstration of mu-opioid receptor association with G α : enhancement following morphine exposure. *Brain Res Mol Brain Res* **135**(1-2): 217-24
- Chavkin C, Goldstein A (1984) Opioid receptor reserve in normal and morphine-tolerant guinea pig ileum myenteric plexus. *Proc Natl Acad Sci U S A* **81**(22): 7253-7

- Chen Y, Mestek A, Liu J, Hurley JA, Yu L (1993) Molecular cloning and functional expression of a mu-opioid receptor from rat brain. *Mol Pharmacol* **44**(1): 8-12
- Cheng PY, Liu-Chen LY, Pickel VM (1997) Dual ultrastructural immunocytochemical labeling of mu and delta opioid receptors in the superficial layers of the rat cervical spinal cord. *Brain Res* **778**(2): 367-80
- Cheng Y, Prusoff WH (1973) Relationship between the inhibition constant (K₁) and the concentration of inhibitor which causes 50 per cent inhibition (I₅₀) of an enzymatic reaction. *Biochem Pharmacol* **22**(23): 3099-108
- Christo PJ, Mazloomdoost D (2008) Cancer pain and analgesia. *Ann N Y Acad Sci* **1138**: 278-98
- Chu J, Zheng H, Zhang Y, Loh HH, Law PY (2010) Agonist-dependent mu-opioid receptor signaling can lead to heterologous desensitization. *Cell Signal* **22**(4): 684-96
- Clapham DE, Neer EJ (1993) New roles for G-protein beta gamma-dimers in transmembrane signalling. *Nature* **365**(6445): 403-6
- Clark MJ, Furman CA, Gilson TD, Traynor JR (2006) Comparison of the relative efficacy and potency of mu-opioid agonists to activate G α (i/o) proteins containing a pertussis toxin-insensitive mutation. *J Pharmacol Exp Ther* **317**(2): 858-64
- Cohen MZ, Easley MK, Ellis C, Hughes B, Ownby K, Rashad BG, Rude M, Taft E, Westbrook JB, JCAHO (2003) Cancer pain management and the JCAHO's pain standards: an institutional challenge. *J Pain Symptom Manage* **25**(6): 519-27
- Colvin LA, Lambert DG (2008) Pain medicine: advances in basic sciences and clinical practice. *Br J Anaesth* **101**(1): 1-4
- Connor M, Christie MD (1999) Opioid receptor signalling mechanisms. *Clin Exp Pharmacol Physiol* **26**(7): 493-9
- Corbett AD, Henderson G, McKnight AT, Paterson SJ (2006) 75 years of opioid research: the exciting but vain quest for the Holy Grail. *Br J Pharmacol* **147 Suppl 1**: S153-62
- Cox BM, Goldstein A, Hi CH (1976) Opioid activity of a peptide, beta-lipotropin-(61-91), derived from beta-lipotropin. *Proc Natl Acad Sci U S A* **73**(6): 1821-3
- Crain SM, Shen KF (1998) Modulation of opioid analgesia, tolerance and dependence by Gs-coupled, GM1 ganglioside-regulated opioid receptor functions. *Trends Pharmacol Sci* **19**(9): 358-65
- Cvejic S, Devi LA (1997) Dimerization of the delta opioid receptor: implication for a role in receptor internalization. *J Biol Chem* **272**(43): 26959-64
- Dang VC, Chieng B, Azriel Y, Christie MJ (2011) Cellular morphine tolerance produced by β arrestin-2-dependent impairment of μ -opioid receptor resensitization. *J Neurosci* **31**(19): 7122-30
- Daniels DJ, Lenard NR, Etienne CL, Law PY, Roerig SC, Portoghese PS (2005) Opioid-induced tolerance and dependence in mice is modulated by the distance between pharmacophores in a bivalent ligand series. *Proc Natl Acad Sci U S A* **102**(52): 19208-13

- Dhawan BN, Cesselin F, Raghbir R, Reisine T, Bradley PB, Portoghese PS, Hamon M (1996) International Union of Pharmacology. XII. Classification of opioid receptors. *Pharmacol Rev* **48**(4): 567-92
- Dighe SV, Madia PA, Sirohi S, Yoburn BC (2009) Continuous morphine produces more tolerance than intermittent or acute treatment. *Pharmacol Biochem Behav* **92**(3): 537-42
- Ding J, Lemieux C, Chung NN, Schiller PW (2012) Bifunctional μ/δ opioid peptides: variation of the type and length of the linker connecting the two components. *Chem Biol Drug Des* **79**(2): 186-93
- Drummond GB (2009) Reporting ethical matters in the Journal of Physiology: standards and advice. *J Physiol* **587**(Pt 4): 713-9
- Duttaroy A, Yoburn BC (1995) The effect of intrinsic efficacy on opioid tolerance. *Anesthesiology* **82**(5): 1226-36
- Eisenberg E, Marinangeli F, Birkhann J, Paladini A, Varassi G (2005) Time to modify the WHO analgesic ladder? *Pain Clinical Updates* **13**: 1-4
- Eisinger DA, Schulz R (2005) Mechanism and consequences of delta-opioid receptor internalization. *Crit Rev Neurobiol* **17**(1): 1-26
- Enquist J, Kim JA, Bartlett S, Ferwerda M, Whistler JL (2011) A novel knock-in mouse reveals mechanistically distinct forms of morphine tolerance. *J Pharmacol Exp Ther* **338**(2): 633-40
- Evans BA, Sato M, Sarwar M, Hutchinson DS, Summers RJ (2010a) Ligand-directed signalling at beta-adrenoceptors. *Br J Pharmacol* **159**(5): 1022-38
- Evans CJ, Keith DE, Morrison H, Magendzo K, Edwards RH (1992) Cloning of a delta opioid receptor by functional expression. *Science* **258**(5090): 1952-5
- Evans RM, You H, Hameed S, Altier C, Mezghrani A, Bourinet E, Zamponi GW (2010b) Heterodimerization of ORL1 and opioid receptors and its consequences for N-type calcium channel regulation. *J Biol Chem* **285**(2): 1032-40
- Fairbanks CA, Wilcox GL (1997) Acute tolerance to spinally administered morphine compares mechanistically with chronically induced morphine tolerance. *J Pharmacol Exp Ther* **282**(3): 1408-17
- Fang L, Knapp RJ, Horvath R, Matsunaga TO, Haaseth RC, Hruby VJ, Porreca F, Yamamura HI (1994) Characterization of [3H]naltrindole binding to delta opioid receptors in mouse brain and mouse vas deferens: evidence for delta opioid receptor heterogeneity. *J Pharmacol Exp Ther* **268**(2): 836-46
- Feuerstein TJ, Gleichauf O, Peckys D, Landwehrmeyer GB, Scheremet R, Jackisch R (1996) Opioid receptor-mediated control of acetylcholine release in human neocortex tissue. *Naunyn Schmiedebergs Arch Pharmacol* **354**(5): 586-92
- Fichna J, do-Rego JC, Chung NN, Lemieux C, Schiller PW, Poels J, Broeck JV, Costentin J, Janecka A (2007) Synthesis and characterization of potent and selective mu-opioid receptor antagonists, [Dmt(1), D-2-Nal(4)]endomorphin-1 (Antanal-1) and [Dmt(1), D-2-Nal(4)]endomorphin-2 (Antanal-2). *J Med Chem* **50**(3): 512-20

- Fields TA, Casey PJ (1997) Signalling functions and biochemical properties of pertussis toxin-resistant G-proteins. *Biochem J* **321** (Pt 3): 561-71
- Filizola M, Laakkonen L, Loew GH (1999) 3D modeling, ligand binding and activation studies of the cloned mouse delta, mu; and kappa opioid receptors. *Protein Eng* **12**(11): 927-42
- Forbes K (2008) *Opioids in Cancer Pain*. UK: Oxford University Press
- Fowler CB, Pogozheva ID, Lomize AL, LeVine H, Mosberg HI (2004) Complex of an active mu-opioid receptor with a cyclic peptide agonist modeled from experimental constraints. *Biochemistry* **43**(50): 15796-810
- Freshney IR (2005) *Culture of animal cells: a manual of basic technique.*, Fifth edition edn: John Wiley & Sons, Inc
- Fundytus ME, Schiller PW, Shapiro M, Weltrowska G, Coderre TJ (1995) Attenuation of morphine tolerance and dependence with the highly selective delta-opioid receptor antagonist TIPP[psi]. *Eur J Pharmacol* **286**(1): 105-8
- George SR, Fan T, Xie Z, Tse R, Tam V, Varghese G, O'Dowd BF (2000) Oligomerization of mu- and delta-opioid receptors. Generation of novel functional properties. *J Biol Chem* **275**(34): 26128-35
- Goldstein A, Tachibana S, Lowney LI, Hunkapiller M, Hood L (1979) Dynorphin-(1-13), an extraordinarily potent opioid peptide. *Proc Natl Acad Sci U S A* **76**(12): 6666-70
- Gomes I, Filipovska J, Jordan BA, Devi LA (2002) Oligomerization of opioid receptors. *Methods* **27**(4): 358-65
- Gomes I, Jordan BA, Gupta A, Trapaidze N, Nagy V, Devi LA (2000) Heterodimerization of mu and delta opioid receptors: A role in opiate synergy. *J Neurosci* **20**(22): RC110
- Green MK, Devine DP (2009) Nociceptin/orphanin FQ and NOP receptor gene regulation after acute or repeated social defeat stress. *Neuropeptides* **43**(6): 507-14
- Greenstein B, Greenstein A (1999) *Color atlas of neuroscience*. New York: Thieme
- Groer CE, Tidgewell K, Moyer RA, Harding WW, Rothman RB, Prisinzano TE, Bohn LM (2007) An opioid agonist that does not induce mu-opioid receptor--arrestin interactions or receptor internalization. *Mol Pharmacol* **71**(2): 549-57
- Grundt P, Jales AR, Traynor JR, Lewis JW, Husbands SM (2003) 14-amino, 14-alkylamino, and 14-acylamino analogs of oxymorphone. Differential effects on opioid receptor binding and functional profiles. *J Med Chem* **46**(8): 1563-6
- Harrison C, McNulty S, Smart D, Rowbotham DJ, Grandy DK, Devi LA, Lambert DG (1999) The effects of endomorphin-1 and endomorphin-2 in CHO cells expressing recombinant mu-opioid receptors and SH-SY5Y cells. *Br J Pharmacol* **128**(2): 472-8
- Harrison C, Rowbotham DJ, Grandy DK, Lambert DG (2000) Endomorphin-1 induced desensitization and down-regulation of the recombinant mu-opioid receptor. *Br J Pharmacol* **131**(6): 1220-6

- Hashimoto Y, Calo G, Guerrini R, Smith G, Lambert DG (2002) Effects of chronic nociceptin/orphanin FQ exposure on cAMP accumulation and receptor density in Chinese hamster ovary cells expressing human nociceptin/orphanin FQ receptors. *Eur J Pharmacol* **449**(1-2): 17-22
- Hawkins KN, Knapp RJ, Gehlert DR, Lui GK, Yamamura MS, Roeske LC, Hruby VJ, Yamamura HI (1988) Quantitative autoradiography of [3H]CTOP binding to mu opioid receptors in rat brain. *Life Sci* **42**(25): 2541-51
- He L, Fong J, von Zastrow M, Whistler JL (2002) Regulation of opioid receptor trafficking and morphine tolerance by receptor oligomerization. *Cell* **108**(2): 271-82
- Hepburn MJ, Little PJ, Gingras J, Kuhn CM (1997) Differential effects of naltrindole on morphine-induced tolerance and physical dependence in rats. *J Pharmacol Exp Ther* **281**(3): 1350-6
- Hirose N, Murakawa K, Takada K, Oi Y, Suzuki T, Nagase H, Cools AR, Koshikawa N (2005) Interactions among mu- and delta-opioid receptors, especially putative delta1- and delta2-opioid receptors, promote dopamine release in the nucleus accumbens. *Neuroscience* **135**(1): 213-25
- Hughes J, Smith TW, Kosterlitz HW, Fothergill LA, Morgan BA, Morris HR (1975) Identification of two related pentapeptides from the brain with potent opiate agonist activity. *Nature* **258**(5536): 577-80
- Jiang M, Spicher K, Boulay G, Wang Y, Birnbaumer L (2001) Most central nervous system D2 dopamine receptors are coupled to their effectors by Go. *Proc Natl Acad Sci U S A* **98**(6): 3577-82
- Jinsmaa Y, Marczak ED, Balboni G, Salvadori S, Lazarus LH (2008) Inhibition of the development of morphine tolerance by a potent dual mu-delta-opioid antagonist, H-Dmt-Tic-Lys-NH-CH2-Ph. *Pharmacol Biochem Behav* **90**(4): 651-7
- Jordan BA, Cvejic S, Devi LA (2000) Opioids and their complicated receptor complexes. *Neuropsychopharmacology* **23**(4 Suppl): S5-S18
- Jordan BA, Devi LA (1999) G-protein-coupled receptor heterodimerization modulates receptor function. *Nature* **399**(6737): 697-700
- Jordan BA, Trapaidze N, Gomes I, Nivarthi R, Devi LA (2001) Oligomerization of opioid receptors with beta 2-adrenergic receptors: a role in trafficking and mitogen-activated protein kinase activation. *Proc Natl Acad Sci U S A* **98**(1): 343-8
- Keith DE, Anton B, Murray SR, Zaki PA, Chu PC, Lissin DV, Montelliet-Agius G, Stewart PL, Evans CJ, von Zastrow M (1998) mu-Opioid receptor internalization: opiate drugs have differential effects on a conserved endocytic mechanism in vitro and in the mammalian brain. *Mol Pharmacol* **53**(3): 377-84
- Keith DE, Murray SR, Zaki PA, Chu PC, Lissin DV, Kang L, Evans CJ, von Zastrow M (1996) Morphine activates opioid receptors without causing their rapid internalization. *J Biol Chem* **271**(32): 19021-4
- Kenakin T (2003) Ligand-selective receptor conformations revisited: the promise and the problem. *Trends Pharmacol Sci* **24**(7): 346-54

- Kenakin T (2007) Functional selectivity through protean and biased agonism: who steers the ship? *Mol Pharmacol* **72**(6): 1393-401
- Kenakin TP (2009) Cellular assays as portals to seven-transmembrane receptor-based drug discovery. *Nat Rev Drug Discov* **8**(8): 617-26
- Kest B, Lee CE, McLemore GL, Inturrisi CE (1996) An antisense oligodeoxynucleotide to the delta opioid receptor (DOR-1) inhibits morphine tolerance and acute dependence in mice. *Brain Res Bull* **39**(3): 185-8
- Kieffer BL (1999) Opioids: first lessons from knockout mice. *Trends Pharmacol Sci* **20**(1): 19-26
- Kieffer BL, Befort K, Gaveriaux-Ruff C, Hirth CG (1992) The delta-opioid receptor: isolation of a cDNA by expression cloning and pharmacological characterization. *Proc Natl Acad Sci U S A* **89**(24): 12048-52
- Kieffer BL, Evans CJ (2002) Opioid tolerance-in search of the holy grail. *Cell* **108**(5): 587-90
- Kim JA, Bartlett S, He L, Nielsen CK, Chang AM, Kharazia V, Waldhoer M, Ou CJ, Taylor S, Ferwerda M, Cado D, Whistler JL (2008) Morphine-induced receptor endocytosis in a novel knockin mouse reduces tolerance and dependence. *Curr Biol* **18**(2): 129-35
- Kissin I, Brown PT, Robinson CA, Bradley EL (1991) Acute tolerance in morphine analgesia: continuous infusion and single injection in rats. *Anesthesiology* **74**(1): 166-71
- Kitayama M, Barnes TA, Carra G, McDonald J, Calo G, Guerrini R, Rowbotham DJ, Smith G, Lambert DG (2003) Pharmacological profile of the cyclic nociceptin/orphanin FQ analogues c[Cys10,14]N/OFQ(1-14)NH₂ and c[Nphe1,Cys10,14]N/OFQ(1-14)NH₂. *Naunyn Schmiedebergs Arch Pharmacol* **368**(6): 528-37
- Kitchen I, Slowe SJ, Matthes HW, Kieffer B (1997) Quantitative autoradiographic mapping of mu-, delta- and kappa-opioid receptors in knockout mice lacking the mu-opioid receptor gene. *Brain Res* **778**(1): 73-88
- Knapp RJ, Malatynska E, Collins N, Fang L, Wang JY, Hruby VJ, Roeske WR, Yamamura HI (1995) Molecular biology and pharmacology of cloned opioid receptors. *FASEB J* **9**(7): 516-25
- Koch T, Höllt V (2008) Role of receptor internalization in opioid tolerance and dependence. *Pharmacol Ther* **117**(2): 199-206
- Koch T, Schulz S, Schroder H, Wolf R, Raulf E, Höllt V (1998) Carboxyl-terminal splicing of the rat mu opioid receptor modulates agonist-mediated internalization and receptor resensitization. *J Biol Chem* **273**(22): 13652-7
- Kulkarni VV, Lee YS, Salibay C, Davis P, Ma SW, Porreca F, Hruby VJ (2009) Novel analogues of bifunctional ligands for opioid and melanocortin 4 receptor. *Adv Exp Med Biol* **611**: 195-6
- Kusmak AJ, Pitchaya S, Anand JP, Mosberg HI, Walter NG, Sunahara RK (2009) Purification and functional reconstitution of monomeric mu-opioid receptors: allosteric modulation of agonist binding by Gi2. *J Biol Chem* **284**(39): 26732-41
- Lambert DG (2008) The nociceptin/orphanin FQ receptor: a target with broad therapeutic potential. *Nat Rev Drug Discov* **7**(8): 694-710

- Lange DG, Fujimoto JM, Fuhrman-Lane CL, Wang RI (1980) Unidirectional non-cross tolerance to etorphine in morphine-tolerant mice and role of the blood-brain barrier. *Toxicol Appl Pharmacol* **54**(2): 177-86
- Law PY, Erickson-Herbrandson LJ, Zha QQ, Solberg J, Chu J, Sarre A, Loh HH (2005) Heterodimerization of mu- and delta-opioid receptors occurs at the cell surface only and requires receptor-G protein interactions. *J Biol Chem* **280**(12): 11152-64
- Ledeboer A, Hutchinson MR, Watkins LR, Johnson KW (2007) Ibudilast (AV-411). A new class therapeutic candidate for neuropathic pain and opioid withdrawal syndromes. *Expert Opin Investig Drugs* **16**(7): 935-50
- Lee MC, Cahill CM, Vincent JP, Beaudet A (2002) Internalization and trafficking of opioid receptor ligands in rat cortical neurons. *Synapse* **43**(2): 102-11
- Lenoir D, Barg J, Simantov R (1984) Characterization and down-regulation of opiate receptors in aggregating fetal rat brain cells. *Brain Res* **304**(2): 285-90
- Levac BA, O'Dowd BF, George SR (2002) Oligomerization of opioid receptors: generation of novel signaling units. *Curr Opin Pharmacol* **2**(1): 76-81
- Li S, Zhu J, Chen C, Chen YW, Deriel JK, Ashby B, Liu-Chen LY (1993) Molecular cloning and expression of a rat kappa opioid receptor. *Biochem J* **295** (Pt 3): 629-33
- Li T, Fujita Y, Shiotani K, Miyazaki A, Tsuda Y, Ambo A, Sasaki Y, Jinsmaa Y, Marczak E, Bryant SD, Salvadori S, Lazarus LH, Okada Y (2005) Potent Dmt-Tic pharmacophoric delta- and mu-opioid receptor antagonists. *J Med Chem* **48**(25): 8035-44
- Li T, Shiotani K, Miyazaki A, Tsuda Y, Ambo A, Sasaki Y, Jinsmaa Y, Marczak E, Bryant SD, Lazarus LH, Okada Y (2007) Bifunctional [2',6'-dimethyl-L-tyrosine¹]endomorphin-2 analogues substituted at position 3 with alkylated phenylalanine derivatives yield potent mixed mu-agonist/delta-antagonist and dual mu-agonist/delta-agonist opioid ligands. *J Med Chem* **50**(12): 2753-66
- Li XY, Sun L, He J, Chen ZL, Zhou F, Liu XY, Liu RS (2010) The kappa-opioid receptor is upregulated in the spinal cord and locus ceruleus but downregulated in the dorsal root ganglia of morphine tolerant rats. *Brain Res* **1326**: 30-9
- Lipkowski AW, Konecka AM, Sadowski B (1982) Double enkephalins. *Pol J Pharmacol Pharm* **34**(1-3): 69-71
- Lipkowski AW, Misicka A, Davis P, Stropova D, Janders J, Lachwa M, Porreca F, Yamamura HI, Hruby VJ (1999) Biological activity of fragments and analogues of the potent dimeric opioid peptide, biphalin. *Bioorg Med Chem Lett* **9**(18): 2763-6
- Liu JG, Prather PL (2001) Chronic exposure to mu-opioid agonists produces constitutive activation of mu-opioid receptors in direct proportion to the efficacy of the agonist used for pretreatment. *Mol Pharmacol* **60**(1): 53-62
- Liu KS, Hu OY, Ho ST, Tzeng JJ, Chen YW, Wang JJ (2004a) Antinociceptive effect of a novel long-acting nalbuphine preparation. *Br J Anaesth* **92**(5): 712-5
- Liu X, Kai M, Jin L, Wang R (2009) Computational study of the heterodimerization between mu and delta receptors. *J Comput Aided Mol Des* **23**(6): 321-32

- Liu YQ, Zhang YZ, Gao PJ (2004b) Novel concentration-killing curve method for estimation of bactericidal potency of antibiotics in an in vitro dynamic model. *Antimicrob Agents Chemother* **48**(10): 3884-91
- Lord JA, Waterfield AA, Hughes J, Kosterlitz HW (1977) Endogenous opioid peptides: multiple agonists and receptors. *Nature* **267**(5611): 495-9
- Lowery JJ, Raymond TJ, Giuvelis D, Bidlack JM, Polt R, Bilsky EJ (2011) In vivo characterization of MMP-2200, a mixed δ/μ opioid agonist, in mice. *J Pharmacol Exp Ther* **336**(3): 767-78
- Mansour A, Khachaturian H, Lewis ME, Akil H, Watson SJ (1987) Autoradiographic differentiation of mu, delta, and kappa opioid receptors in the rat forebrain and midbrain. *J Neurosci* **7**(8): 2445-64
- Martin WR, Eades CG, Thompson JA, Huppler RE, Gilbert PE (1976) The effects of morphine- and nalorphine- like drugs in the nondependent and morphine-dependent chronic spinal dog. *J Pharmacol Exp Ther* **197**(3): 517-32
- Martini L, Whistler JL (2007) The role of mu opioid receptor desensitization and endocytosis in morphine tolerance and dependence. *Curr Opin Neurobiol* **17**(5): 556-64
- Martinka GP, Jhamandas K, Sabourin L, Lapierre C, Lemaire S (1991) Dynorphin A-(1-13)-Tyr14-Leu15-Phe16-Asn17-Gly18-Pro19 : a potent and selective kappa opioid peptide. *Eur J Pharmacol* **196**(2): 161-7
- Mathews JL, Peng X, Xiong W, Zhang A, Negus SS, Neumeyer JL, Bidlack JM (2005) Characterization of a novel bivalent morphinan possessing kappa agonist and micro agonist/antagonist properties. *J Pharmacol Exp Ther* **315**(2): 821-7
- Matlin AJ, Clark F, Smith CW (2005) Understanding alternative splicing: towards a cellular code. *Nat Rev Mol Cell Biol* **6**(5): 386-98
- Matthes HW, Maldonado R, Simonin F, Valverde O, Slowe S, Kitchen I, Befort K, Dierich A, Le Meur M, Dollé P, Tzavara E, Hanoune J, Roques BP, Kieffer BL (1996) Loss of morphine-induced analgesia, reward effect and withdrawal symptoms in mice lacking the mu-opioid-receptor gene. *Nature* **383**(6603): 819-23
- McCarthy RJ, Kroin JS, Tuman KJ, Penn RD, Ivankovich AD (1998) Antinociceptive potentiation and attenuation of tolerance by intrathecal co-infusion of magnesium sulfate and morphine in rats. *Anesth Analg* **86**(4): 830-6
- McCleane GJ (2003) The cholecystokinin antagonist proglumide enhances the analgesic effect of dihydrocodeine. *Clin J Pain* **19**(3): 200-1
- McConalogue K, Grady EF, Minnis J, Balestra B, Tonini M, Brecha NC, Bunnett NW, Sternini C (1999) Activation and internalization of the mu-opioid receptor by the newly discovered endogenous agonists, endomorphin-1 and endomorphin-2. *Neuroscience* **90**(3): 1051-9
- McDonald J, Barnes TA, Okawa H, Williams J, Calo' G, Rowbotham DJ, Lambert DG (2003) Partial agonist behaviour depends upon the level of nociceptin/orphanin FQ receptor expression: studies using the ecdysone-inducible mammalian expression system. *Br J Pharmacol* **140**(1): 61-70

- McNaull B, Trang T, Sutak M, Jhamandas K (2007) Inhibition of tolerance to spinal morphine antinociception by low doses of opioid receptor antagonists. *Eur J Pharmacol* **560**(2-3): 132-41
- McPherson J, Rivero G, Baptist M, Llorente J, Al-Sabah S, Krasel C, Dewey WL, Bailey CP, Rosethorne EM, Charlton SJ, Henderson G, Kelly E (2010) μ -opioid receptors: correlation of agonist efficacy for signalling with ability to activate internalization. *Mol Pharmacol* **78**(4): 756-66
- McVey M, Ramsay D, Kellett E, Rees S, Wilson S, Pope AJ, Milligan G (2001) Monitoring receptor oligomerization using time-resolved fluorescence resonance energy transfer and bioluminescence resonance energy transfer. The human delta -opioid receptor displays constitutive oligomerization at the cell surface, which is not regulated by receptor occupancy. *J Biol Chem* **276**(17): 14092-9
- Meng F, Xie GX, Thompson RC, Mansour A, Goldstein A, Watson SJ, Akil H (1993) Cloning and pharmacological characterization of a rat kappa opioid receptor. *Proc Natl Acad Sci U S A* **90**(21): 9954-8
- Metzger TG, Paterlini MG, Portoghese PS, Ferguson DM (1996) Application of the message-address concept to the docking of naltrexone and selective naltrexone-derived opioid antagonists into opioid receptor models. *Neurochem Res* **21**(11): 1287-94
- Milligan G (2003) Principles: extending the utility of [35S]GTP gamma S binding assays. *Trends Pharmacol Sci* **24**(2): 87-90
- Milligan G (2005) Opioid receptors and their interacting proteins. *Neuromolecular Med* **7**(1-2): 51-9
- Mollereau C, Parmentier M, Mailleux P, Butour JL, Moisand C, Chalon P, Caput D, Vassart G, Meunier JC (1994) ORL1, a novel member of the opioid receptor family. Cloning, functional expression and localization. *FEBS Lett* **341**(1): 33-8
- Morphy R, Rankovic Z (2005) Designed multiple ligands. An emerging drug discovery paradigm. *J Med Chem* **48**(21): 6523-43
- Narita M, Suzuki M, Niikura K, Nakamura A, Miyatake M, Yajima Y, Suzuki T (2006) μ -Opioid receptor internalization-dependent and -independent mechanisms of the development of tolerance to μ -opioid receptor agonists: Comparison between etorphine and morphine. *Neuroscience* **138**(2): 609-19
- Neal CR, Mansour A, Reinscheid R, Nothacker HP, Civelli O, Akil H, Watson SJ (1999) Opioid receptor-like (ORL1) receptor distribution in the rat central nervous system: comparison of ORL1 receptor mRNA expression with (125)I-[(14)Tyr]-orphanin FQ binding. *J Comp Neurol* **412**(4): 563-605
- Neumeyer JL, Peng X, Knapp BI, Bidlack JM, Lazarus LH, Salvadori S, Trapella C, Balboni G (2006) New opioid designed multiple ligand from Dmt-Tic and morphinan pharmacophores. *J Med Chem* **49**(18): 5640-3
- Neumeyer JL, Zhang A, Xiong W, Gu XH, Hilbert JE, Knapp BI, Negus SS, Mello NK, Bidlack JM (2003) Design and synthesis of novel dimeric morphinan ligands for kappa and micro opioid receptors. *J Med Chem* **46**(24): 5162-70

- Nielsen CK, Ross FB, Lotfipour S, Saini KS, Edwards SR, Smith MT (2007) Oxycodone and morphine have distinctly different pharmacological profiles: radioligand binding and behavioural studies in two rat models of neuropathic pain. *Pain* **132**(3): 289-300
- Nielsen CK, Ross FB, Smith MT (2000) Incomplete, asymmetric, and route-dependent cross-tolerance between oxycodone and morphine in the Dark Agouti rat. *J Pharmacol Exp Ther* **295**(1): 91-9
- Nitsche JF, Schuller AG, King MA, Zengh M, Pasternak GW, Pintar JE (2002) Genetic dissociation of opiate tolerance and physical dependence in delta-opioid receptor-1 and preproenkephalin knock-out mice. *J Neurosci* **22**(24): 10906-13
- Okada Y, Tsuda Y, Fujita Y, Yokoi T, Sasaki Y, Ambo A, Konishi R, Nagata M, Salvadori S, Jinsmaa Y, Bryant SD, Lazarus LH (2003) Unique high-affinity synthetic mu-opioid receptor agonists with central- and systemic-mediated analgesia. *J Med Chem* **46**(15): 3201-9
- Ossipov MH, Lai J, King T, Vanderah TW, Malan TP, Jr., Hruby VJ, Porreca F (2004) Antinociceptive and nociceptive actions of opioids. *J Neurobiol* **61**(1): 126-48
- Pan YX (2005) Diversity and complexity of the mu opioid receptor gene: alternative pre-mRNA splicing and promoters. *DNA Cell Biol* **24**(11): 736-50
- Pan YX, Bolan E, Pasternak GW (2002) Dimerization of morphine and orphanin FQ/nociceptin receptors: generation of a novel opioid receptor subtype. *Biochem Biophys Res Commun* **297**(3): 659-63
- Pan YX, Xu J, Mahurter L, Bolan E, Xu M, Pasternak GW (2001) Generation of the mu opioid receptor (MOR-1) protein by three new splice variants of the Oprm gene. *Proc Natl Acad Sci U S A* **98**(24): 14084-9
- Pan YX, Xu J, Xu M, Rossi GC, Matulonis JE, Pasternak GW (2009) Involvement of exon 11-associated variants of the mu opioid receptor MOR-1 in heroin, but not morphine, actions. *Proc Natl Acad Sci U S A* **106**(12): 4917-22
- Pasternak GW (2005) Molecular biology of opioid analgesia. *J Pain Symptom Manage* **29**(5 Suppl): S2-9
- Pasternak GW, Childers SR, Snyder SH (1980) Opiate analgesia: evidence for mediation by a subpopulation of opiate receptors. *Science* **208**(4443): 514-6
- Patel MB, Patel CN, Rajashekara V, Yoburn BC (2002) Opioid agonists differentially regulate mu-opioid receptors and trafficking proteins in vivo. *Mol Pharmacol* **62**(6): 1464-70
- Peng X, Knapp BI, Bidlack JM, Neumeyer JL (2006) Synthesis and preliminary in vitro investigation of bivalent ligands containing homo- and heterodimeric pharmacophores at mu, delta, and kappa opioid receptors. *J Med Chem* **49**(1): 256-62
- Peng X, Knapp BI, Bidlack JM, Neumeyer JL (2007) Pharmacological properties of bivalent ligands containing butorphan linked to nalbuphine, naltrexone, and naloxone at mu, delta, and kappa opioid receptors. *J Med Chem* **50**(9): 2254-8
- Peng X, Neumeyer JL (2007) Kappa receptor bivalent ligands. *Curr Top Med Chem* **7**(4): 363-73
- Pert CB, Snyder SH (1973) Opiate receptor: demonstration in nervous tissue. *Science* **179**(77): 1011-4

- Portenoy RK, Lesage P (1999) Management of cancer pain. *Lancet* **353**(9165): 1695-700
- Portoghese PS (1965) A new concept on the mode of interaction of narcotic analgesics with receptors. *J Med Chem* **8**(5): 609-16
- Portoghese PS (1989) Bivalent ligands and the message-address concept in the design of selective opioid receptor antagonists. *Trends Pharmacol Sci* **10**(6): 230-5
- Portoghese PS (2001) From models to molecules: opioid receptor dimers, bivalent ligands, and selective opioid receptor probes. *J Med Chem* **44**(14): 2259-69
- Portoghese PS, Lunzer MM (2003) Identity of the putative delta1-opioid receptor as a delta-kappa heteromer in the mouse spinal cord. *Eur J Pharmacol* **467**(1-3): 233-4
- Pradhan AA, Walwyn W, Nozaki C, Filliol D, Erbs E, Matifas A, Evans C, Kieffer BL (2010) Ligand-directed trafficking of the δ -opioid receptor in vivo: two paths toward analgesic tolerance. *J Neurosci* **30**(49): 16459-68
- Prado WA (2003) Antinociceptive potency of intrathecal morphine in the rat tail flick test: a comparative study using acute lumbar catheter in rats with or without a chronic atlanto-occipital catheter. *J Neurosci Methods* **129**(1): 33-9
- Purington LC, Sobczyk-Kojiro K, Pogozheva ID, Traynor JR, Mosberg HI (2011) Development and in vitro characterization of a novel bifunctional μ -agonist/ δ -antagonist opioid tetrapeptide. *ACS Chem Biol* **6**(12): 1375-81
- Qiu Y, Law PY, Loh HH (2003) Mu-opioid receptor desensitization: role of receptor phosphorylation, internalization, and representation. *J Biol Chem* **278**(38): 36733-9
- Raehal KM, Bohn LM (2011) The role of beta-arrestin2 in the severity of antinociceptive tolerance and physical dependence induced by different opioid pain therapeutics. *Neuropharmacology* **60**(1): 58-65
- Raffa RB, Martinez RP, Connelly CD (1994) G-protein antisense oligodeoxyribonucleotides and mu-opioid supraspinal antinociception. *Eur J Pharmacol* **258**(1-2): R5-7
- Ramsay D, Carr IC, Pediani J, Lopez-Gimenez JF, Thurlow R, Fidock M, Milligan G (2004) High-affinity interactions between human α 1A-adrenoceptor C-terminal splice variants produce homo- and heterodimers but do not generate the α 1L-adrenoceptor. *Mol Pharmacol* **66**(2): 228-39
- Ramsay D, Kellett E, McVey M, Rees S, Milligan G (2002) Homo- and hetero-oligomeric interactions between G-protein-coupled receptors in living cells monitored by two variants of bioluminescence resonance energy transfer (BRET): hetero-oligomers between receptor subtypes form more efficiently than between less closely related sequences. *Biochem J* **365**(Pt 2): 429-40
- Rana SP, Ahmed A, Kumar V, Chaudhary PK, Khurana D, Mishra S (2011) Successful management of a difficult cancer pain patient by appropriate adjuvant and morphine titration. *Indian J Palliat Care* **17**(2): 162-5
- Rang HP, Dale MM, Ritter JM (1999) *Analgesic Drugs*, Fourth Edition edn. Edinburgh: Churchill Livingstone

- Ribeiro-Neto FA, Rodbell M (1989) Pertussis toxin induces structural changes in G alpha proteins independently of ADP-ribosylation. *Proc Natl Acad Sci U S A* **86**(8): 2577-81
- Ripamonti C, Zecca E, De Conno F (1998) Pharmacological treatment of cancer pain: alternative routes of opioid administration. *Tumori* **84**(3): 289-300
- Rizzi A, Molinari S, Marti M, Marzola G, Calo' G (2011) Nociceptin/orphanin FQ receptor knockout rats: in vitro and in vivo studies. *Neuropharmacology* **60**(4): 572-9
- Rossi GC, Brown GP, Leventhal L, Yang K, Pasternak GW (1996) Novel receptor mechanisms for heroin and morphine-6 beta-glucuronide analgesia. *Neurosci Lett* **216**(1): 1-4
- Roy S, Guo X, Kelschenbach J, Liu Y, Loh HH (2005) In vivo activation of a mutant mu-opioid receptor by naltrexone produces a potent analgesic effect but no tolerance: role of mu-receptor activation and delta-receptor blockade in morphine tolerance. *J Neurosci* **25**(12): 3229-33
- Salvadori S, Fiorini S, Trapella C, Porreca F, Davis P, Sasaki Y, Ambo A, Marczak ED, Lazarus LH, Balboni G (2008) Role of benzimidazole (Bid) in the delta-opioid agonist pseudopeptide H-Dmt-Tic-NH-CH(2)-Bid (UFP-502). *Bioorg Med Chem* **16**(6): 3032-8
- Salvadori S, Trapella C, Fiorini S, Negri L, Lattanzi R, Bryant SD, Jinsmaa Y, Lazarus LH, Balboni G (2007) A new opioid designed multiple ligand derived from the micro opioid agonist endomorphin-2 and the delta opioid antagonist pharmacophore Dmt-Tic. *Bioorg Med Chem* **15**(22): 6876-81
- Sánchez-Blázquez P, Gómez-Serranillos P, Garzón J (2001) Agonists determine the pattern of G-protein activation in mu-opioid receptor-mediated supraspinal analgesia. *Brain Res Bull* **54**(2): 229-35
- Sandrini M, Vitale G, Ruggieri V, Pini LA (2007) Effect of acute and repeated administration of paracetamol on opioidergic and serotonergic systems in rats. *Inflamm Res* **56**(4): 139-42
- Schiller PW (2010) Bi- or multifunctional opioid peptide drugs. *Life Sci* **86**(15-16): 598-603
- Schiller PW, Fundytus ME, Merovitz L, Weltrowska G, Nguyen TM, Lemieux C, Chung NN, Coderre TJ (1999) The opioid mu agonist/delta antagonist DIPP-NH(2)[Psi] produces a potent analgesic effect, no physical dependence, and less tolerance than morphine in rats. *J Med Chem* **42**(18): 3520-6
- Schmidt R, Vogel D, Mrestani-Klaus C, Brandt W, Neubert K, Chung NN, Lemieux C, Schiller PW (1994) Cyclic beta-casomorphin analogues with mixed mu agonist/delta antagonist properties: synthesis, pharmacological characterization, and conformational aspects. *J Med Chem* **37**(8): 1136-44
- Schuller AG, King MA, Zhang J, Bolan E, Pan YX, Morgan DJ, Chang A, Czick ME, Unterwald EM, Pasternak GW, Pintar JE (1999) Retention of heroin and morphine-6 beta-glucuronide analgesia in a new line of mice lacking exon 1 of MOR-1. *Nat Neurosci* **2**(2): 151-6
- Shaheen PE, Legrand SB, Walsh D, Estfan B, Davis MP, Lagman RL, Riaz M, Cheema B (2010) Errors in opioid prescribing: a prospective survey in cancer pain. *J Pain Symptom Manage* **39**(4): 702-11

- Sharif RN, Osborne M, Coderre TJ, Fundytus ME (2002) Attenuation of morphine tolerance after antisense oligonucleotide knock-down of spinal mGluR1. *Br J Pharmacol* **136**(6): 865-72
- Sharman JL, Mpamhanga CP, Spedding M, Germain P, Staels B, Dacquet C, Laudet V, Harmar AJ (2011) IUPHAR DATABASE Vol. 2012.
- Silva-Moreno A, Gonzalez-Espinosa C, León-Olea M, Cruz SL (2012) Synergistic antinociceptive actions and tolerance development produced by morphine-fentanyl coadministration: correlation with μ -opioid receptor internalization. *Eur J Pharmacol* **674**(2-3): 239-47
- Simantov R, Lotem J, Levy R (1984) Selectivity in the control of opiate receptor density in the animal and in cultured fetal brain cells. *Neuropeptides* **5**(1-3): 197-200
- Simon EJ, Hiller JM, Edelman I (1973) Stereospecific binding of the potent narcotic analgesic (3H) Etorphine to rat-brain homogenate. *Proc Natl Acad Sci U S A* **70**(7): 1947-9
- Simonin F, Slowe S, Becker JA, Matthes HW, Filliol D, Chluba J, Kitchen I, Kieffer BL (2001) Analysis of [3H]bremazocine binding in single and combinatorial opioid receptor knockout mice. *Eur J Pharmacol* **414**(2-3): 189-95
- Smart D, Lambert DG (1996) delta-Opioids stimulate inositol 1,4,5-trisphosphate formation, and so mobilize Ca²⁺ from intracellular stores, in undifferentiated NG108-15 cells. *J Neurochem* **66**(4): 1462-7
- Smart D, Smith G, Lambert DG (1994) mu-Opioid receptor stimulation of inositol (1,4,5)trisphosphate formation via a pertussis toxin-sensitive G protein. *J Neurochem* **62**(3): 1009-14
- Smith FL, Dombrowski DS, Dewey WL (1999) Involvement of intracellular calcium in morphine tolerance in mice. *Pharmacol Biochem Behav* **62**(2): 381-8
- Song B, Marvizón JC (2003) Peptidases prevent mu-opioid receptor internalization in dorsal horn neurons by endogenously released opioids. *J Neurosci* **23**(5): 1847-58
- Sora I, Takahashi N, Funada M, Ujike H, Revay RS, Donovan DM, Miner LL, Uhl GR (1997) Opiate receptor knockout mice define mu receptor roles in endogenous nociceptive responses and morphine-induced analgesia. *Proc Natl Acad Sci U S A* **94**(4): 1544-9
- Spampinato S, Baiula M, Calienni M (2007) Agonist-regulated internalization and desensitization of the human nociceptin receptor expressed in CHO cells. *Curr Drug Targets* **8**(1): 137-46
- Storkson RV, Kjorsvik A, Tjolsen A, Hole K (1996) Lumbar catheterization of the spinal subarachnoid space in the rat. *J Neurosci Methods* **65**(2): 167-72
- Surratt CK, Adams WR (2005) G protein-coupled receptor structural motifs: relevance to the opioid receptors. *Curr Top Med Chem* **5**(3): 315-24
- Takayama N, Ueda H (2005) Morphine-induced overexpression of prepro-nociceptin/orphanin FQ in cultured astrocytes. *Peptides* **26**(12): 2513-7
- Tang WJ, Gilman AG (1991) Type-specific regulation of adenylyl cyclase by G protein beta gamma subunits. *Science* **254**(5037): 1500-3

- Tanowitz M, Hislop JN, von Zastrow M (2008) Alternative splicing determines the post-endocytic sorting fate of G-protein-coupled receptors. *J Biol Chem* **283**(51): 35614-21
- Teodorov E, Modena CC, Sukikara MH, Felicio LF (2006) Preliminary study of the effects of morphine treatment on opioid receptor gene expression in brain structures of the female rat. *Neuroscience* **141**(3): 1225-31
- Terenius L (1973) Characteristics of the "receptor" for narcotic analgesics in synaptic plasma membrane fraction from rat brain. *Acta Pharmacol Toxicol (Copenh)* **33**(5): 377-84
- Thompson RC, Mansour A, Akil H, Watson SJ (1993) Cloning and pharmacological characterization of a rat mu opioid receptor. *Neuron* **11**(5): 903-13
- Toll L, Khroyan TV, Polgar WE, Jiang F, Olsen C, Zaveri NT (2009) Comparison of the antinociceptive and antirewarding profiles of novel bifunctional nociceptin receptor/mu-opioid receptor ligands: implications for therapeutic applications. *J Pharmacol Exp Ther* **331**(3): 954-64
- Trescot AM, Datta S, Lee M, Hansen H (2008) Opioid pharmacology. *Pain Physician* **11**(2 Suppl): S133-53
- Ueda H, Yamaguchi T, Tokuyama S, Inoue M, Nishi M, Takeshima H (1997) Partial loss of tolerance liability to morphine analgesia in mice lacking the nociceptin receptor gene. *Neurosci Lett* **237**(2-3): 136-8
- van den Beuken-van Everdingen MH, de Rijke JM, Kessels AG, Schouten HC, van Kleef M, Patijn J (2007) High prevalence of pain in patients with cancer in a large population-based study in The Netherlands. *Pain* **132**(3): 312-20
- van Rijn RM, Whistler JL (2008) The only way is up: preventing opioid tolerance by promoting cell surface expression of MOR-DOR heterodimers? *Mol Interv* **8**(6): 277-80
- van Rijn RM, Whistler JL, Waldhoer M (2010) Opioid-receptor-heteromer-specific trafficking and pharmacology. *Curr Opin Pharmacol* **10**(1): 73-9
- Vergura R, Valenti E, Hebbes CP, Gavioli EC, Spagnolo B, McDonald J, Lambert DG, Balboni G, Salvadori S, Regoli D, Calo G (2006) Dmt-Tic-NH-CH₂-Bid (UFP-502), a potent DOP receptor agonist: in vitro and in vivo studies. *Peptides* **27**(12): 3322-30
- Von Zastrow M, Keith DE, Evans CJ (1993) Agonist-induced state of the delta-opioid receptor that discriminates between opioid peptides and opiate alkaloids. *Mol Pharmacol* **44**(1): 166-72
- von Zastrow M, Kobilka BK (1994) Antagonist-dependent and -independent steps in the mechanism of adrenergic receptor internalization. *J Biol Chem* **269**(28): 18448-52
- Waldhoer M, Fong J, Jones RM, Lunzer MM, Sharma SK, Kostenis E, Portoghesi PS, Whistler JL (2005) A heterodimer-selective agonist shows in vivo relevance of G protein-coupled receptor dimers. *Proc Natl Acad Sci U S A* **102**(25): 9050-5
- Walwyn W, John S, Maga M, Evans CJ, Hales TG (2009) Delta receptors are required for full inhibitory coupling of mu-receptors to voltage-dependent Ca²⁺ channels in dorsal root ganglion neurons. *Mol Pharmacol* **76**(1): 134-43

- Wang HB, Zhao B, Zhong YQ, Li KC, Li ZY, Wang Q, Lu YJ, Zhang ZN, He SQ, Zheng HC, Wu SX, Hökfelt TG, Bao L, Zhang X (2010) Coexpression of delta- and mu-opioid receptors in nociceptive sensory neurons. *Proc Natl Acad Sci U S A* **107**(29): 13117-22
- Wang HL, Hsu CY, Huang PC, Kuo YL, Li AH, Yeh TH, Tso AS, Chen YL (2005) Heterodimerization of opioid receptor-like 1 and mu-opioid receptors impairs the potency of micro receptor agonist. *J Neurochem* **92**(6): 1285-94
- Wang JB, Imai Y, Eppler CM, Gregor P, Spivak CE, Uhl GR (1993) mu opiate receptor: cDNA cloning and expression. *Proc Natl Acad Sci U S A* **90**(21): 10230-4
- Wei LN, Loh HH (2011) Transcriptional and epigenetic regulation of opioid receptor genes: present and future. *Annu Rev Pharmacol Toxicol* **51**: 75-97
- Weltrowska G, Lemieux C, Chung NN, Schiller PW (2004) A chimeric opioid peptide with mixed mu agonist/delta antagonist properties. *J Pept Res* **63**(2): 63-8
- Whistler JL (2012) Examining the role of mu opioid receptor endocytosis in the beneficial and side-effects of prolonged opioid use: From a symposium on new concepts in mu-opioid pharmacology. *Drug Alcohol Depend* **121**(3): 189-204
- Whistler JL, Chuang HH, Chu P, Jan LY, von Zastrow M (1999) Functional dissociation of mu opioid receptor signaling and endocytosis: implications for the biology of opiate tolerance and addiction. *Neuron* **23**(4): 737-46
- Whistler JL, von Zastrow M (1998) Morphine-activated opioid receptors elude desensitization by beta-arrestin. *Proc Natl Acad Sci U S A* **95**(17): 9914-9
- Williams JP, Thompson JP, McDonald J, Barnes TA, Cote T, Rowbotham DJ, Lambert DG (2007) Human peripheral blood mononuclear cells express nociceptin/orphanin FQ, but not mu, delta, or kappa opioid receptors. *Anesth Analg* **105**(4): 998-1005, table of contents
- Wolozin BL, Pasternak GW (1981) Classification of multiple morphine and enkephalin binding sites in the central nervous system. *Proc Natl Acad Sci U S A* **78**(10): 6181-5
- Xu J, Xu M, Rossi GC, Pasternak GW, Pan YX (2011) Identification and characterization of seven new exon 11-associated splice variants of the rat mu opioid receptor gene, OPRM1. *Mol Pain* **7**(1): 9
- Yamamoto T, Nair P, Jacobsen NE, Kulkarni V, Davis P, Ma SW, Navratilova E, Yamamura HI, Vanderah TW, Porreca F, Lai J, Hruby VJ (2010) Biological and conformational evaluation of bifunctional compounds for opioid receptor agonists and neurokinin 1 receptor antagonists possessing two penicillamines. *J Med Chem* **53**(15): 5491-501
- Yamazaki M, Suzuki T, Narita M, Lipkowski AW (2001) The opioid peptide analogue biphalin induces less physical dependence than morphine. *Life Sci* **69**(9): 1023-8
- Yang CH, Huang HW, Chen KH, Chen YS, Sheen-Chen SM, Lin CR (2011) Antinociceptive potentiation and attenuation of tolerance by intrathecal β -arrestin 2 small interfering RNA in rats. *Br J Anaesth* **107**(5): 774-81
- Yoshikawa K, Sabol SL (1986) Expression of the enkephalin precursor gene in C6 rat glioma cells: regulation by beta-adrenergic agonists and glucocorticoids. *Brain Res* **387**(1): 75-83

- Yu X, Mao X, Blake AD, Li WX, Chang SL (2003) Morphine and endomorphins differentially regulate micro-opioid receptor mRNA in SHSY-5Y human neuroblastoma cells. *J Pharmacol Exp Ther* **306**(2): 447-54
- Zadina JE, Hackler L, Ge LJ, Kastin AJ (1997) A potent and selective endogenous agonist for the mu-opiate receptor. *Nature* **386**(6624): 499-502
- Zastawny RL, George SR, Nguyen T, Cheng R, Tsatsos J, Briones-Urbina R, O'Dowd BF (1994) Cloning, characterization, and distribution of a mu-opioid receptor in rat brain. *J Neurochem* **62**(6): 2099-105
- Zhang X, Wang F, Chen X, Li J, Xiang B, Zhang YQ, Li BM, Ma L (2005) Beta-arrestin1 and beta-arrestin2 are differentially required for phosphorylation-dependent and -independent internalization of delta-opioid receptors. *J Neurochem* **95**(1): 169-78
- Zheng H, Chu J, Zhang Y, Loh HH, Law PY (2011) Modulating {micro}-opioid receptor phosphorylation switches agonist-dependent signaling as reflected in PKC{epsilon} activation and dendritic spine stability. *J Biol Chem* **286**(14):12724-33
- Zhu Y, King MA, Schuller AG, Nitsche JF, Reidl M, Elde RP, Unterwald E, Pasternak GW, Pintar JE (1999) Retention of supraspinal delta-like analgesia and loss of morphine tolerance in delta opioid receptor knockout mice. *Neuron* **24**(1): 243-52
- Zimprich A, Simon T, Höllt V (1995) Cloning and expression of an isoform of the rat mu opioid receptor (rMOR1B) which differs in agonist induced desensitization from rMOR1. *FEBS Lett* **359**(2-3): 142-6
- Zuo Z (2005) The role of opioid receptor internalization and beta-arrestins in the development of opioid tolerance. *Anesth Analg* **101**(3): 728-34, table of contents